Dissertation

Cyclic GMP signaling during the lytic cycle of *Toxoplasma gondii*

zur Erlangung des akademischen Grades
doctor rerum naturalium
(Dr. rer. nat.)

im Fach Biologie

eingereicht an der

Lebenswissenschaftlichen Fakultät

der Humboldt-Universität zu Berlin

von

M. Sc. Özlem Günay-Esiyok

Präsidentin der Humboldt-Universität zu Berlin
Prof. Dr.-Ing. Dr. Sabine Kunst

Dekan der Lebenswissenschaftlichen Fakultät
Prof. Dr. Bernhard Grimm

Gutachter: 1. Prof. Dr. Friedrich W. Herberg
2. Prof. a. D. Dr. Richard Lucius
3. PD Dr. Nishith Gupta

eingereicht am: 06.08.2019
Datum der mündlichen Verteidigung: 05.11.2019

https://doi.org/10.18452/20740

Abstract

Infection and pathogenesis of *Toxoplasma gondii* depend on well-coordinated and cGMP-mediated regulation of subcellular events. Cyclic GMP signaling is known as one of the master regulators of diverse functions in eukaryotes; however, its architecture and functioning in protozoans including *T. gondii* remain poorly understood. In the scope of this thesis, an exclusive guanylate cyclase coupled with N-terminal P4-ATPase was reported in a common and clinically relevant obligate intracellular parasite *T. gondii* that can infect almost all nucleated cells of warm-blooded organisms. *In silico* analysis indicated an activation of the guanylate cyclase by heterodimerization of its two cyclase domains and offered valuable insights into possible functions of its ATPase domain. This bulky protein (477-kDa), termed in this study as *Tg*ATPase$_{P}$-GC to fairly reflect its envisaged multifunctionality, localizes in the plasma membrane at the apical pole of the parasite, whereas the corresponding cGMP-dependent protein kinase (*Tg*PKG) is distributed in the cytomembranes. *Tg*ATPase$_{P}$-GC is refractory to genetic deletion, and its CRISPR/Cas9-assisted disruption aborts the lytic cycle of *T. gondii*. Besides, Cre/loxP-mediated knockdown of *Tg*ATPase$_{P}$-GC reduced the synthesis of cGMP in the fast-replicating tachyzoite stage and inhibited the parasite growth due to impairments of motility-dependent egress and invasion events. Equally, repression of *Tg*PKG by a similar strategy recapitulated phenotypes of the *Tg*ATPase$_{P}$-GC-depleted mutant. Notably, despite its temporally restricted function, *Tg*ATPase$_{P}$-GC is expressed constitutively throughout the lytic cycle, entailing a post-translational regulation of cGMP signaling. Not least, the occurrence of *Tg*ATPase$_{P}$-GC orthologs in several other alveolates implies a divergent functional repurposing of cGMP signaling in protozoans.

Besides native signaling, an optogenetic approach was also utilized by expressing a light-activated rhodopsin-guanylate cyclase (RhoGC) from an aquatic fungus *Blastocladiella emersonii* in *T. gondii*. The system enabled a light-control of cGMP elevation on crucial steps of lytic cycle in a fast, spatial and reversible manner. Excitation of RhoGC which was expressed under different conditions resulted in at least 2-fold increase in motile fraction and three times longer average trail lengths of parasites in comparison to dark cultures. The impact of gliding motility was also observed in host-cell invasion and egress, which is consistent with the genetic knockdown studies of *Tg*ATPase$_{P}$-GC and *Tg*PKG mentioned above. Having established optogenetically modified parasite strains now allows to identify mediators of cGMP signaling *via* phosphoproteomic analysis.

Keywords: Egress, guanylate cyclase, invasion, motility, optogenetics, P4-ATPase, *Toxoplasma*

Zusammenfassung

Infektion und Pathogenese von *Toxoplasma gondii* beruhen auf einer gut koordinierten und cyclisches GMP-vermittelten Regulierung subzellulärer Ereignisse. Der cGMP-Signalweg ist als einer der Hauptregulatoren von diversen Funktionen in Eukaryoten bekannt; allerdings ist seine Architektur und Funktionsweise in Protozoen wie *T. gondii* immer noch wenig verstanden. Im Rahmen dieser Arbeit wurde eine exklusive Guanylatcyclase, gekoppelt mit einer N-terminalen P4-ATPase, in einem weit verbreiteten und klinisch relevanten, obligat intrazellulären Parasiten *T. gondii*, der fast alle Kern-haltigen Zellen warmblütiger Tiere infizieren kann, gemeldet. Eine *in silico*-Analyse wies auf eine Aktivierung der Guanylatcyclase durch Heterodimerisierung ihrer beiden Cyclasedomänen hin und ermöglichte wertvolle Einsichten in mögliche Funktionen ihrer ATPase-Domäne. Um die vorgestellte Multifunktionalität dieses massigen Proteins (477 kDa) gerecht widerzuspiegeln, wurde es in dieser Studie als *Tg*ATPase$_{P}$-GC bezeichnet. Es ist in der Plasmamembran am apikalen Pol des Parasiten lokalisiert, während die entsprechende cGMP-abhängige Proteinkinase (*Tg*PKG) in den Zellmembranen verbreitet ist. *Tg*ATPase$_{P}$-GC ist unempfänglich gegenüber genetischer Deletion und seine CRISPR/Cas9 unterstützte Spaltung beendet den lytischen Zyklus von *T. gondii* vorzeitig. Darüber hinaus reduzierte ein Cre/loxP-vermittelter Knockdown von *Tg*ATPase$_{P}$-GC die Synthese von cGMP im sich schnell-replizierenden Tachyzoiten-Stadium und inhibierte das Parasitenwachstum aufgrund von Beeinträchtigungen Motilitäts-abhängiger Prozesse des Austretens und Eindringens. Die Phänotypen des *Tg*ATPase$_{P}$-GC-armen Mutanten wiederholten sich durch eine ähnliche Strategie der Hemmung von *Tg*PKG. Trotz seiner zeitlich beschränkten Funktion ist *Tg*ATPase$_{P}$-GC konstitutiv während des ganzen lytischen Zyklus exprimiert, welches eine post-translationale Regulierung des cGMP-Signalweges bedingt. Nicht zuletzt impliziert das Vorhandensein von *Tg*ATPase$_{P}$-GC-Orthologen in anderen Alveolata eine divergente Umfunktionierung der cGMP-Signalwege in Protozoen.

Neben dem natürlichen Signalweg wurde auch ein optogenetischer Ansatz genutzt, indem eine Licht-aktivierte Rhodopsin-Guanylatcyclase (RhoGC) aus dem aquatischen Pilz *Blastocladiella emersonii* in *T. gondii* exprimiert wurde. Dieses System erlaubte eine kontrollierte Erhöhung von cGMP durch Licht an entscheidenden Schritten des lytischen Zyklus in einer schnellen, räumlich-beschränkten und reversiblen Weise. Die Anregung von RhoGC, das unter verschiedenen Bedingungen exprimiert wurde, steigerte den motilen Anteil mindestens ums doppelte und verlängerte die mittlere Spurlänge ums dreifache im Vergleich zu den dunklen Kulturen. Der Einfluss der Gleitmotilität wurde auch beim Eindringen in sowie Austreten aus den

Wirtszellen beobachtet und befindet sich in Einklang mit den oben genannten Knockdown-Studien von *Tg*ATPase$_{P}$-GC und *Tg*PKG. Die Etablierung optogenetisch modifizierter Parasitenstämme ermöglicht es jetzt, die Vermittler des cGMP-Signalwegs durch phosphoproteomische Analysen zu identifizieren.

Schlagwörter: Austreten, Guanylatcyclase, Eindringen, Motilität, Optogenetik, P4-ATPase, *Toxoplasma*

Table of Contents

List of Abbreviations

%	Percentage	**FCS**	Fetal calf serum
°C	Celsius degree	**FUDR**	5-fluoro-2'-deoxyuridine
µ	Micro	**g**	Gravity or gram
AC	Adenylate cyclase	**GAP45**	Glideosome-associated protein 45
Amp	Ampicillin	**GC**	Guanylate cyclase
Approx.	Approximately	**GCaMP6s**	Circularly permuted GFP-calmodulin-M13 peptide 6
ATP	Adenosine triphosphate	**gDNA**	Genomic deoxyribonucleic acid
APH	Acylated-peleckstrin-homology domain	**GECI**	Genetically encoded calcium indicators
au	Arbitrary units	**GFP**	Green fluorescent protein
bp	Base pair	**GRA**	Dense granule protein
BSA	Bovine serum albumin	**GSH**	Glutathione
C2	Compound 2	**GTP**	Guanosine triphosphate
Ca^{2+}	Calcium	**h**	Hour
$CaCl_2$	Calcium chloride	**HA**	Hemagglutinin
CaM	Calmodulin	**HBBS**	Hanks balanced salt solution
cAMP	Cyclic adenosine monophosphate	**HEPES**	4-(2-hxdroxyethyl)-1-piperazineethane-sulfonic acid
cDNA	Complementary deoxyribonucleic acid	**HFF**	Human foreskin fibroblasts
CDPK	Ca^{2+}-dependent protein kinase	**hpi**	Hours post infection
cGMP	Cyclic guanosine monophosphate	**HPLC**	High Performance Liquid Chromatography
cNMP	Cyclic nucleotide monophosphate	**IFA**	Immunofluorescence assay
cm^2	Centimeter square	**iFCS**	Inactivated fetal calf serum
CO_2	Carbon dioxide	**IMC**	Inner membrane complex
cpEGFP	Circularly-permuted enhanced green fluorescent protein	**IP_3**	Inositol 1,4,5-trisphosphate
DAG	Diacylglycerol	**kb**	Kilo bases
DAPI	4',6-diamidino-2-phenylindole	**l**	Liter
DD	Destabilization domain	**LB**	Luria-bertani
DGK	DAG-kinase	**M**	Molar
dH_2O	Distilled water	**m-**	Milli
DHFR	Dihydrofolate reductase	**-m**	Meter
DMEM	Dulbecco's modified eagle medium	**MeOH**	Methanol
DMSO	Dimethylsulfoxide	**$MgCl_2$**	Magnesium chloride
DNA	Deoxyribonucleic acid	**MIC**	Microneme protein
dNTP	Deoxyribonucleotide triphosphate	**min**	Minute
DTT	Dithiothreitol	**MOI**	Moiety of infection
E. coli	*Escherichia coli*	**ms**	Milliseconds
EDTA	Ethylenediaminetetraacetic acid	**n-**	Nano
eGFP	Enhanced green fluorescent protein	**NaCl**	Sodium chloride
ER	Endoplasmic reticulum	**ORF**	Open reading frame

PA	Phophatidic acid
PAGE	Polyacrylamide gel electrophoresis
PBS	Phosphate buffered saline
PCR	Polymerase chain reaction
PDE	Phosphodiesterase
PFA	Paraformaldehyde
PI-PLC	Phosphatidylinositol phospholipase
PKA	Protein kinase A
PKG	Protein kinase G
PLP	Perforin-like protein
PV	Parasitophorous vacuole
PVM	Parasitophorous vacuole membrane
RhoGC	Rhodopsin-guanylate cyclase
RNA	Ribonucleic acid
ROP	Rhoptry bulb protein
rpm	Rotations per minute
RT	Room temperature
SAG	Surface antigen
SDS	Sodium dodecyl sulfate
sec	Second
SOB	Super optimal broth
SOC	Super optimal broth with catabolite repression
T. gondii	*Toxoplasma gondii*
TAE	Tris base, acetic acid and edta
TEMED	Tetramethylethylenediamine
Tg	*Toxoplasma gondii*
TM	Transmembrane helix
U	Units
UPRT	Uracil phosphoribosyltransferase
UTR	Untranslated region
V	Volt
W	Watt
WB	Western Blot

List of Figures

1 Introduction

1.1 Apicomplexa: The group of obligate intracellular parasites

The phylum Apicomplexa (lat. *apex* + *complexus*) is a diverse taxonomic group of single-celled protists that comprises more than 6000 obligate intracellular parasite species infecting a large number of organisms including livestock and humans (1). The infection by most common members of apicomplexan parasites, *i.e*. *Plasmodium sp*., *Cryptosporidium sp*., *and Toxoplasma gondii* has considerable impact on the global health since they cause severe diseases in human. For example, malaria caused by *Plasmodium sp.* alone inflicts about 0.45 million deaths per year according to the latest WHO report (2). Besides, many other members of this phylum, such as *Neospora*, *Eimeria*, *Theileria*, *Babesia* are known to have a significant veterinary importance (3).

Apicomplexan parasites have a complex life cycle including both sexual and asexual reproduction. While some of the members maintain the entire life in one host (*e.g., Eimeria*, *Cryptosporidium*), some of the others (*e.g., Toxoplasma, Plasmodium*) need two different hosts (one is usually defined for sexual reproduction) to complete their development (4). Extracellular, infective stages of parasites are named as “zoite”, which are found at various phases of life cycle. One successful round of life cycle can only be ensured by processing three distinct processes; sporogony, merogony (schizogony) and gamogony that lead to the production of sporozoites (infectious), merozoites (infectious) and gametes, respectively (Figure 1) (5).

All life cycle forms hold a haploid genome except for the zygote/ookinete formation but differ by morphological features and organelle compositions. Apicomplexan parasites have a distinctive structure called “apical complex” that consists of a group of secretory organelles, micronemes and rhoptries, as well as microtubules connected to a polar ring. The apical complex plays a crucial role in gliding motility and host-cell invasion by the parasite (6,7). Besides, most of apicomplexans possess a unique, non-photosynthetic but plastid-like organelle termed apicoplast, which is needed for several essential metabolic pathways (8).

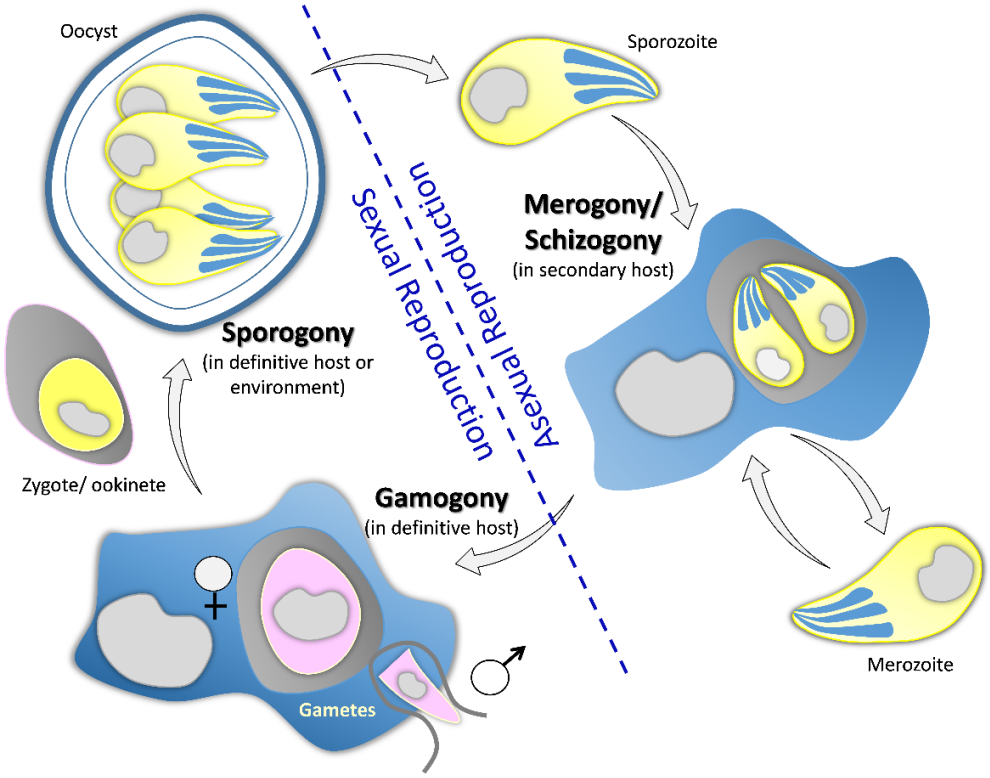

Figure 1. Summarized schematics of life cycle stages and developmental processes in Apicomplexa. Complex life cycle of apicomplexan parasites can be completed either in one host or in two hosts containing sexual and asexual developmental stages, as depicted. Host cell infection starts typically with releasing of sporozoites (infective stage) which are formed in thick-walled oocyst *via* sporogony (sexual reproduction) process. Following infection, sporozoites develop into merozoites (infective form) and multiply themselves by schizogony/merogony (asexual reproduction). Some of the merozoites can differentiate into male and female gametes by means of gamogony that allows fertilization to generate a zygote. Modified from Striepen *et al.* 2007 (5).

1.2 *Toxoplasma gondii*: One of the most common zoonotic parasites

1.2.1 Global distribution, pathogenesis and prevention strategies

Toxoplasma gondii was first isolated from a North African rodent in 1908 and called as *Ctenodactylus gundi* by Nicolle and Manceaux (9). The first *T. gondii* infection case in human was recognized however at the end of 1930s (9,10). It is one of the most prevalent and successful species of the phylum apicomplexa, which can infect almost all nucleated cells of warm-blooded vertebrates including wild and domesticated animals (11). Although seroepidemiology substantially varies between countries, even between different geographical areas within a country based on nutritional and hygienic conditions, an estimated 30% of the human population has been exposed to this pathogen worldwide. The prevalence of *Toxoplasma* infection in Africa and South America is notably much higher

revealing clinical importance of this parasite (9). While *T. gondii* is the only species in *Toxoplasma* genus, molecular analysis showed that globalization and differences between population structures caused a genetic diversity within the species, that resulted in arising four ancestral clonal lineages (type I-IV) including six recently identified major clades (12-14). The majority of the *Toxoplasma* isolates (I, II, III) are distributed in the Europe and North America. Although only <5% natural genetic recombination is observed amongst ancestral lineages, the severeness of infectivity considerably varies between each other (12,15). On the other hand, the clonality of parasites in South America has been found reflecting more recombination frequency, which gives rise to a separation to distinct clades (13-15).

T. gondii is the causative agent of toxoplasmosis. In most of the cases, the infection of parasite remains asymptomatic or emerges as flu-like mild symptoms in immunocompetent individuals (16), which is usually controlled by Th1 cytokine interferon gamma (IFN-γ) mediated adaptive immune response (17). The immune response forces parasite to differentiate into a dormant cyst form (bradyzoite) (16,18). However, in case of debilitated immune response, the tissue cyst can be reactivated. In immunocompromised people, such as AIDS patients or transplant recipients, acute or reactivating infections by fast replicating tachyzoite stage may cause severe complications including encephalitis and psychiatric disorders, ocular diseases like retinitis and retinochoroiditis, sepsis syndrome, myocarditis and hepatitis (9,16). The morbidity caused by *Toxoplasma* infection imposes an extraordinary burden of public health (19). If the primary infection of *T. gondii* takes place during the pregnancy, the parasite can be transmitted to the fetus leading a congenital toxoplasmosis with severe neurological disabilities, retinal lesions in infants or even stillbirths and abortions (9,19,20).

The most common pathways proposed for the transmission of parasite are through the consumption of (i) raw or undercooked meat containing tissue cysts and (ii) oocyst-contaminated water, raw vegetables or fruits in the environment; that makes toxoplasmosis a food- and/or waterborne disease (21). So far, several strategies have been applied to cope with toxoplasmosis. For instance, a vaccination using live but attenuated tachyzoites in sheep and goat successfully generated protective immunity against acute infection however was not able to prevent tissue cyst formation (22). Such a vaccine with avirulent parasite strain is not accepted as an appropriate protection method for humans, since the attenuated strain can be reverted, which leads to a disease and side effects on fetus (21). An oral vaccine was

developed for cats as they are definitive host reservoirs of *T. gondii*, however the commercial production of this vaccine was ceased shortly after because of the high cost and less interest by owners of cats (21,23). Recently, a mutant parasite that is unable to produce oocysts due to defective fertilization was generated and inoculated to cats as a potential transmission-blocking vaccine (24). Apart from that, a combination therapy of pyrimethamine, sulfadiazine and folic acid is recommended to treat acute toxoplasmosis, although it is ineffective against the chronic infection (25).

1.2.2 Life cycle of *T. gondii*

The life cycle of *T. gondii* includes sexual and asexual reproduction as depicted in Figure 2. Sexual development takes place only in the members of the genus *Felidae* as definitive hosts, whereas asexual propagation can be performed in a wide range of intermediate hosts including humans and farm animals (18). Successful pathogenesis as an opportunistic parasite can partly be assured by its ability to switch between fast-multiplying tachyzoite stage (acute phase of infection) and latent bradyzoite-containing tissue cyst form (chronic phase of infection) during the asexual reproduction (Figure 2), which enables the parasite to spread in a wide range of hosts (26).

Sexual reproduction starts in the intestine of felids when they ingest prey animals harboring tissue cysts (27). After ingestion, bradyzoites (Greek, *brady* = slow; slowly multiplying form into tissue cyst) (28) are released from the cysts, penetrate themselves to the epithelial cells of small intestine and replicate themselves *via* several rounds of merogony during 3 to 7 days (29). Following asexual proliferation, the merozoites differentiate into male (micro) and female (macro) gametes by gamogony. Microgametes swim by means of their flagella to fertilize mature macrogametes. The fusion of micro- and macrogametes forms a zygote that later develops into an environment-resistant oocyst with five-layered wall (30) (Figure 2). The oocysts shed in the environment sporulate under proper aeration and temperature conditions to constitute two sporocysts each containing four sporozoites (30). The sporulated oocysts are quite infectious for intermediate hosts, and they can survive for years under harsh environmental conditions (16,31).

In case of the sporulated oocyst uptake from contaminated vegetables or water, the sporozoites are released to the intestine of intermediate host during digestion. They invade the epithelial cells of gut and differentiate into fast-replicating tachyzoite stage (Greek, *tachy*

= fast) (32). Tachyzoites are the agents of acute infection. They multiply themselves in an intermediate host, followed by spreading through the body *via* blood or lymph (16). In immunocompetent individuals, upon immune stress tachyzoites turn into slowly replicating bradyzoites which are surrounded by a thick wall (<0.5 μm) and form tissue cysts (Figure 2).

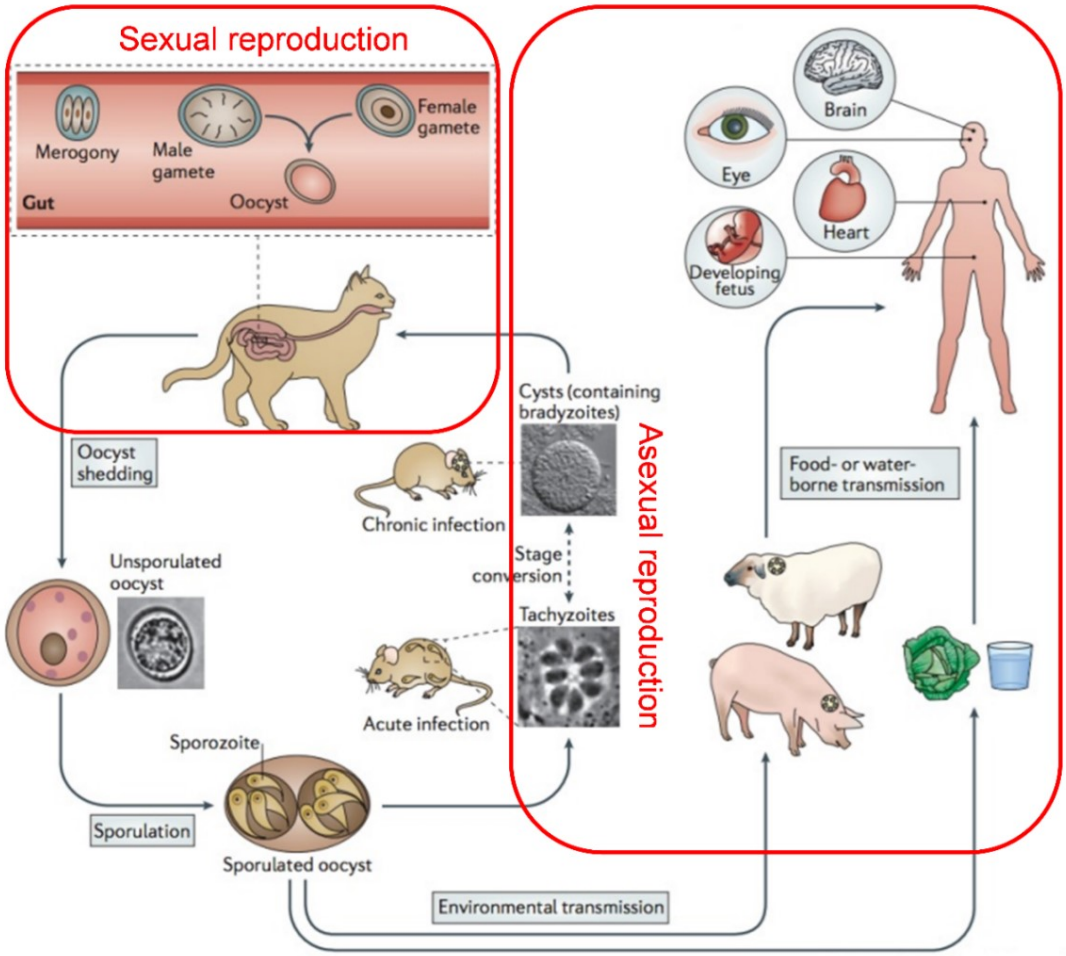

Figure 2. Life cycle of *T. gondii*. Sexual and asexual reproduction of *Toxoplasma* take place in felids and warm-blooded intermediate hosts, respectively. Oocysts are formed by the fusion of micro- and macrogametes in the gut epithelium of cats, followed by shedding to the environment. Oocyst sporulation occurs under convenient climate conditions. The uptake of sporulated oocyst by intermediate host *via* food- or waterborne transmission initiates asexual reproduction. Following ingestion, sporozoites are released from oocyst, penetrate to the epithelial cells of small intestine and differentiate into tachyzoites causing acute infection. Short after, tachyzoites are disseminated to the whole body and turn into bradyzoite-containing cysts leading chronic infection mostly in neural and muscular tissues. Predation of a cyst-containing animal by cat followed by merogony process completes the life cycle of parasite. Adapted from Hunter and Sibley 2012 (18).

Tissue cysts can be developed in all visceral organs, such as lung, liver or kidney; however parasite has a tropism mostly to neural (brain-eyes) and muscular (skeletal-cardiac) tissues (32). Chronic infection caused by such cysts does not harm the healthy people and persists for the entire life (26,32). However, a relapse into acute infection because of the

immunosuppression can be fatal. Another ingestion of cyst-containing animal by cat causes the completion of full life cycle. Predation of an infected animal by another intermediate host is another way of parasite transmission that increases the prevalence of toxoplasmosis.

1.2.3 Lytic cycle and parasite organelles

Toxoplasmosis occurs by proliferation and persistence of the two asexual stages of *T. gondii.* The acute infection caused by tachyzoite stage is hallmarked by successive rounds of lytic cycles, which starts with the invasion of the host cell, proceeds with intracellular replication and ends by lysing the cell in order to infect neighboring host cells. 7-10 days post-infection, fast-replicating tachyzoites differentiate into bradyzoite-containing tissue cysts, which is the onset of chronic phase (33). Successful lytic cycle events and interconversion between tachyzoite and bradyzoite stages are tightly regulated by signaling pathways (34) (Figure 3).

Tachyzoites are around 2-6 µm long crescent-shaped developmental forms of *T. gondii*, which have a pointed anterior (conoidal) and rounded posterior ends (30). The morphological features of tachyzoites include a flexible cytoskeletal structure containing (i) a spirally arranged fibrillary conoid, (ii) a pellicle that consists of an outer plasma membrane (PM) and inner membrane complex (IMC), and (iii) longitudinal subpellicular microtubules originating from apical polar ring, all of which coordinate a specialized form of parasite motility called "gliding motility" (35-37) (Figure 4). Gliding enables the parasite to navigate through the host and penetrate to the host-cell surface, followed by an active invasion. These events rely on the coordinated release of adhesion proteins and regulation of actin-myosin motor/complex (36,37). Once invaded, parasite resides within a non-fusogenic membranous structure called "parasitophorous vacuole (PV)" which is initially formed using the lipids of the host cell, plasma membrane along with secreted proteins and lipids of the parasite (38,39). Three distinct secretory organelles *i.e.* micronemes, rhoptries and dense granules (Figure 4) excrete their protein contents to facilitate invasion, PV maturation and establishment of a parasite-friendly environment in the host cytoplasm that allows the parasite replication in the PV (6,30).

Tachyzoites utilize a unique way of cell division in the PV known as "endodyogeny", in which two daughter cells are formed by a specialized mitosis of nucleus and organelle division within the cytoplasm of mother cell (5,34,40) (Figure 3). Each endodyogeny varies

between 6 to 8 h and continues successively inside the mother cell until reaching 32-64 progeny per vacuole, that leads to burst of host cell (egress), and thereby completing one round of lytic cycle process (33) (Figure 3). Egress process requires a synchronized secretion of proteins from secretory organelles. Besides, it is known to be regulated by multiple signaling pathways (41,42).

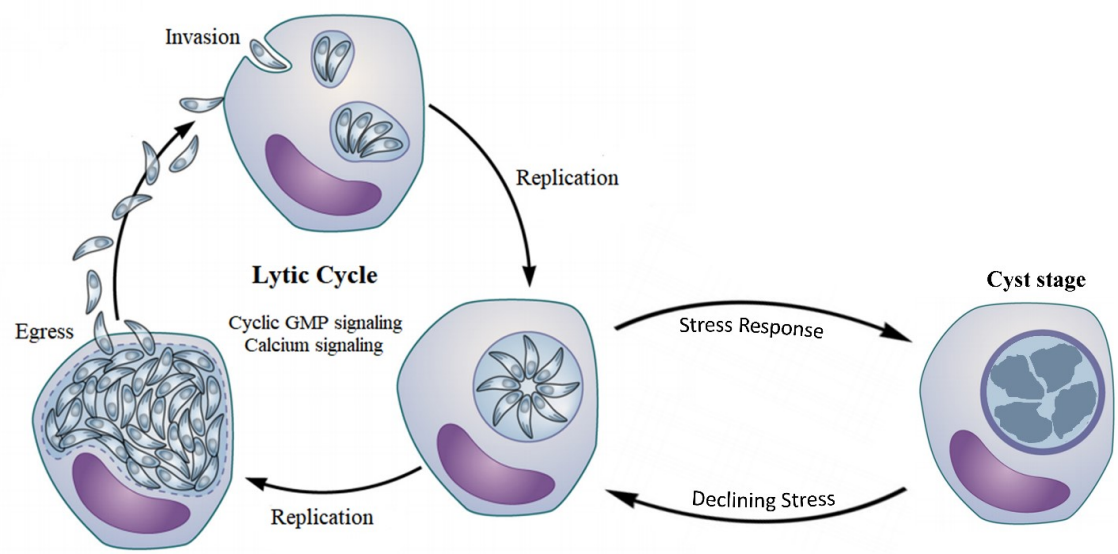

Figure 3. Lytic cycle and stage differentiation of *T. gondii*. During acute infection of *T. gondii*, motile tachyzoites actively invade their host cell, followed by formation of a parasitophorous vacuole. Parasite replicates itself exponentially in parasitophorous vacuole to generate 32-64 progenies in 48 h time frame, which leads to the lysis and egress out of host (*left*). Immune stress compels the parasites to differentiate into thick-walled dormant bradyzoite stage, which can reconvert to acute stage in declining stress conditions (*right*). The cooperation of cyclic nucleotide and calcium signaling regulates both lytic cycle and stage conversion during asexual replication. Modified from Zhang *et al*. 2013 (43).

Formation of a non-fusogenic PV is an essential task for tachyzoites to assure the parasite survival from lysosomal activity of hosts (44,45). The membrane of PV also functions as an interface to facilitate the exchange between the parasite and host, allowing nutrient acquisition from host to the parasite and discharge from the parasite to its host cell (44,46). Small molecules, whose uptake is crucial for *T. gondii* tachyzoites, can be scavenged from the host cell by crossing through the membrane of the PV. These precursors are used for *de novo* synthesis of macromolecules in various organelles (47,48).

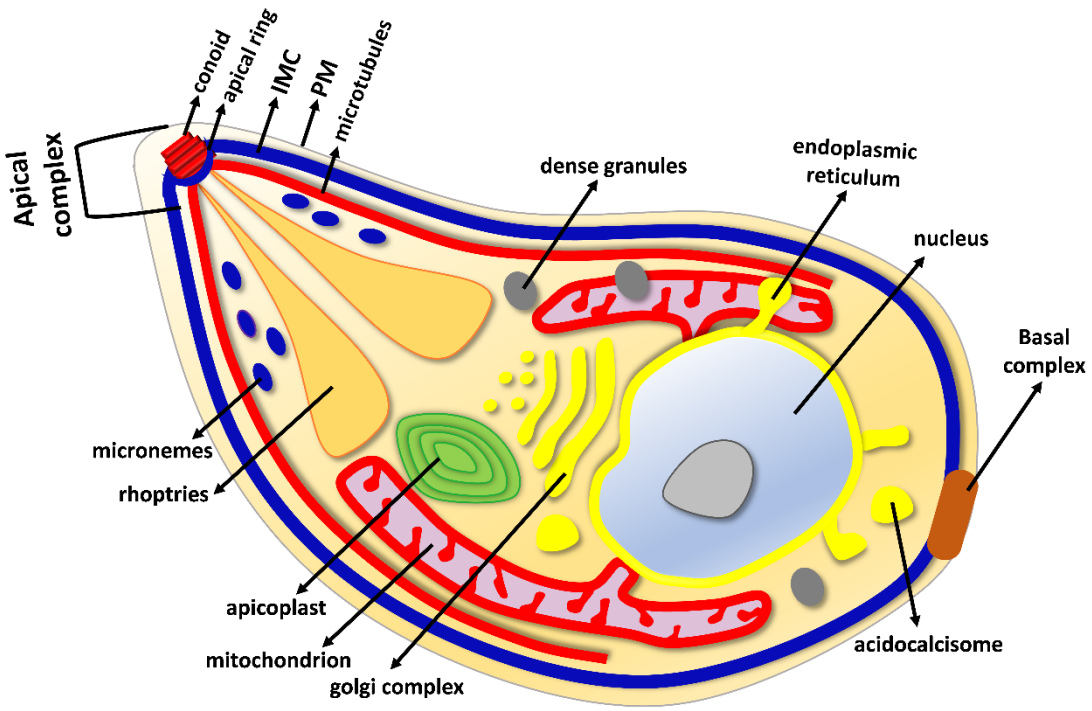

Figure 4. The major organelle structures of *T. gondii* tachyzoite. Tachyzoite is a crescent-shaped parasite stage with a pointed anterior (conoidal) and rounded posterior ends. It has a complex membrane structure containing an outer plasma membrane (PM) and a bilayer inner membrane complex (IMC). The apical complex structure consists of a spirally organized conoid, secretory organelles (micronemes and rhoptries) and microtubules connected to a polar ring. Besides, tachyzoites contain a four-membranous plastid-like organelle, apicoplast, which plays a major role in carbon metabolism. Acidocalcisomes are acidic compartments responsible for ion flux and calcium storage. Additionally, tachyzoites include a full set of eukaryotic cell organelles like nucleus, mitochondrion, endoplasmic reticulum and Golgi complex. Adapted from Gupta 2018 (49).

1.2.4 Genetic manipulation of the parasite genome

T. gondii is the most common model organism used to study intracellular parasitism by virtue to its (i) well-established *in vitro* culturing techniques, (ii) proficiency to invade almost all types of nucleated cells, (iii) feasibility to apply a range of molecular approaches to manipulate the target genes, (iv) available complete genome sequence information in an accessible database (ToxoDB) (50), which allows a direct comparison with other members of apicomplexans.The first manipulation of *T. gondii* was performed by chemical mutagenesis approach to make temperature-sensitive clonal lines. This pioneer study formed a basis for the optimization of basic protocols for *in vitro* cultivation and making clonal lines of tachyzoites (51). Afterwards, classic genetic recombination method was applied in cats to correlate observed phenotype with single or multiple genomic loci to find out gene functions (52). Following this forward genetics approach, the restriction fragment length

polymorphism linkage map was constructed using 64 markers for *T. gondii*, which resulted in defining genes responsible for drug resistance as distributed in different regions of 11 chromosomes (53). In another research, *T. gondii* chromosomes were separated by pulsed field gel electrophoresis. The linkage groups were assigned by hybridization to construct a molecular karyotype of the parasite, which reveals that *T. gondii* has a ~80 Mb haploid nuclear genome (54). The applications of modern reverse genetics approach to understand the roles of genes became possible only after developing electroporation technologies.

First electroporation trials were performed for introducing exogenous DNA fragments in *T. gondii* (55,56). Several expression vectors have been designed to enable both tagging or deletion of genes by homologous recombination and non-homologous random integration of transgenes. For this purpose, a wide range of selectable markers were developed to choose only successfully transfected parasites from the stable drug-resistant pool. The most common selection markers available for *T. gondii* include dihydrofolate reductase/thymidylate synthase (DHFR/TS) conferring pyrimethamine resistance (56); hypoxanthine-xanthine-guanine phosphoribosyltransferase (HXGPRT) which can be used both for positive and negative selection using mycophenolic acid-xanthine and 6-thioxanthine treatments, respectively (57); uracil-phosphoribosyltransferase (UPRT) that can be negatively selected by 5-fluorouracil (FudR) (58); and chloramphenicol acetyltransferase (CAT) providing a resistance to chloramphenicol (59). Cre-loxP mediated recombination system from bacteriophage P1 has also been successfully adapted to *T. gondii* to excise the target DNA fragment flanked between loxP sites and/or introduction of aforementioned selectable markers by the activity of site-specific Cre-recombinase (Figure 5A) (60). Yet, the success rate of homologous recombination for gene replacement was still quite low in wild-type parasites. To overcome this problem, non-homologous end joining (NHEJ) pathway, which repairs double-strand DNA breaks, was inactivated by deleting Ku80 protein first in type I (61,62) and then in type II (63) strains to increase the efficiency of homologous-recombination-mediated gene- tagging and knockout without effecting the virulence features of parasites.

On the other hand, studying the function of essential genes that are refractory to direct genetic deletion required a conditional system. The implementation of RNA interference (RNAi) technology, which was applicable in many other organisms, did not work in *T. gondii* due to the absence of DICER complex (64). Another milestone occurred in the research field when tetracycline repressor based transactivator system (TetR) was reported for

downregulation of essential genes (65). A parasite line carrying transactivator elements (TATi-1) was generated to perform conditional knockdown of a gene of interest (GOI) by anhydrotetracycline (aTc) treatment. Soon after, DD/Shield1 conditional system was implemented successfully in *T. gondii* (66). In principle, human rapamycin-binding protein FKBP12-derived destabilization domain (ddFKBP) was used as an epitope, whose fusion with GOI causes a rapid, efficient and reversible degradation of a protein of interest. On the contrary, the supplement of Shield1, a cell-permeable analogue of rapamycin, can stabilize the protein expression in a dose-dependent manner (Figure 5B) (67).

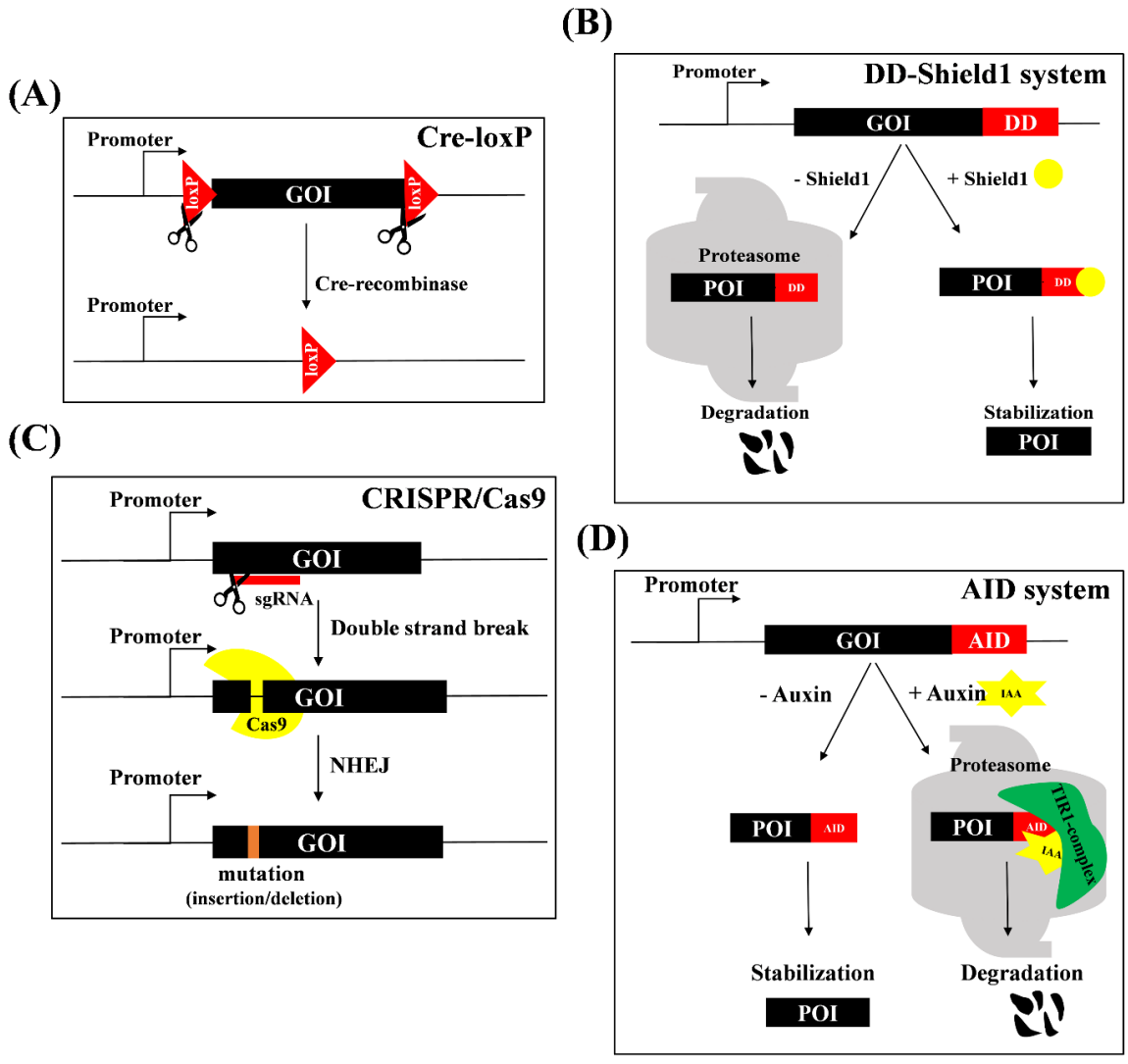

Figure 5. Illustration of commonly used genetic manipulation strategies applied in *T. gondii*. **(A)** Simplified example of Cre-loxP site-specific recombination method for gene deletion. A GOI is flanked by 34 bp long loxP sequences. Parasite is transfected with a Cre-recombinase expressing vector, which will recognize loxP sites, resulting in excision of floxed sequence. **(B)** Conditional protein expression using DD/Shield1 system. A GOI is tagged with destabilization domain (DD). The fusion of DD to a POI causes a rapid protein degradation by the proteasome in the absence of its ligand. However, the supplement of Shield1 stabilizes a DD-fused POI. **(C)** CRISPR/Cas9 technology for introducing a mutation in the genome *via* non-homologous end joining (NHEJ). A single-guide

RNA (sgRNA) is designed to target a particular genomic locus and direct Cas9 protein to induce site-directed double strand break, which is repaired by NHEJ causing random insertion and/or deletion. **(D)** The auxin-inducible degron (AID) system for conditional protein depletion. The protein expression of an AID-tagged GOI within the auxin receptor (TIR1-complex as shown in green) expressing parasite can be successfully performed in the absence of auxin (IAA). However, 15 min IAA treatment causes proteasomal degradation of POI. GOI: gene of interest, POI: Protein of interest

Clustered regularly interspaced short palindromic repeats (CRISPR) naturally exist in *Bacteria* and *Archaea* as an adaptive defense system (68), which can recognize the foreign phage DNA and break double strands of DNA by means of CRISPR-associated protein 9 (Cas9). The targeted site for the genome cleavage is guided by a single RNA (sgRNA) which contains a site-specific complementary sequence (Figure 5C) (69). Modifying prokaryotic CRISPR/Cas9 system and thereby adapting as a large spectrum of genome editing tool in *T. gondii* was the recent breakthrough in the field. Recently, two pioneer studies were successfully performed in *T. gondii* using CRISPR/Cas9-based genome editing system and paved the way for high-throughput genome engineering to investigate the function of genes:

1) For gene insertion or deletion in laboratory-adapted *T. gondii* strains as well as in natural isolates, *i.e.* type I GT1 strain by homology-directed repair (HDR) approach (70),

2) For introducing mutations as well as epitope-tagging of a target gene by non-homologous end joining (NHEJ) and HDR approaches, respectively (Figure 5C) (71).

The latest, a state of the art method has emerged and been adapted to *T. gondii* research by coupling CRISPR/Cas9 technology with a conditional expression system called auxin-inducible degron (AID) to study essential proteins (Figure 5D) (72-74). Auxins are plant hormones which are involved in a signaling transduction pathway to induce degradation of auxin-family transcription repressors (75). A research group from Japan found out that other eukaryotes apart from plants also contain the same degradation pathway (TIR1 complex) without auxin. From this point of view, they expressed the small AID molecule in a various of non-plant cells to conditionally control of the protein stability (76). Following that, a *T. gondii* strain stably expressing the auxin receptor (ΔKu80/TIR1) was generated in 2017, and certain essential gene of interests were tagged with AID-3xHA using CRISPR/Cas9 technology to downregulate their expression by auxin (indole-3-acetic acid, IAA) treatment (Figure 5D) (72,74). The efficient combination of novel systems for genome editing and analysis of importance of proteins have become pivotal to understand the parasite biology.

1.3 Signal transduction *via* cyclic nucleotides

Signal transduction pathways are critical for regulation of essential cellular processes, such as neurotransmission, muscle contraction/relaxation, chemotaxis, optical perception or phototransduction in higher organisms as well as sensing and adaption to the changing environment conditions in microorganisms (77). The complex signal transduction pathways are initiated by the recognition of signals through receptors and processed with the production of second messengers, such as cyclic nucleotides (cNMPs), Ca^{2+} (77), diacylglycerol (DAG) or inositol triphosphate (IP_3) (78). The signal transduction mechanisms typically proceed with the phosphorylation or dephosphorylation of target proteins by kinases to relay the effect of second messengers.

Cyclic nucleotides [3'5'- cyclic adenosine monophosphate (cAMP) and 3'5'- cyclic guanosine monophosphate (cGMP)] are universal single-phosphate nucleotides (Figure 6), existing from prokaryotic bacteria to humans in almost all organisms. They convey the endogenous and exogenous cues to the downstream mediators (kinases, ion channels *etc.*), and thereby regulate a wide range of important events (79,80). Initiating a physiological response to a biological cue requires a complex mechanism based on the modulation of intracellular level of cNMPs that is tightly controlled by mainly three distinct type of enzymes (Figure 6):

(1) Nucleotide cyclases: cAMP and cGMP are synthesized from the adenosine- or guanosine triphosphate (ATP or GTP) by the catalytic action of adenylate (adenylyl)- and guanylate (guanylyl) cyclase (AC and GC), respectively (Figure 6).

(2) cNMP-dependent protein kinases: Protein kinase G (PKG or cGMP-dependent protein kinase) and protein kinase A (PKA or cAMP-dependent protein kinase) are the major mediators of cNMP signaling. They phosphorylate a repertoire of effector proteins to exert a consequent subcellular response. Besides, cyclic-nucleotide gated (CNG) ion channels can also be directly activated by cNMPs to balance ion concentrations by changing polarization of the membrane to control physiological events in many eukaryotes (80,81). An additional cAMP-binding protein called "Exchange protein directly activated by cAMP (ePAC)" is also described as one of the direct effectors of cAMP signaling, which fulfils the need for diverse biological functions in mammalian cells (Figure 6) (82).

(3) cNMP-specific phosphodiesterases (PDEs): The levels of cGMP and cAMP are strictly counterbalanced by phosphodiesterase enzymes which degrade cGMP into 5'-GMP and cAMP into 5'-AMP by hydrolyzing the 3'-phosphoester bonds (83) (Figure 6).

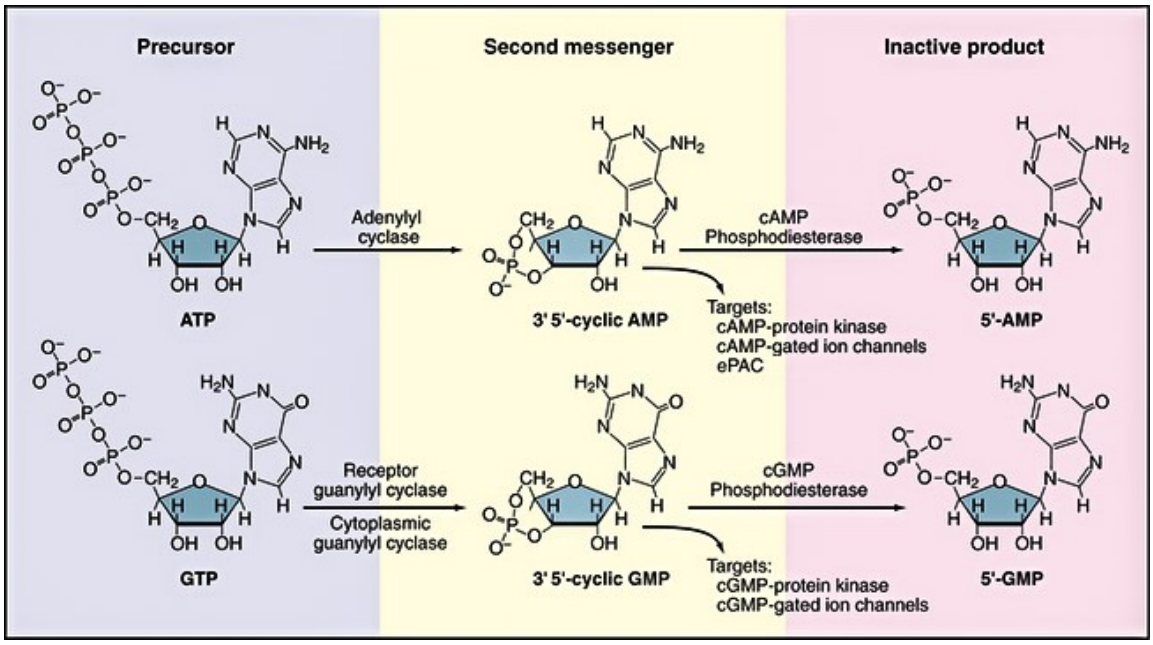

Figure 6. Molecular structures of cyclic nucleotides (cAMP and cGMP), their precursors and degraded products. 3'5'-cyclic AMP and 3'5'-cyclic GMP are single-phosphate nucleotides that are produced by adenylyl- (adenylate) and guanylyl- (guanylate) cyclases from ATP and GTP, respectively. They contain a cyclic bond between the hydroxyl group of the ribose sugar and the phosphate group. cNMP-dependent protein kinases and cyclic nucleotide-gated ion channels are downstream targets of cyclic nucleotides. The intracellular concentration of cAMP and cGMP are counterbalanced by cNMP-phosphodiesterases which degrade them to 5'-AMP and 5'-GMP depending on their substrate specificity. Adapted from https://basicmedicalkey.com/second-messengers/

1.3.1 Cyclic nucleotide signaling in mammalian cells

Much of our understanding about cNMP-induced signal transduction is derived from higher organisms, namely mammalian cells which harbor 4 soluble guanylate cyclase subunits ($\alpha_1, \alpha_2, \beta_1, \beta_2$) and seven membrane-bound guanylate cyclases (GC-A to GC-G). The soluble guanylate cyclase (sGC) isoforms function as heterodimers and consist of an amino-terminal heme-binding regulatory domain, a dimerization region and a carboxyl-terminal catalytic domain (Figure 7A). In contrast, all known particulate GC (pGC) proteins occur as homodimers except for GC-C which exists as a homotrimer in the basal state. pGCs typically possess the successive domains: An extracellular ligand binding site formed by two amino terminal domains followed by a transmembrane, a kinase homology, a dimerization and finally a catalytic domain comprising two functional catalytic sites (80,84,85) (Figure 7A).

Nitric-oxide (NO) is the best-characterized activator of sGCs, while a variety of the ligands, such as atrial natriuretic peptides (ANPs), guanylin or bicarbonate were reported for the activation of pGCs (80,84) (Figure 7B). The cGMP produced can be used consequently by three classes of intracellular target proteins: PKGs and CNG channels as effectors, cGMP-specific PDEs as regulators of cGMP (85). CNG channels are usually described as photoreceptors, being activated by cGMP in phosphorylation-independent manner and play important role in visual perception by regulating influx/efflux of Ca^{2+} and Na^{+} ions (85,86). The closure of CNG ion channels in response to light leads to the activation of PDEs. Not only cGMP-specific PDEs but also cAMP-specific PDEs which use cGMP as a substrate for activation but hydrolyze specifically cAMP to AMP, can be stimulated by CNG channels (Figure 7B). Besides, phosphorylation events performed by PKGs can also activate PDEs (83,85).

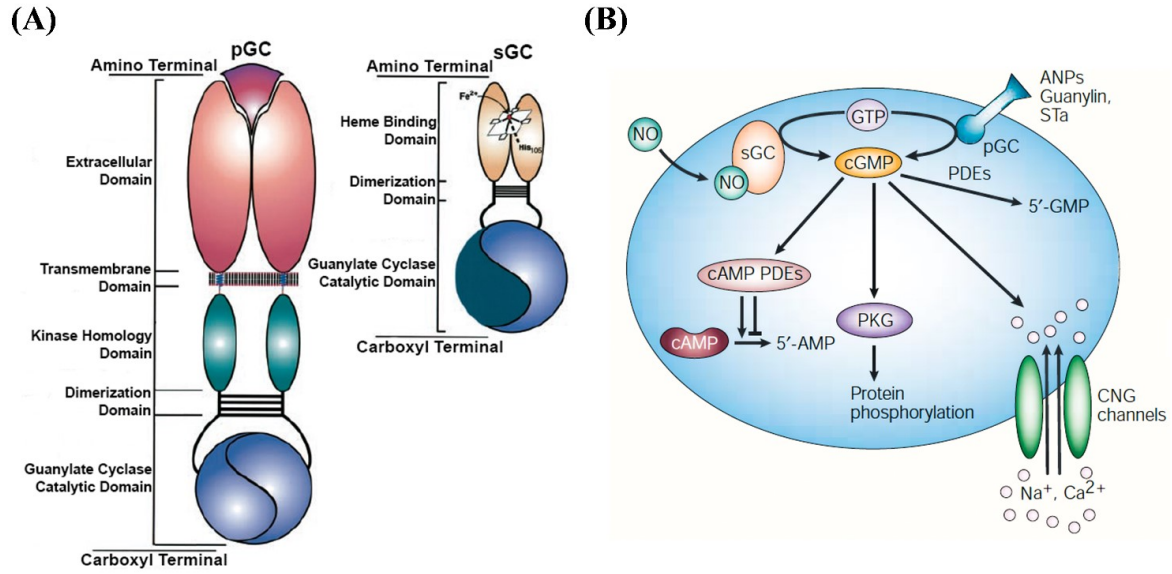

Figure 7. The basic mechanism of cGMP signaling and its regulation in mammalian cells. (A) Molecular structures of particulate and soluble guanylate cyclases (pGC and sGC) including the domain structure from N-terminal (amino) to the C-terminal (carboxyl) end. Adapted from Lucas *et al.* 2000 (80). **(B)** Simplified illustration of cGMP signaling involving the extracellular stimulus (NO and/or ANPs, guanylin) and major downstream mediators responsible from its synthesis (pGC and/or sGC), function (PKG and/or CNG channels) and degradation (PDEs), respectively. ANPs, atrial natriuretic peptides; NO, nitric oxide; pGC, particulate guanylate cyclase; sGC, soluble guanylate cyclase; PKG, cGMP-dependent protein kinase; CNG channels, cyclic nucleotide gated ion channels; PDEs, phosphodiesterases. From Beavo and Brunton 2002 (77).

On the other hand, 9 closely related-adenylate cyclase isoforms (AC1-AC9) with 2 splice variants of AC8 have been identified, all of which are membrane-anchored (87). Only one soluble AC has been reported in the male germ cells so far (88). Each AC isoform contains two hydrophobic domains at the N-terminal, which consist of six transmembrane

spans, and follows two catalytic regions at the C-terminal in the cytosol (87,89). All known PKAs and PKGs belong to the serine/threonine kinases. In mammals, there are 2 variants of PKG (PKG I and PKG II) described, while a single PKA has been identified (90,91). The type I PKGs with two soluble alternatively-spliced isoforms (α and β) is expressed more generally and function as homodimers. It is employed as a major regulator of the cardiovascular system and often associated with the pathways controlling subcellular Ca^{2+} levels (85,91,92). The type II PKGs are membrane-bound proteins that are predominantly expressed in the epithelial cells of intestine to regulate ion and water transport (91,93). Although type II PKG protein isolated from pig intestine was shown to behave as a monomeric membrane protein (94), the same recombinant protein in rat intestine was found as a dimer (91). In contrast, human PKA protein is a tetrameric holoenzyme when it is in the inactive state. It includes a dimeric regulatory subunit at the N-terminal and two catalytic subunits at the C-terminal (90).

1.3.2 cGMP signaling in *T. gondii*

Unlike mammalian cells, little is understood about the overall architecture and functioning of cyclic nucleotide signaling in protozoans. The cyclic GMP signaling pathway in the parasite *T. gondii* is the particular focus of this thesis.

The cGMP pathway in protozoans shows a marked divergence from mammalian cells (95-97), which is suggested to underlie microbial pathogenesis (95). Apicomplexa, as one of the protozoan phyla, exhibits an even more intriguing design of cGMP signaling. *Toxoplasma*, *Plasmodium* and *Eimeria* as key apicomplexan parasites display a complex life cycle regulated by interconnected signaling pathways in nature, assuring their successful infection, reproduction, stage-conversion, adaptive persistence and inter-host transmission. Cyclic GMP cascade has been shown as one of the most central mechanisms to coordinate the key steps during the parasitic life cycle (95,98-101). In particular, the motile parasitic stages, *e.g.,* sporozoite, merozoite, ookinete and tachyzoite deploy cGMP signaling to enter or exit host cells (98,100) or traverse tissues by activating secretion of micronemes which are the apicomplexan-specific secretory organelle (102-104). Micronemes secrete adhesive proteins required for the parasite motility and subsequent invasion and egress events (100,102-104). Microneme secretion was shown to be triggered in *in vitro* cultures by external stimuli, such as low level of potassium (105) or pH (106), and a host protein serum albumin (103). The process is mainly controlled by a programmed PKG activity.

The work of Gurnett *et al.* (107) demonstrated that *T. gondii* and *E. tenella* harbor a single PKG gene encoding for two alternatively-translated isoforms (soluble and membrane-bound). The physiological essentiality of PKG for the asexual reproduction of both parasites was first revealed by a chemical-genetic approach (108), whereas the functional importance of this protein for secretion of micronemes, motility and invasion of *T. gondii* tachyzoites and *E. tenella* sporozoites was proven by Wiersma *et al*.(109). Successive works in *T. gondii* have further endorsed a critical requirement of *Tg*PKG for its asexual reproduction by various methods (42,72,108,110). PKG is also needed for the hepatic and erythrocytic development of *Plasmodium* species (98,111,112). It was shown that PKG triggers the release of calcium from endoplasmic reticulum and other storage organelles, such as Golgi apparatus, mitochondria or endosome-like compartments like plant like vacuoles, in *Plasmodium* (113) and *Toxoplasma* (103). Calcium can in turn activate calcium dependent protein kinases (CDPK1 and CDPK3) (42,114), and thereby exocytosis of micronemes as shown in the Figure 8. The Ca^{2+} stores can be stimulated to be released into the cytosol *via* calcium ionophores, such as A23187 or ethanol, eventually inducing microneme exocytosis (115). On the contrary, chelating intracellular Ca^{2+} by BAPTA-AM treatment causes a blockage of microneme discharge (116), which subsequently leads to an inhibition of gliding motility (117) as well as host-cell invasion (118).

The effect of cGMP signaling on calcium depends on inositol 1,4,5-triphosphate (IP_3) that is produced by phosphoinositide-phospholipase C (PI-PLC), a downstream mediator of PKG (Figure 8) (102). Besides IP_3, diacylglycerol (DAG) is also generated as a product of PI-PLC and converted to phosphatidic acid (PA) by diacylglycerol kinase1 (DGK1) to induce microneme secretion *via* an alternative way (104). The *Tg*APH protein (acylated-peleckstrin-homology domain) located onto the microneme surface has been identified as the first PA-sensor. Once PA is recognized by *Tg*APH, DOC2.1 protein anchored in plasma membrane of *T. gondii* gets involved to initiate membrane fusion during exocytosis (104,119) (Figure 8). The membrane fusion machinery is also known to take place in a Ca^{2+}-dependent manner for exocytosis of micronemes (119).

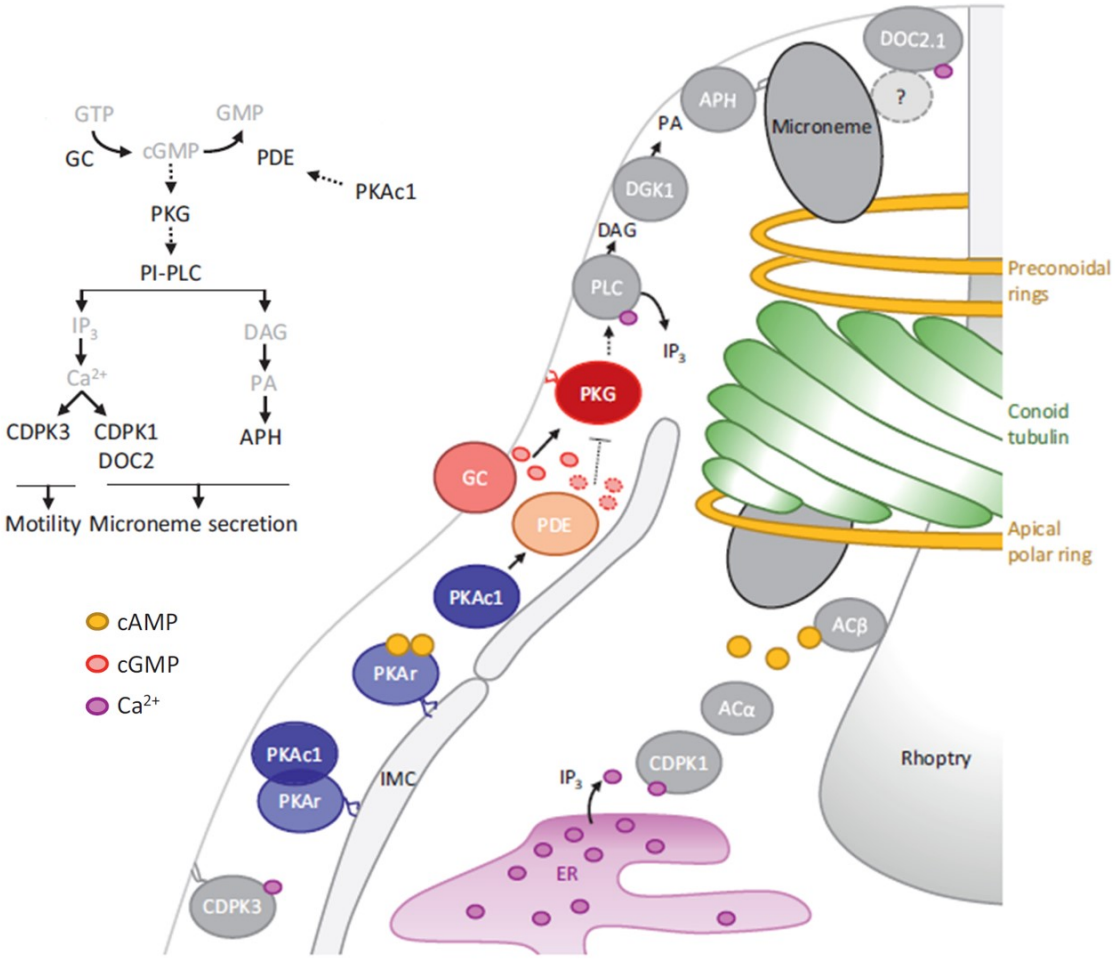

Figure 8. Coordinated control of microneme secretion *via* interconnected network of cAMP, cGMP, calcium and lipid signaling pathways. In the presence of cGMP synthesized by GC, PKG activates PLC to produce both IP_3 and DAG, and thereby stimulating microneme exocytosis. While IP_3 can be recognized by yet unknown receptor in the ER to release calcium in the cytoplasm, DAG is phosphorylated by DGK1 to generate PA. Eventually, microneme secretion and gliding motility of parasites are induced by both pathways. ACs (ACα and ACβ) produce cAMP, which is bound by PKAr causing the release of PKAc1. cGMP-specific PDE is phosphorylated by active PKAc1 to degrade cGMP, which in turn blocks the PKG and subsequent microneme secretion. (Abbreviations: AC, adenylate cyclase; APH, acylated-peleckstrin-homology domain containing protein; CDPK, calcium dependent protein kinase; DAG, diacylglycerol; DGK, diacylglycerol kinase; ER, endoplasmatic reticulum; GC, guanylate cyclase; PA, phosphatidic acid; PDE, phosphodiesterase; PKAc1, catalytic subunit of protein kinase A; PKAr, regulatory subunit of protein kinase A; PKG, protein kinase G; PLC, phospholipase C; IMC, inner membrane complex; IP_3, inositol 1,4,5-triphosphate) Image adapted from Jia *et al.* 2017 (120).

Recently, a crosstalk between *Tg*PKA and *Tg*PKG was revealed to regulate timely egress of *T. gondii* tachyzoites (120). The catalytic and regulatory subunits of PKA (PKAc1 and PKAr) are present as linked with each other in the parasite membrane when PKAc1 is inactive as depicted in the Figure 8. The increase of cAMP level by the action of ACs in the parasite is employed by PKAr, which induces the release of PKAc1. The active PKAc1 phosphorylates the cGMP-specific PDE causing a decline in the cGMP level of parasite,

which blocks *Tg*PKG and subsequently inhibit microneme secretion (Figure 8). Downregulation of PKAc1 in contrast, triggers premature egress from host cells by modulating phosphorylation profile of a putative cGMP-dependent PDE. Besides, the inhibition of *Tg*PKG by specific compounds (compound 1 and 2) (121) ceases the egress event stimulated by PKAc1 inactivation. However, the treatment with a cGMP-specific PDE inhibitor, BIPPO (122) rescues the egress blocked by activation of PKAc1 (Figure 8) (120). Consequently, PKAc1 acts as a balancing regulator of PKG and Ca^{2+} signaling, and thereby negatively controlling microneme secretion and egress (120). PKA was also shown to suppress cytosolic calcium after invasion immediately, leading to a repressed motility before the onset of intracellular replication (123).

In brief, cAMP, cGMP, lipid and Ca^{2+} signaling pathways constitute a complex and an interconnected network to regulate crucial events during the lytic cycle.

1.3.3 Optogenetic tools to manipulate cGMP-mediated signaling

Optogenetics is a rapidly developing discipline that combines techniques of Optics and Genetics to tightly control cellular processes both in living cells and in the whole organism in a cell-specific manner. The term "Optogenetics" was first coined by Deisseroth *et al.* (124) to designate genetically-encoded photoreceptor proteins in neuron cells for manipulating (either activate or inhibit) neuronal activities. The research techniques of this field have been improved greatly in the last decade and overridden conventional chemical methods to study cellular signaling in spatial and temporal manner (125). This has become feasible by means of a variety of bioengineered photosensitive proteins serving as actuators (to light-dependently control the cell actions) and sensors (to monitor ongoing actions in cell) (125,126). Currently, more than 40 actuators and about 30 biosensors are present in the "Addgene" data repository (www.addgene.org), most of which are substantially applied in Neurobiology research (127).

Optogenetic actuators, also known as sensory photoreceptors, enable fast, non-invasive and reversible modulation of second messenger signaling, membrane potential, gene expression and protein-protein interaction (128). There are seven such protein classes: rhodopsins, photoactive-yellow proteins, light-oxygen voltage (LOV) sensors, blue-light receptors containing flavine adenine dinucleotide (BLUF), cryptochromes, phytochromes and UV-B receptors (UVR8). All aforesaid photoreceptors except for UVR8 rely on their

respective chromophore that absorbs a specific frequency of light ranging between 300 and 800 nm and subsequently undergo a conformational change to initiate the catalytic activation (125).

For cyclic nucleotide signaling research, two naturally existing photoreceptors possessing soluble adenylate cyclase/s were firstly described as potential optogenetic tools in *Euglena gracilis* (129) and *Beggiatoa sp*.(130), both of which comprise a N-terminal BLUF domain involved in blue-light (455 nm) sensing. Photo-activated AC from *Beggiatoa* (bPAC) is the most commonly used optogenetic tool due to its simple design and soluble nature to stimulate cAMP production by blue light in various models. The mutagenized version of this protein acting as a light-activated guanylate cyclase (bPGC) was generated by Ryu *et al*. (131). Although cGMP synthesis could be induced by blue light in bPGC-expressing systems, a minor increase in cAMP level was also detected, which limited its application. Subsequently, light-activated phosphodiesterases (LAPDs), which can be activated by red light to degrade cNMPs, (132) were engineered by combining bacterial phytochrome from *Deinococcus radiodurans* with the human phosphodiesterase 2A as effector. However, they have not yet gained wider application due to dual specificity of both cyclic nucleotides.

Rhodopsins constitute one of the main photoreceptor groups expressed in the great majority of all living organisms (133). They are classified into two groups; type I (microbial) and type II (metazoan), both of which are membrane proteins containing seven transmembrane α-helices. They use all-*trans* retinal as the chromophore (134). Lately, a microbial rhodopsin class with an enzymatic activity to regulate cGMP concentration with an additional output domain has been explored. One of the representatives of this fusion proteins containing a C-terminal GC catalytic domain and N-terminal microbial rhodopsin domain linked *via* 40 aa long coiled coil (RhoGC) was discovered in an aquatic fungus *Blastocladiella emersonii* (Figure 9A) (135). It was shown that the green light (520-530 nm) can activate RhoGC to synthetize cGMP in various systems with a negligible dark activity, which proposes RhoGC as an excellent optogenetic tool (128,136,137). Another rhodopsin protein with a C-terminal cytoplasmic PDE domain, which are connected to each other by a linker (40-50 aa) (RhoPDE), was reported in a Choanoflagellate, *Salpingoeca rosetta.* RhoPDE was found to degrade cGMP 10 fold more than cAMP as substrate; however, its hydrolytic activity is also observed in the dark (Figure 9B). Besides, the illumination with

blue-green light (492 nm) did not show any additional induction of cNMP degradation in mammalian systems (138,139).

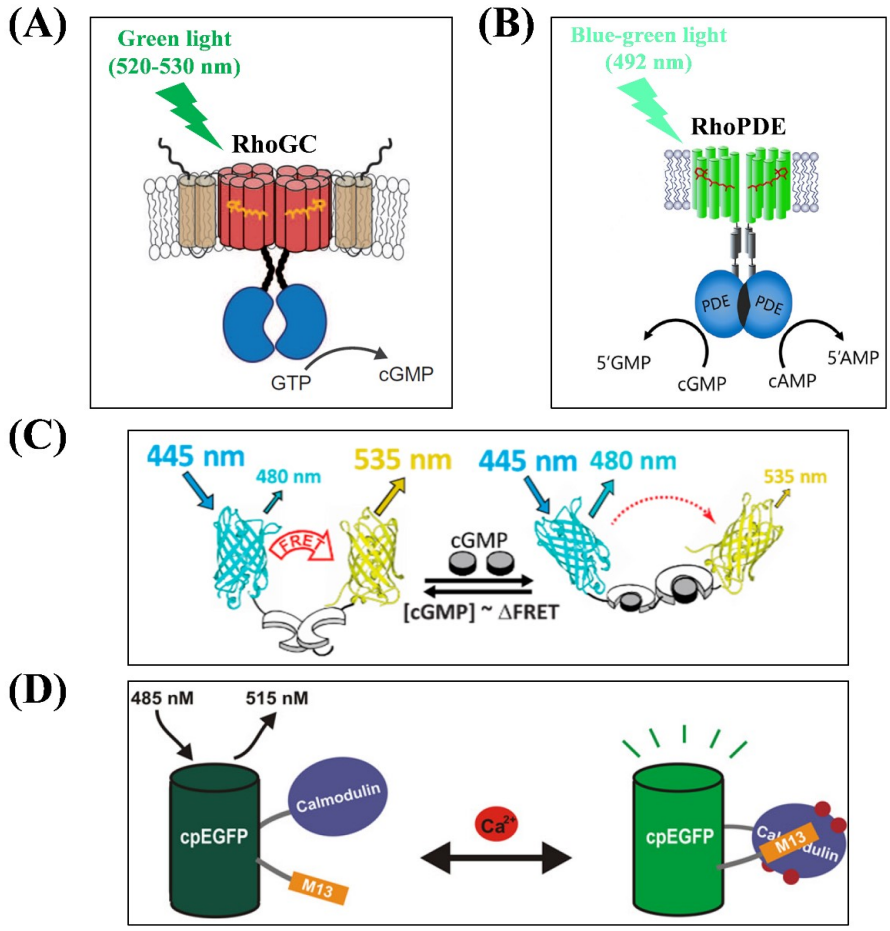

Figure 9. Schematic structures of representative optogenetic tools. (A) Model of dimeric photo-activated rhodopsin-guanylate cyclase gene fusion (RhoGC) from fungus *Blastocladiella emersonii.* Microbial rhodopsin containing 7 transmembrane domains (red) is linked to soluble guanylate cyclase (blue) through a coiled-coil domain (black). Two additional membrane-spanning helices were shown in beige. Rhodopsin senses green light (520-530 nm) and activates guanylate cyclase to synthesize cGMP from GTP. Adapted from Scheib *et al.* 2015 (136). **(B)** Illustration of membrane-anchored rhodopsin (green) with phosphodiesterase (blue) of RhoPDE from *Salpingoeca rosetta* in dimer form. PDE catalytic domain constantly hydrolyses cAMP and cGMP in the dark condition. The blue-green light illumination (492 nm) does not show an additional increase in its activity. Adapted from Yoshida *et al.* 2017 (139). **(C)** Demonstration of working principle of cGi500 sensor to detect cGMP. FRET-based indicator depicting cGMP-binding domain of protein kinase G, which is sandwiched between cyan- and yellow- fluorescent proteins, CFP and YFP, respectively. The bound of cGMP (gray) leads to a conformational change of protein and decrease in FRET, causing reduced emission from YFP (535 nm) and increased emission from CFP (480 nm). Figure source is Paolillo *et al.* 2018 (140). **(D)** The structure of single fluorophore calcium sensor GCaMP. Calcium (Ca^{2+}) binding causes a conformational change in calmodulin-M13 complex, leading to an increase in the fluorescence of circularly permuted enhanced GFP (cpEGFP). Figure was acquired from Knöpfel *et al*. 2010 (141).

On the other hand, optical sensor proteins including environment-sensitive fluorescent proteins, *e.g.,* pH-sensitive GFP, and bioluminescent indicators allow the monitoring of a vast number of cellular factors, such as membrane voltage, changes in metabolite or ion

concentrations and enzyme activities. Besides, several sensors engineered by mutation, permutation or integration of two fluorescent proteins are also available to track dynamics of the molecules of interest (125,142). Interaction with a specific-molecule leads to a structural change in protein-complex, causing an alteration in fluorescence -spectra, -intensity or -resonance energy transfer (FRET) efficacy between acceptor and donor (125). Hence, the fluorescence response can be monitored either according to the intensity change or ratiometrically (FRET-based) with two-different wavelengths (one excitation and two emission or two excitation and one emission) (142).

The designing and application of gene encoded cGMP-sensitive biosensors facilitate real time monitoring of cGMP changes in living cells, which is difficult otherwise because of the transient nature of cGMP. Recently engineered FRET-based cGMP-sensors (Figure 9C) (named as cGi500, cGi3000 and cGi6000 depending on their sensitivity to cGMP concentrations) (143) were designed based on the type I PKG flanked by cyan- and yellow-fluorescent proteins, CFP and YFP, respectively. The bound of cGMP causes a conformational change leading a decrease of FRET from CFP to YFP as seen in Figure 9C. The estimation of cGMP concentration is done by calculation of CFP/YFP emission ratio. Although these cGMP indicators showed fast binding kinetics and an excellent specificity to cGMP in mammalian systems (140), FRET-based sensors have not yet been widely utilized because of the complexity of multiple emission parameters by a dual emission fluorescence microscopy. Instead, circularly permuted GFP-based cGMP sensors, such as FlincG3, are employed to timely monitor cGMP dynamics (144). Similarly, the usage of genetically-encoded calcium indicators (GECI) with single fluorophore (Figure 9D) has been also found pretty valuable to monitor intracellular Ca^{2+} homeostasis of various cell types (145-147). GCaMPs family proteins, the most widely used GECIs, are composed of a circularly permuted enhanced green fluorescent protein (cpEGFP), the calcium binding calmodulin (CaM) and CaM-interacting myosin light-chain kinase domain (M13) (146). An enhance in calcium level causes a conformational change in CaM, followed by activation of M13 and blocking the hole in the cpEGFP β-barrel, which leads to an increase in the fluorescence of cpEGFP as shown in Figure 9D (147,148).

Despite the fact that optogenetic technologies seem to provide several advantages to address convoluted questions, their application in infection research remained quite limited. A few years ago, Hartmann *et al.* (149) successfully expressed bPAC (130) to regulate cAMP

signaling by light in *T. gondii*. Recently, possible applications of available tools were proposed by Arroyo-Olarte *et al.* (127) to study various paradigms in intracellular pathogens. Given the benefits, such as (i) specific and quantitative regulation of cNMP levels within the parasite, (ii) efficient and reversible modulation of cNMP, (iii) rapid and spatiotemporal induction of signaling pathways, wider implementation of optogenetics in infection biology is very much expected.

1.4 Objective of this study

Cyclic GMP is a universal second messenger, regulating vital processes in the parasite. The function of PKG in *T. gondii* has been studied in details up to now. However, the onset of cGMP cascade remains underappreciated, partly due to complex structure of guanylate cyclases, as described in *Plasmodium* (97,150). Two distinct guanylate cyclases, *Pf*GCα and *Pf*GCβ (96,150,151), were identified in *P. falciparum*. Lately, Gao *et al.* (152) demonstrated the essential role of GCβ for the motility and transmission of *P. yoelii*. It was aimed in this thesis to characterize the native guanylate cyclase of *T. gondii* and test the physiological importance of cGMP signaling for the asexual reproduction of its acutely infectious tachyzoite stage. Our findings along with other independent studies published during the course of this work (99,153,154) as discussed elsewhere in this thesis, provide significant new insights into cGMP signaling during the lytic cycle of *T. gondii*.

Much of the cyclic-nucleotide signaling research is so far based on the usage of chemical activators and inhibitors targeting protein kinases and phosphodiesterases in conjunction with reverse genetics approach. The implementation of such chemical modulators is not optimal in this kind of two-organism (host-parasite) system to examine the organism-specific pathways, because they target proteins in both organisms due to the ubiquitous nature of cNMP signaling. As a consequence, there is no evidence yet showing real-time induction of cGMP cascade within the parasite and its direct relationship with the lytic cycle. To overcome such issues, we intended to take advantage of optogenetics by recombinantly expressing a light-activated rhodopsin-guanylate cyclase fusion protein (RhoGC) (135,136) in *T. gondii* tachyzoites to modulate only the parasite-specific cGMP pathways by light without perturbing its host cell. It allowed a rapid, reversible and spatial regulation of cGMP during the lytic cycle of parasite.

2 Materials and Methods

2.1 Materials

2.1.1 Biological resources

Cell line	Source
Human foreskin fibroblasts (HFFs)	Carsten Lüder, Georg-August University, Göttingen, Germany
T. gondii tachyzoites (RHΔ*ku80-hxgprt*⁻ strain)	Vern Carruthers, University of Michigan, Ann Arbor, USA (62)
E.coli (XL-1blue)	Stratagene, Germany
E. coli (M15/pREP4)	Qiagen, Germany
E.coli (BTH101)	Qiagen, Germany

2.1.2 Vectors

Vectors	Source
p3'IT-HXGPRT	John Boothroyd, Stanford School of Medicine, USA
pSAG1-Cre (Cre-recombinase expressing vector)	John Boothroyd, Stanford School of Medicine, USA
pTKO-DHFR/TS	modified from *p3'IT-HXGPRT*
pGRA1-UPKO	modified from *p3'IT-HXGPRT*
pDHFR-UPKO	modified from *p3'IT-HXGPRT*
pGP-SIU-GCaMP6s-GFP	Loren Looger, Howard Hughes Medical Institute, USA
pU6-Universal	Sebastian Lourido, White Institute for Biomedical research, USA (71)
pQE60	Qiagen, Germany
pGEM-RhoGC	Suely L. Gomes, Universidade de Sao Paulo, Brazil (135)

2.1.3 Oligonucleotides

All oligonucleotides used in this study were synthesized by Thermo Fisher Scientific (Germany) and listed in Table 1.

Table 1. Oligonucleotides used in this study

Primer name (Restriction site)	**Primer Sequence (Restriction site underlined)**	**Objective (Cloning vector)**
3'HA tagging of selected *Toxoplasma* genes (Δ*ku80*-Δ*hxgprt* strain)		
*Tg*ATPase$_P$-GC-COS-F1 (*Xcm*I)	CTCATCCCACCGGTCACCTGGGC ATGAGTGTGGCGGAGT	Cloning of crossover sequence for 3'-HA tagging (*p3'IT-HXGPRT*)
*Tg*ATPase$_P$-GC-HA$_{3'IT}$-COS-R1 (*EcoR*I)	CTCATCGAATTCCTACGCGTAGT CCGGGACGTCGTACGGGTACGA CCCGAGTGCAGAGC	
*Tg*PKG-COS-F1 (*Nco*I)	CTCATCCCATGGGAAAACTCGTT TTCCCGC	
*Tg*PKG-HA$_{3'IT}$-COS-R1 (*EcoR*I)	CTCATCGAATTCCTACGCGTAGT CCGGGACGTCGTACGGGTAGAA ATCCTTGTCCCAGTCATACT	
3'UTR cloning in the *Tg*ATPase$_P$-GC-HA$_{3'IT}$ and *Tg*PKG-HA$_{3'IT}$ vector constructs		
*Tg*ATPase$_P$-GC-3`UTR-F1 (*EcoR*I+loxP)	CTCATCGAATTCATAACTTCGTAT AGCATACATTATACGAAGTTATAA CGCAGCTTTTGTCAGC	Cloning of 3'UTR for the native expression (*p3'IT-HXGPRT)*
*Tg*ATPase$_P$-GC-3`UTR-R1 (*Spe*I)	CTCATCACTAGTTTATGTACGTAT ATACGCACATGTATG	
*Tg*PKG-3`UTR-F1 (*EcoR*I+loxP)	CTCATCGAATTCATAACTTCGTAT AGCATACATTATACGAAGTTATTT TTTCAGCTTAGGTGTTTGTTCC	
*Tg*PKG-3`UTR-R1 (*Spe*I)	CTCATCACTAGTGCTTTTCTGCG ACTCTGCTC	
Screening for 3'UTR excision of *Tg*ATPase$_P$-GC-HA$_{3'IT}$ and *Tg*PKG-HA$_{3'IT}$ mutants		
*Tg*ATPase$_P$-GC-HA$_{3'IT}$-Scr-F1	CTGGTCTCCGCAGAGATGCT	Screening primers of 3'UTR excision for the gene knockdown *(p3'IT-HXGPRT)*
Scr-*Tg*PKG-HA$_{3'IT}$-Scr-F1	GTTCATGTGCGGACCTCTCC	
3`UTR$_{excised}$-loxP-Scr-R1 (*Tg*ATPase$_P$-GC/*Tg*PKG)	CAGTGAGCGCAACGCAATTA	
Overexpression of catalytic domains GC1 and GC2 of *Tg*ATPase$_P$-GC in *E. coli*		
*Tg*ATPase$_P$-GC1-F1 (*Bgl*II)	CTCATCAGATCTATGCTCGATAAG AAGTACTTGCCCCCAC	Cloning of *Tg*ATPase$_P$-GC cyclase catalytic domains for *E. coli* expression (*p*QE60-6xHis)
*Tg*ATPase$_P$-GC1-R1 (*Bgl*II)	CTCATCAGATCTCGACGACGCAC CCGCAGT	
*Tg*ATPase$_P$-GC2-F1 (*Bgl*II)	CTCATCAGATCTATGACGATGAG CTTAACGTTCATCATC	
*Tg*ATPase$_P$-GC2-R1 (*Bgl*II)	CTCATCAGATCTTTGAGGGATCG CACCGCC	
*Tg*ATPase$_P$-GC1+2-F1 (*Bgl*II)	CTCATCAGATCTATGCTCGATAAG AAGTACTTGCCCCCAC	
*Tg*ATPase$_P$-GC1+2-R1 (*Bgl*II)	CTCATCAGATCTTTGAGGGATCG CACCGCC	

*p*QE60-Sequencing-F1	CGGATAACAATTTCACACAG	
*p*QE60-Sequencing-R1	GTTCTGAGGTCATTACTGG	
Making the Δ*Tg*ATPase$_P$-GC mutant (*Tg*ATPase$_P$-GC-HA$_{3'IT}$ strain)		
*Tg*ATPase$_P$-GC-KO-5'UTR-F1 (*Xcm*I)	CTCATCCCACCGGTCACCTGGTG CTTGGCTGATTGATGG	Cloning of 5'UTR for the *Tg*ATPase$_P$-GC knockout (*pTKO-DHFR/TS*)
*Tg*ATPase$_P$-GC-KO-5'UTR-R1 (*Spe*I)	CTCATCACTAGTTTTCGTCGTATT CGATAGCTCC	
*Tg*ATPase$_P$-GC-KO-5'Scr-F1	CGAGACGAGATTCTTGAACGA	Screening of 5' recombination
*Tg*ATPase$_P$-GC-KO-3'UTR-F1 (*Hind*III)	CTCATCAAGCTTAACGCAGCTTT TGTCAGCG	Cloning of 3'UTR for the *Tg*ATPase$_P$-GC knockout (*pTKO-DHFR/TS*)
*Tg*ATPase$_P$-GC-KO-3'UTR-R1 (*Apa*I)	CTCATCGGGCCCGACGGCTAGTC GAGACCCTG	
*Tg*ATPase$_P$-GC-KO-3'Scr-R1	AAGGATGATATTGCACCTCACA	Screening of 3' recombination
Genetic disruption of *Tg*ATPase$_P$-GC by CRISPR/Cas9 in *Tg*ATPase$_P$-GC-HA$_{3'IT}$ strain		
*Tg*ATPase$_P$-GC-sgRNA-F1	AAGTTCGTTGACTCTGTTCACCG CCG	Cloning of sgRNA for editing of *Tg*ATPase$_P$-GC (*pU6-sgRNA-Cas9*)
*Tg*ATPase$_P$-GC-sgRNA-R1	AAAACGGCGGTGAACAGAGTCA ACGA	
Making of optogenetic strain expressing RhoGC in *T. gondii* (Δ*ku80*-Δ*hxgprt*)		
RhoGC-F1 (*Nsi*I)	CTCATCATGCATATGAAAGATAA GGATAATAACCTGAGA	Cloning of RhoGC-HA in *pTKO-DHFR/TS* for randomly insertion
RhoGC-HA-R1 (*PacI*)	CTCATCTTAATTAACTACGCGTAG TCCGGGACGTCGTACGGGTATTT TCTGCCCAGCACCCAAT	
Making of optogenetic strain conditionally expressing RhoGC in *T. gondii* (Δ*ku80*-Δ*hxgprt*)		
ddFKBP-F1 (*Nsi*I)	CTCATCATGCATATGGGAGTGCA GGTGGAA	Cloning of ddFKBP to the N-terminal of RhoGC in *pTKO-DHFR/TS*
ddFKBP-R1 (*Pst*I)	CTCATCCTGCAGAGGTTCCGGTT TTAGAAGCTCC	
Sequencing for full-length of RhoGC in *pTKO-DHFR/TS*		
pTKO-EsPri-F1	TATAGACGCAACTCGGTTTGCT	Sequencing primers for verification
RhoGC-Rho-EsPri-R1	GTTCTCCAGTTCCTCTGCGA	
RhoGC-GC-EsPri-F1	CTTGGAGCCTGTTCCCCATT	
pTKO-EsPri-R1	CTGATCGGCTTTGTAGACTTCTC	
Ectopic expression of RhoGC in *T. gondii* (Δ*ku80*-Δ*hxgprt*)		
RhoGC-F1 (*Nsi*I)	CTCATCATGCATATGAAAGATAA GGATAATAACCTGAGA	Cloning of RhoGC-3xHA in *pDHFR-UPKO* vector for
RhoGC-3xHA-R1 (*Pac*I)	CTCATCTTAATTAATTAGGCATAA TCTGGAACATCGTAAGGATACGC	

	ATAATCGGGCACATCATAGGGATAGCCAGCGTAGTCCGGGACGTCGTACGGGTATTTTCTGCCCAGCACCCAAT	moderate expression
pDHFR-UPKO-EsPri-F1	ATTTTACCACACGGCAGTG	Sequencing primers of *pDHFR-UPKO* for verification
pDHFR-UPKO-EsPri-R1	GGGTCTCTGGCACCCCCT	
Screening of RhoGC expression in optogenetic strains		
RhoGC-Scr-F1	ATGAAAGATAAGGATAATAACCTGAGAGG	Primers for gDNA and cDNA screening
RhoGC-Scr-R1	TTTTCTGCCCAGCACCCAATAAG	
Ectopic expression of GCaMP6s in *T. gondii* (Δ*ku80*-Δ*hxgprt* strain)		
GCaMP6s-F1 (*Nsi*I)	CTCATCATGCATTCTCATCATCATCATCAT	Cloning of GCaMP6s-ORF in *pGRA1-UPKO* vector
GCaMP6s-R1 (*Pac*I)	CTCATCTTAATTAATCACTTCGCTGTCATC	
Co-expression of GCaMP6s with RhoGC-3xHA in *T. gondii* (*pDHFR-RhoGC-3xHA* strain)		
GCaMP6s- cassette-F1 (*Not*I)	CTCATCGCGGCCGCCGTCTCAGCTGCGCGAGGC	Cloning of GCaMP6s-cassette flanked with *Tg*Gra1-5'UTR and *Tg*Gra2-3'UTR to *pDHFR-RhoGC-3xHA* vector
GCaMP6s-cassette-R1 (*Not*I)	CTCATCGCGGCCGCCACCGCGGTGGGATCCGT	

2.1.4 Antibodies

Antibody	Dilution	Source
α-*Tg*Sag1 (mouse)	1:10000	Dubremetz *et al.* 1985 (155)
α-*Tg*ISP1 (mouse)	1:2000	Beck *et al.* 2010 (156)
α-*Tg*Gap45 (rabbit)	1: 3000	Plattner *et al*. 2008 (157)
α-*Tg*Rop2 (mouse)	1:1000	Sadak *et al*. 1988 (158)
α-*Tg*HSP90	1:1000	Echeverria *et al*. 2005 (159)
α-GFP (mouse)	1:1000	Thermo Fisher Scientific, Germany
α-GFP (rabbit)	1:5000	Thermo Fisher Scientific, Germany
α-HA (mouse)	1:3000	Invitrogen, Germany
α-HA (rabbit)	1:200	Thermo Fisher Scientific, Germany
α-6xHis mAb IgG1 (mouse)	1:2000	Dianova, Germany
Alexa Fluor 488 α-mouse IgG (goat)	1:3000	Thermo Fisher Scientific, Germany
Alexa Fluor 488 α-rabbit IgG (goat)	1:3000	Thermo Fisher Scientific, Germany
Alexa Fluor 594 α-rabbit IgG (goat)	1:3000	Thermo Fisher Scientific, Germany
Alexa Fluor 594 α-mouse IgG (goat)	1:3000	Thermo Fisher Scientific, Germany

IRDye 680RD α-rabbit (goat)	1:15000	LI-COR Biosciences, USA
IRDye 800CW α-mouse (goat)	1:15000	LI-COR Biosciences, USA

2.1.5 Enzymes

Enzyme	Company
Anza™ Alkaline Phosphatase	Invitrogen, Germany
Dream Taq™ Polymerase	Fermentas, Germany
Restriction Endonucleases	New England Biolabs, USA
Q5-High Fidelity DNA Polymerase	New England Biolabs, USA
T4 Ligase	New England Biolabs, USA
Proteinase K	Sigma Aldrich, Germany

2.1.6 Chemical reagents

Chemicals	Manufacturer
1,4-Dihydro-5-(2-propoxyphenyl)-7H-1,2,3-triazolo(4,5-d)pyrimidin-7-one (Zaprinast)	Sigma-Aldrich, Germany
1,4-Dithiothreitol (DTT)	AppliChem, Germany
4',6'-Diamidino-2-phenylindol-dihydrochloride (DAPI)/Fluoromount G®	Southern Biotech, USA
4-[7-[(dimethylamino) methyl]-2-(4-fluorophenyl) imidazo [1,2-*α*] pyridin-3-yl] pyrimidin-2-amine (Compound 2)	Oliver Billker, Wellcome Trust Sanger Institute, UK (160)
5-Benzyl-3-isopropyl-1H-pyrazolo [4,3*d*] pyrimidin-7(*6H*)-one (BIPPO)	Philip Thompson, Monash University, Melbourne, Australia (122)
5-Fluoro-2'-deoxyuridine (FudR)	Sigma-Aldrich, Germany
6-thioxanthine (6-TX)	Sigma-Aldrich, Germany
Acetic acid 96%	Merck, Germany
Acrylamide (Rotiphorese gel 30)	Carl Roth, Germany
Adenosine triphosphate (ATP)	Sigma-Aldrich, Germany
Agarose	Carl Roth, Germany
All-trans retinal	Sigma-Aldrich, Germany
Ammonium persulfate (APS)	Carl Roth, Germany
Ampicillin (Amp)	Carl Roth, Germany
Bovine serum albumin (BSA)	Carl Roth, Germany
Bromophenol blue	Merck, Germany
Calcium chloride ($CaCl_2$)	Carl Roth, Germany
Chloroform	Carl Roth, Germany

Crystal violet	Sigma-Aldrich, Germany
Deoxynucleotide-triphosphate(dNTPs)	Rapidozym, Germany
Dimethyl sulfoxide (DMSO)	Carl Roth, Germany
Disodium phosphate (Na_2HPO_4)	Sigma-Aldrich Chemie GmbH, Germany
Distilled water (HPLC-purified)	Carl Roth, Germany
Dithiothreitol (DTT)	Carl Roth, Germany
DNA loading dye (6x)	Thermo Fisher Scientific, Germany
Dulbecco's Modified Eagle medium (DMEM)	PAN-Biotech, Germany
Dulbecco's phosphate buffered saline (PBS)	PAN-Biotech, Germany
Ethanol ≥ 99,8% p.a.	Roth, Germany
Ethylenediaminetetraacetic acid (EDTA)	Sigma-Aldrich, Germany
Fetal bovine serum (FBS)	PAN-Biotech, Germany
Gene Ruler DNA-Ladder (1 kb)	Thermo Fisher Scientific, Germany
Glucose	Carl Roth, Germany
Glutathione (GSH)	Sigma-Aldrich, Germany
Glycerol	Carl Roth, Germany
Glycine	Sigma-Aldrich, Germany
Guanosine triphosphate (GTP)	Thermo Fisher Scientific, Germany
Hank's balanced salt solution (HBSS)	PAN-Biotech, Germany
HEPES (4-(2-hxdroxyethyl)-1-piperazineethane-sulfonic acid)	Carl Roth, Germany
Iodoacetamide (IAA)	Sigma-Aldrich, Germany
Isopropanol	AppliChem, Germany
Isopropyl-beta-D-thiogalactopyranoside (IPTG)	AppliChem, Germany
Kanamycin sulfate	AppliChem, Germany
L-glutamine (200mM)	PAN-Biotech, Germany
MacConkey-Agar	Carl Roth, germany
Magnesium chloride ($MgCl_2$)	Carl Roth, Germany
MEM non-essential amino acids (100x stock)	PAN-Biotech, Germany
Methanol ≥ 99,9% p.a.	Carl Roth, Germany
Milk powder	Carl Roth, Germany
Mycophenolic acid (MPA)	AppliChem, Germany
PageRuler-Prestained protein ladder	Thermo Fisher Scientific, Germany
Paraformaldehyde (PFA)	Merck, Germany

Penicillin/Streptomycin (100x)	PAN-Biotech, Germany
Phenylmethylsulfonyl fluoride (PMSF)	Carl Roth, Germany
Phosphatase inhibitor cocktail	Sigma Aldrich, Germany
Potassium chloride (KCl)	Carl Roth, Germany
Potassium dihydrogen phosphate (KH_2PO_4)	Carl Roth, Germany
Pyrimethamine	Sigma-Aldrich, Germany
Roti®Safe-GelStain	Carl Roth, Germany
Shield1	Chemin Pharma, USA
Sodium chloride (NaCl)	Carl Roth, Germany
Sodium dodecyl sulfate (SDS)	Carl Roth, Germany
Sodium pyruvate, 100mM	PAN-Biotech, Germany
Streptomycin sulfate	AppliChem, Germany
Tetramethylethylenediamine (TEMED)	Carl Roth, Germany
Trifluoroacetic acid (TFA)	Sigma-Aldrich, Germany
Tris-Hydrochloride	Promega, USA
Triton-X100	Carl Roth, Germany
TRIzol® Reagent	Life Technologies Corporation, USA
Trypsin (TPCK-treated)	Thermofisher Scientific, Germany
Trypsin/ EDTA	PAN-Biotech, Germany
Tryptone	AppliChem, Germany
Tween 20	AppliChem, Germany
Xanthine	Sigma-Aldrich, Germany
Yeast extract	AppliChem, Germany
α-Toxin from *Clostridium septicum*	List Biological Laboratories, USA
β-mercaptoethanol	Carl Roth, Germany

2.1.7 Instruments

Instrument	Manufacturer
Camera system (E.A.S.Y. RH)	Herolab, Germany
Cell counting chamber (Neubauer-improved)	Carl Roth, Germany
Centrifuges (5417R, 5424, 5810R)	Eppendorf, Germany
Cryo container (Nalgene, Mr. Frosty)	Thermo Fisher Scientific, Germany
Electric pipetting aid (Accu-jet Pro)	Brand GmbH, Germany
Electrophoresis Power Supply (EPS 200/300)	Pharmacia Biotech, Sweeden

Electroporator (Amaxa Nucleofector)	Lonza, Switzerland
ELISA microplate reader	Biotek, Germany
Freezer (-80°C) (UF85-360T)	Colora, Germany
Gel electrophoresis system (Easy Phor)	Biozym, Germany
Gel documentation system (E.A.S.Y.®-CAST)	Herolab, Germany
High performance liquid chromatograph (HPLC)-LC-20AD	Shimadzu, Japan
Ice machine (ZBE 110-35)	Ziegra, Germany
Incubator- CO_2 (HERACELL 150i)	Thermo Fisher Scientific, Germany
Incubators (SE200-400)	Memmert, Germany
Infrared imaging system (Odyssey FC)	LI-COR Biosciences, USA
Microscope-fluorescence (Axio Image.Z2)	Carl Zeiss, Germany
Microscope-inverted (LABOVERT)	Leica, Germany
Microscope-light optical (DM750)	Leica, Germany
Microwave (M805 Typ KOR-6115)	Alaska, Germany
Mini centrifuge (Sprout® Mini-Centrifuge)	Heathrow Scientific, USA
Mini vertical SDS-PAGE electrophoresis system (Hoefer™ Mighty Small™ II)	Hoefer Inc., USA
Multichannel pipette (Transferpipette® -8/-12) (50-200 µl)	Brand, Germany
NanoDrop® spectral photometer (ND-1000)	Peqlab, Germany
PCR Thermocycler (Flex Cycler)	Analytic Jena, Germany
PerfectBlue™ 'Semi-Dry' blotter (SEDEC M)	Peqlab, Germany
Photometer (BioPhotometer)	Eppendorf, Germany
Pipettes	Eppendorf, Germany
pH-meter (pH528 MultiCal®)	Xylem Analytics, Germany
Precision scale (PCB 1000-2)	Kern & Sohn, Germany
Precision scale (BP 110 S)	Sartorius, Germany
Safety work benches (HERA safe)	Heraeus Instruments, Germany
Shaker (WS5)	Edmund Bühler, Germany
Shaking incubator (Innova 4000)	New Brunswick, Germany
Steam-sterilizer (VARIOKLAV)	Thermo Fisher Scientific, Germany
Ultrasonic bath (Biorupter Sonication System)	Diogenode, Belgium
UV-transilluminator (UVT-20 M/W)	Herolab, Germany
Thermoshaker (Thermomixer comfort/ 5436)	Eppendorf, Germany
Vortex (MS 1 shakers)	IKA®-Werke, Germany
Waterbath (1002)	GFL, Germany
Waterbath (U 3/8)	Julabo, Germany

2.1.8 Commercial kits

Kit	Company
Direct cGMP ELISA kit (ADI-900-014)	Enzo Life Sciences GmbH, Germany
DetectX High Sensitivity Direct cGMP (K020-C1)	Arbor Assays Headquarters, USA
innuPREP DNA Mini Kit 2.0	Analytik Jena AG, Germany
innuPREP DOUBLEpure Kit	Analytik Jena AG, Germany
innuPREP Plasmid Mini Kit 2.0	Analytik Jena AG, Germany
innuPREP RNA Mini Kit 2.0	Analytik Jena AG, Germany
Pierce BCA Protein Assay Kit	Thermo Fisher Scientific, Germany
PureLink HiPure Plasmid Midiprep Kit	Invitrogen, Germany
RevertAid H Minus First Strand cDNA Synthesis Kit	Thermo Fisher Scientific, Germany

2.1.9 Plastic ware and other disposables

Consumable items	Company
24 well glass bottom plate-black wall	IBL Baustoff + Labor GmbH, Austria
Cell culture dishes (60x15 mm)	Sarstedt, Germany
Cell culture flasks (T25, T75, T175, T300)	Sarstedt, Germany
Cell culture plate (6, 24, 96 well)	Sarstedt, Germany
Cell scraper (30 cm)	TPP™, Switzerland
Centrifugal filters (0.22-µm, Corning Costar Spin-X)	Sigma Aldrich, Germany
Cryotube preservation tubes (2 ml)	Greiner Bio One, Germany
Disposable Sterican™ blunt end needles, (27 G, 23 G)	Braun, Germany
DuraSeal laboratory sealing film	Diversified Biotech, USA
Electroporation cuvettes (2 mm)	PEQLAB, Germany
Falcon Tubes (15 ml/ 50 ml), CELLSTAR™	Greiner Bio One, Germany
Filter (5 µm), Millex® syringe-compatible	Merck Millipore, Germany
Filter sterilizer (0.22 µm)	Schleicher Schuell, Germany
Filter tubes (Amicon Ultra-0.5 ml)	Merck Millipore, Germany
Glass cover slips (10 mm diameter)	VWR International, Germany
Glass slides, microscopic (76x26 mm)	Carl Roth, Germany
Latex gloves AQL 1.5	Sempermed™, Austria
Microtube (8x0.2 ml)	Biozym, Germany
Microtube lid (8x0.2 ml)	Biozym, Germany
Ni-NTA columns for protein purification (Novex)	Thermo Fisher Scientific, Germany
Nitrile gloves AQL 1.5	Sempermed™, Austria
Nitrocellulose transfer membrane	AppliChem, Germany
Parafilm®	Pechiney Plastic Packaging, USA
PCR-tube-stripes (0.2 ml)	Biozym, Germany

Pipette-pasteur	A. Hartenstein, Germany
Pipette tips (10 µl, 20 µl, 200 µl, 1ml)	Sarstedt, Germany
Protein low bind reaction tube (0030108116)	Eppendorf, Germany
Reaction tubes (0.2 ml, 0.5 ml, 1.5 ml, 2 ml)	Sarstedt, Germany
RNAase free barrier tips (10-1000 µl)	Biozym, Germany
Rotilab blotting paper	Carl Roth, Germany
Serological pipettes, sterile (5 ml, 10 ml, 25 ml)	Sarstedt, Germany
Size exclusion columns (10-kDa, 30-kDa cut-off)	Merck Millipore, Germany
Syringes Omnifix® (3 ml, 5 ml, 10 ml)	B. Braun Melsungen AG, Germany
UV-cuvettes	Carl Roth, Germany
Whatman paper (3 MM)	A. Hartenstein, Germany

2.1.10 Buffer and medium compositions

Medium or buffers		Composition
T. gondii - D10 medium	500 ml	DMEM (high glucose 5g/l without L-glutamine)
	50 ml	iFCS (heat-inactivated)
	5.5 ml	penicillin/streptomycin (100x)
	5.5 ml	non-essential amino acids (100x)
	5.5 ml	sodium pyruvate (100 mM)
	5.5 ml	L-glutamine (200 mM); stored at 4 °C
T. gondii - freezing medium		10% DMSO in heat-inactivated FBS; stored at -20 °C
Lysogeny Broth (LB) medium	10 g	tryptone
	5 g	yeast extract
	10 g	NaCl
	15 g	agar (optional for plates)
		in 1 liter of deionized autoclaved water
Super Optimal Broth with Catabolite repression (SOC) medium	20 g	tryptone
	5 g	yeast extract
	0.5 g	NaCl
	0.186 g	KCl
	0.952 g	$MgCl_2$
		in 1 liter of deionized water, autoclaved
	20 mM	glucose; filter-sterilized with 0.22 µm filter
Cytomix	120 mM	KCl
	25 mM	HEPES (pH 7.6)
	5 mM	$MgCl_2$
	2 mM	EDTA
	0.15 mM	$CaCl_2$
	10 mM	K_2HPO_4/KH_2PO_4 (pH 7.6)
		in deionized autoclaved water
		adjusted to pH: 7.6, filter-sterilized with 0.22 µm filter

4% paraformaldehyde (PFA)	10 g	PFA in 0,25 liter of PBS (heat-treatment at 60 °C) adjusted to pH: 7.6
PBS (10x)	25,6 g 80 g 2 g 2 g	$Na_2HPO_4 \cdot 7H_2O$ NaCl KCl KH_2PO_4 adjusted to pH: 7.4 in 1 liter of deionized water, autoclaved
TAE-Buffer (1x)	40 mM 0.1% 1 mM	Tris-HCl acetic acid EDTA in deionized water
SDS-loading buffer (5x)	0.25% 0.5 M 50% 10% 0.25 M	bromophenol blue dithiothreitol (DTT) glycerol sodium dodecyl sulfate (SDS) Tris-HCl (pH 6.8) in deionized water
SDS-running buffer (5x)	1.25 M 0.5% 125 mM	glycine SDS Tris-HCl (pH 8.3); in 1 liter of deionized water
5% stacking gel (SDS-PAGE)	1.4 ml 0.33 ml 0.25 ml 20 µl 20 µl 10 µl	dH_2O 30% acrylamide 1 M Tris-HCl (pH:6.8) 10% SDS 10% APS TEMED
12% resolving gel (SDS-PAGE)	1.6 ml 2 ml 1.3 ml 50 µl 50 µl 2 µl	dH_2O 30% acrylamide 1.5 M Tris-HCl (pH:8.8) 10% SDS 10% APS TEMED
8% resolving gel (SDS-PAGE)	2.3 ml 1.3 ml 1.3 ml 50 µl 50 µl 3 µl	dH_2O 30% acrylamide 1.5 M Tris-HCl (pH:8.8) 10% SDS 10% APS TEMED

Semi-dry blot transfer buffer	38 mM	glycine
	20%	methanol
	0.0037%	SDS
	48 mM	Tris-HCl (pH:8.3); in deionized water
TBS buffer (10x)	1.5 M	NaCl
	0.5 M	Tris-HCl (pH:7.6); in deionized water
TBS-T buffer (1x)	10%	10x TBS buffer
	0.2%	Tween 20; in deionized water

2.1.11 Software and web resources

Software/ website	Company/ address
AxioVision Rel. 4.8.	Carl Zeiss Mikroskopie GmbH, Germany
Geneious® 6.1	Biomatters Ltd., New Zealand
GraphPad Prism 6.0	GraphPad Software Inc, USA
ImageJ win 32	https://github.com/fiji
Ligation calculator tool	http://www.insilico.uni-duesseldorf.de/Lig_Input.html
Protein molecular weight calculator	https://www.bioinformatics.org/sms/prot_mw.html
FigTree v1.4.3	http://tree.bio.ed.ac.uk/software/figtree/
MS Office 2010	Microsoft Cooperation, USA
Arduino 1.8.8	Arduino AG, Italy
ToxoDB: Toxoplasma Genomic Resource	http://toxodb.org/toxo/
ZEN 2012 (*blue edition*)	Carl Zeiss Mikroskopie GmbH, Germany
TMHMM Server, v. 2.0	DTU Bioinformatics, Denmark
SMART (Simple Modular Architecture Research Tool)	http://smart.embl-heidelberg.de/
Phobius	http://phobius.sbc.su.se/
NCBI conserved domain search	https://www.ncbi.nlm.nih.gov/Structure/cdd/wrpsb.cgi
TmPred server -EMBnet	https://embnet.vital-it.ch/software/TMPRED_form.html
Clustal Omega-Sequence alignment	https://www.ebi.ac.uk/Tools/msa/clustalo/
UniProt	https://www.uniprot.org/
SWISS-MODEL-homology modelling	https://swissmodel.expasy.org/
CLC Genomics Workbench v12.0	Qiagen Bioinformatics, USA

2.2 Methods – Molecular cloning and nucleic acid isolation

2.2.1 Polymerase chain reactions (PCR)

All targeted DNA fragments were amplified by Q5 polymerase (New England Biolabs) either from a vector or genomic DNA of *T. gondii* RHΔ*ku80-hxgprt*$^-$ strain. Template concentrations ranged between 10-200 ng for standard reactions as manufacturer's recommendation. Dream Taq^{TM} Polymerase (Fermentas) was only used for colony PCR to detect positive *E. coli* colonies following transformation. Briefly, single bacterial colonies were resuspended in 20 µl of sterile dH_2O, and only 2 µl of suspension was used as template for the screening. The mastermix and PCR samples were prepared according to the manufacturer's protocols, and reactions were run by setting programs based on the amplicon size and primer features in Thermocycler (FlexCycler, Analytik Jena).

2.2.2 Agarose gel electrophoresis

The PCR amplicons, digested vectors or DNA fragments were mixed with DNA loading buffer (1:6 volume) and run on 1% agarose gel stained with Roti®Safe-GelStain at 120 V in TAE buffer. Visualization was performed using Herolab camera system and UV-transilluminator.

2.2.3 Purification of DNA fragments

After verification with agarose gel electrophoresis, PCR products showing expected band sizes were directly purified by passing through column or extracted from gel using the innuPREP DOUBLEpure kit (Analytik Jena) according to the manufacturer's instruction. The purified insert was eluted in sterile dH_2O followed by measuring the concentration *via* NanoDrop® spectral photometer (ND-1000).

2.2.4 Restriction endonuclease digestion

Vector DNA was isolated from overnight *E. coli* cultures by innuPREP Plasmid Mini Kit 2.0 (Analytik Jena); the purity and concentration of DNA were determined at 260 nm using NanoDrop. 1-15 µg of purified PCR product and vector DNA were digested using corresponding restriction enzymes, 5 units of which was used to cut 1 µg of DNA in 1x enzyme specific reaction buffer. Reaction tube was incubated for 3 h in an appropriate temperature as it is suggested by manufacturers. Dephosphorylation was performed by

alkaline phosphatase (Invitrogen) during vector digestion for non-directional cloning (using the same restriction enzyme for N-terminal and C-terminal sites). Subsequently, vector was run on agarose gel to see the digestion efficiency, and backbone was purified from gel; whereas digested insert was exposed to column purification as stated in section 2.2.3 followed by elution in sterile dH_2O.

2.2.5 Ligation and transformation of *E. coli*

Digested plasmid DNA and insert were ligated in a molar ratio 1:3 (fmol of plasmid:fmol of insert) by using 5 units of T4 DNA ligase in a ligase buffer. The vector amount was always set as 45 ng, and insert amount was calculated depending component's size using online ligation calculator tool (http://www.insilico.uni-duesseldorf.de/Lig_Input.html). Ligation mixture was incubated either for 1 h at 22 °C or overnight at 4 °C prior to transformation. 10 µl of ligation reaction was mixed with 100 µl of fresh-thawed competent cells immediately. *E. coli* XL-1blue (Stratagene) cells were used for regular cloning prepared for *T. gondii* transfections, whereas M15 and BTH101 (Qiagen) strains were deployed for recombinant expression of *T. gondii* proteins. Bacterial cells were incubated on ice for 30 min and heat-shocked for 45 sec at 42 °C followed by chilling on ice for 3-5 min. Thereafter, 700 µl of pre-warmed SOC medium was added into the reaction tube and incubated for 1 h by shaking at 450 rpm, 37 °C. Cells were centrifuged at 8000xg for 2 min, and pellet was dissolved in 100 µl SOC. Cell suspension was plated on selective LB-agar containing ampicillin (100 µg/ml), kanamycin (50 µg/ml) and/or streptomycin (100 µg/ml) depending on the resistance of strain or plasmid. Plates were incubated then overnight at 37 °C, and single colonies were screened for plasmid expression. Colony PCR was set using insert specific primers, and overnight cultures of selected positive colonies were prepared for plasmid isolation.

2.2.6 Isolation of plasmid DNA and preparation of freezer stocks

5 ml of overnight cultures prepared from positive colonies were used for both preparing freezer stocks and plasmid DNA isolation. 500 µl of bacterial culture was mixed with an equal volume of autoclaved 50% glycerol in a cryo-preserving tube under sterile work bench and stored at -80 °C. Afterwards, plasmid DNA was isolated from the left over overnight culture by innuPREP Plasmid Mini Kit 2.0 (Analytik Jena) following the instructions, which yields 4-5 µg of DNA in general. The constructed plasmid was verified by DNA sequencing

to eliminate any mutation risk. 200 ml of overnight cultures were prepared for large-scale plasmid isolation by PureLink HiPure Plasmid Midiprep Kit (Invitrogen). Plasmid DNA was eluted in 120-150 µl of sterile dH_2O and stored at -20 °C.

2.2.7 Precipitation of plasmid DNA

The vectors were precipitated by adding 200 µl of isopropanol in a reaction tube and centrifuged at 18000xg, 4 °C for 30 min following incubation for 1 h at -20 °C. Supernatant was discarded after centrifugation, and the pellet was washed with 200 µl of 70% ethanol (ice cold). After a short centrifugation (18000xg, 4 °C, 5 min) supernatant was discarded again, and pellet was dried inside a sterile work bench. Eventually, the pellet was dissolved in 20 µl of sterile dH_2O and stored at -20 °C.

2.2.8 Isolation of genomic DNA from *T. gondii* tachyzoites

Fresh lysed out parasites (5-10x10^6) were pelleted at 12000xg for 10 min from the cultures. The parasite pellet was then either stored at -80 °C or directly processed by innuPREP DNA Mini Kit 2.0 (Analytic Jena). At first, parasite pellet was resuspended in lysis buffer (400 µl), and proteinase K treatment was performed by incubating samples for 30 min at 50 °C. Afterwards, kit protocol was applied to isolate genomic DNA. DNA concentration was measured by nanodrop and used as a template for PCR.

2.2.9 Extraction of RNA from *T. gondii* tachyzoites and cDNA synthesis

Total RNA was extracted from extracellular or freshly syringe-released parasites, and RNAase free plastic wares were used during the extraction. Briefly 5-20x10^6 parasites were pelleted and lysed in 1 ml of TRIzol followed by either storing at -80 °C or directly processed by innuPREP RNA Mini Kit 2.0 (Analytic Jena). Briefly, 200 µl of chloroform was added into eppendorf and vortexed for 15 sec by holding the lid tightly. Sample was centrifuged at 12000xg for 15 min at 4 °C, causing separation of two layers. The upper aqueous layer containing RNA was transferred into another reaction tube and mixed with an equal volume of 70% ethanol (diluted with DEPC-treated water) by mixing thoroughly for 5 sec. This composition was transferred into spin filter R supplied by RNA kit, and kit protocol was followed. The RNA was eluted eventually in 20 µl of DEPC-treated sterile water and used immediately as a template for cDNA synthesis. RevertAid H Minus First Strand cDNA synthesis kit protocol (Thermo Fisher Scientific) was applied using oligo-dT primers

provided by kit. Synthesized cDNA was used for screening of protein transcripts and stored at -20 °C.

2.3 Methods – Overexpression, purification and functional assays of *T. gondii* proteins in *E. coli*

2.3.1 Heterologous expression of proteins in *E. coli*

Heterologous expression of *Tg*ATPase$_P$-GC nucleotide cyclase domains, termed as GC1 and GC2, was performed in the M15 and BTH101 strains of *E. coli*. The open reading frames of GC1 (2850-3244 bp), GC2 (3934-4242 bp) and GC1+GC2 (2850-4242 bp) domains starting with the first upstream start codon (ATG) were amplified from the mRNA of RHΔ*ku80-hxgprt*$^-$ strain. The first-strand cDNA used for ORF-specific PCR was generated from the total RNA by oligo-dT primers as described in section 2.2.9. The ORFs were cloned into the *pQE60* vector at the *Bgl*II restriction site resulting in a C-terminal 6xHis-tag fusion (see vector maps in Appendix 8). To express the indicated proteins, 5 ml culture of the recombinant M15 strains (grown overnight at 37°C) were diluted to an OD_{600} of 0.1 in 100 ml of LB medium containing 100 µg/ml ampicillin and 50 µg/ml kanamycin, and incubated at 37°C until OD_{600} reached to 0.4-0.6 (4-5 h). The cultures were then induced with 0.1 mM Isopropyl β-D-1-thiogalactopyranoside (IPTG) overnight at 25°C. The OD_{600} of cultures then normalized for protein purification.

2.3.2 Recombinant protein purification from *E. coli*

The recombinant proteins expressed in *E. coli* M15 strain were purified under denaturing conditions using Ni-NTA column according to the manufacturer's protocol (Novex, Thermo Fisher Scientific). Briefly, cells were harvested by centrifugation at 3000x*g*, 20 min, 4 °C, and pellet was resuspended in 8 ml of lysis buffer containing 6 M guanidine-HCl, 20 mM NaH_2PO_4, 500 mM NaCl, (pH 7.8) followed by incubation at 4 °C by shaking for 10 min. Subsequently, probe sonication (5 pulses, each for 30 sec, with intermittent cooling on ice-water) was performed in order to disrupt the cells. Sonicated samples were flash-frozen in liquid nitrogen and thawed at 37°C in three iterations. Intact cells were eliminated by pelleting at 3000x*g* for 15 min. Lysate-containing supernatant (cell-free extract) was loaded on Ni-NTA column pretreated with binding buffer (8 M urea, 20 mM NaH_2PO_4, 500 mM NaCl, pH 7.8) and washed twice by 4 ml of washing buffer (8 M urea,

20 mM NaH_2PO_4, 500 mM NaCl) with pH 6.0 and pH 5.3, respectively. Proteins were eluted in 5 ml of elution buffer (20 mM NaH_2PO_4, 100 mM NaCl, 10% Glycerol, pH 7.8) by incubating tubes on ice, and protease inhibitor cocktail (50 µl) was added to the eluate. The eluate was then concentrated and dialyzed by 30-kDa cut-off centrifugal filters (Amicon ultra filters, Merck Millipore, Germany). A refolding of the purified proteins led to precipitation. The amount of urea was thus gradually reduced down to 0.32 M by adding 4x volume of buffer including 20 mM NaH_2PO_4, 100 mM NaCl and 10% glycerol in successive centrifugation steps. The final purified protein preparation was stored at -80°C until using. The quantitation of protein in samples was specified by bicinchoninic acid (BCA) assay that was performed by a commercial kit (Thermo Fisher Scientific). 5 µg of purified proteins were exposed to SDS-PAGE and following Western Blot analysis by using α-His antibody.

2.3.3 Making of bacterial cell lysates

5 ml of overnight cultures from GC1, GC2 and GC1+GC2 expressing *E. coli* M15 strains were grown overnight at 37 °C, and cultures were handled as stated in 2.3.1 until the last step. When OD_{600} reached to 0.5 at 37 °C incubation, the cultures were kept at 4 °C for 30 min and then induced with 0.1 mM IPTG in 10 ml LB medium overnight at 25°C. After OD_{600} was adjusted to 1.0 for all strains, cells were pelleted at 3000x*g* for 20 min (4 °C) and incubated in 500 µl of lysis buffer containing 50 mM HEPES (pH 7.5), 100 mM NaCl, 1 mM PMSF, 10 mM β-mercaptoethanol and 10 mM imidazole at 4 °C for 1 h by shaking (600 rpm). The samples were sonicated for 30 sec with successive 5 pulses including intervals between each pulse for cooling on ice-water. Following centrifugation at 15000xg, 4 °C for 20 min, the pellet was discarded, and the supernatant was used immediately to set *in vitro* functional assay. 20 µl of remaining lysate was run on SDS gel and following Western Blot by staining with α-His antibody.

2.3.4 Guanylate cyclase assay with purified proteins and cell lysates

5 µg of purified GC1 and GC2 proteins and 50 µl of cell lysates from *E. coli* M15 strain (preparation of samples was described in section 2.3.2 and 2.3.3, respectively) were examined by *in vitro* guanylate cyclase assay. The enzymatic reaction was carried out in 50 mM HEPES buffer (pH, 7.5) containing 100 mM NaCl, 2 mM $MnCl_2$ and 2 mM GTP. The reaction volume was completed to 100 µl, and the assay was performed at 22 °C for 10 min. Negative controls (-protein/+GTP and +protein/-GTP) were also included in both cases to the

assay. The reaction was quenched by adding 200 µl of 0.1 M HCl, and samples were stored at -20 °C until measurement by high performance liquid chromatography (HPLC).

2.3.5 Adenylate cyclase assay on MacConkay agar

The function of GC1, GC2 and GC1+GC2 as being potential adenylate cyclases was tested in the *E. coli* BTH101 strain lacking an adenylate cyclase (*cya*), and thus unable to utilize maltose as a carbon resource (161). The *pQE60* constructs encoding indicated ORF sequences were transformed into the BTH101 strain. The bacterial cultures were grown overnight in 5 ml of LB medium containing 100 µg/ml ampicillin and 100 µg/ml streptomycin at 37 °C. Protein expression was induced by 200 µM of IPTG (2 h, 30 °C) followed by serial dilution plating on MacConkey agar (pH 7.5) supplemented with 1% maltose, 200 µM IPTG and 100 µg/ml of each antibiotic. The strain harboring the empty *pQE60* vector served as a negative control, whereas the plasmid expressing *Cya*A (native bacterial adenylate cyclase) was included as a positive control. Agar plates were incubated at 30 °C (~32 h) to examine the appearance of colonies. cAMP could be produced if the catalytic domains are functioning as adenylate cyclase, causing the complement of maltose pathway. This will result in formation of red colonies on MacConkey agar. If the pathway is not complemented, the bacteria strains are expected to form slow growing white colonies.

2.4 Methods – Cell culture and transfection

2.4.1 Cultivation of host cells

Human foreskin fibroblast (HFF) cells were cultivated in Dulbecco's modified Eagle's medium (DMEM) with glucose (4.5 g/L) supplemented with 10% heat-inactivated fetal bovine serum (iFBS, PAN Biotech, Germany), 2 mM glutamine, 1 mM sodium pyruvate, 1x minimum Eagle's medium non-essential amino acids (100 µM each of serine, glycine, alanine, asparagine, aspartic acid, glutamate, proline), penicillin (100 U/ml), and streptomycin (100 µg/ml) in a humidified incubator (37 °C, 5% CO_2). Briefly, host cells were cultured in T300 flasks and grown to confluence. They were harvested by trypsinization (0.25% trypsin-EDTA) every 2-3 weeks and seeded in flasks, plates or dishes, as a requirement of experiments.

2.4.2 Parasite culture and preparation of extracellular parasites for assays

T. gondii tachyzoites were propagated by serial passaging routinely every 2-3 days in confluent HFF monolayers. Cultures were incubated in D10 medium at 37 °C with 5% CO_2 supplement. All experiments were set by using fresh syringe-released extracellular parasite, unless otherwise specified. Host cells grown as confluent monolayers in standard culture medium in dishes, flasks or plates were infected with *T. gondii* tachyzoites in multiplicity of infection (MOI) of 1.5 and incubated for 40-42 h. Late stage cultures with mature parasite vacuoles were washed with PBS to eliminate extracellular parasites and host debris. Cells were scraped in fresh medium and mechanically extruded through 27G syringe (2x) followed by filter-passing (5 µm) to eliminate host cell debris. Eventually, number of extracellular parasites were counted using Neubauer counting chamber after an appropriate dilution in medium.

2.4.3 Transfection of *T. gondii* tachyzoites

To make transgenic lines, fresh egressed or syringe released parasites (10-20x10^6) were washed with PBS, pelleted by centrifugation at 420xg for 10 min and suspended in filter-sterile cytomix (100 µl) supplemented with fresh ATP (2 µM) and glutathione (5 µM). After adding 15 µg of circular or linearized vector, parasite suspension was transferred into an electroporation cuvette followed by transfection of tachyzoites using the Amaxa Nucleofector electroporator (T-016 program; voltage, 1700 V; resistance, 50 Ω; pulse duration, 176 µs; number of pulses, 2; interval, 100 ms; polarity, unipolar). Transfection mixture was then swiftly transfused to a dish containing an HFF monolayer. The medium was changed to fresh D10 8-16 h post-transfection to eliminate dead parasite and remaining transfection reagents. Drug selection was performed depending on the selection cassette introduced into expression vector. Transgenic parasites expressing HXGPRT (hypoxanthine phosphoribosyltransferase) selection cassette were selected with mycophenolic acid (MPA, 25 µg/ml) and xanthine (50 µg/ml) (57). On the other hand, 6-thioxanthine was used for negative selection of HXGPRT cassette (162). Similarly, for DHFR/TS (dihydrofolate reductase/thymidylate synthase) and UPRT (uracil phosphoribosyltransferase) selectable markers, 1 µM pyrimethamine (56) and 5 µM FudR (58) were added into the cultures, respectively. MPA + xanthine and pyrimethamine selections were applied 24 h post-transfection, while 6-thioxanthine treatment was done after first passage (~48 h post-transfection). For FudR selection, parasites were maintained in D10 medium ~96 h (two

passages) prior to drug selection. Transfected and drug-selected cultures were kept in the same dish until having a stable pool, which usually takes 7-15 days.

2.4.4 Making of clonal transgenic lines

Stable and drug-resistant transgenic parasite cultures were then subjected to limiting dilution in 96-well plates with confluent HFF cells to obtain single clonal lines. 1000 parasites were diluted in 1 ml of D10 medium containing selection. The first columns of 96-well plate were infected with 100 µl of parasite suspension (100 parasites) followed by sequential 1:2 dilutions until sixth well. Afterwards, plate was kept at 37 °C in 5% CO_2 containing incubator for 7 days without any movement. Wells containing single plaques were selected from the plate and transferred into 24-well plate for further analysis and future assays.

2.5 Methods – Lytic cycle assays

All assays were set up essentially with fresh syringed-released parasites as described in section 2.4.2.

2.5.1 Plaque assay

HFF monolayers grown in 6-well plates were infected with extracellular tachyzoites (150 parasites/well) and incubated for 7 days without perturbation (37 °C, 5% CO_2). Cultures were fixed with ice-cold methanol (-80°C, 10 min) after removing media and stained with crystal violet solution (12.5 g dye in 125 ml ethanol mixed with 500 ml 1% ammonium oxalate) for 15 min followed by washing with PBS. Plaque numbers of each strains were counted under an inverted microscope (Leica), and plaque sizes of all single plaques were measured by using ImageJ software (NIH, USA).

2.5.2 Replication assay

In order to check replication rate of parasites, host cells grown on glass coverslips placed in 24-well plate were infected with $3x10^4$ parasites and incubated 24 h and 40 h before fixation with 4% PFA. Following permeabilization, neutralization, blocking and immunostaining steps with α-*Tg*Gap45(1:8.000) and Alexa594 antibodies were performed

the same as explained in section 2.6.1 for indirect immunofluorescence assay. The cell division was assessed by enumerating parasite numbers replicating in their vacuoles.

2.5.3 Motility assay

To measure the gliding motility, $4x10^5$ freshly syringe-released parasites were suspended in calcium-free Hank's balanced salt solution (HBSS) with or without drug treatment (BIPPO, 55 µM; zaprinast, 500 µM; compound 2, 2 µM). Parasites were incubated at room temperature for 15 min to let them settle down before gliding on BSA-coated (0.01%) coverslips (37 °C, 15 min). Afterwards, parasite samples were fixed with 4% PFA and subjected to standard IFA protocol using α-*Tg*Sag1 (1:10.000) and Alexa488 antibodies, as mentioned in 2.6.1. Motile fractions were counted on the microscope, and trail lengths were quantified by using the ImageJ software.

2.5.4 Invasion and egress assays

For invasion and egress assays, host-cell monolayers cultured on glass coverslips were infected with MOI: 10 for 1 h, or with MOI: 1 for 40, 48 and 64 h, respectively. The effect of BIPPO (55 µM), zaprinast (500 µM) and compound 2 (2 µM) treatments on the invasion rate of parasites were tested over the 1 h incubation time, while samples were treated with aforementioned drugs only for 5 min 30 sec 40 h post-infection to observe the change of egress profile. After incubation, cells were fixed with 4% PFA for 15 min, neutralized by 0.1 M glycine/PBS for 5 min, and then blocked in 3% BSA/PBS for 30 min. Afterwards, non-invading parasites or egressed vacuoles were stained with α-*Tg*Sag1 antibody (mouse, 1:10.000, 1 h) prior to detergent permeabilization. Cultures were washed 3x with PBS, permeabilized with 0.2% Triton-X 100/PBS for 20 min, and stained with α-*Tg*Gap45 antibody (rabbit, 1:3.000, 1 h) to visualize intracellular parasites (invaded parasites and intact vacuoles). Samples were then washed with 0.2% Triton-X 100/PBS three times and immunostained with Alexa488 and Alexa594-conjugated antibodies (1:10.000, 1 h). Eventually, the fraction of invaded parasites was counted by immunostaining with α-*Tg*Gap45/Alexa594 (red), but not with α-*Tg*Sag1/Alexa488 (green). The percentage of lysed vacuole on the other hand was scored directly by counting α-*Tg*Sag1/Alexa488 (green) and dual-colored parasites.

2.5.5 Sample collection for cGMP measurements by commercial kit

Confluent HFF monolayers were infected with MOI: 1.3-2 depending on the growth of the *T. gondii* parasite strain and incubated for 40 hours. For sample collection, infected cells containing mature parasite vacuoles were washed twice with ice-cold PBS to eliminate free parasites, scraped by adding 2 ml of colorless DMEM, and extruded through a 27G syringe (2x). Parasite suspension was centrifuged (420x*g*, 10 min, 4°C), and the pellet was then dissolved in 100 µl of cold colorless DMEM for counting of parasites. The parasite number was adjusted to $5x10^6$ in 100 µl volume for cGMP extraction and mixed with 200 µl of ice-cold 0.1 M HCl to lyse the cells (20 min). Samples were then flash-frozen in liquid nitrogen and thawed before they were squirted through pipette to disrupt the parasite membranes. The colorless DMEM and HFF cells, treated similarly, were used as negative controls. Samples were transferred onto centrifugal filters (0.22 µm, Corning Costar Spin-X, CLS8169, Sigma) to eliminate the membrane particulates (20800x*g*, 10 min, 4 °C). The flow-through was filtered once more *via* 10-kDa filter units (Amicon Ultra-0.5 ml filters, Millipore) (20800x*g*, 30 min, 4°C), and samples were subjected to ELISA using the commercial 'Direct cGMP ELISA kit' (ADI-900-014, Enzo Life Sciences) to measure basal cGMP levels of parasites.

2.6 Methods – Biochemical assays

2.6.1 Indirect Immunofluorescence assay (IFA)

Immunofluorescence assay was performed both with intracellular and extracellular parasites. For extracellular parasite staining, fresh egressed tachyzoites were incubated for 20 min on the BSA-coated (0.01%) coverslips. On the other hand, intracellular parasites were stained within confluent monolayers of HFFs grown on glass coverslips (24 h post-infection). Samples were fixed with 4% paraformaldehyde (PFA) for 15 min and neutralized with 0.1 M glycine in PBS for 5 min. In the ongoing process of standard IFA of extra-and intracellular parasites, samples were permeabilized with 0.2% triton-X 100/PBS (20 min), and nonspecific binding was blocked by 2% BSA in 0.2% triton X-100/PBS (20 min). Afterwards, coverslips were stained with specified primary antibodies diluted in 2% BSA in 0.2% triton-X 100/PBS for 1 h. Samples were then washed 3x with 0.2% triton X.100/PBS and incubated with appropriate Alexa488- and 594-conjugated secondary antibodies for 1 h. Following 3x

washing steps with PBS, coverslips were mounted with Fluoromount G including DAPI for nuclei staining and then imaged with Zeiss Apotome microscope (Zeiss, Germany).

To resolve the C-terminal topology of *Tg*ATPase$_P$-GC, about 5x10^4 parasites were released on BSA-coated coverslips, incubated for 20 min and fixed using 4% PFA with 0.05% glutaraldehyde. Samples were stained either with the combination of rabbit α-HA (1:200) and mouse α-*Tg*Sag1 (1:10.000) antibodies or with rabbit α-*Tg*Gap45 (1:3.000) and mouse α-*Tg*Sag1 (1:10.000) before and after permeabilization. Permeabilized cells were subjected to immunostaining as indicated above, while all solutions were substituted to PBS for non-permeabilized staining (*i.e.* no detergent triton X-100 and BSA). To detect the exact membrane distribution of *Tg*ATPase$_P$-GC, extracellular parasites were treated with α-toxin from *Clostridium septicum* (20 nM) (List Biological Laboratories, USA) for 2 h to separate plasma membrane from inner membrane complex. Subsequently, samples were fixed on BSA-coated coverslips and exposed to standard immunostaining.

2.6.2 SDS-PAGE and immunoblot analysis

Both recombinant proteins of GC1 and GC2 catalytic domains of *Tg*ATPase$_P$-GC purified from *E. coli* M15 strains (5 µg) and probe-sonicated bacterial cell lysates (20 µl) were exposed to SDS-PAGE and following western blot to verify the size and expression of proteins, respectively. Briefly, sample suspensions were mixed with SDS sample buffer (5x) and boiled at 99 °C for 5 min. Samples were then loaded to each lane of 5% stacking gel and separated by 12% resolving gel (120 V, 2 h). Afterwards, proteins were transferred from SDS-gel onto a nitrocellulose membrane by semi-dry blotting (85 mA/cm^2, 2 h). The membrane was blocked with 5% skimmed milk solution prepared in 0.2% tween 20/TBS (1 h with shaking at room temperature or overnight at 4 °C) and then stained with mouse α-6xHis (1:1.000) antibody.

To detect protein expression levels in *T. gondii* tachyzoites, standard western blot protocol was applied. However, dot blot analysis was performed for *Tg*ATPase$_P$-GC-HA$_{3'IT}$ due to its large size (477-kDa). For standard western blot, the protein samples prepared from extracellular parasites (2-3 x10^7) were separated by 8% SDS-PAGE (120 V, 2 h), followed by semi-dry blotting onto a nitrocellulose membrane (85 mA/cm^2, 3 h). The membrane was blocked as described above and stained with appropriate primary antibodies diluted in 0.2%

tween 20/TBS/5% skimmed milk powder. For the dot blot, protein samples equivalent to 10^7 parasites were spotted directly onto nitrocellulose membrane. The membrane was blocked in a solution containing 1% BSA and 0.05% tween 20 in TBS for 1 h, followed by immunostaining with rabbit α-HA (1:1.000) and/or rabbit α-*Tg*Gap45 (1:3.000) antibodies diluted in the same buffer. After primary antibody staining, membranes were washed three times with tween 20/TBS buffer in all cases. Eventually, proteins were visualized by Li-COR imaging after staining with IRDye® 680RD and IRDye® 800CW (1:15.000) antibodies. Densitometric analysis was performed using the Image J software.

2.6.3 cGMP measurement by ELISA-based kits

Parasite samples collected for cGMP measurement were thawed from -80 °C and subjected to ELISA using the commercial 'Direct cGMP ELISA kit' (ADI-900-014, Enzo Life Sciences). The acetylated (2 hours) format of the assay was run for all samples including the standards and controls, as described by manufacturers to increase the sensitivity of kit. Briefly, cGMP standard (5,000 pmol/ml) provided by kit was serially diluted in 0.1 M HCl to prepare standards whose cGMP concentrations range between 50 pmol/ml and 0.08 pmol/ml. Acetylation reagent was prepared by mixing acetic anhydride with trimethylamine at 1:2 (v/v) ratio. As suggested in kit manual, 10 µl of acetylation reagent was added into each 200 µl volume of sample and standard by mixing thoroughly for 5 sec. Following ELISA, cGMP levels of samples were measured at 405 nm absorbance, and the data were analyzed using the microplate analysis tool by adjusting dilution factor to 1:3 (www.myassays.com).

2.6.4 cGMP measurement by High Performance Liquid Chromatography (HPLC)

cGMP production potentials of GC1 and GC2 domains of *Tg*ATPase$_P$-GC, purified from *E. coli* M15 strains or by directly using bacterial lysates, were tested by *in vitro* cyclase assays prior to measurement of cGMP contents by HPLC. Frozen samples were thawed and filtered by 0.22-µm centrifugal filters (Corning Costar Spin-X, Sigma) at 14.000xg for 30 min (4 °C) prior to measurement. 2 mM of GTP and 2 mM of cGMP (final concentration) were resuspended in 0.1 M HCl and used as standards. 200 µl of each sample including standards were prepared for running on HPLC device, and injection volume was adjusted to 20 µl. Nucleotides were separated by HPLC with a C18 reversed phase column (SUPELCOSIL™ LC-18-T, 3 µm particle size, 15 cm × 4.6 mm, Sigma Aldrich) at a flow

rate of 1 ml/min in an eluent buffer containing 100 mM potassium phosphate (pH: 5.9), 4 mM tetra-butylammonium iodide and 10% (v/v) methanol. Analyte elution was recorded *via* absorbance at 260 nm. The peak areas of GTP and cGMP in standard was detected and compared with sample retention times (for GTP ~5 min and for cGMP ~7.5 min, respectively). cGMP and GTP concentrations of samples were quantified by peak analysis in Geneious® 6.1 (Biomatters Ltd., New Zealand).

2.7 Methods – Optogenetic manipulation of *T. gondii*

Optogenetic parasite strains were cultured in standard D10 medium supplemented with appropriate selection in dark conditions by wrapping aluminium foil. Regular passaging of parasites was performed under red light (635 nm) using RGB-LED Strip (Paulmann) installed on the safety cabinet. Before setting an assay, cultures were incubated by adding 1 µM all-trans retinal as chromophore of rhodopsin that makes photo-regulated fusion protein RhoGC sensitive to the light.

2.7.1 Design of 24-well plate illumination device for optogenetic studies

Light activation of RhoGC in *T. gondii* tachyzoites was performed for all functional assays using a 24-well plate compatible illumination device designed specifically for this study by Willi Weber as a bachelor thesis project (HU, Berlin) (Figure 10). Briefly, LEDs with Red-Green-Blue (RGB) light emitting feature (Adafruit Breadboard-friendly RGB Smart NeoPixel), which are in the emission wavelengths of 620-630 nm, 515-530 nm and 465-475 nm, respectively, were placed on the printed circuit board to make a LED-plate. Afterwards, the control unit of LED-plate was assembled. A real time clock module which will ensure the accurate timing of LEDs and an infrared receiver module for the remote actuation of device were integrated into the breadboard. Subsequently, the breadboard with all circuit components was connected to an Arduino Mega 2560 as a micro controller and a LED-plate, which enables data transfer between micro controller and LED-plate (Figure 10A).

The user interface of the software to enter the information of intended illumination pattern and time sequence was developed as a Microsoft Excel sheet (Figure 10B), that allows to adjust the light intensity and exposure time of each well individually. Because information transfer size between software and Arduino micro controller is limited to 8 bit data, it is not

possible to transfer light intensity values more than 256 µW/cm². Thus, excel configuration file of software was constructed using assigned digital values represented in Appendix 1 instead of real light intensity values. In order to activate RhoGC, the 24-well specific LED-device program was set at green light (530 nm) with 197,4 µW/cm² intensity (adjusted to 250 as digital value) for 5 min illumination as depicted in Figure 10B for all assays. The excel configuration file is processed by clicking "Run Script" button, which transfers the configuration to the micro controller. Bottom light illumination was performed by placing 24-well plates on the LED-device. Black wall glass bottom plates (IBL Baustoff + Labor GmbH, Austria) were used in order to prevent neighbor wells from light scattering during all functional assays.

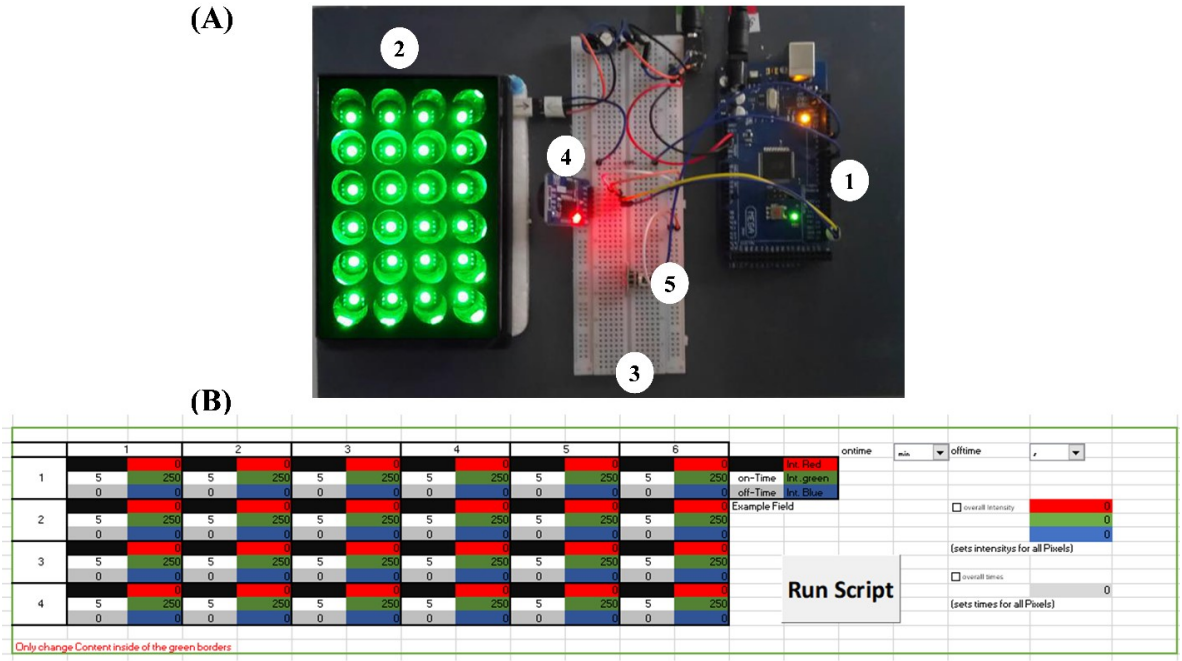

Figure 10. 24-well plate compatible LED-device used for optogenetic assays. A) The set-up of 24-well illumination device including important circuit components. 1-Arduino Mega 2560 as micro controller; 2-LED-plate containing 24 Red-Green-Blue (RGB) Smart NeoPixel LEDs in 620-630 nm, 515-530 nm and 465-475 nm emission wavelengths, respectively; 3-Breadboard; 4-Real time clock module; 5-Infrared receiver module to remote control. **B)** Graphical user interface. An excel script was used for programming illumination device with an intended light colour, intensity and period. During this study, green light (530 nm) exposure was performed for 5 min with 197,4 µW/cm² intensity by adjusting digital values to 250 as shown on the script. (designed by Willi Weber, within the scope of bachelor thesis, HU, Berlin)

2.7.2 Lytic cycle assays

Cell culture dishes were infected with optogenetic parasite strains (MOI:1.5) and incubated 40 h by adding 1 µM of retinal and 0.5 µM of Shield1 (if required). Cultures were scraped and syringe-released in 2 ml of colorless DMEM media to extrude parasites as described in section 2.4.2. Subsequently, functional assays were set in black wall glass

bottom 24-well plates. For all assays, dark samples were kept in a separate plate to secure their protection from light exposure. In order to set motility assay, 40 µl of parasite suspension (including ~$8x10^5$ parasites) was diluted in 1 ml of HBSS buffer containing 1 µM retinal and released immediately on two BSA-coated (0.01%) coverslips (500 µl in each) in separate black wall plates (for dark and light samples). Plates were then centrifuged at 420xg for 5 min at 37 °C to settle parasites down. Afterwards, one plate was kept in the dark by covering with aluminium foil, and the other was exposed to the green light (530 nm) for 5 min. Subsequently, both plates were incubated for 15 min at 37 °C to let them glide on coverslips. Standard motility assay protocol was followed after sample fixation with 4% PFA as explained in section 2.5.3.

For invasion assay, $2x10^6$ parasites were diluted in 1 ml of colorless DMEM medium including 1 µM retinal and 0.5 µM of Shield1 (if required). 10^6 parasites diluted in 500 µl of colorless DMEM was used to infect a HFF-monolayer grown on glass coverslip in dark and light conditions. Both samples in two conditions were incubated for 15 min at 37 °C to let them invade host cells following light illumination. On the other hand, tachyzoite infected HFF-monolayers ($5x10^4$, 24 h) cultured on glass coverslips were either kept in the dark or exposed to the light (530 nm, 5 min) after medium replacement with colorless DMEM supplemented by 1 µM of retinal and 0.5 µM of Shield1 (if required) to examine egress profile of parasites in response to light. Coverslips were fixed with 4% PFA after 15 min incubation (37 °C, 5% CO_2). The following protocol procedures both for egress and invasion assays were applied as stated in subtitle 2.5.4.

2.7.3 Sample collection and cGMP measurement by ELISA-based kit

As described in section 2.5.5, HFF monolayers grown in dishes were infected with optogenetic *T. gondii* parasite strains (MOI:1.5) and incubated for 40 hours by including 1 µM retinal and 0.5 µM of Shield1 (if required) into the culture medium. For sample collection, dishes containing mature parasite vacuoles were washed twice with PBS, scraped in 2 ml of colorless DMEM and filter-passed (5 µm) following syringe-release (2x27G). Parasite numbers were adjusted to $2.5x10^6$ in 100 µl of colorless DMEM for each sample. Dark samples were always kept in the dark by covering with aluminium foil. Other samples were exposed to the green light (530 nm, 197,4 µW/cm² intensity) for specified time periods. Afterwards, 100 µl of sample diluent supplemented by 'DetectX High Sensitivity Direct cGMP' kit (K020-C1, Arbor Assays) was applied (at RT for 10 min) directly onto the samples

to quench the reaction and lyse the parasites. Samples were then centrifuged (2000xg, 15 min, 4 °C), and supernatants were either assayed directly following kit instructions to measure cGMP levels or frozen at -80 °C until measurement. Luminescence of each well was read in chemiluminescent mode using a 0.1 sec read time per well. The obtained data was subsequently analyzed by the help of online web tool (www.myassays.com).

2.8 Structure modelling

The membrane topology of *Tg*ATPase$_P$-GC and *Tg*PKG was predicted according to the data obtained from TMHMM (163), SMART (164), Phobius (165), NCBI conserved domain search (166) and TMpred (167). To detect conserved residues of active sites in *Tg*ATPase$_P$-GC, GC1 and GC2 regions were aligned with the cyclase domains of representative organisms using Clustal Omega program (https://www.ebi.ac.uk/Tools/msa/clustalo/) (168). Similarly, conserved motifs in the ATPase domain of *Tg*ATPase$_P$-GC were obtained by alignment with members of human P4-ATPases using MAFFT online alignment server (v7) (169). Conserved residues were color-coded by the Clustal Omega program.

The conserved motifs and cyclase domains for the tertiary model were predicted using UniProt (https://www.uniprot.org/). The catalytic units of GC1 (aa 2929-3200, lacking the loop from aa 3038 to 3103) and GC2 (aa 3989-4195) were modeled by SWISS-MODEL (https://swissmodel.expasy.org/), based on a ligand-free tmAC as the structural template (UniProt ID: 1AZS). The Qualitative Model Energy ANalysis (QMEAN) and the Global Model Quality Estimation (GMQE) scores were determined as -3.44 and 0.59 respectively, reflecting the accuracy of the model. Subsequently, the ligand GTPαS was positioned into the model of pseudo-heterodimer corresponding to the location of ATPαS in tmAC (Protein Data Bank ID: 1CJK).

2.9 Phylogenetic analysis

The open reading frame sequences of *Tg*ATPase$_P$-GC orthologs were obtained from the NCBI database. Briefly, the whole sequences of 30 proteins were aligned, and a consensus tree was generated using the CLC Genomics Workbench v12.0 (Qiagen Bioinformatics). Maximum likelihood method was utilized for clustering; bootstrap analysis was performed with 100 iterations; neighborhood joining was used for construction; and JJT model was

selected for amino acid substitutions. The eventual tree was visualized as a cladogram by Figtree v1.4.3, followed by text annotation in the Microsoft PowerPoint.

2.10 Data analysis and statistics

All experiments were performed at least three independent times, unless otherwise specified. Figures illustrating images or transgenic strains typically show a representative of three biological replicates. Graphs and statistical significance were generated using GraphPad Prism v6.0. The error bars in graphs represent means with S.E.M. from multiple assays, as indicated in figure legends. The p-values were calculated by Student's t-test (*, $p \leq 0.05$; **, $p \leq 0.01$; ***, $p \leq 0.001$; ****, $p \leq 0.0001$).

3 Results

3.1 The native cGMP signaling mediators of *T. gondii*

The genome searches identified a single putative guanylate cyclase and a corresponding protein kinase G in the parasite database (ToxoDB) (50) as the main cGMP signaling mediators (Table 2). Besides, 18 cNMP-dependent phosphodiesterases were detected in the *Toxoplasma* genome; however, they were excluded from the scope of this study. Sequence analysis revealed that *T. gondii* guanylate cyclase comprises multiple P-type ATPase like domains at its N-terminus and two nucleotide cyclase catalytic regions (termed as GC1 and GC2 based on the evidence herein, see section 3.1.1.2) at the C-terminus. It was named as *Tg*ATPase$_P$-GC in this study given the predicted multi-functionality of this protein. The entire gene size of *Tg*ATPase$_P$-GC is about 38.3-kb, consisting of 53 introns and 54 exons. On the other hand, cGMP-specific protein kinase (*Tg*PKG) is composed of four ligand-binding domains at the N-terminal and a kinase domain at its C-terminal. The gene size is 15-kb containing 19 introns and 20 exons (Table 2). *Tg*PKG has been characterized extensively in an earlier work (72). This thesis primarily focused on *Tg*ATPase$_P$-GC.

Table 2. The features of cGMP signaling mediators of *T. gondii* worked in this study (Resource: ToxoDB)

ToxoDB accession no.	Gene description	Gene size (bp)	Protein length (aa)	Phenotype score (log2) by CRISPR assay	Abbreviations used in this study
TGGT1_254370	Guanylate cyclase	38286	4367	-3.56	***Tg*ATPase$_P$-GC**
TGGT1_311360	Protein kinase G	15055	994	-2.18	***Tg*PKG**

3.1.1 An alveolate-specific guanylate cyclase conjugated to P-type ATPase

A variety of *in silico* tools were applied to get functional insight into *Tg*ATPase$_P$-GC as described in sections 2.8 and 2.9. The open reading frame of *Tg*ATPase$_P$-GC encodes for a remarkably large protein (4367 aa, 477-kDa), including multiple P-type ATPase motifs (270-kDa) and nucleotide cyclase domains (207-kDa) with 22 transmembrane helices (Figure 11A and B). The first half of this huge protein (1-2480 aa) contains 10 α-helices and 4 conserved ATPase-like subdomains: (a) the region from Lys^{110} to His^{174} encodes a lipid-translocating ATPase; (b) the residues from Leu^{207} to Gly^{496} are predicted to form a

bifunctional E1-E2 ATPase binding to both metal ions and ATP, and thus functioning like a cation-ATPase; (c) the amino acids from Thr[1647] to Ser[1748] harbor yet another metal-cation transporter with an ATP-binding region; (d) the subdomain from Cys[2029] to Asn[2480] contains a haloacid dehalogenase-like (HAD-like) hydrolase, or otherwise a second lipid-translocating ATPase (Figure 11A).

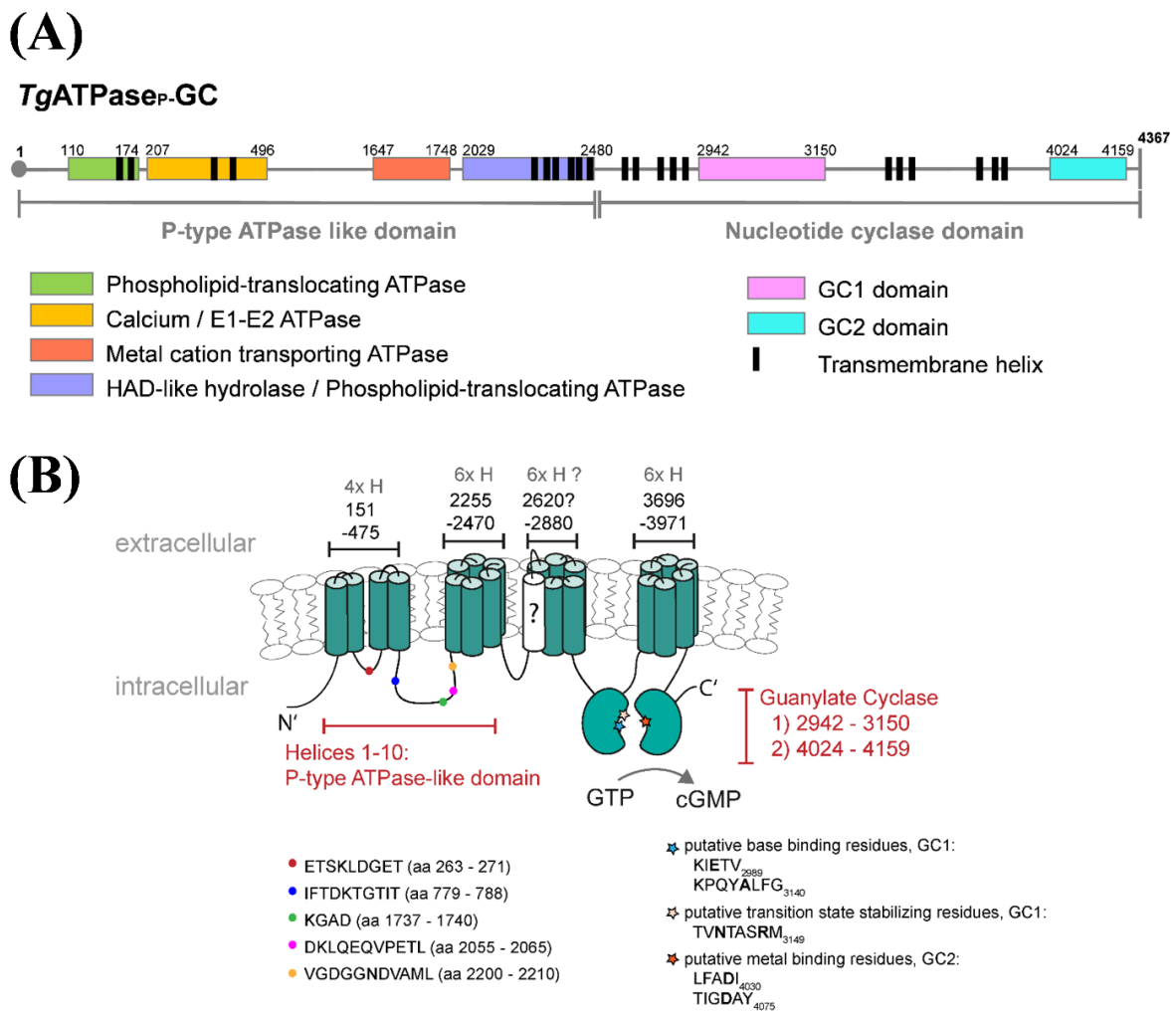

Figure 11. The genome of *T. gondii* harbors an unusual guanylate cyclase conjugated to P-type ATPase-like structures. **(A-B)** The primary and secondary topology of *Tg*ATPase$_P$-GC were predicted using TMHMM, SMART, TMpred, Phobius and NCBI domain search tools. The model was constructed by consensus across algorithms regarding the position of domains and transmembrane spans. The N-terminal (1-2480 aa) containing 10 α-helices resembles P-type ATPase with at least four domains (color-coded). The C-terminal (2481-4367 aa) harbors two potential nucleotide cyclase catalytic regions, termed GC1 and GC2, each follows 6 transmembrane helices. The question-marked (?) helix was predicted only by Phobius tool (probability score, 752). **(B)** To detect conserved residues of the active sites and ATPases in *Tg*ATPase$_P$-GC, sequence alignment was performed using Clustal Omega program. The color-coded signs on secondary structure show the position of highly conserved sequences in the ATPase and cyclase domains. The key residues involved in the base binding and catalysis of cyclases are also depicted in bold letters (Structure model in B was drawn with the help of Ulrike Scheib, Humboldt University of Berlin).

The second half of *Tg*ATPase$_P$-GC (2481-4367 aa) includes a potential guanylate cyclase comprising GC1 and GC2 domains from Ser^{2942}-Lys^{3150} and Thr^{4024}-Glu^{4159} residues, respectively (Figure 11A). Both GC1 and GC2 follow a transmembrane region, each with six helices. The question-marked helix (2620-2638 aa) antecedent to GC1 has been detected with low probability (score, 752) (Figure 11B). An exclusion of this helix from the envisaged model however results in a reversal of GC1 and GC2 topology (facing outside the parasite), which is unlikely given the intracellular transduction of cGMP signaling *via* *Tg*PKG. Moreover, our experimental outcomes suggest that C-terminal of *Tg*ATPase$_P$-GC faces inwards (see figure 15B). Phylogenetic study performed by entire protein sequence of 30 different guanylate cyclases from several organisms indicated an evident clading of *Tg*ATPase$_P$-GC with homologs from parasitic (*Hammondia, Eimeria*, *Plasmodium*) and free-living (*Tetrahymena*, *Paramecium*, *Oxytricha*) alveolates (Figure 12). In contrast, GCs from the metazoan organisms (soluble and receptor-type) and plants formed their own distinct clusters. Quite intriguingly, the protist clade contained two groups, one each for apicomplexans and ciliates, implying a phylum-specific evolution of *Tg*ATPase$_P$-GC orthologous.

3.1.1.1 P-type ATPase domain of *Tg*ATPase$_P$-GC resembles to P4-ATPases

The N-terminal of *Tg*ATPase$_P$-GC covering 10 transmembrane helices (TM) and 4 conserved motifs is comparable to P4-ATPases, a subfamily of P-type ATPases involved in translocation of phospholipids across the membrane bilayer and vesicle trafficking in the secretory pathways (170,171). The human genome contains 14 different genes for P4-ATPases clustered in 5 classes (1a, 1b, 2, 5, 6), all of which have five functionally distinct domains (170). A-(actuator), N-(nucleotide binding), and P-(phosphorylation) domains are cytoplasmic; whereas T-(transport) and S-(class-specific support) domains are membrane-anchored. Besides, a regulatory (R-) domain usually exists either at the N- or C-terminal or at both ends (171). In mammalian orthologs, the region between TM1-TM6 constitutes a functional unit for lipid flipping, and the segment between TM7-TM10 undertakes a supportive role. ATPases have an intrinsic kinase activity to phosphorylate itself at the aspartate residue located in the P-domain while catalytic cycle is taking place, and later it gets dephosphorylated by A-domain when transportation is terminated (171,172). The phosphorylated Asp located in Asp-Lys-Thr-Gly (DKTG) sequence is highly conserved in P-type ATPases. The consensus residue region has been formulized as

DKTG[T/S][L/I/V/M][T/I]. The A-domain has Asp-Gly-Glu-Thr (DGET), P4-ATPase-specific signature residues that facilitate dephosphorylation (173).

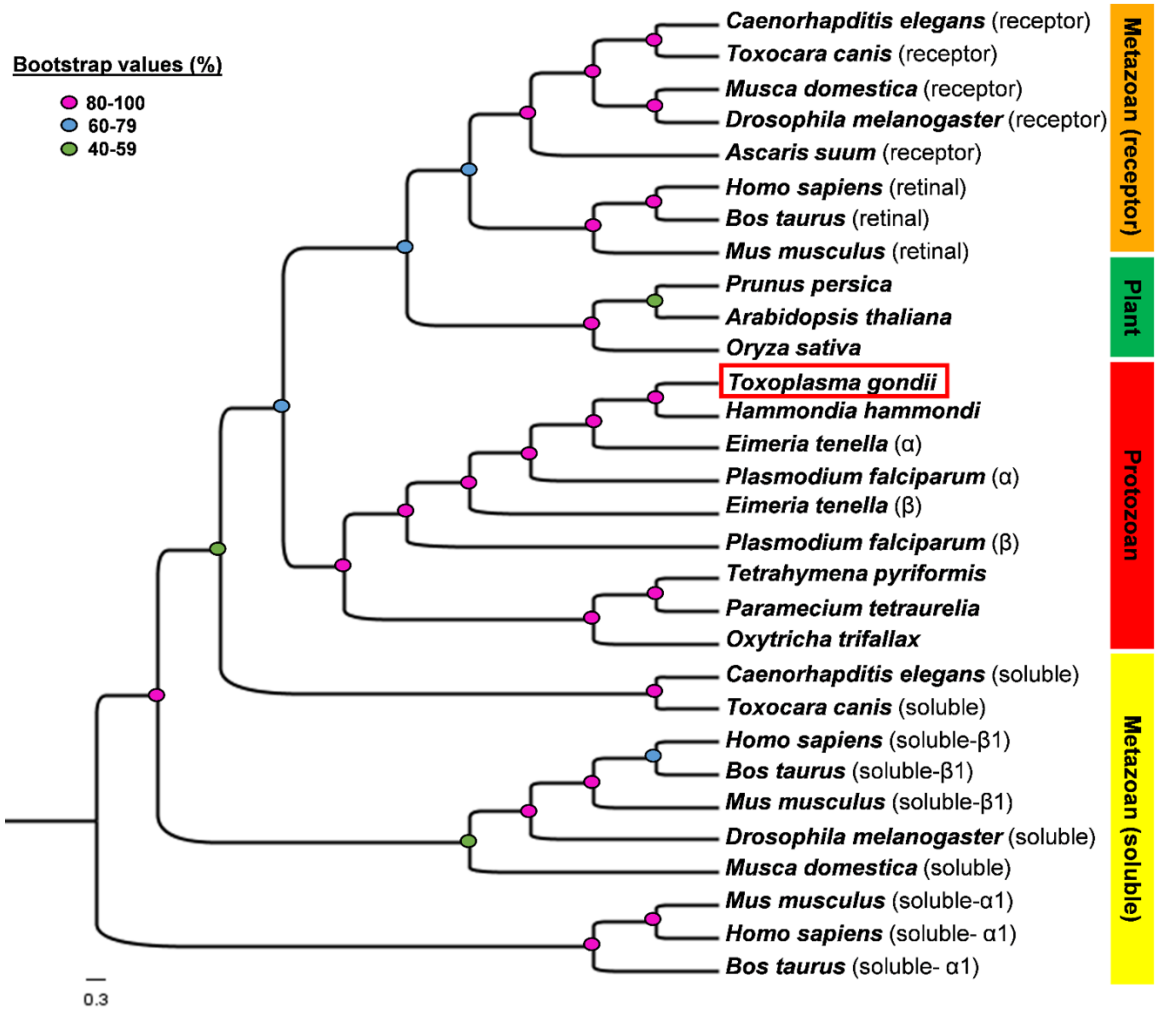

Figure 12. Phylogenetic analysis reveals a protozoan-specific clading of *Tg*ATPase$_P$-GC. The tree shows the evolutionary relationship of *Tg*ATPase$_P$-GC from *T. gondii* with respective orthologs from various organisms signifying various domains of life. The image represents a single most parsimonious cladogram generated by maximum likelihood method. Sequence alignment and construction of the tree were performed by CLC Genomics Workbench v12.0, followed by visualization using Figtree v1.4.3. The colored dots on branching nodes show the bootstrap values. NCBI accession numbers of proteins: *Arabidopsis thaliana*, AAM51559.1; *Ascaris suum* (receptor-type), ERG86823.1; *Bos taurus* (retinal-type) NP_776973.2; *Bos taurus* (soluble α1-subunit), P19687.1; *Bos taurus* (soluble β1-subunit), P16068.1; *Caenorhabditis elegans* (receptor-type), NP_494995.2; *Caenorhabditis elegans* (soluble), NP_510557.3; *Drosophila melanogaster* (receptor-type), AAA85858.1; *Drosophila melanogaster* (soluble β-subunit), NP_524603.2; *Eimeria tenella* (soluble α), XP_013229212.1; *Eimeria tenella* (particulate β), XP_013235760.1; *Hammondia hammondi*, XP_008885058.1; *Homo sapiens* (retinal-type), NP_000171.1; *Homo sapiens* (soluble α1-subunit), NP_001124157.1; *Homo sapiens* (soluble β1-subunit), NP_001278880.1; *Musca domestica* (receptor-type), XP_005177218.1; *Musca domestica* (soluble), XP_019895151.1; *Mus musculus* (retinal-type), NP_001007577.1; *Mus musculus* (soluble α1-subunit), AAG17446.1; *Mus musculus* (soluble β1-subunit), AAG17447.1; *Oryza sativa*, ABD18448.1; *Oxytricha trifallax*, EJY85073.1; *Paramecium tetraurelia*, XP_001346995.1; *Plasmodium falciparum* (soluble α), AJ245435.1; *Plasmodium falciparum* (particulate β), AJ249165.1; *Prunus persica*, AGN29346.1; *Tetrahymena pyriformis*, AJ238858.1; *Toxoplasma gondii*, EPR59074.1; *Toxocara canis* (receptor-type), KHN81453.1; *Toxocara canis* (soluble), KHN85312.1.

Besides, two other conserved sequences, Thr-Gly-Asp-Asn (TGDN) and Gly-Asp-Gly-x-Asn-Asp (GDGxND), are located in the P-domain that bind Mg^{2+} and connect ATP-binding region to the transmembrane segments (173). T-domain includes the ion-binding site, which has a conserved proline in Pro-Glu-Gly-Leu (PEGL) sequence located usually between TM4 and TM5 (170).

The alignment of ATPase domains from *Tg*ATPase$_P$-GC, *Pf*GCα and *Pf*GCβ with five different members of human P4-ATPases revealed several conserved residues (Appendix 2). For example, the second subdomain of *Tg*ATPase$_P$-GC (defined as Ca^{2+}-ATPase, yellow colored in Figure 11A) carries DGET signature of A-domain albeit with one altered residue in the region (ETS**K**LDGET instead of ETSNLDGET). *Pf*GCα contains two amino acid mutations in the same region (ETS**L**LN**N**GET) when compared to the human ATP8A1, which translocates phosphatidylserine as its main substrate (174). Another replacement (Ser to Thr^{781}) was observed both in *Tg*ATPase$_P$-GC and *Pf*GCα at the IF**T**DKTGTIT motif, which harbors the consensus phosphorylated aspartate residue (D) in P-domain. The nucleotide binding sequence KGAD in N-domain (third region indicated as cation-ATPase) – the most conserved signature among P4-ATPases – is preserved in *Tg*ATPase$_P$-GC but substituted by a point mutation in *Pf*GCα (Ala to Ser^{1739}, KG**S**D). Additional mutation (D to E) was detected in the DKLQ**E**QVPETL sequence located in the last ATPase subdomain of *Tg*ATPase$_P$-GC (highlighted with blue in Figure 11A). Not least, the GDGxND signature is conserved in *Tg*ATPase$_P$-GC but degenerated in *Pf*GCα (Appendix 2). Notably most signature residues could not be identified in *Pf*GCβ, which signifies a degenerated ATPase domain. Taken together, *in silico* analysis suggests that N-terminal ATPase domain of *Tg*ATPase$_P$-GC belongs to the P4-ATPase subfamily, and thus it is likely involved in lipid translocation.

3.1.1.2 GC1 and GC2 domains of *Tg*ATPase$_P$-GC form a pseudo-heterodimer

The arrangement and architecture of GC1 and GC2 domains in *Tg*ATPase$_P$-GC correspond to mammalian transmembrane adenylate cyclase (tmAC) of the class III (89). tmACs are activated by G-proteins to produce cAMP following extracellular stimuli (*e.g.,* hormones). The cyclase domains of tmACs, C1 and C2, form an antiparallel pseudo-heterodimer with one active and one degenerated site at the dimer interface (89). Amino acids from both domains contribute to the binding site, and seven conserved residues were identified to play essential roles for nucleotide binding and catalysis (89,175,176). These include two aspartate residues which bind two divalent metal cofactors (Mg^{+2}, Mn^{+2}) crucial

for substrate placement and turnover. An arginine and asparagine stabilize the transition state, while another arginine binds the terminal phosphate (Pγ) of the nucleotide. A lysine/aspartate pair underlies the selection of ATP over GTP as the substrate. In contrast, the existence of a glutamate/cysteine or glutamate/alanine pair defines the substrate as GTP in guanylate cyclases. The nucleotide binding and transition-state stabilization are conferred by one domain, while the other domain directly or *via* bound metal ions interacts with the terminal phosphate of the nucleotide in tmACs (175-177).

The sequence alignment of GC1 and GC2 domains from *Tg*ATPase$_P$-GC to their orthologous GCs/ACs (Appendix 3) showed that GC1 contains a 74-residues long loop insertion (3033-3107 aa) unlike other cyclases. A shorter insertion (~40 amino acids) was also found in *Pf*GCα. The tertiary model structure (depleted for the loop inserted between α3 and β4 of GC1) shows that both domains consist of a seven-stranded β-sheets surrounded by three helices (Appendix 3, Figure 13B). The key functional amino acid residues with some notable substitutions could be identified as distributed across GC1 and GC2 (Figure 13). In GC1 domain, one of the two metal binding (Me) aspartates is replaced by glutamate (E2991), while both are conserved in GC2 (D4029 and D4073) (Figure 13A-C). The transition-state stabilizing (Tr) asparagine (N3144) and arginine (R3148) residues are located within GC1 domain (Figure 13A-C), however both are replaced by leucine (L4153) and methionine (M4157), respectively in GC2 motif (Figure 13A). Another arginine (R4125) that is responsible for phosphate binding (Pγ) in tmACs is conserved in the GC2 domain (Figure 13A-C), whereas it is substituted by K3116 in GC1 (Figure 13A).

The cyclase specificity defining residues (B) are glutamate/alanine (E2987/A3137) and cysteine/aspartate (C4069/D4146) pairs in GC1 and GC2, respectively (Figure 13A-C). The E/A identity of the nucleotide binding pair in GC1 is indicative of specificity towards GTP. Thus, we propose that GC1 and GC2 form a pseudo-heterodimer and function as a guanylate cyclase (Figure 13A). Similar to tmACs, one catalytically active and one degenerated site are allocated at the dimer interface to make *Tg*ATPase$_P$-GC functional. However, the sequence of GC1 and GC2 is inverted in *Tg*ATPase$_P$-GC, which means that, unlike tmAC, GC1 domain contributes to the nucleotide and transition state binding residues of the active site, whilst GC2 harbors two aspartates crucial for metal ion binding. Guanylate cyclase function of *Tg*ATPase$_P$-GC was also experimentally validated by showing the involvement in cGMP synthesis by mutagenesis studies in parasite tachyzoites (see section 3.1.4.2).

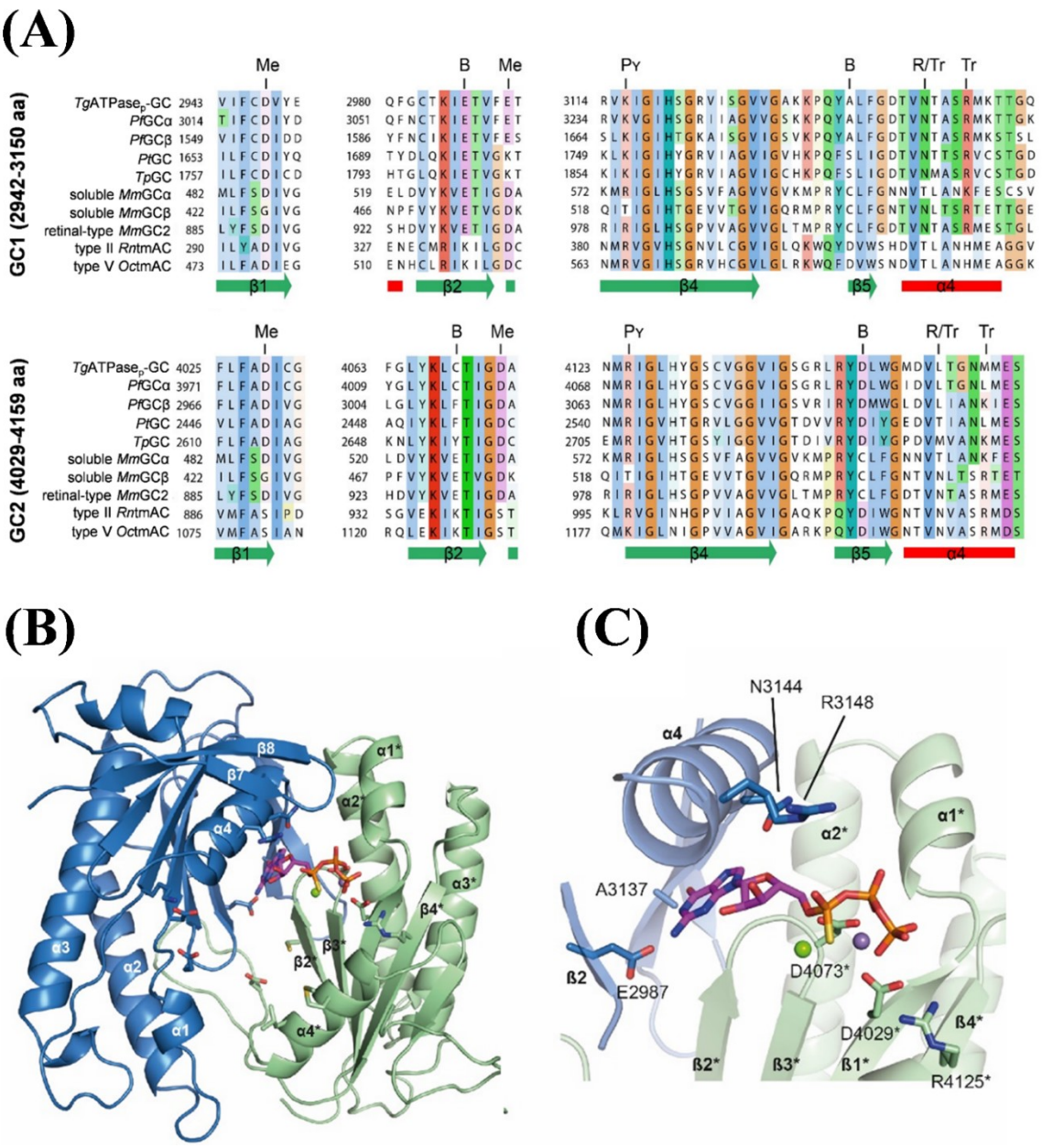

Figure 13. The sequence alignment of GC1 and GC2 domains from *Tg*ATPase$_P$-GC with other cyclases identifies signature residues. **(A)** Amino acid sequences were obtained from Uniprot and aligned with the Clustal Omega program. Only conserved residues containing regions were shown in the figure with color-codes. (See full-length sequence alignment in appendix 3). The secondary α-β structures depicted underneath the alignment correspond to transmembrane type III adenylate cyclases (tmAC) (UniProt-Protein Data Bank ID: 1AZS, *Oryctolagus cuniculus* for GC1, *Rattus norvegicus* for GC2; DSSP hydrogen bond estimation algorithm). In type III cyclases, 7 residues are involved in cofactor binding for the catalysis, which are indicated above in the alignments as 'Me' for metal, 'B' for base, 'Pγ' for phosphate, 'R' for ribose, and 'Tr' for transition state binding. Note that alignment of GC1 and GC2 domains from *Tg*ATPase$_P$-GC to their orthologous GCs/ACs showed that, unlike other cyclases, a 74-residues long segment (3033-3107 aa) is inserted between α3 and β4 of GC1 (not shown). Organism abbreviations and accession numbers: *Tg*ATPase$_P$-GC, *Toxoplasma gondii* (Uniprot; S7VVK4); *Pf*GCα, *Plasmodium falciparum* (AJ245435.1); *Pf*GCβ, *P. falciparum* (AJ249165.1); *Pt*GC, *Paramecium tetraurelia* (XP_001346995.1; *Tp*GC, *Tetrahymena pyriformis* (AJ238858.1); soluble *Mm*GCα, *Mus musculus* (AAG17446.1); soluble *Mm*GCβ, *M. musculus* (AAG17447.1); retinal-type *Mm*GC2, *M. musculus* (NP_001007577.1); type II *Rn*tmAC, *Rattus norvegicus* (P26769.1) and; type V *Oc*tmAC, *Oryctolagus cuniculus* (CAA82562.1). **(B-C)** Tertiary structure of GC1 and GC2 domains based on sequence alignment. The catalytic units of GC1 and

GC2 were modelled by SWISS-MODEL (https://swissmodel.expasy.org/) using a ligand-free tmAC as the structural template (UniProt ID: 1AZS). The ribbon diagrams of GC1 and GC2 suggest a functional activation by pseudo-heterodimerization similar to transmembrane adenylate cyclases (tmACs). The model shows an antiparallel arrangement of GC1 and GC2, where each domain harbors a 7-stranded β-sheet surrounded by 3 α-helices. The image in *panel C* illustrates a GC1-GC2 heterodimer interface bound to GTPαS. The residues of GC2 labelled with asterisk (*) interact with the phosphate backbone of the nucleotide.

3.1.1.3 Overexpression and purification of recombinant GC1 and GC2 domains

With an objective to determine the functionality of *Tg*ATPase$_P$-GC, we expressed ORFs of GC1 (M^{2850}-S^{3244}), GC2 (M^{3934}-Q^{4242}) and GC1+GC2 (M^{2850}-Q^{4242}) in *E. coli* (Figure 14A). Transgenic bacterial strains showed expected 1185, 927 and 4176 bp ORF-specific PCR-bands for GC1, GC2 and GC1+GC2 domains, respectively, by PCR screening (Figure 14B). Positive clones were further verified by sequencing of PCR amplicons. An overexpression of GC1 and GC2 proteins as 6xHis-tagged in the M15 strain resulted in inclusion bodies, which did not allow us to use native conditions in order to purify proteins. We nevertheless purified them through a Ni-NTA column under denaturing conditions. Purified GC1 and GC2 proteins exhibited an expected molecular weight of 47 and 38-kDa, respectively (Figure 14C). Our attempts to purify GC1+GC2 protein were futile however. To test the catalytic activity of purified GC1 and GC2 domains, we executed an *in vitro* guanylate cyclase assay. Neither for GC1 nor for GC2 any functionality was detected when tested separately or together. Further optimization of protein purification process yielded no detectable GC activity. By considering the possibility of obtaining misfolded or unfolded purified proteins, the guanylate cyclase assay was repeated with bacterial lysates expressing specified domains (Appendix 4A); yet, no cGMP production was observed either as judged by HPLC (Appendix 4B).

Furthermore, it was examined whether GC1 and GC2 can function as adenylate cyclase using a bacterial complementation assay, as described by Karimova *et al*. (161) (Figure 14D). GC1, GC2 and GC1+GC2 proteins were expressed in the BTH101 strain of *E. coli*, which is deficient in the adenylate cyclase activity and so unable to utilize maltose as a carbon source. The BTH101 strain produced white colonies on MacConkey agar containing maltose, which would otherwise be red-colored upon induction of cAMP-dependent disaccharide catabolism. It was observed that, unlike the positive control (adenylate cyclase from *E. coli*), BTH101 strains expressing GC1, GC2 or GC1+GC2 produced only white colonies in each case (Figure 14D), which could either be attributed to inefficient expression

or a lack of adenylate cyclase activity in accordance with the presence of signature residues defining the specificity for GTP in indicated domains (Figure 13A).

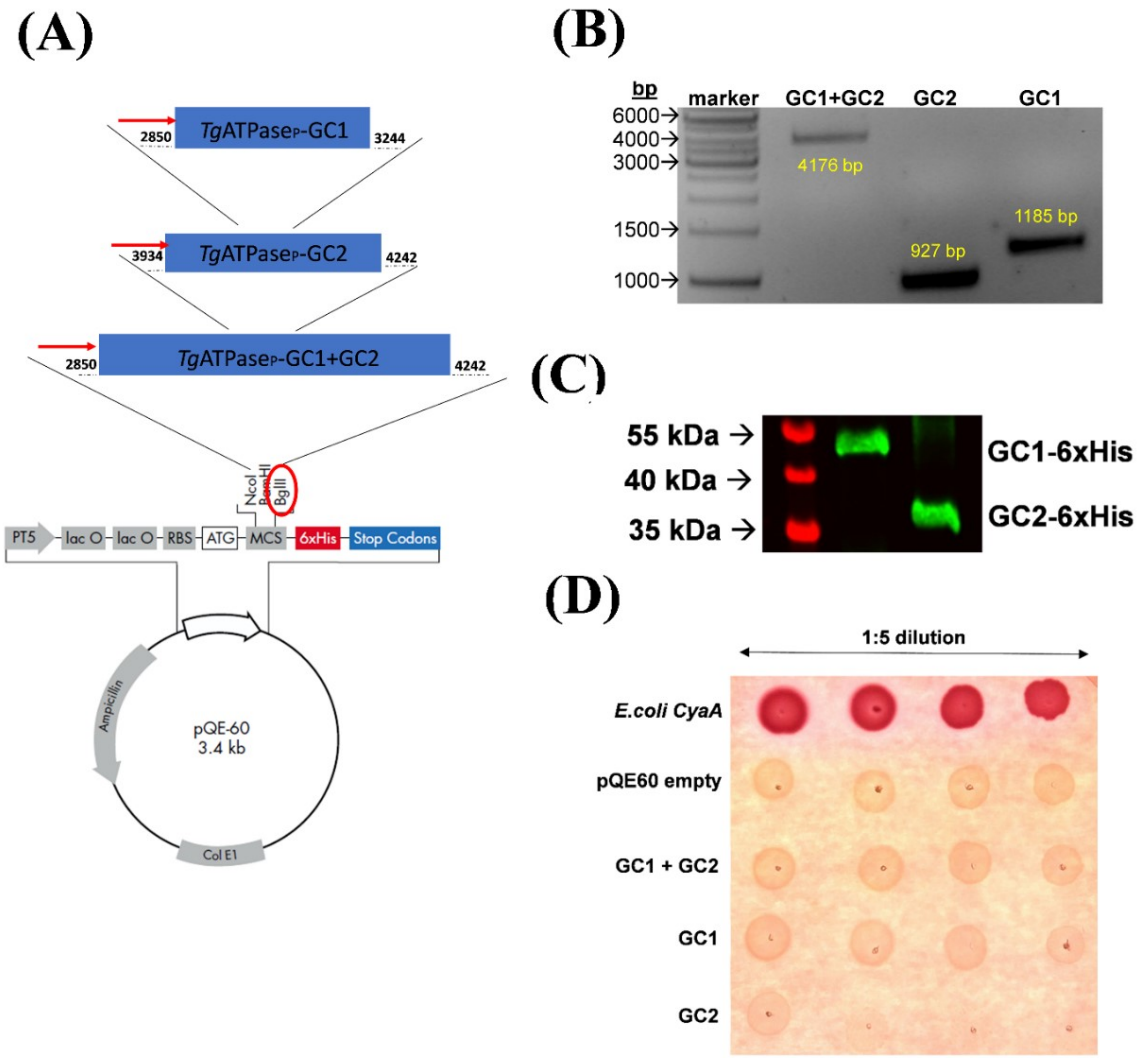

Figure 14. Expression of *Tg*ATPase$_P$-GC1 and GC2 domains in the M15 and BTH101 strains of *Escherichia coli*. (A) Scheme depicting the molecular cloning of GC1, GC2 and GC1+GC2 domains in the *pQE60* expression vector. The open reading frames of indicated domains were amplified starting from the first upstream start codon (ATG) using the tachyzoite-derived RNA, and ligated into *Bgl*II-digested *pQE60* plasmid. Proteins were fused with a C-terminal 6xHis-tag for subsequent detection by immunoblot and purification by virtue of the Ni-NTA column. **(B)** PCR screening of genomic DNA of transgenic M15 strains resulted in obtaining of 1185, 927 and 4176 bp ORF-specific PCR-amplicons, which verifies successful transformation of GC1, GC2 and GC1+GC2 domains, respectively. **(C)** Immunoblot of purified GC1-6xHis and GC2-6xHis proteins (5 µg) using the mouse α-His antibody. The protein bands of 47-kDa and 38-kDa correspond to GC1 and GC2 domains, respectively. Purification was performed under denaturing conditions from the M15 strain, as described in *methods,* section 2.3. However, GC1+GC2 protein could not be purified. **(D)** Functional testing of GC1, GC2 and GC1+GC2 domains in the BTH101 strain. Bacterial strains expressing GC1, GC2, GC1+GC2 were grown in LB medium (OD_{600},1.6; 37°C), and then plated on MacConkey agar containing 1% maltose (carbon source) and 200 µM IPTG (inducer) by dilutions. Bacteria strain expressing *Ec*CyaA (adenylate cyclase) or harboring the empty *pQE60* vector were used as positive and negative controls, repectively. The appearance of red colonies is indicative of cAMP-dependent catabolism of disaccharide following a functional expression of *Ec*CyaA, but not others.

Notwithstanding technical issues with our expression model or enzyme assay, it is plausible that the P4-ATPase domain is required for the functionality of cyclase domains in *Tg*ATPase$_P$-GC, as also suggested by two recent studies (99,153). In similar experiments conducted with *Plasmodium* guanylate cyclases, *Pf*GCα and *Pf*GCβ, the guanylate cyclase activity could only be confirmed for *Pf*GCβ, but not for *Pf*GCα (151), which happens to be the nearest ortholog of *Tg*ATPase$_P$-GC (refer to phylogeny in Figure 12).

3.1.2 *Tg*ATPase$_P$-GC is expressed in the plasma membrane at the apical pole

To gain insight into the endogenous expression and localization of *Tg*ATPase$_P$-GC protein, epitope tagging of the gene was performed in tachyzoites of *T. gondii* (Figure 15A). The parental (RHΔ*ku80-hxgprt*$^-$) strain was transfected with a plasmid construct which allows 3'-insertional tagging of *Tg*ATPase$_P$-GC with a hemagglutinin (HA) tag by single homologous crossover (see the vector map in Appendix 8). The resulting transgenic strain (P_{native}-*Tg*ATPase$_P$-GC-HA$_{3'IT}$-*Tg*Gra1-3'UTR) encoded HA-tagged *Tg*ATPase$_P$-GC under the control of its native promoter but *Tg*Gra1-3'UTR. Notably, the fusion protein localized predominantly at the apex of the intracellularly growing parasites, as deduced by its co-staining with *Tg*Gap45, a marker of the IMC (178) (Figure 15A, *left*). The apical location of *Tg*ATPase$_P$-GC-HA$_{3'IT}$ was confirmed by its co-localization with the IMC sub-compartment protein 1 (*Tg*ISP1) (156) (Figure 15A, *right*). Besides, a significant expression of *Tg*ATPase$_P$-GC-HA$_{3'IT}$ outside the parasite periphery within the residual body (Figure 15A, marked with *arrows*) was noted, which has also been observed for several other proteins, such as Rhoptry Neck 4 (RON4) (179). To assess the membrane location and predicted C-terminal topology of the protein, extracellular parasites were stained with α-HA antibody prior to and after detergent permeabilization of the parasite membranes (Figure 15B). The HA-staining was detected only after the permeabilization, indicating that C-terminus of *Tg*ATPase$_P$-GC faces the parasite interior, as shown in the model (Figure 11B).

Then, extracellular parasites were treated with α-toxin as described in section 2.6.1 to split the plasma membrane from inner membrane complex, which enabled to distinguish the distribution of *Tg*ATPase$_P$-GC-HA$_{3'IT}$ between both entities. By staining of tachyzoites with two markers, *i.e. Tg*Gap45 for the IMC and *Tg*Sag1 for the PM, the association of *Tg*ATPase$_P$-GC-HA$_{3'IT}$ was shown with the plasma membrane (Figure 15C). Making of a transgenic line encoding *Tg*ATPase$_P$-GC-HA$_{3'IT}$ also enabled to evaluate its expression pattern by immunoblot analysis throughout the lytic cycle, which recapitulates the successive

events of gliding motility, host- cell invasion, intracellular replication, and egress leading to host-cell lysis.

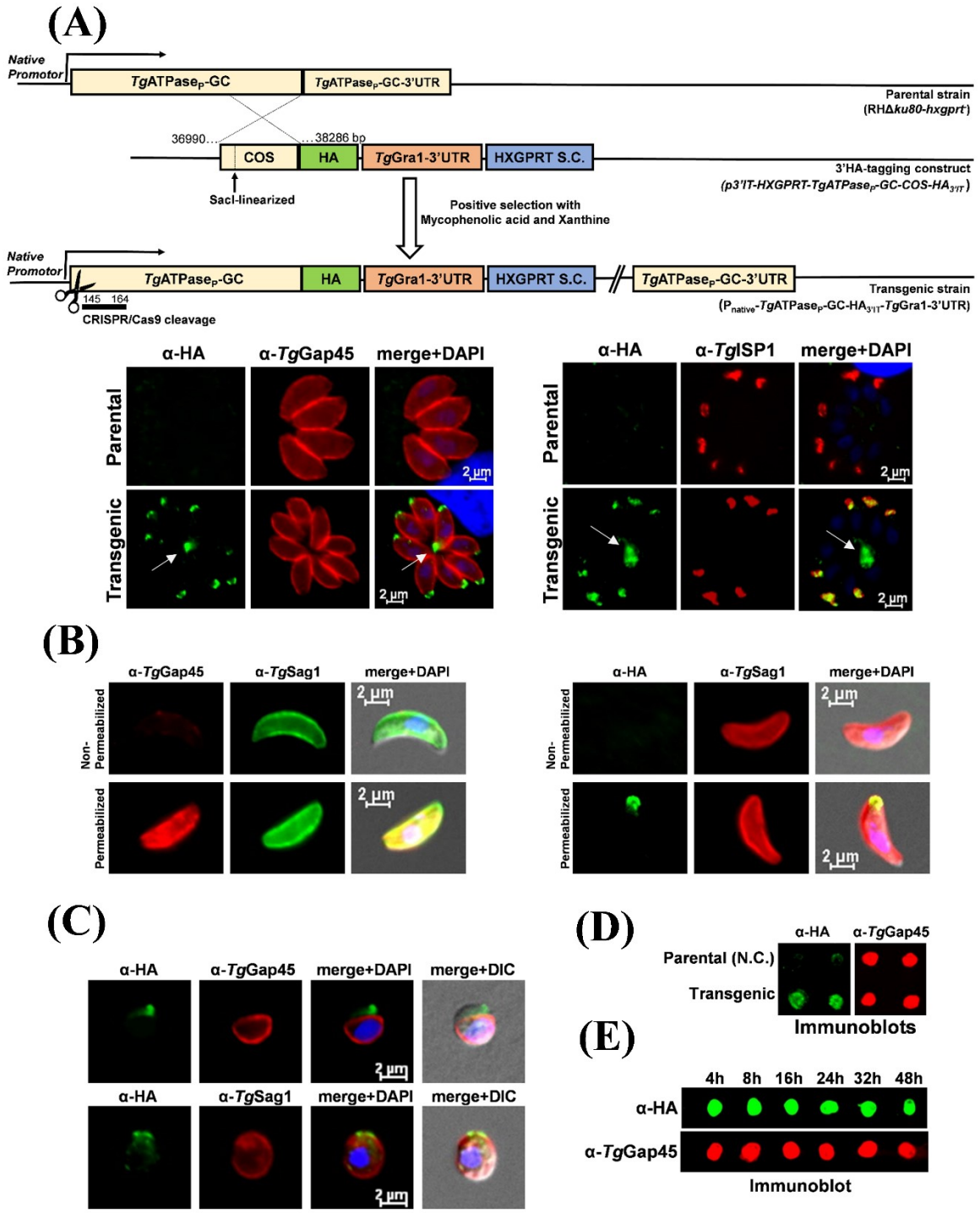

Figure 15. *Tg*ATPase$_P$-GC is a constitutively expressed protein located at the apical end in the plasma membrane of *T. gondii*. (A) Scheme for the genomic tagging of *Tg*ATPase$_P$-GC with a 3'-end HA epitope. The *Sac*I-linearized plasmid for 3'-insertional tagging (*p3'IT-HXGPRT-TgATPase$_P$-GC-COS-HA$_{3'IT}$*) was transfected into the parental (RHΔ*ku80-hxgprt*$^-$) strain, followed by drug selection. Intracellular parasites of the resulting transgenic strain (P$_{native}$-*Tg*ATPase$_P$-GC-HA$_{3'IT}$-*Tg*Gra1-3'UTR) were subjected to immunostaining with specified antibodies (24 h post-infection). *Arrows* indicate the location of the residual body. The host-cell and parasite nuclei were stained by DAPI. *COS*, crossover sequence; *S.C.*, selection cassette. **(B)** Immunofluorescence staining of

extracellular parasites expressing *Tg*ATPase$_P$-GC-HA$_{3'IT}$. The α-HA immunostaining of the free parasites was performed before or after membrane permeabilization either using PBS without additives or with BSA dissolved in detergent-supplemented PBS, respectively. The appearance of *Tg*Gap45 signal (located in the inner membrane complex) only after permeabilization confirms functionality of the assay. *Tg*Sag1 is located in the plasma membrane and thus visible under both conditions. **(C)** Immunostaining of extracellular parasites encoding *Tg*ATPase$_P$-GC-HA$_{3'IT}$ after drug-induced splitting of the inner membrane complex (IMC) from the plasma membrane (PM). Tachyzoites were incubated with α-toxin (20 nM, 2 h) prior to immunostaining with α-HA antibody in combination with primary antibodies recognizing IMC (α-*Tg*Gap45) or PM (α-*Tg*Sag1), respectively. **(D-E)** Immunoblots of tachyzoites expressing *Tg*ATPase$_P$-GC-HA$_{3'IT}$, and of the parental strain (RHΔ*ku80-hxgprt*$^-$, negative control). The protein samples prepared from extracellular parasites (10^7) were directly loaded onto membrane blot, followed by staining with α-HA and α-*Tg*Gap45 antibodies. Samples in *panel E* were collected at different time periods during the lytic cycle and stained with α-HA and α-*Tg*Gap45 (loading control) antibodies.

*Tg*ATPase$_P$-GC is a bulky protein (477-kDa) with several transmembrane regions; hence it was not possible for us to successfully resolve it by gel electrophoresis and transfer onto nitrocellulose membrane for immunostaining. Thus, we performed the dot-blot analysis by loading protein samples directly onto an immunoblot membrane (Figure 15D-E). Unlike the parental strain (negative control), which showed only a faint (background) α-HA staining, we observed a strong signal in the *Tg*ATPase$_P$-GC-HA$_{3'IT}$-expressing strain (Figure 15D). Samples of transgenic strains collected at various periods embracing the entire lytic cycle indicated a constitutive and steady expression of *Tg*ATPase$_P$-GC-HA$_{3'IT}$ in tachyzoites (Figure 15E).

3.1.3 *Tg*ATPase$_P$-GC is essential for the parasite survival

Having established the expression profile and location, next the physiological importance of *Tg*ATPase$_P$-GC for tachyzoites was examined. Multiple efforts to knockout the *Tg*ATPase$_P$-GC gene by double homologous recombination were unrewarding, suggesting its essentiality during the lytic cycle (lethal phenotype). Hence, the strain expressing *Tg*ATPase$_P$-GC-HA$_{3'IT}$ was utilized to monitor the effect of genetic disruption immediately after the transfection of the plasmid for gene disruption (Figure 16). To achieve this, a CRISPR/Cas9-directed cleavage were executed in *Tg*ATPase$_P$-GC gene, and then parasites were immunostained at various periods to determine a time-elapsed loss of HA-signal (Figure 16A). Within a day of transfection, about 4% of vacuoles had lost the apical staining of *Tg*ATPase$_P$-GC-HA$_{3'IT}$ (Figure 16B). Parasites losing the HA-signal remained constant until the 1st passage (P1, 24-40 h). However, their growth reduced gradually down to 2% during the 2nd passage (P2, 72-88 h) and fully seized by the 3rd passage (P3, 120-136 h).

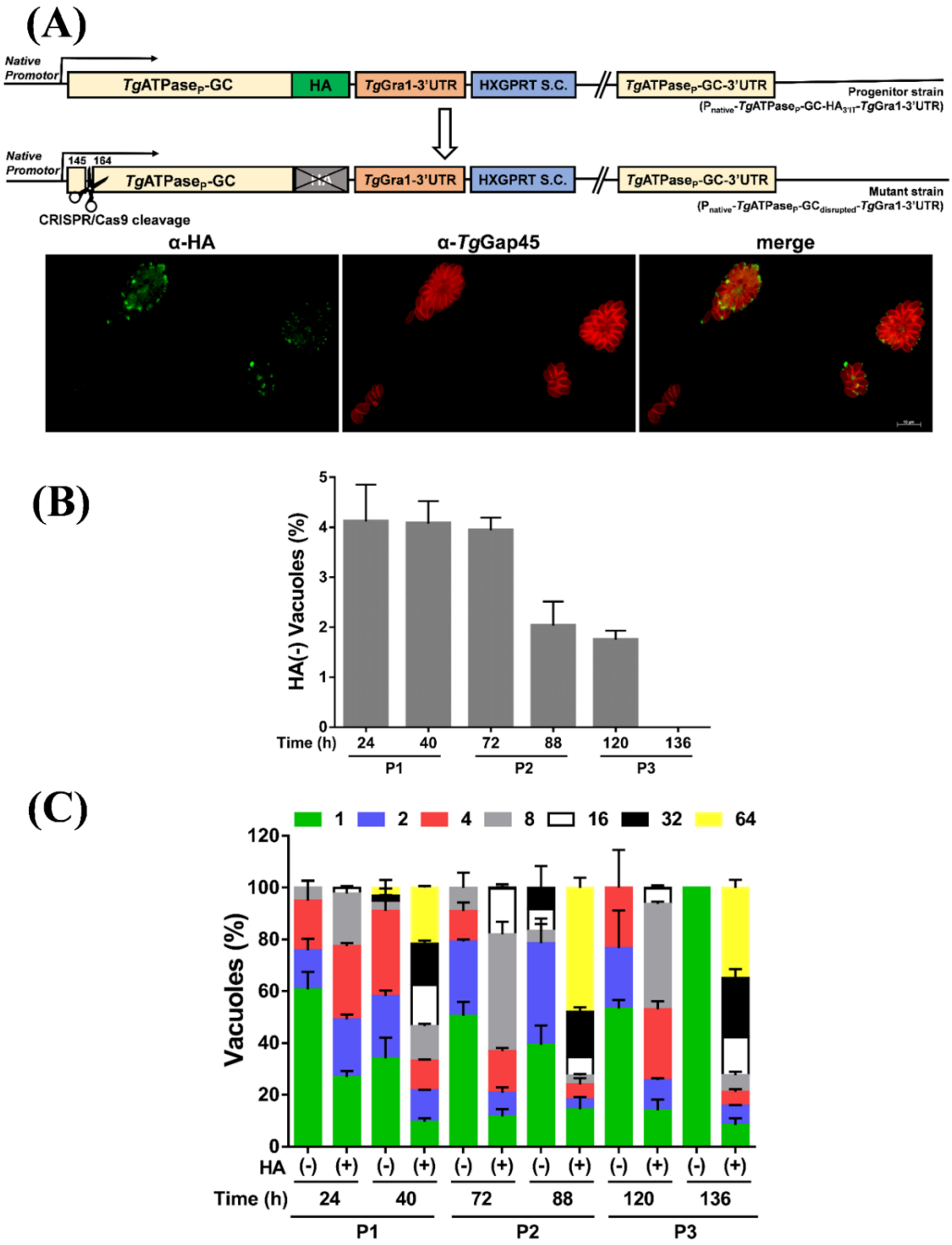

Figure 16. Genetic disruption of *Tg*ATPase$_P$-GC is lethal to tachyzoites of *T. gondii.* (A) Scheme for the CRISPR/Cas9-mediated disruption of the gene in parasites expressing *Tg*ATPase$_P$-GC-HA$_{3'IT}$. The guide RNA was designed to target the nucleotides between 145 and 164 bp in the progenitor strain (P_{native}-*Tg*ATPase$_P$-GC-HA$_{3'IT}$-*Tg*Gra1-3'UTR). Image shows the loss of HA signal in some vacuoles after CRISPR/Cas9-cleavage. Parasites were transfected with the *pU6-TgATPase$_P$-GC$_{sgRNA}$-Cas9* vector, and then stained with α-HA and α-*Tg*Gap45 antibodies at specified periods. **(B)** Quantitative illustration of *Tg*ATPase$_P$-GC-HA$_{3'IT}$-disrupted mutant parasites from *panel A*. The HA-negative vacuoles harboring at least 2 parasites were scored during successive passages (P1-P3) of culture. **(C)** The replication rates of the HA (+) and HA (-) tachyzoites, as evaluated by immunostaining (*panel A*). About 500-600 vacuoles were enumerated for the parasite numbers per vacuole (n=3 assays, means ± S.E.M.).

The same assay also allowed to quantify the replication rates of HA-negative parasites in relation to the HA-positive parasites by counting their numbers in intracellular vacuoles (Figure 16C). As expected, the fraction of single parasites and small vacuoles comprising 2 parasites were much higher in the nonexpression (HA-negative) parasites. Inversely, the progenitor strain expressing *Tg*ATPase$_P$-GC-HA$_{3'IT}$ showed predominantly a higher percentage of bigger vacuoles with 16-64 parasites. By 3rd passage, only single-parasites without HA-signal were detected, which demonstrates an essential role of *Tg*ATPase$_P$-GC for the asexual reproduction. It must also be mentioned that the off-target activity caused by Cas9 toxicity is a well-documented problem of this system in a variety of cell-lines (180-182) as well as in *Toxoplasma* (110) and cannot be ruled out here. However, the effect of Cas9 toxicity, if any, should not only be seen in the parasites without HA signal but also with HA-positive parasites at all of time points. As shown in Figure 16A-B, we detected about 4% vacuoles without HA signal with normally replicating parasites, which gradually disappeared in the entire population over a week period. These results are consistent with a refractory nature of guanylate cyclase.

3.1.4 Genetic knockdown of *Tg*ATPase$_P$-GC in *T. gondii* tachyzoites

Although an indispensable nature of *Tg*ATPase$_P$-GC for tachyzoites could be established, the above mentioned CRISPR/Cas9-mediated gene disruption strategy did not yield a clonal mutant for in-depth biochemical and phenotypic analyses due to an eventual mortal phenotype. Therefore, a knockdown approach was applied on the basis of Cre/LoxP-mediated native 3'UTR deletion of *Tg*ATPase$_P$-GC to lower the protein expression that allowed to examine the physiological importance of this mega gene during the lytic cycle of the parasite.

3.1.4.1 Excision of *Tg*ATPase$_P$-GC-3'UTR reduces cGMP synthesis

Following successful expression of the *Tg*ATPase$_P$-GC-HA$_{3'IT}$ under the regulation of its native promoter and *Tg*Gra1-3'UTR (Figure 15A), an additional transgenic strain, in which *Tg*Gra1-3'UTR was replaced by the 3'UTR of *Tg*ATPase$_P$-GC, was generated to designate native protein expression. To achieve this, 1 kb part of the *Tg*ATPase$_P$-GC-3'UTR following stop codon was amplified from the genomic DNA of parental RHΔ*ku80-hxgprt*$^-$ strain, and amplicon was substituted for *Tg*Gra1-3'UTR in our expression construct by flanking with two loxP sites (see vector map in Appendix 8). Subsequently, transfection and

drug selection were performed as described (section 3.1.2). In the eventually engineered parasite strain, *Tg*ATPase$_P$-GC-HA$_{3'IT}$ was expressed under its natural regulatory elements; however, the 3'UTR of gene was loxP-flanked (floxed) (P$_{native}$-*Tg*ATPase$_P$-GC-HA$_{3'IT}$-3'UTR$_{floxed}$) (Figure 17A). The transfection of this strain culture with a Cre recombinase expressing vector permitted the Cre/loxP-mediated excision of the 3'UTR as well as and HXGPRT selection cassette. Mutant parasites were selected by 6-thioxanthine treatment (80 µg/ml) (Figure 17A).

Genomic screening using specific primers (indicated with red arrows in Figure 17A) confirmed a successful generation of the mutant (P$_{native}$-*Tg*ATPase$_P$-GC-HA$_{3'IT}$-3'UTR$_{excised}$), which yielded 2.2-kb amplicons as opposed to 5.2-kb in the progenitor strain (P$_{native}$-*Tg*ATPase$_P$-GC-HA$_{3'IT}$-3'UTR$_{floxed}$) (Figure 17B). The sequencing of amplicons further verified the accomplished 3'UTR excision. Immunoblots of a clonal mutant by α-HA antibody staining showed the evidence of downregulation of the *Tg*ATPase$_P$-GC-HA$_{3'IT}$ protein expression (Figure 17C). Densitometric analysis of *Tg*ATPase$_P$-GC-HA$_{3'IT}$ protein revealed about 65% reduction in the mutant when compared to the progenitor strain. Knockdown of the protein was also endorsed by loss of HA-staining in immunofluorescence assay (Figure 17D), where about 94% vacuoles lost their HA-signal, and the rest (~6%) displayed only a faint HA-staining (Appendix 5A).

Next, it was evaluated if the repression of *Tg*ATPase$_P$-GC translated into a declined cGMP synthesis by the parasite. Indeed, ~60% regression was measured in the steady-state levels of cGMP in the mutant (Figure 17E), equating to the decay at the protein level (Figure 17C-D). The average cGMP level of mutant strain was detected as about 67 fmol/10^6 parasites, while this value was measured as ~153 and ~216 fmol/10^6 parasites in progenitor and parental strains, respectively (Figure 17E). The progenitor strain (P$_{native}$-*Tg*ATPase$_P$-GC-HA$_{3'IT}$-3'UTR$_{floxed}$) also showed a decreased cGMP level in comparison to parental strain likely due to epitope tagging and introduction of loxP sites between the last gene exon and 3'UTR. Overall, these results indicate that *Tg*ATPase$_P$-GC functions as a guanylate cyclase to serve for cGMP production.

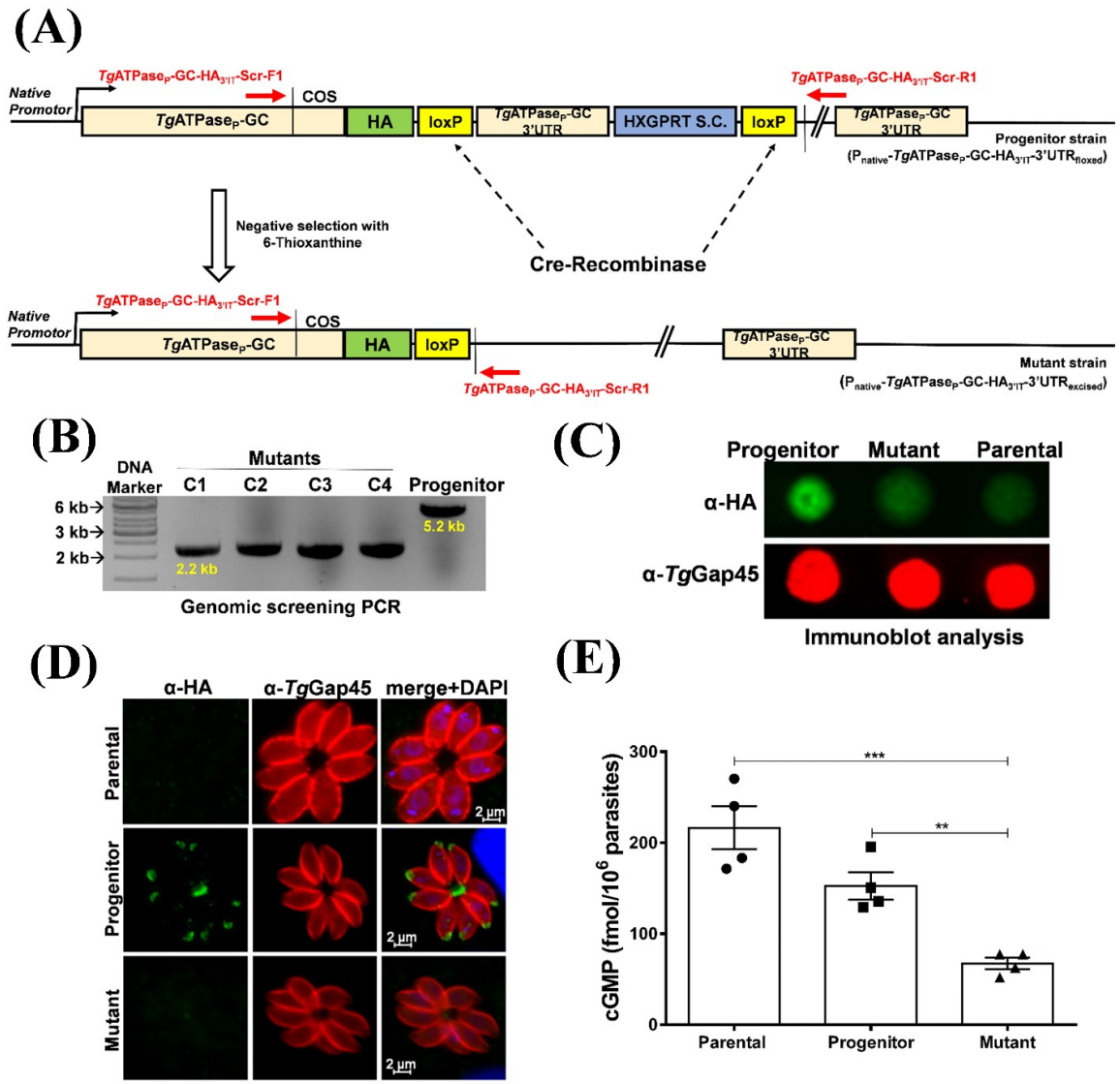

Figure 17. Cre recombinase-mediated downregulation of *Tg*ATPase$_P$-GC-HA$_{3'IT}$ declines cGMP synthesis in *T. gondii*. **(A)** Schematics for making the parasite mutant (P_{native}-*Tg*ATPase$_P$-GC-HA$_{3'IT}$-3'UTR$_{excised}$). A vector expressing Cre recombinase was transfected into the progenitor strain (P_{native}-*Tg*ATPase$_P$-GC-HA$_{3'IT}$-3'UTR$_{floxed}$), in which 3'UTR of the *Tg*ATPase$_P$-GC gene was flanked with two loxP sites. Parasites involving Cre recombinase expressing vector were selected for the loss of HXGPRT selection cassette (S.C.) using 6-thioxanthine. **(B)** Genomic screening of the *Tg*ATPase$_P$-GC mutant confirming Cre-mediated excision of 3'UTR and HXGPRT. Primers, indicated as red *arrows* in *panel A*, were used to PCR-screen of the gDNA isolated from four different mutant clones (C1-C4) along with the progenitor strain. **(C)** Immunoblot showing a repression of *Tg*ATPase$_P$-GC-HA$_{3'IT}$ in 3'UTR- excised parasites with respect to the progenitor and parental (RHΔ*ku80-hxgprt*$^-$) strains. Parasites (10^7) were subjected to the dot blot analysis using α-HA and α-*Tg*Gap45 (loading control) antibodies. **(D)** Immunostaining of the mutant (*Tg*ATPase$_P$-GC-HA$_{3'IT}$-3'UTR$_{excised}$) and progenitor parasites revealing the loss of HA-signal in the former strain. Parental strain was used as a negative control for the background staining. Parasites were stained with α-HA and α-*Tg*Gap45 antibodies 24 h post infection. **(E)** Changes in total steady-state cGMP level of the mutant compared to the parental and progenitor strains. Fresh syringe-released extracellular parasites ($5x10^6$) were subjected to ELISA-based cGMP measurements (n=4 assays, the means are with ±S.E.M.). **, p ≤0.01; ***, p ≤0.001 (Student's t-test)

3.1.4.2 Downregulation of cGMP synthesis impairs the parasite growth

The growth fitness of *Tg*ATPase$_{P}$-GC-HA$_{3'IT}$-3'UTR$_{excised}$ mutant was examined by comparing it with the progenitor (P$_{native}$-*Tg*ATPase$_{P}$-GC-HA$_{3'IT}$-3'UTR$_{floxed}$) and parental (RHΔ*ku80-hxgprt*$^{-}$) strains (Figure 18A). A significant impairment in the plaque number of mutant was observed in comparison to parental strain (Figure 18B). As anticipated, the mutant exhibited about 65% and 35% reduction in plaque area when compared to the parental and progenitor strains, respectively (Figure 18C), which correlated rather well with its residual expression of *Tg*ATPase$_{P}$-GC in the immunoblot, immunofluorescence as well as in cGMP assays (Figure 17C-E). However, the progenitor strain also showed lesser plaque formation and ~30% impairment in plaque sizes (Figure 18B-C), which corresponds again to the observed reduction in cGMP level when compared to the parental strain (Figure 17E).

Next, we checked the replication rate of the mutant to determine whether observed growth defect in plaque assay is due to the affected replication. Parasites released on HFF-monolayers were incubated for 24- and 40 h to replicate themselves in parasitophorous vacuoles, followed by counting of the parasite numbers in vacuoles across strains. The replication assay revealed a modestly higher fraction of smaller vacuoles with two parasites in early culture (24 h) of the mutant compared to the control strains; however, the effect was assuaged at the later culture stage (40 h) (Figure 18D). The average parasite numbers in each vacuole were also scored to ascertain the obtained data. Indeed, no significant difference was observed in the average parasite numbers of the *Tg*ATPase$_{P}$-GC mutant (33 parasites/vacuole) with respect to the control strains (37-38 parasites/vacuole) in late stage cultures (40 h), although a slight delay was observed in early culture stage (6-7 parasites/vacuole in mutant *versus* 10 and 8 parasites/vacuole in progenitor and parental strains, respectively) (Figure 18E), which suggests a nonessential function of *Tg*ATPase$_{P}$-GC for the cell division. All together, these results show that the knockdown of *Tg*ATPase$_{P}$-GC protein causes a significant decrease in cGMP synthesis of mutant parasites. The effect of cGMP decline was observed on the growth profile of tachyzoites, which indicates that *Tg*ATPase$_{P}$-GC is necessary for the lytic cycle of parasite.

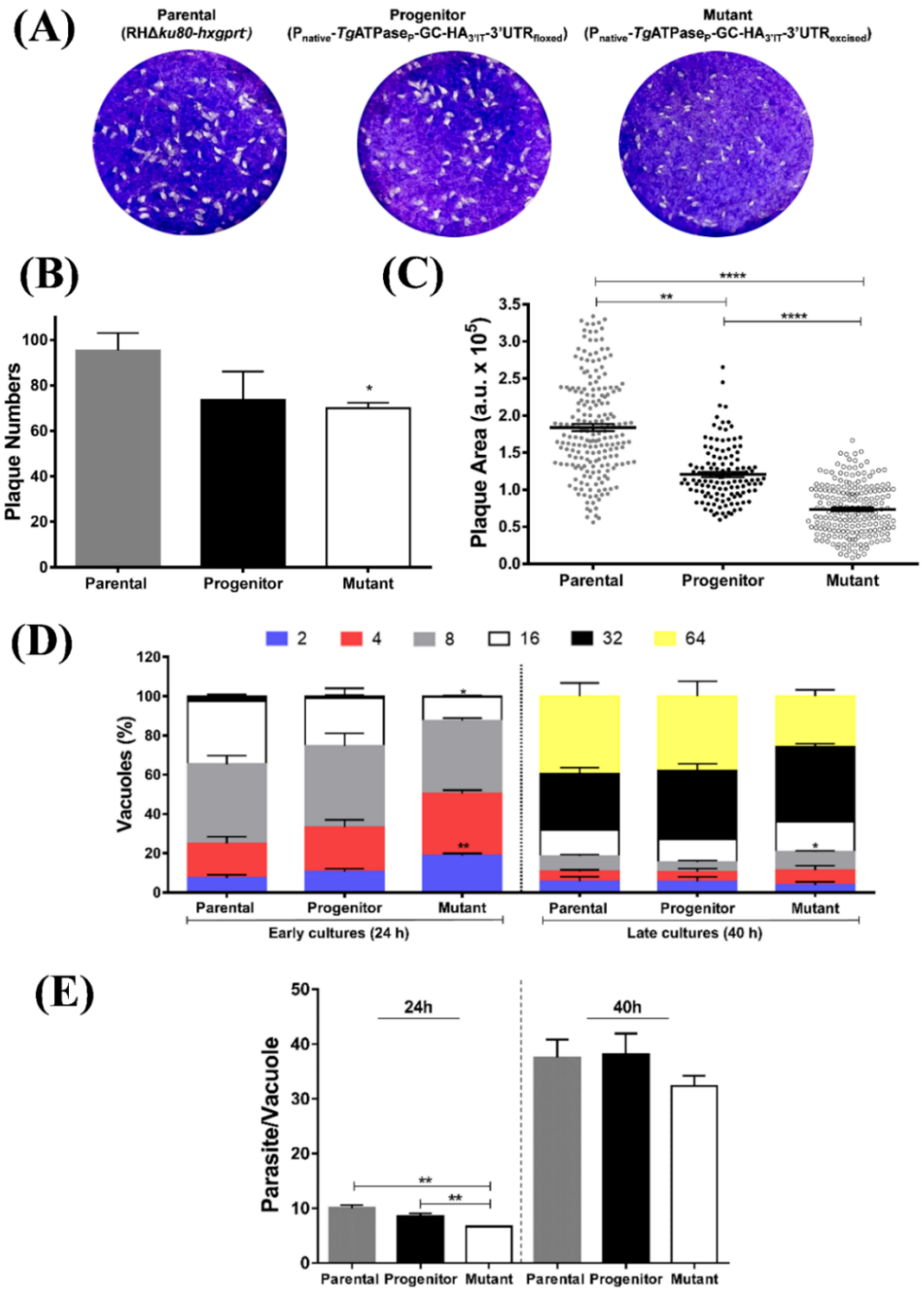

Figure 18. **A declined cGMP synthesis causes a defect in parasite growth. (A-C)** Plaque assays using the *Tg*ATPase$_P$-GC mutant (P_{native}-*Tg*ATPase$_P$-GC-$HA_{3'IT}$-3'$UTR_{excised}$), progenitor (P_{native}-*Tg*ATPase$_P$-GC-$HA_{3'IT}$-3'UTR_{floxed}) and parental (RHΔ*ku80-hxgprt*$^-$) strains. **(A)** The dotted white areas and blue staining signify plaques formed by parasites and intact host-cell monolayers, respectively. **(B)** The score of the plaque numbers revealing the comparative growth of mutant with respect to parental and progenitor strains (n=3 assays). **(C)** The area of each plaque (arbitrary units, a.u.) embodies the growth fitness of indicated strains. 150-200 plaques of each strain were evaluated from 3 independent assays. **(D-E)** Replication assays of mutant, progenitor and parental strains (n=4 assays). **(D)** The intracellular replication rates were analyzed 24 h and 40 h post-infection by scoring the parasite numbers in a total of 500-600 vacuoles after staining with α-*Tg*Gap45 antibody. **(E)** The average parasite numbers per vacuole were also depicted in two time points for all strains. Statistics was performed by Student´s *t*-test; *, $p \leq 0.05$; **, $p \leq 0.01$; ****, $p \leq 0.0001$ (the means with ±S.E.M).

3.1.4.3 *Tg*ATPase$_P$-GC regulates the crucial events of lytic cycle

The availability of an effective mutant encouraged to study also the importance of *Tg*ATPase$_P$-GC for the critical steps of lytic cycle including invasion, egress and gliding motility, all of which contribute eventually to the parasite virulence (Figure 19). About 30% decline was quantified in the invasion efficiency of the 3'UTR-excised *Tg*ATPase$_P$-GC-mutant down from 80% to 53% (Figure 19A). Hence, we presume that a minor replication defect observed at 24 h (Figure 18D-E) may be a consequence of a poor host-cell invasion by the mutant parasite. Besides, the effect of protein repression was more pronounced in egress assay, where the mutant showed 70% decline in natural egress when compared to the parental strain and 40% defect in relation to the progenitor strain at 40 h and 48 h post-infections (Figure 19B). Notably though, the egress defect was compensated and not apparent upon prolonged (64 h) culture. Such compensation at the later stage is probably caused by alternative (CDPKs) signaling cascades (42).

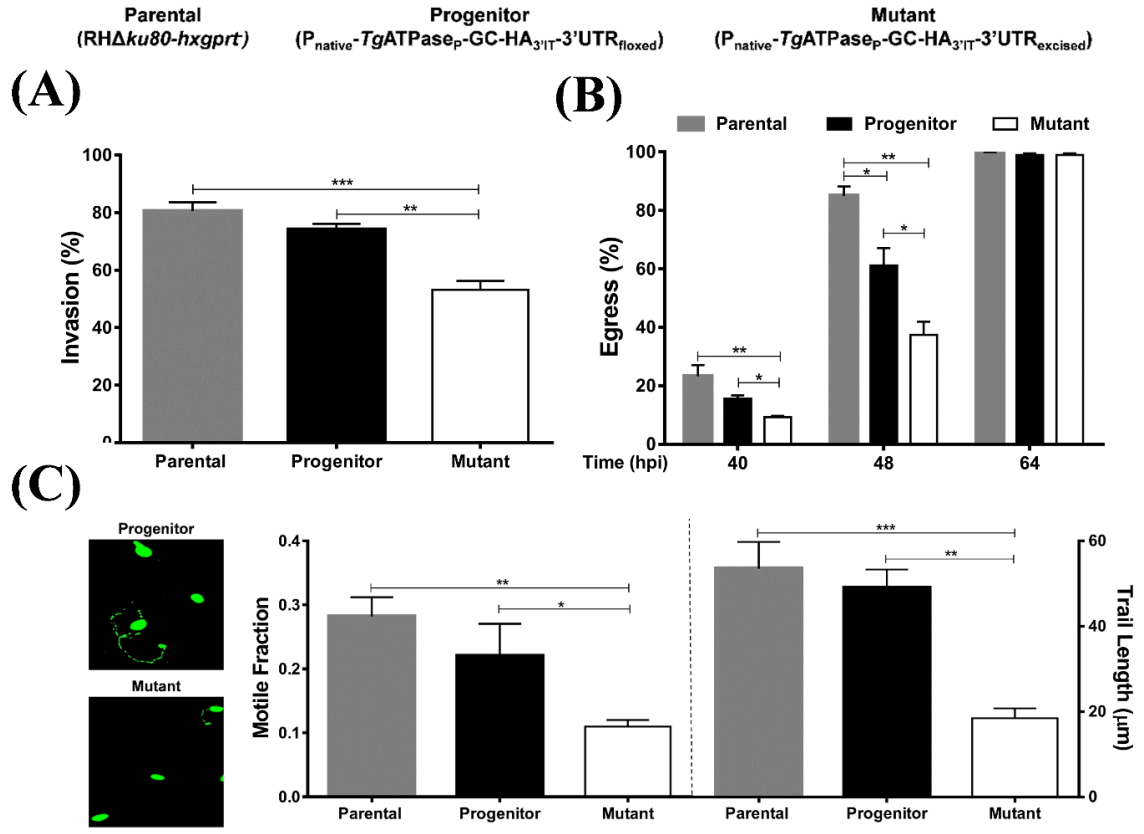

Figure 19. Cyclic GMP signaling governs the key events during the lytic cycle of *T. gondii*. **(A-C)** *In vitro* phenotyping of the *Tg*ATPase$_P$-GC mutant and its progenitor compared with parental strain. **(A)** Host-cell invasion, **(B)** Parasite egress and **(C)** Gliding motility were assessed using standard phenotyping methods described in section 2.5. Invasion and egress rates were calculated by dual staining with α-*Tg*Gap45 and α-*Tg*Sag1 antibodies. In total, 1000 parasites for each strain from 4 independent assays were examined to estimate the invasion efficiency. The natural egress of tachyzoites was measured after 40 h, 48 h and 64 h by scoring 500-600 vacuoles of each strain (n=3

assays). To estimate the gliding motility, fluorescent images stained with α-*Tg*Sag1 antibody were analyzed for the motile fraction (500 parasites of each strain, n=3 assays), and 100-120 trail lengths per strain were measured (the means with ±S.E.M; the significance with Student's *t*-test, *, p ≤0.05; **, p ≤0.01; ***, p ≤0.001).

Because invasion and egress are considered to be mediated by gliding motility (100), *in vitro* motility assay was performed to test the phenotype of our *Tg*ATPase$_P$-GC mutant strain. We determined that the average motile fraction was reduced by more than half in the mutant (from ~25-30% to ~10%), and trail lengths of moving parasites were remarkably shorter (~18 µm) than the control strains (~48 µm) (Figure 19C). Not least, as witnessed in plaque assays (Figure 18 A-C), it was also found a steady, albeit not significant, decline in the invasion and egress rates of the progenitor when compared to the parental strain, which further confirms a correlation across all phenotypic assays.

3.1.4.4 Pharmacological modulation of cGMP signaling in the *Tg*ATPase$_P$-GC mutant

A partial phenotype prompted us to pharmacologically inhibit the residual cGMP signaling *via* PKG in the 3'UTR-excised *Tg*ATPase$_P$-GC mutant. An inhibitor called compound 2 (C2), which has been shown to block mainly *Tg*PKG but also calcium-dependent protein kinase 1 (CDPK1) (183), was used to assess the effect of cGMP signaling on the lytic cycle steps of mutant by comparison with its progenitor strain (P_{native}-*Tg*ATPase$_P$-GC-$HA_{3'IT}$-$3'UTR_{floxed}$) (Figure 20). Conversely, *Tg*ATPase$_P$-GC mutant was also treated with two cGMP-specific PDE inhibitors, namely zaprinast and BIPPO, which are known to inhibit parasite enzymes along with human PDE5 and PDE9, respectively (122,184), to complement the depletion of *Tg*ATPase$_P$-GC by drug-mediated elevation of cGMP (Figure 21).

The gliding motility of *Tg*ATPase$_P$-GC mutant was completely suppressed by 2 µM of C2 treatment. Besides, a remarkable reduction was also detected in progenitor strain (Figure 20A). Approximately, 6-fold decrease was observed in motile fraction of both strains. The length of trails in motile parasites was extremely short (in turn, ~16 and ~ 8 µm in progenitor and mutant strains). The impact of C2 was more accentuated on the motility of mutant strain, likely due to the cumulative effect of genetic repression and drug inhibition.

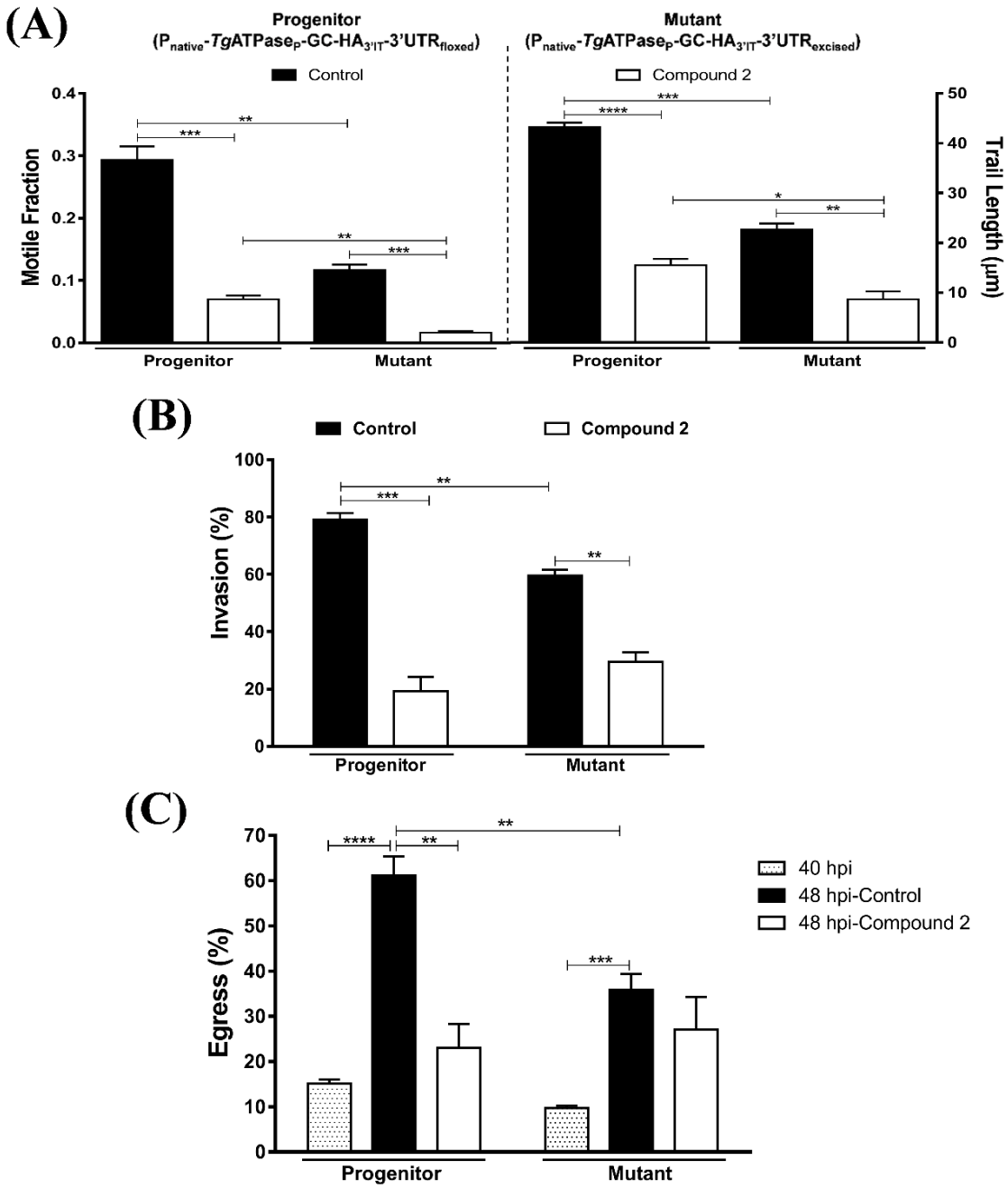

Figure 20. Inhibition of residual cGMP signaling in the *Tg*ATPase$_P$-GC mutant by Compound 2 augments the defective phenotype. The effect of PKG inhibitor Compound 2 (2 µM) on the **(A)** Motility, **(B)** Invasion and **(C)** Egress of *Tg*ATPase$_P$-GC mutant and its progenitor. **(A)** The impact of compound 2 treatment on gliding motility was analyzed using the fluorescent images stained with α-*Tg*Sag1 antibody following 15 min incubation to let parasites making trails on BSA-coated glass coverslips. For the motile fraction, 500 parasites of each strain were considered (n=3 assays). A total of 50 trails in the progenitor and 15 trails of the mutant (due to severe defect) were measured by ImageJ. **(B-C)** Invasion and egress rates were scored after staining with α-*Tg*Gap45 and α-*Tg*Sag1 antibodies. For invasion, freshly extracellular parasites (10^6) were released on HFF-monolayers grown on glass coverslips with or without compound 2 treatment following 1 h incubation. 450-500 parasites were scored (n=3 assays). For egress, parasite cultures grown to the mature vacuoles in HFF-monolayers were treated with Compound 2 40 hpi and incubated 8 more hours to observe the effect of drug. 500-600 vacuoles were counted for each strain from 4 independent assays. Mean values are shown with S.E.M. Statistical significance was calculated for each pair of columns individually by Student's *t*-test. (*, p ≤0.05; **, p ≤0.01; ***, p ≤0.001; ****, p ≤0.0001.)

The impairment observed in motility was also detected in invasion and egress after C2 treatment (Figure 20B-C). Invasion efficiency dropped from ~80% to 20% and from ~60% to 30% in the progenitor and mutant strains, respectively (Figure 20B). On the other hand, C2 treatment did not influence the egress phenotype of the mutant significantly, while egress rate of the progenitor strain declined from ~60% to ~25% (Figure 20C). The inhibitory potential of C2 was evidently stronger on the invasion and egress events of the progenitor strain than on the *Tg*ATPase$_P$-GC mutant, which can be attributed to the already-activated compensatory mechanisms in the mutant parasite after genetic attenuation of *Tg*ATPase$_P$-GC.

To further validate our findings, zaprinast (500 µM) and BIPPO (55 µM) were applied to the cultures to check if the elevation of cGMP *via* drug treatment could alleviate the phenotypic defects in the *Tg*ATPase$_P$-GC knockdown mutant (Figure 21). As shown in Figure 21A, both drugs led to a dramatic increase in the motile fraction and trail lengths of the progenitor (P_{native}-*Tg*ATPase$_P$-GC-$HA_{3'IT}$-3'UTR_{floxed}) and mutant (P_{native}-*Tg*ATPase$_P$-GC-$HA_{3'IT}$-3'$UTR_{excised}$) strains expectedly. The latter parasites were as competent as the former after drug exposure. A similar restoration of phenotype in the mutant was detected in egress assays. The effect of BIPPO was much more pronounced than zaprinast, leading to egress of nearly all parasites (Figure 21B).

In contrast to the motility and egress, a treatment of BIPPO and zaprinast resulted in a surprisingly divergent effect on the invasion rates of both strains (Figure 21C). Indeed, BIPPO exerted an opposite effect, *i.e.* a reduction in invasion efficiency of both progenitor and mutant strains. Impairment was stronger in the former strain; hence a reversal of the phenotype was noted when compared to the control (untreated) samples. A similar effect was seen on the progenitor strain after zaprinast treatment; although, it was much less potent than BIPPO, as implied previously (122). However, invasion rate of the mutant could be increased by zaprinast treatment. These observations can be ascribed to differential elevation of cGMP (overabundance or above certain threshold) caused by PDE-inhibitors which might inhibit the host-cell invasion, but promotes the parasite motility and egress.

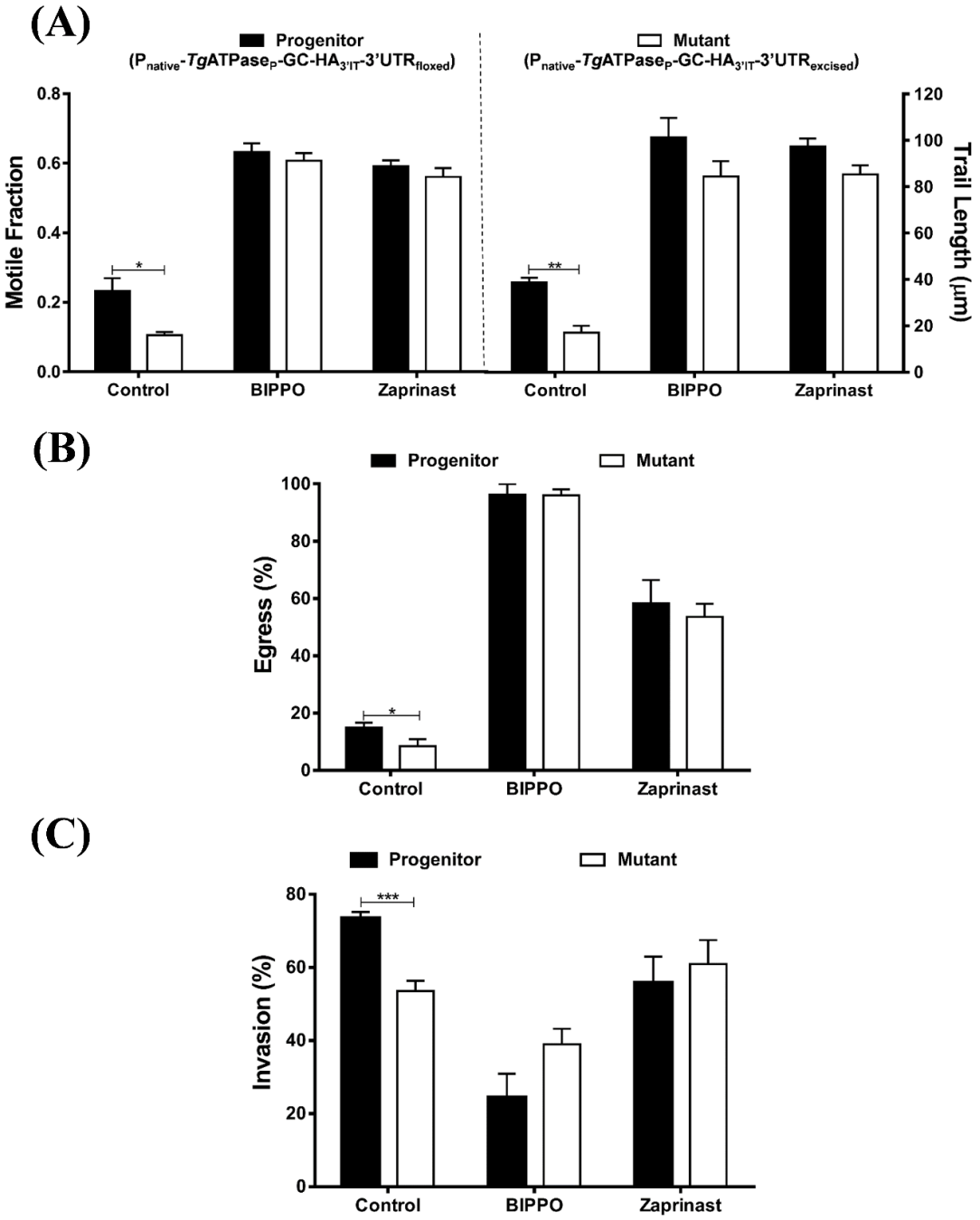

Figure 21. cGMP-specific PDE inhibition can repair phenotypic defects of *Tg*ATPase$_P$-GC mutant. **(A)** Gliding motility of the P_{native}-*Tg*ATPase$_P$-GC-$HA_{3'IT}$-3'$UTR_{excised}$ mutant and progenitor (P_{native}-*Tg*ATPase$_P$-GC-$HA_{3'IT}$-3'UTR_{floxed}) strains in the presence of two inhibitors of cGMP-specific phosphodiesterases, zaprinast (500 μM) and BIPPO (55 μM). Fresh syringe-released parasites were treated with drugs for 15 min during the assay, followed by fixation and staining with α-*Tg*Sag1 antibody. 500-600 parasites of each strain were evaluated for the motile fraction, and 100-120 trail lengths were measured by ImageJ (n= 3 assays, mean with S.E.M.). **(B-C)** Egress and invasion rates of indicated parasite strains after exposure to zaprinast and BIPPO. Intracellular and extracellular parasites were differentially stained with α-*Tg*Gap45 and α-*Tg*Sag1 antibodies, as described in *methods*. Drug treatment during invasion assay was performed for 1 h. For egress, parasitized cells (MOI, 1; 40 h post-infection) were stimulated with either zaprinast (500 μM) or BIPPO (55 μM) for 5 min 30 sec prior to fixation and staining. In total, 1000 parasites and 500-600 vacuoles were scored for each strain in *panel B* and *C,* respectively (n= 3 assays, mean with S.E.M.). Statistics was performed for individual pair of columns using Student's *t*-test (*, $p \leq 0.05$; **, $p \leq 0.01$; ***, $p \leq 0.001$).

3.1.5 *T. gondii* harbors a single gene expressing two isoforms of Protein kinase G

cGMP-dependent protein kinase of *T. gondii* (*Tg*PKG) is a member of serine/threonine-specific protein kinases which largely regulate signal transduction pathways *via* phosphorylation of target proteins to coordinate core cellular processes. In *Toxoplasma*, only a single cGMP-dependent protein kinase gene was detected in the database (ToxoDB) (50). The entire gene size is about 15-kb which consists of 19 introns and 20 exons. The ORF encodes for a 994 amino acids-long protein including a regulatory subunit at its C-terminus and a serine/threonine kinase catalytic domain at its N-terminus (Figure 22A). The first half of *Tg*PKG (1-670 aa) constitutes the regulatory region containing four cGMP-binding domains positioned between the amino acids from Val^{198} to Gln^{290}, from Phe^{308} to Ile^{417}, from Leu^{430} to Gly^{539} and from Ile^{561} to Lys^{661}, respectively. The second half (670-994 aa) involves a catalytic domain encoded from the region between Leu^{684} and Phe^{941} amino acids. As opposed to *Tg*ATPase$_P$-GC, *Tg*PKG does not contain any transmembrane helix (Figure 22A).

Because *Tg*PKG is known as the main effector of cGMP signaling in *T. gondii,* the same abovementioned genomic-tagging (section 3.1.2), knockdown (section 3.1.4.1) and phenotyping (section 3.1.4.2 and 3.1.4.3) approaches were also implemented to *Tg*PKG in order to consolidate aforesaid work on *Tg*ATPase$_P$-GC. Briefly, 1 kb from the 3' end of *Tg*PKG gene was amplified with C-terminal HA-tag between *Nco*I and *EcoR*I restriction enzyme recognition sites and introduced into the expression vector that includes 1 kb part of native *Tg*PKG-3'UTR. Thereafter, a parasite strain expressing *Tg*PKG with HA-epitope under the control of its endogenous regulatory elements was generated by 3'-insertional tagging strategy. The 3'UTR and HXGPRT selection cassette were floxed in the expression construct (Figure 22B-Step 1) (please see vector map in Appendix 8). The resultant progenitor strain (P_{native}-*Tg*PKG-$HA_{3'IT}$-$3'UTR_{floxed}$) was then exposed to a Cre-mediated knockdown of *Tg*PKG-$HA_{3'IT}$ by excising the loxP-flanked 3'UTR and selection cassette, which resulted in a generation of *Tg*PKG-$HA_{3'IT}$-knockdown mutant (P_{native}-*Tg*PKG-$HA_{3'IT}$-$3'UTR_{excised}$) (Figure 22B-Step 2). As intended, genomic screening with specified primers in Figure 22B yielded 1.9-kb amplicons in the isolated clonal mutants (P_{native}-*Tg*PKG-$HA_{3'IT}$-$3'UTR_{excised}$) as opposed to a 4.8-kb band in the progenitor strain (P_{native}-*Tg*PKG-$HA_{3'IT}$-$3'UTR_{floxed}$) (Figure 22C). The excision of 3'UTR and HXGPRT marker was further confirmed by DNA sequencing of PCR amplicons.

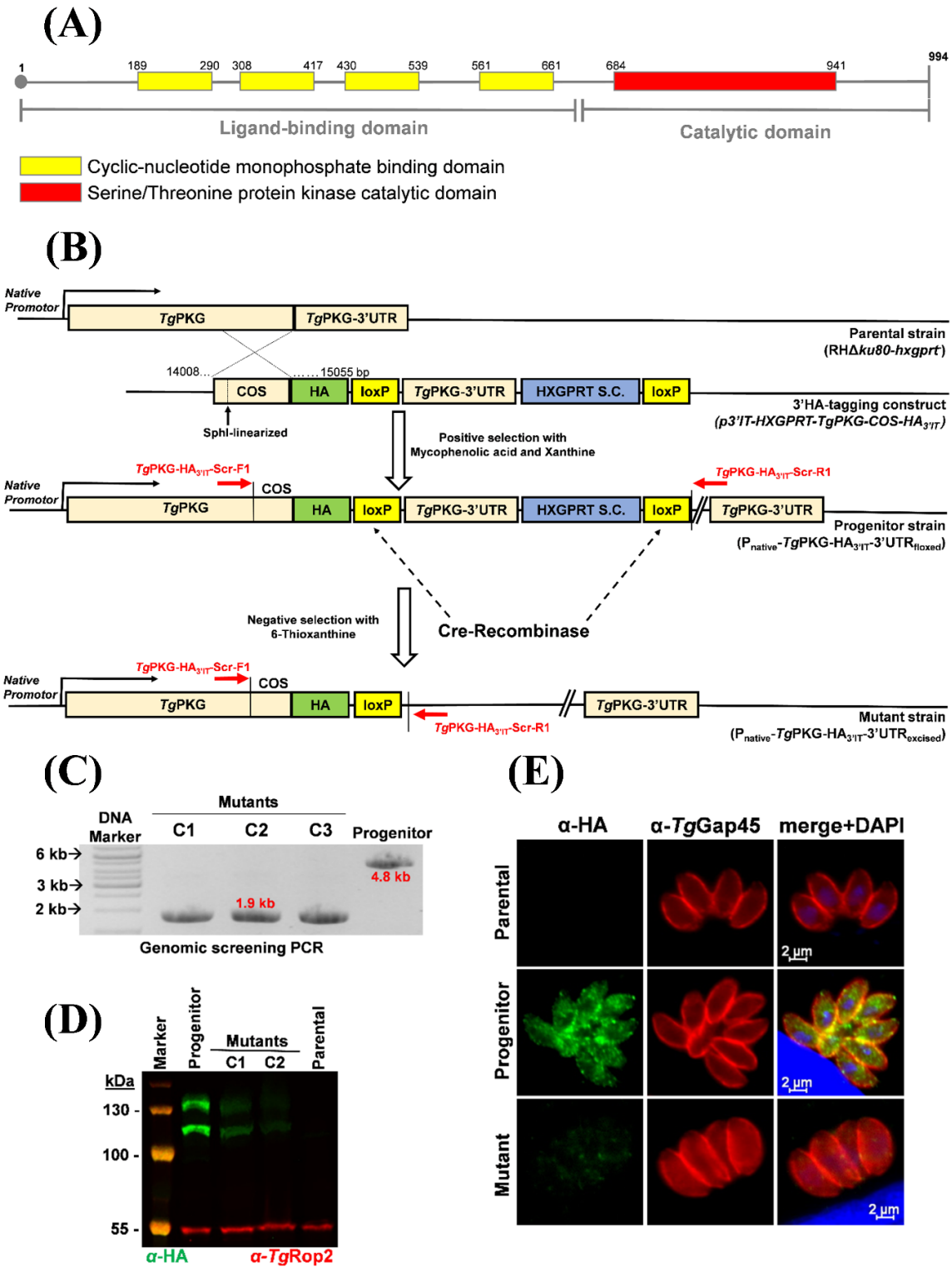

Figure 22. C-terminal epitope-tagging and Cre recombinase-mediated knockdown of *Tg*PKG in *T. gondii*. (A) The primary structure of *Tg*PKG as predicted by SMART and NCBI domain search online tools. The N-terminal (1-670 aa) comprises a ligand-binding domain with four subunits. C-terminal (670-994 aa) contains a serine/threonine protein kinase domain. **(B)** 3'-insertional tagging of the *Tg*PKG gene with an HA-epitope (step 1) and subsequent deletion of loxP-flanked (floxed) native 3'UTR by Cre recombinase (step 2). The construct for 3'-insertional tagging (3'IT) was transfected into the parental strain (RHΔ*ku80-hxgprt*$^-$) through crossover sequence (COS) and drug-selected for the HXGPRT selection cassette (S.C.). The eventual progenitor strain (P_{native}-*Tg*PKG-$HA_{3'IT}$-3'UTR_{floxed}) expressed *Tg*PKG-$HA_{3'IT}$ under its own regulatory elements. In the second step,

the progenitor strain was transfected with a vector expressing Cre-recombinase under *Tg*SagI promoter (60) to cutoff the floxed 3'UTR and HXGPRT by negative selection, which resulted in downregulation of *Tg*PKG in mutant (P_{native}-*Tg*PKG-$HA_{3'IT}$-3'$UTR_{excised}$). **(C)** Genomic screening PCR validating the integrity of the *Tg*PKG mutant generated by the excision of 3'UTR. Primers indicated as red-color arrows in *panel B* were used to test gDNAs isolated from the mutant clones (C1-C3) and progenitor strain. The mutagenesis was further confirmed by sequencing of amplicons (1.9-kb). **(D)** Immunoblot depicting the expression of *Tg*PKG isoforms in clonal mutants (C1 and C2) along with the progenitor and parental strains. Extracellular tachyzoites ($2x10^7$) of each strain were subjected to protein sample preparation, followed by immunoblotting with α-HA antibody. Expression of 112-kDa and 135-kDa isoforms in the progenitor and mutants, but not in the parental strain, confirms efficient 3'-HA tagging and successful knockdown of the *Tg*PKG protein, respectively. *Tg*Rop2 served as loading control. **(E)** The fluorescence images demonstrating the expression of *Tg*PKG-$HA_{3'IT}$ in the progenitor strain, and its downregulation in the 3'UTR-excised mutant. The parental strain was included as a negative control. Intracellular parasites (24 h post-infection) were stained with α-HA and α-*Tg*Gap45 antibodies. The merged image shows DAPI-stained host and parasite nuclei in blue.

Besides, 3'UTR excision gave rise to the reduced *Tg*PKG-$HA_{3'IT}$ expression which was validated by immunofluorescence and immunoblot assays (Figure 22D-E). Moreover, immunoblot of both *Tg*PKG-$HA_{3'IT}$ progenitor and *Tg*PKG-$HA_{3'IT}$-3'$UTR_{excised}$ mutant strains demonstrated two isoforms of *Tg*PKG, where the expression of smaller isoform (112-kDa/PKG^{II}) was found stronger than the larger one (135-kDa/PKG^{I}). Besides, excision of 3'UTR resulted in a marked reduction of both *Tg*PKG isoforms in the mutant. Densitometry analysis of immunoblots revealed a similar decline in the both isoforms of the mutant clones (135-kDa isoform, ~70%; 112-kDa isoform, ~85%) (Figure 22D). The expression of *Tg*PKG-$HA_{3'IT}$ was detected by immunofluorescence assay in cytoplasm and parasite membrane of intracellular parasites, as also reported earlier for PKG^{II} and PKG^{I} isoforms, respectively (72,107,108) (Figure 22E). Knockdown of *Tg*PKG-$HA_{3'IT}$ caused a residual HA-staining in IFA of the mutant parasites when compared to the progenitor strain, which is also in a harmony with immunoblot assay. Besides, the efficiency of Cre-loxP recombination was observed at about 93%, as judged by scoring HA^+ and HA^- vacuoles (Appendix 5B).

3.1.6 Knockdown of *Tg*PKG phenocopies the *Tg*ATPase$_P$-GC mutant

The *Tg*PKG knockdown mutant was examined during the lytic cycle of *T. gondii* tachyzoites for any phenotypic consequences (Figure 23 and 24). Cre recombinase-mediated 3'UTR excision of *Tg*PKG protein led to an analogous inhibition of the parasite growth in plaque assays of P_{native}-*Tg*PKG-$HA_{3'IT}$-3'$UTR_{excised}$ mutant (Figure 23A-C). The mutant formed smaller plaques (35% growth defect) when compared with the parental (RHΔ*ku80-hxgprt*$^-$) and progenitor (P_{native}-*Tg*PKG-$HA_{3'IT}$-3'UTR_{floxed}) strains (Figure 23C), whereas plaque numbers did not show any significant difference (Figure 23B). Yet again, comparable

to the *Tg*ATPase$_P$-GC mutant (Figure 18D), cell division of the *Tg*PKG mutant was only moderately affected, as judged by a smaller fraction of bigger vacuoles containing 16, 32 or 64 parasites both in early (24 h) and in late (40 h) cultures in comparison to its progenitor strain (Figure 23D). When considered together with the results obtained from *Tg*ATPase$_P$-GC mutant, the data indicates that cGMP signaling is not required for the parasite replication.

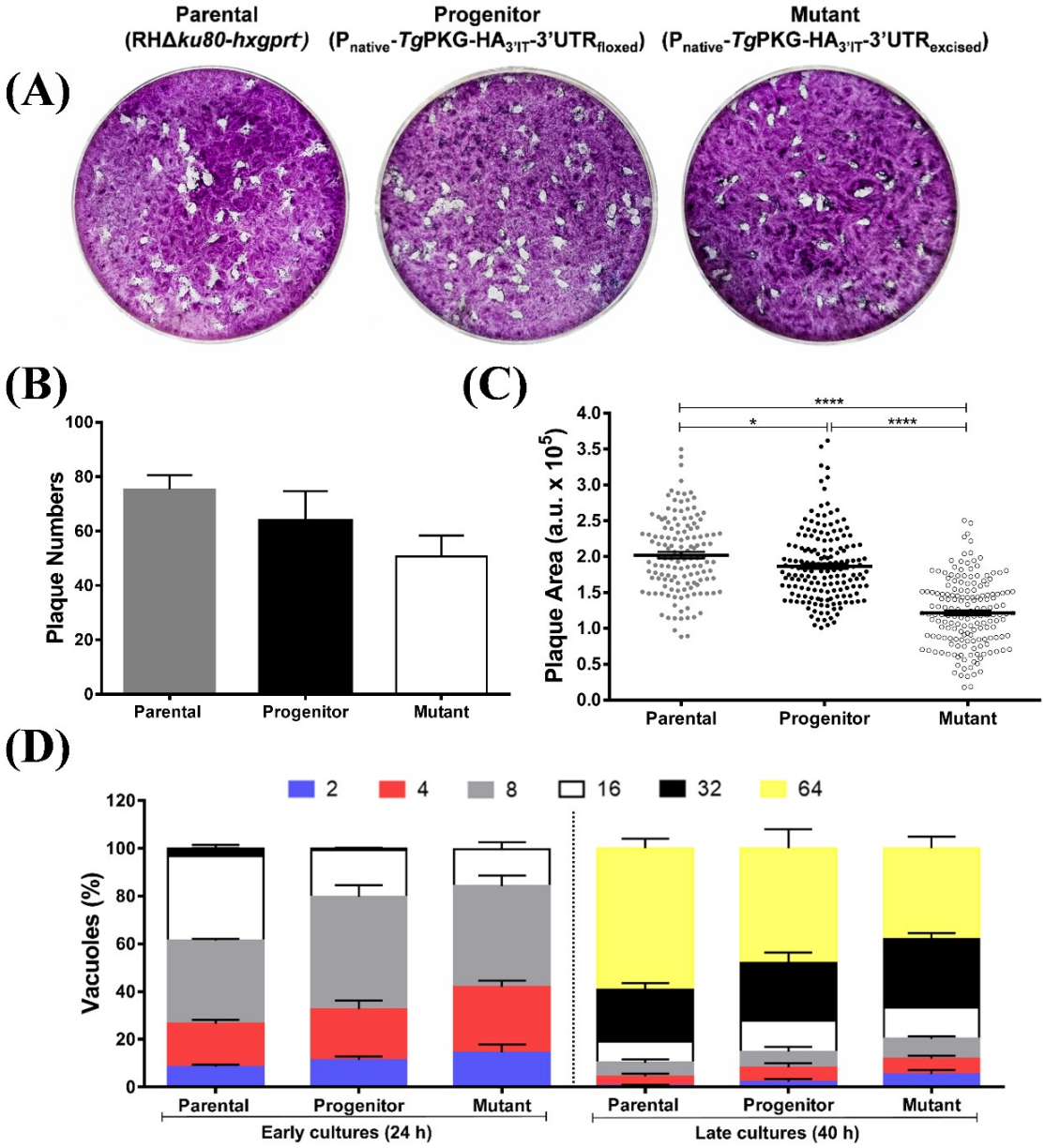

Figure 23. *Tg*PKG mutant showed an analogous growth inhibition phenotype with *Tg*ATPase$_P$-GC mutant. The progenitor (P_{native}-*Tg*PKG-$HA_{3'IT}$-3'UTR_{floxed}) and the mutant (P_{native}-*Tg*PKG-$HA_{3'IT}$-3'$UTR_{excised}$) strains were generated as illustrated in the Figure 22B. **(A-C)** Plaque assay revealing comparative growth of the mutant, progenitor and parental (RHΔ*ku80-hxgprt*$^-$) strains (n=3). **(A)** HFF monolayers grown in 6-well plates were infected with 150 fresh extracellular parasites following 7 days incubation, methanol fixation and crystal violet staining as described in *methods.* **(B)** The number of plaques of each strain was calculated. **(C)** The plaque area is shown in arbitrary units (a.u.). A total of 140-170 plaques for each strain were scored by ImageJ. Statistics was done by Student's *t*-test (*, p ≤0.05; ****, p ≤0.0001). **(D)** Replication rates of indicated strains during early

(24 h) and late (40 h) cultures. Intracellular tachyzoites proliferating in their vacuoles were stained with α-*Tg*Gap45 antibody. The numbers of tachyzoites per vacuole were counted from 400-500 vacuoles for each strain (n=3 assays). The means are shown with ±S.E.M.

Next, the significance of *Tg*PKG for the key points of lytic cycle; *i.e.* motility-dependent invasion and egress processes was investigated. A noteworthy invasion defect (~45%) was observed in the *Tg*PKG mutant (Figure 24A). In accord, the mutant exhibited a significant decrease in egress, which is noticeable at all tested time points (40-, 48- and 64-h) when compared to the parental and its progenitor strains. The defective egress of mutant was scored at least 50% in the early incubation times (40- and 48- h), which was more outstanding in 48 hpi, though this value was assuaged to 20% in 64 hpi (Figure 24B). It is also worth mentioning here that the progenitor *Tg*PKG-$HA_{3'IT}$ itself revealed about 42% egress delay (from ~85% to ~50%) in 48 h time point, as observed in the egress profile of the *Tg*ATPase$_P$-GC mutant. However, the delay was compensated at the later time (64 hpi) as opposed to *Tg*ATPase$_P$-GC mutant. Similarly, the motile fraction dropped by almost 50% in the *Tg*PKG knockdown mutant, and trail lengths were accordingly shorter (~24 µm) compared to the control strains (~55 µm) (Figure 24C).

Not least, the treatment with C2 (2 µM) further blocked the lytic cycle assays (Appendix 6), as expected. The motile fraction went down to ~4% both in the progenitor and in the mutant strains. Concordantly, the trail lengths were measured as the average of ~5 and ~10 µm for the mutant and its progenitor, respectively (Appendix 6A). The impact of C2 on the invasion and egress was somewhat stronger in the mutant (Appendix 6B-C), but none of the two strains exhibited a complete inhibition, which resonates again with the results of *Tg*ATPase$_P$-GC mutant (Figure 20). Collectively, the results clearly show that individual repression of *Tg*ATPase$_P$-GC and *Tg*PKG using a 3'UTR excision approach for the protein knockdown imposes nearly identical phenotypic defects on the lytic cycle.

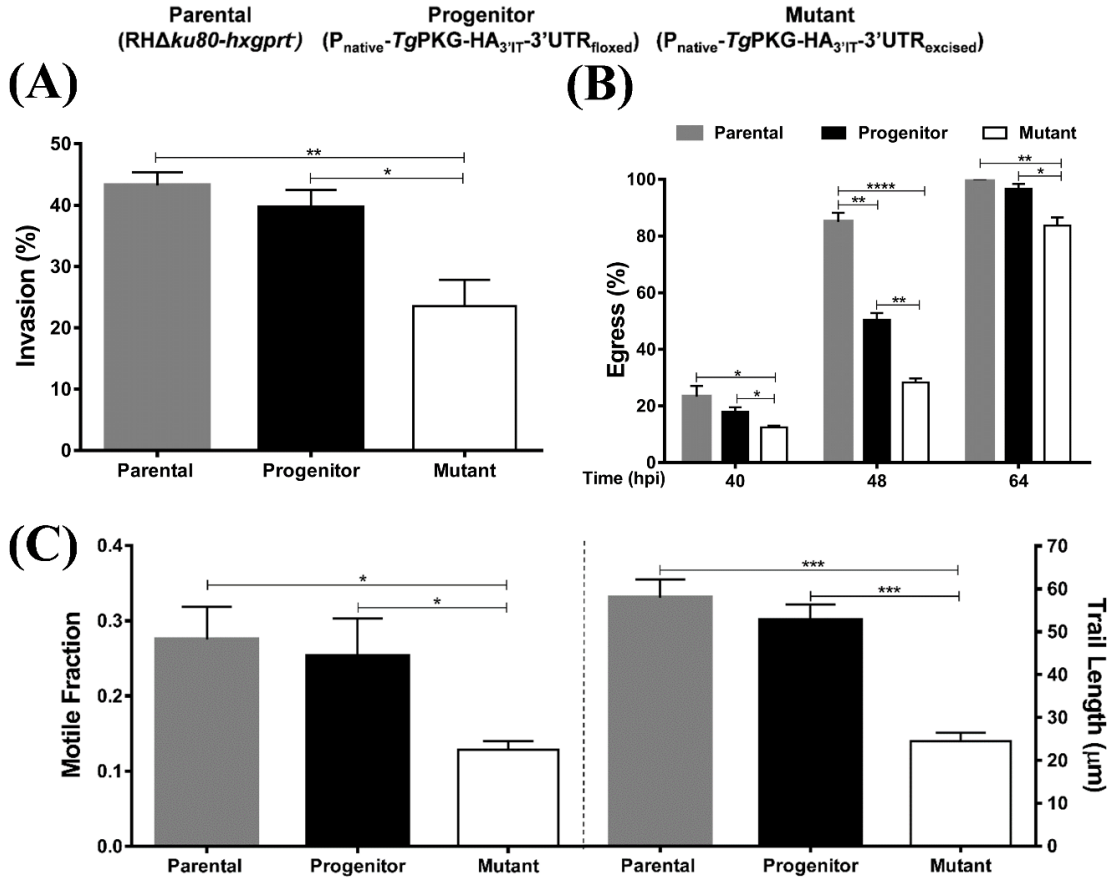

Figure 24. Mutagenesis of *Tg*PKG recapitulates the phenotype of the *Tg*ATPase$_P$-GC mutant. Progenitor (P_{native}-*Tg*PKG-$HA_{3'IT}$-3'UTR_{floxed}) and mutant (P_{native}-*Tg*PKG-$HA_{3'IT}$-3'$UTR_{excised}$) strains were generated as illustrated in the Figure 22B. **(A-B)** Invasion and egress profiles of the *Tg*PKG mutant along with the parental and progenitor parasites, as judged by dual-color staining. Intracellular tachyzoites were immunostained red using α-*Tg*Gap45 antibody, while extracellular ones appeared two-colored (red and green) stained with both α-*Tg*Gap45 and α-*Tg*Sag1 antibodies. **(A)** In total, 1000-1200 parasites were evaluated to score the invasion rate of each strain (n= 5 assays). **(B)** The percentage of ruptured vacuoles at indicated periods was determined by observing 400-500 vacuoles for each strain from 3 experiments. **(C)** The motile fraction and trail lengths of the indicated parasite strains. About 600 parasites were analyzed for the motile fraction, and 100 trail lengths were measured using ImageJ software, following immunostaining with α-*Tg*Sag1 (n= 3 assays). Numerical values in all graphs show the means with S.E.M. Statistical significance in individual assays was measured by comparing the mutant against the parental and progenitor strains (*, p ≤0.05; **, p ≤0.01; ***, p ≤0.001).

3.2 Optogenetic modulation of cGMP signaling in *T. gondii*

So far, cyclic nucleotide signaling research has been performed utilizing chemical modulators (*i.e.* activators and inhibitors) in combination with reverse genetics, as also applied in this study. Although it is a universal way to examine nucleotide signaling pathways, the aforesaid commercial drug usage is not the best method in two-organism systems, since it does not allow to selectively modulate the parasite-specific signaling. Furthermore, phenotypic consequences of genetic knockouts might be due to the non-specific

"knock-on effect" on downstream mediators and do not necessarily reflect the actual importance of the target protein, given the very rapid and transient nature of signaling. Notwithstanding the existing knowledge of cGMP signaling in the parasite, the affirmative evidence demonstrating a direct relationship between the specific induction of signaling within the parasite and subsequent activation of downstream molecular and phenotypic events is still lacking, because of the inadequacy of routine methods.

In this thesis, the application of optogenetics was integrated in *T. gondii* research with intent to (i) modulate and/or monitor cGMP signaling in real-time and adjustable manner in intracellular parasites without perturbing its host cells, (ii) determine the correlation between the activation of cGMP cascade and the onset of phenotypic events (motility-driven egress or invasion), (iii) evaluate the downstream impact of cGMP induction on calcium homeostasis. In accordance with these purposes, a photo-activated guanylate cyclase (RhoGC) from an aquatic fungus *Blastocladiella emersonii* (135,136) was stably expressed in *T. gondii* tachyzoites which permitted a fast, efficient and spatiotemporal control of cGMP signaling by green light (530 nm) exposure in a time-dependent manner during the lytic cycle of parasite.

3.2.1 Stable expression of light-activated RhoGC in tachyzoites

The RHΔ*ku80-hxgprt*⁻ strain of *T. gondii* was transfected with various plasmid constructs carrying RhoGC-ORF (please see the primer sequences in Table 1 and vector maps in the appendix 8) to examine whether RhoGC can be functionally expressed in the parasite. Four transgenic strains expressing RhoGC under different conditions were generated by following strategies (Figure 25):

1. The full length of RhoGC was tagged with HA-epitope from its C-terminal end. The RhoGC-HA fusion was then cloned into the *pTKO-DHFR/TS* vector whose transfection allowed random integration of expression cassette driven by *Tg*Gra1 promoter in *T. gondii* genome. Transgenic parasites were selected for the DHFR/TS expression using pyrimethamine (1 μM) (56). The resulting strain following limiting dilution from the stable pool was named as "RhoGC-HA" in this thesis (Figure 25A).

2. The HA-tagged RhoGC-ORF was firstly cloned into the above-mentioned *pTKO-DHFR/TS* plasmid as described in point 1. In the second step of cloning, a ligand-

controlled ddFKBP destabilization domain (DD) was inserted to the N-terminal of RhoGC, which enabled conditional expression of protein. The fusion of DD domain caused degradation of RhoGC protein in the absence of its ligand, Shield1, during regular culturing of transfected parasites (67). The transgenic strain termed as "DD-RhoGC-HA" in this study was supplemented with Shield1 (0.5 µM) 24 h prior to setting experiment to ensure protein expression (Figure 25B).

3. The ORF of RhoGC was fused with 3xHA-epitope at the C-terminus and cloned into *pDHFR-UPKO* plasmid, which permitted a weak to moderate expression of RhoGC flanked by *Tg*DHFR/TS regulatory elements (5'- and 3'- UTR). The transfection of this vector into tachyzoites enabled a single copy insertion of RhoGC-3xHA expression cassette to the UPRT locus. The transgenic strains named as "RhoGC-3xHA" were selected for the loss of UPRT using 5-fluorodeoxyuridine (FudR) (5 µM) (58) (Figure 25C).

4. To monitor the relationship between cGMP signaling and Ca^{+2} homeostasis within the parasite, a genetically-encoded calcium sensor GCaMP6s (146) was co-expressed with RhoGC-3xHA, both targeted at the UPRT locus. To achieve this, GCaMP6s-ORF was first cloned into *pGRA1-UPKO* vector to express it under strong *Tg*Gra1 promoter since it is known from a former study conducted in our group that the high expression of GECI does not affect the parasite growth (147). Thereafter, the whole GCaMP6s expression cassette was amplified and inserted into the constructed *pDHFR-UPKO-RhoGC-3xHA* plasmid described in point 3 from the end of RhoGC-3xHA expression cassette within the UPRT locus (Figure 25D). The orientation of GCaMP6s cassette was confirmed by DNA sequencing. The eventual vector was introduced into the RHΔ*ku80-hxgprt*⁻ strain to generate an optogenetic parasite termed "RhoGC-3xHA-GCaMP6s" in this study (Figure 25D).

The successful insertion and transcription of full length ORF of RhoGC and/or GCaMP6s were confirmed by PCR screening using cDNAs of clonal optogenetic strains (Appendix 7). Positive clones were further verified by the sequencing of PCR amplicons whose size were detected as 1900 and 1354 bp for RhoGC and GCaMP6s, respectively (Appendix 7).

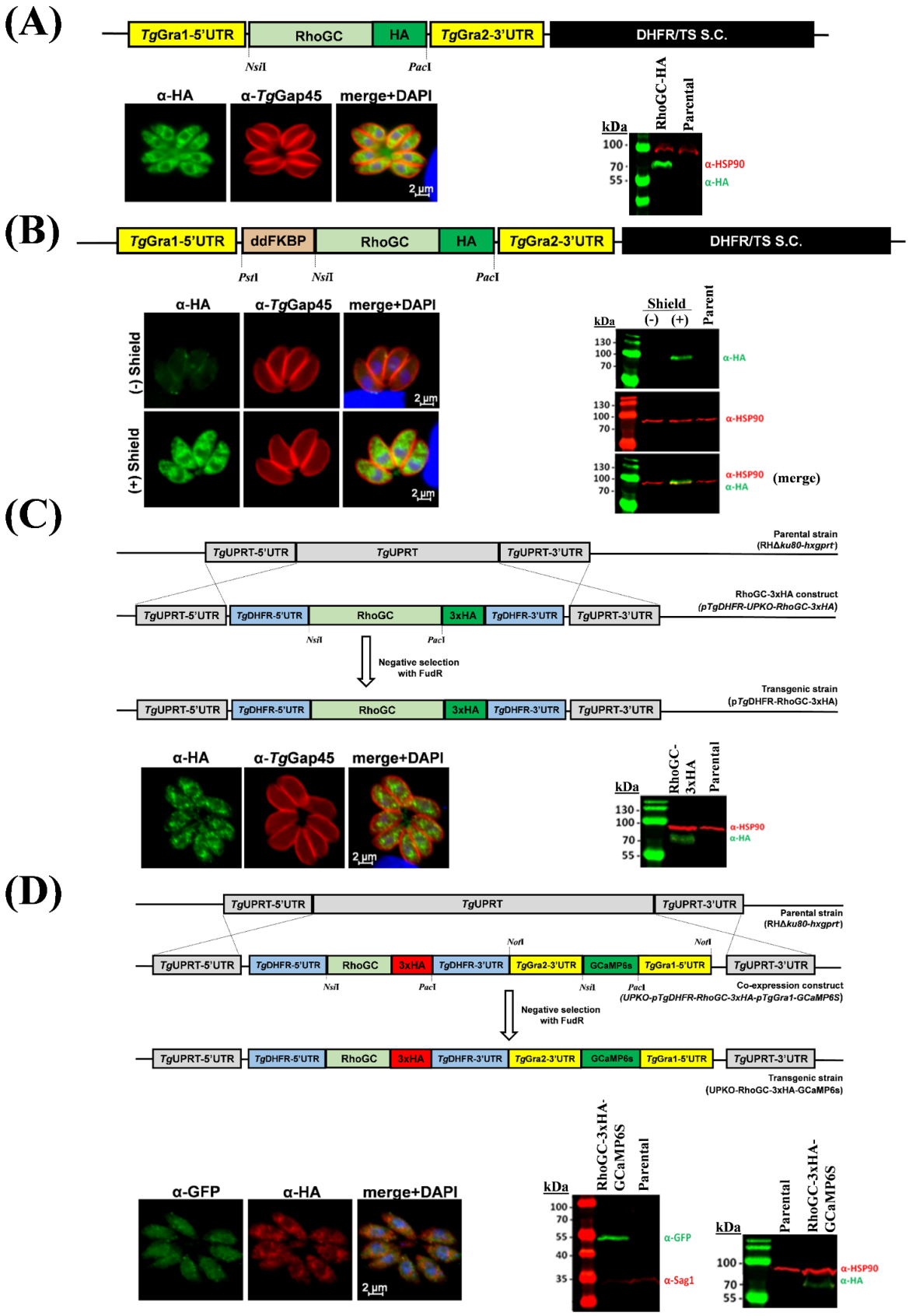

Figure 25. Different strategies for expression of photo-activated guanylate cyclase (RhoGC) in *T. gondii* tachyzoites. (A-B) Schematic illustrations for random integration of HA-tagged RhoGC (RhoGC-HA) driven by *Tg*Gra1 promoter and TgGra2-3'UTR. The *Nae*I-linearized plasmids were transfected into the parental strain (RHΔ*ku80-hxgprt*) to express RhoGC-HA either constitutively

(A), or conditionally **(B)** by introducing destabilization domain (ddFKBP) at the N-terminus of RhoGC, which enables RhoGC expression in the presence of Shield1. The optogenetic strains were selected by pyrimethamine (1 µM) for DHFR/TS selection cassette (S.C). **(C)** Scheme for a single copy insertion of 3xHA-tagged RhoGC (RhoGC-3xHA) by double homologous recombination targeting the *Tg*UPRT locus. The transgenic strain expressed RhoGC-3xHA under a weaker *Tg*DHFR/TS promotor, following drug-selection by FudR (5 µM) (The strain was generated by Claudia Ufermann in the scope of her project module studies under my lab supervision). **(A-C)** The resulting transgenic lines were immunostained by α-HA antibody for RhoGC co-localization. α-*Tg*Gap45 antibody was used as a control to stain IMC (24 h post infection). The merged images include DAPI-stained host and parasite nuclei in blue. Immunoblots using α-HA antibody exhibit the successful expression of RhoGC in all transgenic lines. DD-RhoGC-HA strain showed Shield1-dependent RhoGC expression both in IFA and immunoblot assays. Shield1 (0.5 µM) treatment was performed for 24 h prior to assays. Protein samples of the parental strain (RHΔ*ku80-hxgprt*$^-$) were used as a negative control, and α-*Tg*HSP90 antibody served as a loading control. **(D)** Scheme depicting tail-to-tail expression strategy of RhoGC-3xHA flanked by *Tg*DHFR/TS regulatory elements and GCaMP6s-ORF expressed under the *Tg*Gra1-5'UTR and *Tg*Gra2-3'UTR, both targeted at the *Tg*UPRT locus. Positive strains were subjected to IFA and immunoblot with α-HA (for RhoGC) and α-GFP (for GCaMP6s) antibodies. α-*Tg*HSP90 and α-*Tg*SagI antibodies were used as loading controls (The transgenic strain was made by Elena Pies during her master studies under my lab supervision).

Subsequently, all aforesaid optogenetic strains were subjected to immunostaining assay with the IMC marker *Tg*Gap45 antibody, resulted in cytosolic as well as perinuclear localization of HA-tagged RhoGC in intracellular parasites (Figure 25A-D). The intensity of HA-staining explicitly differed between the strains generated by random integration under strong promoter (RhoGC-HA and DD-RhoGC-HA) and a single gene copy insertion under weaker promoter (RhoGC-3xHA and RhoGC-3xHA-GCaMP6s) strategies. The perinuclear staining of RhoGC was more obvious in RhoGC-3xHA and RhoGC-3xHA-GCaMP6s strains. On the other hand, co-staining of EGFP domain of GCaMP6s sensor with RhoGC-3xHA revealed the distribution of GCaMP6s in the parasite cytosol of RhoGC-3xHA-GCaMP6s strain (Figure 25D), as reported earlier (147).

The successful expression of RhoGC was also demonstrated by an immunoblot analysis using α-HA antibody (Figure 25A-D). An apparent protein band of approximately 76-kDa was detected for RhoGC expression in all optogenetic strains apart from DD-RhoGC-HA, in which an expected band size of ~88-kDa was determined due to the fusion of DD-tag. Besides, DD-RhoGC-HA strain showed a Shield1-dependent expression of RhoGC both in immunofluorescence and immunoblot assays as a proof of concept for conditional regulation of protein, although a weak background of HA-staining could still be observed in the absence of Shield1 (Figure 25B). The number of parasites used to prepare protein samples for western blot analysis varied between the strains. While 10^7 parasites were enough to show the RhoGC expression in RhoGC-HA and DD-RhoGC-HA strains (Figure 25A-B), this

number was increased to $2x10^7$ for RhoGC-3xHA and RhoGC-3xHA-GCaMP6s strains due to relatively weaker RhoGC expression under *Tg*DHFR/TS promoter (Figure 25C-D). Similarly, the immunoblot of GCaMP6s using α-GFP antibody resulted in a ~55-kDa protein band on the membrane blot from 10^7 parasites of RhoGC-3xHA-GCaMP6s co-expressing culture (Figure 25D).

Taken together, these data confirmed the integrity of RhoGC and/or GCaMP6s constructs in newly engineered transgenic strains of *T. gondii,* which was essential to establish an optogenetic system in the parasite tachyzoites. Having multiple optogenetic strains provided the flexibility of different target-oriented applications.

3.2.2 Expression of RhoGC is not detrimental to tachyzoites

The overall growth fitness of the aforementioned transgenic parasite strains expressing light-activated RhoGC were examined by plaque assays which comprise 3-4 consecutive lytic cycles of parasite cultures. The parental strain (RHΔ*ku80-hxgprt*$^-$) was also included into the assays as a control (Figure 26). 150 parasites were counted from each cultures and released into a 6-well plate seeded with confluent host cells without any supplement, *i.e.* retinal, drug-selection or Shield1, which allowed to compare all strains under the standard culturing conditions. Cultures were incubated for 7 days without perturbation to let parasites producing plaques. Methanol-fixed and crystal violet-stained wells were evaluated by relative plaque numbers and plaque area (Figure 26A). The average plaque numbers of all strains including parental strain ranged from 75 to 85 without any significant difference (Figure 26B). Importantly, the expression of RhoGC did not cause any negative impact on the plaque size produced by optogenetic strains in comparison to the parental strain (Figure 26C). Considering these data, it can be said that the expression of RhoGC or co-expression of RhoGC with GCaMP6s does not have any toxic effect on the parasite growth, which permitted further comparison and testing of subsequent optogenetic assays.

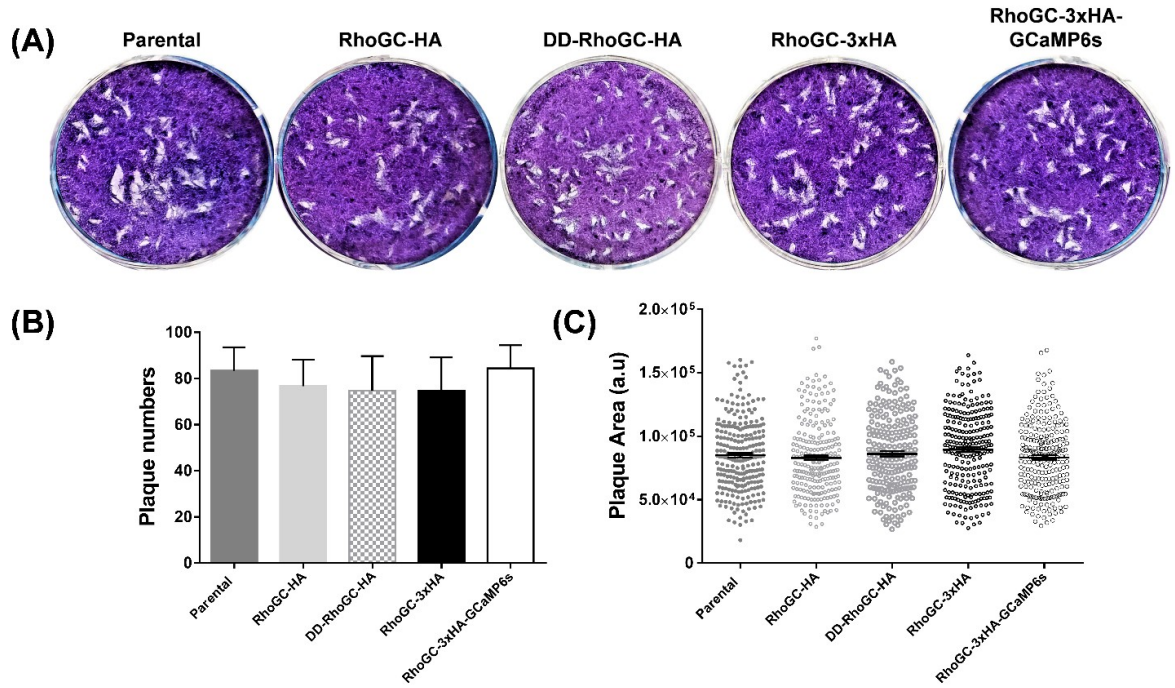

Figure 26. Expression of light-activated RhoGC does not affect the growth of tachyzoites. (A) Images illustrating a representative plaque assay of RhoGC-expressing optogenetic strains in comparison to the parental (RHΔ*ku80-hxgprt*) strain. 6-well plates with confluent HFF monolayers were infected with freshly syringe-released parasites (150) and then incubated for 7 days in a standard culture medium without intervention. Following incubation, cultures were fixed with methanol and stained with crystal violet. Blank areas represent plaques formed by each infective parasite, and purple staining denotes host cell monolayers. **(B)** The average plaque numbers were scored for all parasite strains from three independent assays. **(C)** The area of each plaque (arbitrary units, a.u.) was measured by ImageJ software. About 200-250 plaques for each strain (n=3) were evaluated for the growth phenotype. Statistical analysis was performed by Student's *t* test (mean with ±S.E.M). (Assays were performed by Elena Pies and counted by Anika Freitag within the scope of their master theses under my lab supervision).

3.2.3 Kinetics of GMP induction in RhoGC-expressing tachyzoites

To test whether RhoGC is functional in *T. gondii* tachyzoites, the optogenetic strains were investigated for induction of cGMP by green light (530 nm, 197,4 µW/cm^2) (Figure 27). Among four optogenetic strains (section 3.2.1), two strains were selected for functional testing: (i) DD-RhoGC-HA strain expressing RhoGC conditionally under a strong *Tg*Gra1 promoter, (ii) RhoGC-3xHA parasite strain expressing a single RhoGC copy driven by weaker *Tg*DHFR/TS regulatory elements. The effect of green light-exposure was evaluated in fresh syringe-released extracellular parasites supplemented with retinal (1 µM) and Shield1 (0.5 µM, if required) prior to experiment. Seven samples, each containing 2.5x10^6 parasites in 100 µl of colorless DMEM aliquot, were prepared from optogenetic cultures. In principle, one sample aliquot was always kept in the dark to determine the steady-state cGMP level of parasites. Each of the remaining samples was then released in a well of a black-wall

24 well-plate, followed by a light illumination from the bottom using the LED device described elsewhere (section 2.7.1). Parasite samples were stimulated by the light pulses at 530 nm in 197,4 μW/cm^2 intensity, but with different durations (varies from 30 sec to 5 min). The assay was immediately quenched following light illumination, and cGMP levels of parasites were measured by commercial "DetectX High Sensitivity Direct cGMP kit" (Figure 27A).

As seen in Figure 27A, optogenetic strains (DD-RhoGC-HA and RhoGC-3xHA) responded disparately to the green light exposure as reflected by cGMP levels of the parasites over the illumination time. cGMP amount in dark sample was about 220 fmol/10^6 parasites in DD-RhoGC-HA strain (Figure 27A-B). The RhoGC expressed in DD-RhoGC-HA strain was activated within 1 min of light exposure, thus 2-fold increase (~450 fmol/10^6 parasites) in cGMP level was observed when compared to the basal state (dark) measurement (Figure 27A). The longer photo-stimulation gradually elevated cGMP amount in the DD-RhoGC-HA strain, which was measured as ~1.48 pmol/10^6 parasites after 3 min illumination (Figure 27A). A 5 min green light exposure to the optogenetic strain caused ~16.5-fold increase in the cGMP level (~3.45 pmol/10^6 parasites) (Figure 27A-B). A nearly linear increase in cGMP induction (as a result of light illumination from 1 min to 5 min) suggests that the level of cGMP is not saturated yet in the DD-RhoGC-HA strain. Besides, GTP as a cellular resource is not a limiting factor to restrict cGMP induction in extracellular parasites.

On the other hand, cGMP level in dark sample of RhoGC-3xHA strain was slightly less (~180 fmol//10^6 parasites) than the measured in the DD-RhoGC-HA (Figure 27A). A 1 min green light exposure was not enough to activate RhoGC expressed under the weaker *Tg*DHFR/TS promoter in the RhoGC-3xHA strain. However, cGMP level increased slightly in culture after 2 min illumination (~235 fmol//10^6 parasites). A 3 min exposure caused to double the amount of cGMP (~398 fmol//10^6 parasites) in comparison to dark sample. After 4 min light illumination, ~1055 fmol of cGMP per a million extracellular parasites was quantified (Figure 27A). Additional light exposure did not show any significant influence in cGMP level, indicating a maximal catalytic activity of RhoGC in the RhoGC-3xHA strain. A 5 min green light exposure of RhoGC-3xHA strain revealed about 6.3-fold induction of the basal cGMP level in the extracellular parasites (Figure 27B).

These data confirm that the light-activated RhoGC was functional in *T. gondii* tachyzoites, which allowed an optogenetic control of cGMP in time-dependent manner.

Working with extracellular parasites enabled to evaluate the intrinsic cGMP levels in *T. gondii* without an involvement of host-cell originated cGMP. The effect of light illumination was stronger in DD-RhoGC-HA when compared to the RhoGC-3xHA strain, which is also consistent with the level of RhoGC expression. Besides, the cGMP profile of RhoGC-3xHA permitted to select the optimal duration of light illumination (5 min) for downstream assays.

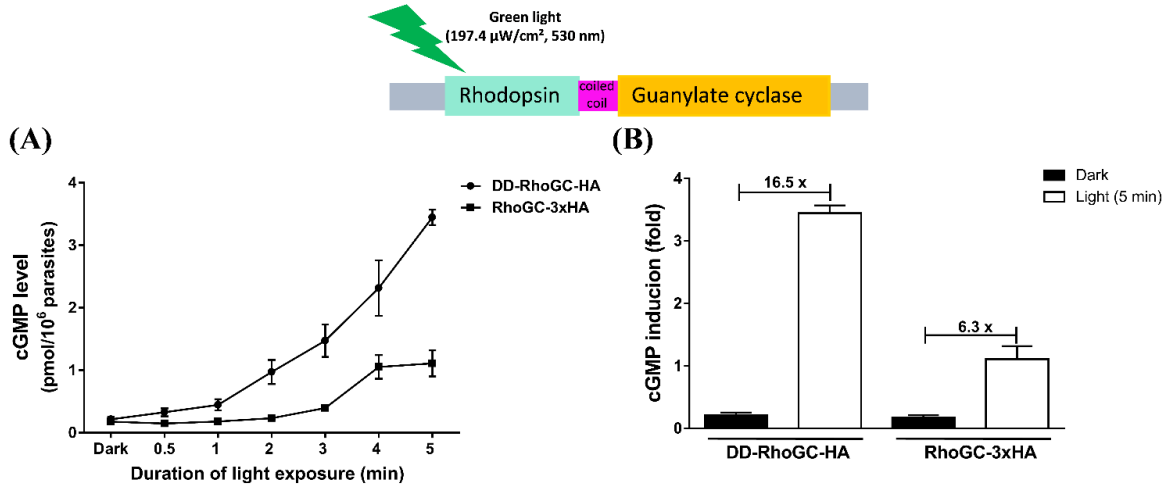

Figure 27. Expression of RhoGC in tachyzoites allows cGMP induction by green light. HFFs grown in Petri dishes were infected (MOI:1.5) with RhoGC-expressing transgenic lines (DD-RhoGC-HA, RhoGC-3xHA) and incubated for 38-40 h in D10 medium supplemented by 1 µM of retinal and 0.5 µM of Shield1 (if required). Mature parasite cultures were scraped, syringe-released (2x27G) to set parasites free and filter-passed (5 µm) to eliminate host-cell debris. **(A)** Fresh extracellular parasites ($2.5x10^6$) were exposed to green light (530 nm, 197,4 µW/cm^2 intensity) in colorless DMEM medium for indicated durations, followed by cell lysis immediately by sample diluent provided by commercial "DetectX High Sensitivity Direct cGMP kit" (K020-C1, Arbor Assays). cGMP amounts were measured following kit instructions, and the data was normalized per 10^6 parasites (n=2). **(B)** Induction of cGMP in two different RhoGC-expressing transgenic parasite strains following 5 min green light exposure (n=2). The bars show the mean with ± S.E.M.

3.2.4 Photo-stimulation of RhoGC induces motility, invasion and egress

The importance of native cGMP signaling for the successful lytic cycle of *T. gondii* has been already described by experimental evidences in the first part of this thesis (section 3.1). Having functional optogenetic strains enabled to investigate the direct effect of increased subcellular cGMP levels on distinct steps of lytic cycle. Prior to setting up experiments, intracellular tachyzoites were incubated for 38-40 h with 1 µM of retinal. DD-RhoGC-HA strain was also supplemented with 0.5 µM of Shield1 to stabilize the expression of RhoGC. Fresh syringe-released parasites were subjected to motility, invasion and egress assays. A 5 min light illumination (530 nm) with defined intensity (197,4 µW/cm^2) was performed on the RhoGC-HA, DD-RhoGC-3xHA, RhoGC-3xHA and RhoGC-3xHA-GCaMP6s strains.

Besides the dark samples of optogenetic strains, the parental strain (RHΔ*ku80-hxgprt*$^{-}$) was also included in all assays as a negative control (Figure 28).

Figure 28A shows the representative gliding motility images of all strains in dark and light conditions. The fraction of motile parasites in the parental culture was not affected by light, as expected. Besides, the average motile fraction of dark samples of all transgenic strains was also similar to the parental strain, which indicates the absence of dark activity in RhoGC-expressing strains (Figure 28B). The excitation of RhoGC by light stimulated the gliding motility of optogenetic strains leading at least 2-fold increase (from ~30% to ~60%) in the motile fraction of all four optogenetic parasite strains when compared to their respective dark cultures (Figure 28B). Likewise, the average trail lengths of moving parasites in dark samples of all strains including the parental line ranged from 22 to 25 μm without any significant difference. The light exposure resulted in making three times longer trails (~60-63 μm) in all RhoGC-expressing parasite strains (Figure 28C).

Next, the invasion and egress efficiencies of RhoGC-expressing strain were tested (Figure 28D-E) in response to the green light because these events are dependent on the gliding motiliy (42,100,106). The invasion rate of dark samples of optogenetic strains was scored quite similar to the invasion efficiency of the parental strain, exhibiting approximately 36-42% invading parasites (Figure 28D). This rate was enhanced to ~60% (as the observed highest level) in RhoGC-HA strain after light exposure, corresponding to 1.5-fold increase, when compared to dark samples of all strains. On the other hand, DD-RhoGC-HA, RhoGC-3xHA and RhoGC-3xHA-GCaMP6s strains behaved similarly to the green light illumination showing an enhanced invasion (~55-57%) in comparison to their respective dark samples (Figure 28D).

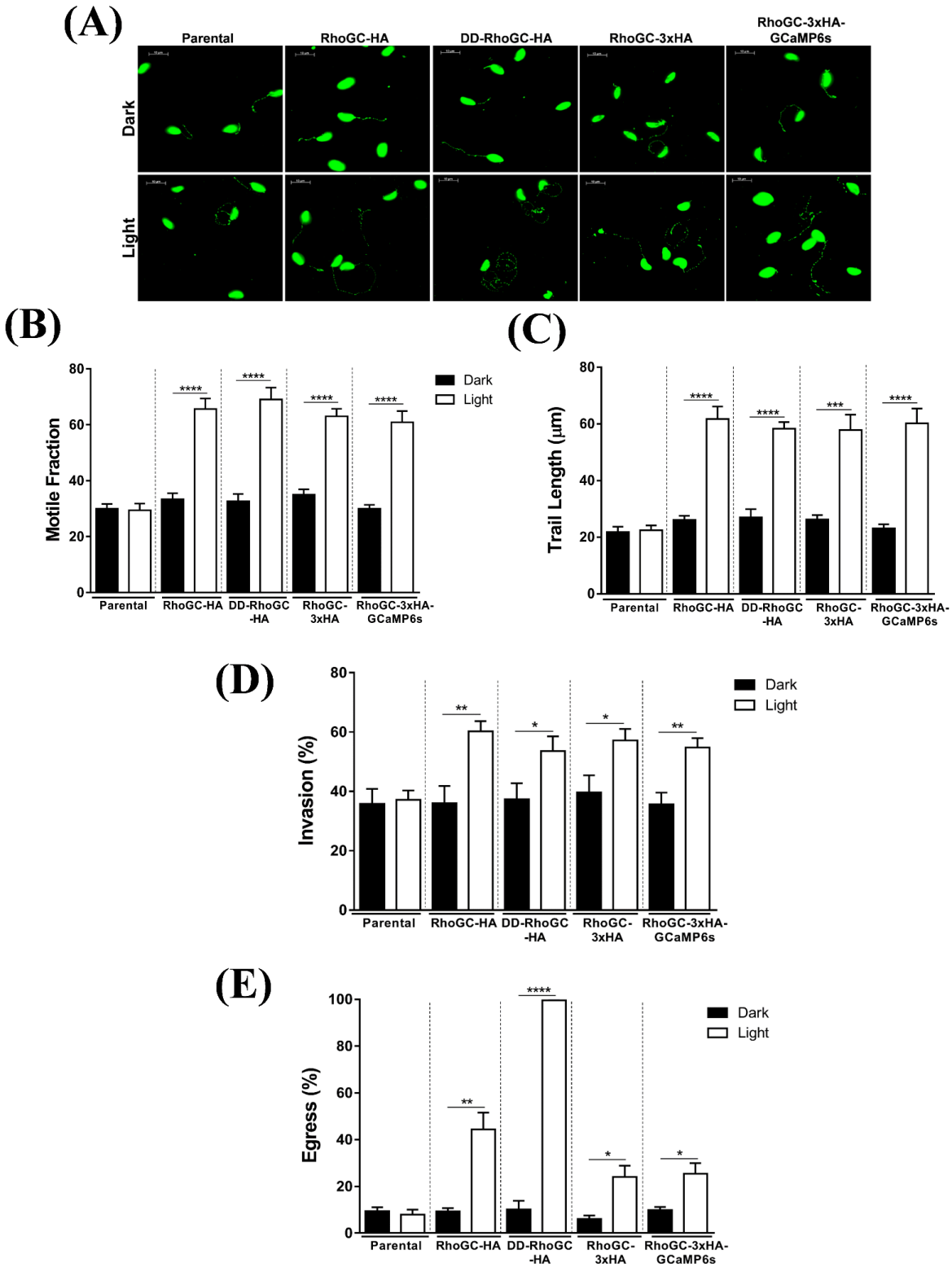

Figure 28. Activation of RhoGC stimulates motility-dependent invasion and egress. Tachyzoites of the indicated strains were used to examine the impact of RhoGC activation in **(A-C)** motility, **(D)** invasion and **(E)** egress as described in section 2.7.2. Optogenetic strains were induced by the green light (197.4 μW/cm² intensity, 530 nm wavelength) or kept in the dark for the assays. Parental (RHΔ*ku80-hxgprt*) strain was included as a negative control. **(A)** Representative images of the gliding motility on the BSA-coated glass coverslips. Parasites and their trails were immunostained with α-*Tg*Sag1 antibody. The scale bars represent 10 μm. **(B-C)** To evaluate gliding motility, around 1000 parasites were analyzed for motile fraction, and a total of 500-600 trail lengths for each strain

was measured by ImageJ under each condition. **(D-E)** Invasion and egress rates were scored by counting of parasites and vacuoles, respectively, after the dual staining with α-*Tg*Gap45 and α-*Tg*Sag1 antibodies as explained in *methods* section. At least 800 parasites or vacuoles per each strain were examined for invasion and egress efficiency, respectively. The data were evaluated from three independent experiments, each with two replicates, for the motility, invasion and egress assays. (Lytic cycle assays were set by Elena Pies and Anika Freitag followed by evaluation of results individually from one replicate within the context of their master thesis under my supervision. The obtained data were pooled in this thesis). Statistical comparing light and dark samples was performed by Student's *t* test. The significance was measured of each individual strain (*, $p \leq 0.05$; **, $p \leq 0.01$; ***, $p \leq 0.001$; ****, $p \leq 0.0001$; the means with ±S.E.M).

Although invasion profiles of optogenetic strains conform with the motility data by showing almost the same proportion of increase in response to light, the egress phenotypes of strains differed from each other (Figure 28E). All dark samples of studied parasite strains including the parental exhibited an about 8-13% natural egress 24 h post infection. The light-exposed transgenic parasite samples demonstrated an explicitly higher but different rates of egress in comparison to their dark samples. Almost all parasites were egressed in DD-RhoGC-HA strain after 5 min illumination. However, the percentage of egressed vacuoles in light-stimulated RhoGC-HA strain was only counted as ~40%, although it shares features (*i.e*. promoter strength, random insertion) with DD-RhoGC-HA line except for ddFKBP-tagging. On the other hand, RhoGC-3xHA and RhoGC-3xHA-GCaMP6s lines were consistent in their light-illuminated egress profile, both revealing ~2.5-fold increase with 25-27% egressed vacuole (Figure 28E).

Collectively, these results reveal that the photo-activation of RhoGC in tachyzoites augments the motility, invasion and egress events. Besides, the data are consistent with the genetic knockdown studies of *Tg*ATPase$_P$-GC and *Tg*PKG, which indicates the importance of cGMP regulation for the lytic cycle of parasite.

3.2.5 Co-expression of RhoGC and GCaMP6s in tachyzoites to study the impact of cGMP on Ca^{2+}

cGMP and Ca^{2+} signaling pathways are essential for the asexual reproduction of *T. gondii.* They are tightly coordinated with each other to assure the successful lytic cycle (42,115,185). The optogenetic strain co-expressing RhoGC-3xHA and GCaMP6s was used to measure the cytosolic Ca^{2+} in response to light activation of RhoGC in tachyzoites. In this regard, intracellular parasites of RhoGC-3xHA-GCaMP6s strain were tested whether the induction of cGMP by light also leads to an increase in calcium level. Binding of calcium to

GCaMP6s causes an enhancement in EGFP fluorescence, which allows dynamic monitoring of cytosolic calcium in the parasite (Figure 29).

HFF-monolayers grown on the glass coverslips were infected with RhoGC-3xHA-GCaMP6s strain (MOI:1.5) and incubated for 40 h. Intracellular parasites within mature vacuoles were illuminated by light (530 nm, 197,4 μW/cm² intensity) from the bottom with different durations (1 min, 2 min or 5 min) using the LED device described in section 2.7.1 or kept in dark, followed by immediate fixation of samples. The GFP fluorescence of vacuoles was analyzed under the microscope empirically (low-medium-high) to examine whether cGMP induction can promote Ca^{2+} increase in tachyzoites (Figure 29A).

As shown in Figure 29B, ~60% of the vacuoles in RhoGC-3xHA-GCaMP6s strain exhibited the background GFP signal in the dark (standard culture) condition. The fraction of vacuoles with high signal intensity was only about 8%. Exposure to light for 1 min had a minor influence on cGMP induction (Figure 27A), which also correspondingly monitored on calcium levels (Figure 29B). The percentage of the vacuoles with low, medium and high GFP fluorescence was scored as about 40%, 44% and 16%, respectively in response to 1 min light exposure. The fluorescence profile did not change much after 2 min illumination (Figure 29B), as also similarly observed in cGMP levels (Figure 27A). However, 5 min exposure caused a significant 5-fold increase (up to 40%) in the fraction of vacuoles with high GFP signal when compared to the dark sample, which is yet again compatible with the cGMP measurement assay (Figure 27). Accordingly, the rate of vacuoles with low GFP intensity decreased from ~60% to ~18% after 5 min illumination (Figure 29B).

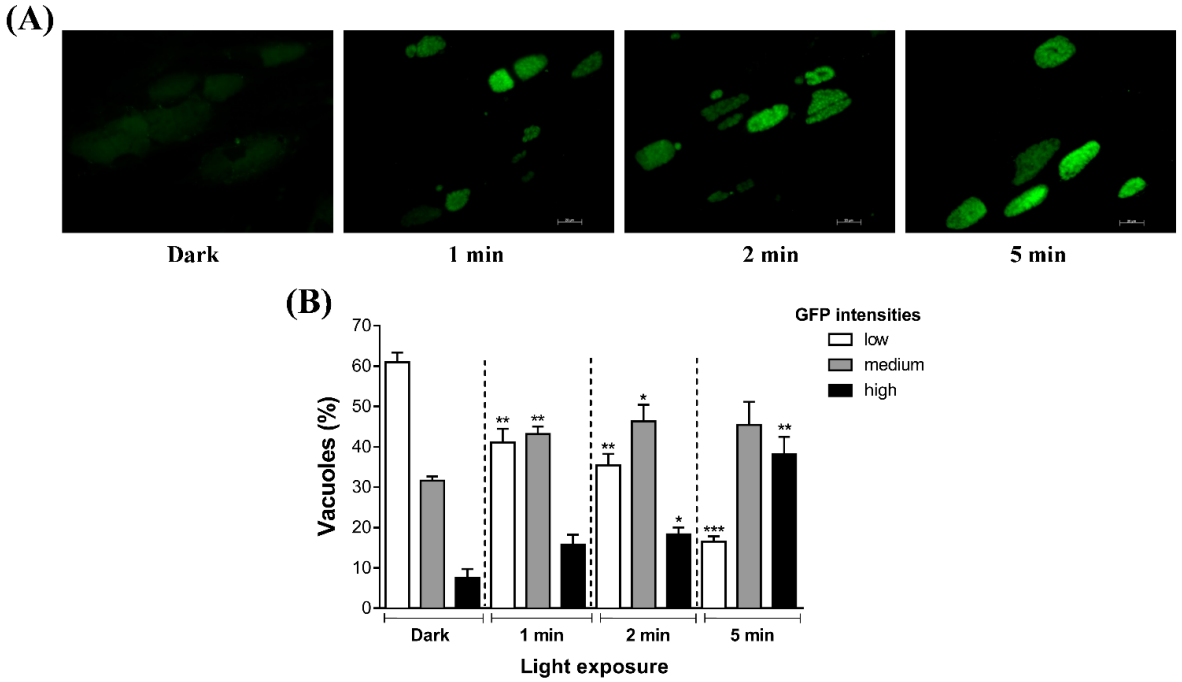

Figure 29. Light induction of RhoGC leads to increased cytosolic calcium. An optogenetic strain co-expressing the light-activated RhoGC and calcium sensor GCaMP6s was generated as described in section 3.2.1. **(A)** Representative pictures of mature vacuoles (36-42 hpi) of RhoGC-3xHA-GCaMP6s strain exhibiting EGFP-derived fluorescence of GCaMP6s in response to the green light (530 nm, 197,4 µW/cm²). The samples of transgenic strain were exposed to the green light for 1 min, 2 min, or 5 min or kept in the dark, followed by gently fixation. The images were created at 250 msec exposure time. The scale bars represent 20 µm. **(B)** In total, 500 vacuoles from 3 assays were scored empirically for GFP fluorescence intensity as low, medium or high. Statistical analysis was performed using the Student's *t*-test. Significance refers to the dark samples; *, $p \leq 0.05$; **, $p \leq 0.01$; ***, $p \leq 0.001$, the means with ±S.E.M. (The assay was performed by Elena Pies in the scope of master thesis under my supervision).

These data indicate a direct linkage between cGMP and Ca^{2+} signaling and support to the notion that calcium is released from the storage organelles to the cytosol, once intracellular cGMP level is increased in the parasites. It also seems that a threshold induction of cGMP is required to stimulate calcium release in the parasite. The successful application of optogenetic approach provides an opportunity to discern the effect of cGMP on calcium homeostasis during the lytic cycle.

4 Discussion

4.1 Evolutionary characteristics and possible multi-functionality of *Tg*ATPase$_P$-GC

The first part of this study (186) characterized an alveolate-specific protein, termed *Tg*ATPase$_P$-GC herein, which imparts a central piece of cGMP signaling conundrum in *T. gondii*. The research conducted within this thesis provides a comprehensive functional and structural insight into the initiation of cGMP signaling in *T. gondii* in conjunction with three recently published independent studies while this work has been performed (99,153,154). The parasite encodes an unusual and multifunctional protein (*Tg*ATPase$_P$-GC) primarily localized in the plasma membrane at the apical pole of the tachyzoite stage. Previous reports have concluded a surface localization of *Tg*ATPase$_P$-GC by inference, which we reveal to be the plasma membrane as opposed to the inner membrane complex (Figure 15C).

Interestingly, a confined localization of GCβ in a unique spot of the ookinete membrane was recently reported to be critical for the protein function in *P. yoelii* (152). Similar work in *T. gondii* (99) demonstrated that deletion or mutation of ATPase domain in *Tg*ATPase$_P$-GC mislocalized the protein to the ER and cytosol, whereas deletion or mutation of GC domains did not affect the apical localization. An impaired secretion of micronemes was observed in both cases, suggesting the importance of ATPase domain both for localization and function. Earlier, it was reported that the long isoform of *Tg*PKG (*Tg*PKG^I) associated with the plasma membrane is essential and sufficient for PKG-dependent events during the lytic cycle, however the shorter cytosolic isoform (*Tg*PKG^{II}) is inadequate and dispensable (72). It was illustrated in this thesis that C-terminal of *Tg*ATPase$_P$-GC faces inside the plasmalemma bilayer (Figure 15B), where it should be in spatial proximity with *Tg*PKG^I to allow efficient induction of cGMP signaling. Moreover, it was also shown that *Tg*ATPase$_P$-GC is expressed throughout the lytic cycle of tachyzoites but required only for their entry or exit from host cells, which implies a post-translational activation of cGMP signaling.

This work along with others (99,153,154) reveals that *Tg*ATPase$_P$-GC is essential for a successful lytic cycle. Its knockdown by 3'UTR excision using Cre/loxP method confirmed a physiological role of cGMP for the invasion and egress. The effect however was reflected at most in motility of parasite. The treatment of cGMP agonists, BIPPO and zaprinast, resulted in a fast rescue of motility defect; while inhibition of *Tg*PKG by compound 2 further

blocked the gliding motility in *Tg*ATPase$_P$-GC mutant, which indicates once more the regulatory effect of cGMP signaling on the infectivity of tachyzoites. On the contrary, the knockdown of *Tg*ATPase$_P$-GC revealed that the protein is not required for parasite replication, as also confirmed by two recent studies (99,154). In further work, the depletion of *Tg*PKG by using the same knockdown approach phenocopied the *Tg*ATPase$_P$-GC knockdown mutant, which resonates again with a previous work (72).

The predicted topology of *Tg*ATPase$_P$-GC harboring 22 transmembrane helices within this thesis differs from the work of Yang *et al.* (154) suggesting the occurrence of 19 helices, but echoes with the two other reports (99,153). The similar organization of the transmembrane helices was also reported previously for GCα and GCβ of *P. falciparum* as well as GC of *Paramecium* (97,150). Besides, *in silico* analysis of *Tg*ATPase$_P$-GC offers valuable insights into bifunctional arrangement as well as regulatory and catalytic functions of ATPase and GC domains in *Tg*ATPase$_P$-GC, respectively. GC1 and GC2 of *Tg*ATPase$_P$-GC dimerize to form only one pseudo-symmetric catalytic center in contrast to the homodimer formation in mammalian pGCs (89,176,177). GC1 and GC2 have probably evolved by gene duplication causing degeneration of the unused second regulatory binding site in protists, as reported in tmACs (176,177,187). Contrary to tmACs, the conserved residues that are involved in heterodimerization are found as inverted in GC1 and GC2 of *Tg*ATPase$_P$-GC, which is consistent with the previous report of *Pf*GCα and *Pf*GCβ (150). The function of *Tg*ATPase$_P$-GC as a guanylate cyclase aligns rather well with its predicted substrate specificity for GTP, though its contribution for cAMP synthesis (if any) remains to be tested. Several attempts to functionally complement maltose metabolism of an adenylate cyclase-deficient *E. coli* mutant (161) by expressing only guanylate cyclase domain of *Tg*ATPase$_P$-GC were not fruitful in this study; however it could still be demonstrated that the repression of *Tg*ATPase$_P$-GC leads to a comparable reduction in cGMP level of parasite (Figure 17E), which indicates its guanylate cyclase function.

Unlike the C-terminal guanylate cyclase of *Tg*ATPase$_P$-GC, the exact function of N-terminal ATPase domain remains rather obscure. The latter resembles P4-ATPases similar to other alveolate GCs (97,98,151). Lipids and cation homeostasis have been shown to influence the gliding motility and associated protein secretion, which in turn drives the egress and invasion events (100,102,104,188,189). There is a little evidence though, how lipid and cation-dependent pathways embrace each other. It thus tempts to propose a nodal role of

*Tg*ATPase$_P$-GC in asymmetric distribution of phospholipids in the lipid bilayer, and cation flux (*e.g.*, Ca^{2+}, K^+, Na^+) across the plasma membrane. The recent studies (99,153) also entail a regulatory role of P4-ATPase domain on the functioning of GC domain. Conversely, the GC domain of GCβ was found sufficient to produce cGMP independently of the ATPase domain in *P. yoelii* (152). This may be due to degenerated conserved sequences in the ATPase domain of *Pf*GCβ, as shown in the sequence alignment (Appendix 2). Equally, the expression of *Pf*GCα and *Pf*GCβ resulted in the functional protein only for *Pf*GCβ, but not for *Pf*GCα (151). Likewise, the heterologous expression of GC catalytic domains of *Tg*ATPase$_P$-GC in *E. coli* and subsequent GC assays did not yield to cGMP production in this study. As shown by phylogeny (Figure 12), *Tg*ATPase$_P$-GC is more homologous to *Pf*GCα (Identity, 43%; E value, $3E^{-140}$), which may explain the differences in the *Pf*GCβ and *Tg*ATPase$_P$-GC mutants.

Two additional components, cell division component 50 (CDC50.1) and unique GC organizer (UGO), were suggested to secure the functionality of *Tg*ATPase$_P$-GC by interacting with ATPase and GC domains, respectively (153). It was already known that most of the mammalian P4-ATPases require CDC50 proteins as accessory subunits which are transmembrane glycoproteins ensuring formation of active P4-ATPase complex (170,190). A similar interaction between GCβ and CDC50A protein was also shown in *P. yoelii* (152). The CDC50.1 expressed in *T. gondii* was also found in connection with the P4-ATPase domain of *Tg*ATPase$_P$-GC to facilitate the recognition of phosphatidic acid, and thereby regulating the activation of GC domain. The second interacting partner UGO on the other hand was proposed to be essential for the activation of GC domain after phosphatidic acid binding (153). Additionally, the study of Yang *et al.* (154) showed that the depletion of *Tg*ATPase$_P$-GC impairs the production of phosphatidic acid, which is consistent with our postulated lipid flipping function of P4-ATPase domain in *Tg*ATPase$_P$-GC. However, a systematic experimental analysis is still required to understand the intramolecular coordination of ATPase and guanylate cyclase domains.

The topology, subcellular localization, modelled structure as well as depicted multi-functionality of *Tg*ATPase$_P$-GC strikingly differ from the particulate GCs of mammals. Other distinguished features of mammalian pGCs, such as extracellular ligand binding and regulatory kinase-homology domains, are also absent in *Tg*ATPase$_P$-GC, which exhibits an evolutionary specialization of cGMP signaling in *T. gondii.* Likewise, other PKG-independent effectors of cGMP, *i.e.* nucleotide-gated ion channels as reported in mammalian

cells (80,85,191), could not be identified in the genome of *T. gondii*, which suggests a rather linear transduction of cGMP pathways through PKG. Notably, the topology of *Tg*ATPase$_P$-GC is shared by the members of another alveolate phylum Ciliophora (*e.g., Paramecium*, *Tetrahymena*) (97) which exhibits an entirely different lifestyle. Also, a guanylate cyclase with 2 catalytic domains but lacking ATPase-like region is present in *Dictyostelium* (member of amoebozoa) (192). Such a conservation of cGMP signaling architecture in several alveolates with diverse lifestyles signifies a convoluted repurposing of signaling within the protozoan kingdom. A divergent origin and essential requirement of cGMP cascade can be exploited to selectively inhibit the asexual reproduction of the parasitic protists.

4.2 Optogenetic control of cGMP in *T. gondii* tachyzoites

The previous work performed by Hartmann *et al.* (149) has successfully produced optogenetic *T. gondii* strains to modulate cAMP signaling using a photo-activated adenylate cyclase (bPAC) (130). It was the first study pioneering the application of optogenetics in infection research. Though several applications have been proposed meanwhile (127), there has not been any study conducted in this direction. The attempts were made in earlier work to express mutagenized version of bPAC (bPGC), which produces cGMP in response to light exposure (131), to regulate cGMP signaling in *T. gondii*. The expression of bPGC however resulted in the cAMP production alongside cGMP, which is not optimal when specifically targeting to control of cGMP signaling. After a while, a light-activated guanylate cyclase (RhoGC) (135) was discovered from an aquatic fungus. The electrophysiological characterization of RhoGC in different heterologous expression systems revealed its cyclase specificity for cGMP production (136). In this regard, we believed that RhoGC should prove particularly useful to study cGMP signaling in *T. gondii* tachyzoites.

Within the scope of this thesis, four different transgenic *Toxoplasma* strains expressing RhoGC under different conditions were generated. The expression of RhoGC showed a cytosolic as well as perinuclear, presumably ER, localization in tachyzoite stage of parasite (Figure 25), due to the presence of multiple transmembrane helices in the protein structure (136). The insertion of RhoGC did not exert any detrimental effect on the parasite growth. The functional expression enabled the induction of cGMP simply by light within the parasite without affecting the sheltering host cells. Shining green light on extracellular parasites of two different transgenic strains (DD-RhoGC-HA and RhoGC-3xHA) showed a differential

and dynamic regulation of cGMP in the parasite (Figure 27). Having multiple optogenetic strains enabled to make some inferences and optimize several parameters during this work. Some of them are summarized below:

1) The expression level of RhoGC influences the induction of cGMP in proportion. For instance, a single copy of RhoGC under a relatively weak *Tg*DHFR/TS regulatory elements in RhoGC-3xHA strain delivered a moderate expression when compared to its expression under stronger *Tg*Gra1 promoter in DD-RhoGC-HA strain (Figure 25). Although the basal (dark) levels of cGMP were almost the same in these aforesaid strains, light exposure resulted in differential induction of cGMP (6.3-fold increase *versus* 16.5-fold-increase) after 5 min illumination (530 nm, 197.4 $\mu W/cm^2$ intensity). These strains can therefore serve for a flexible and goal-oriented modulation of cGMP in diverse experimental setups. Besides, DD-RhoGC-HA allows to regulate the expression of RhoGC by chemical treatment in ligand-dependent manner, which prevents an unintended expression in regular cultures. The conditional expression of RhoGC also exhibited much stronger cGMP induction in DD-RhoGC-HA in comparison to the RhoGC-3xHA strain.

2) Light intensity-dependent control of RhoGC does not seem so critical for the performance of RhoGC. Previous studies have shown that cGMP production by RhoGC remained the same in *Xenopus* oocytes (136) and *in vitro* activity assays (128) even when the light was gradually increased after reaching the half-maximal light intensity value in a given expression model. After some optimization steps, the light intensity was fixed to 197.4 $\mu W/cm^2$ throughout this study.

3) The duration of illumination is another important determinant in the assays. Variable exposure times were utilized from 0.5 to 5 min for the cGMP assay performed with extracellular parasites of optogenetic *T. gondii* strains (Figure 27). The assay results revealed that RhoGC differentially responds to light exposure in different strains, accordingly the exposure time to reach the maximal cGMP induction varies between strains. 30 sec light pulse was not enough to stimulate cGMP production in neither DD-RhoGC-HA nor RhoGC-3xHA strains, although flashing light for few seconds was sufficient to induce cGMP levels in other heterologous systems; such as in *Xenopus* oocytes, HEK293T or Chinese hamster ovary cells (128,136). Both DD-RhoGC-HA and RhoGC-3xHA strains exhibited a moderate cGMP induction until reaching 0.4-0.45 pmol (per 10^6 parasites) cGMP levels after 1 min and 3 min exposure, respectively. The subsequent illumination (from 1 min to 5 min) showed

almost a linear increase of cGMP in DD-RhoGC-HA strain. In addition, this strain had still a tendency to increase cGMP level, which suggests that the amount of cGMP is not saturated yet in DD-RhoGC-HA strain after 5 min illumination. However, the maximal induction of cGMP in RhoGC-3xHA was limited with 1 pmol/10^6 parasite after 4 min illumination. An additional exposure did not increase cGMP level in RhoGC-3xHA strain. Consequently, at least 3 min light pulse is required to reach a minimum threshold to assure an exponential cGMP induction in our optogenetic strains. Based on the cGMP profile of RhoGC-3xHA strain, 5 min light illumination was applied to test the functional effect of RhoGC in all optogenetic strains during lytic cycle assays.

Designing an optogenetic device offered an easy control of illumination parameters. A 24-well plate compatible LED-device built specifically for this study (section 2.1.7) facilitated the application of optogenetics in *T. gondii* research. It enabled to minimize the variations between independent assays by stabilizing the assay conditions, such as excitation wavelengths, light intensity and durations *via* a designed graphical user interface. Such low-cost devices also allow to standardize the research parameters between laboratories. Although some optogenetic setups are available specifically for Neurobiology researches (193-195), development of new target-oriented devices compatible to different systems is an emergent requirement nowadays to integrate the application of optogenetics in wider fields.

Application of optogenetics in *T. gondii* showed a direct link between induction of cGMP signaling in the parasite and regulation of lytic cycle events. The percentage of motility, invasion and egress in dark samples of different optogenetic strains were quite similar with the parental strain, which confirms functional stability and robust light-dependent cyclase activity of RhoGC in *T. gondii*. Expression of RhoGC in different models also did not display any dark activity (128,136,137). Furthermore, light-induced phenotypes were consistent across all optogenetic strains. The comparison of cGMP induction assay and phenotype data of DD-RhoGC-HA and RhoGC-3xHA strains also reveals a relationship between cGMP thresholds and phenotypic consequences. cGMP levels were measured as ~1.1 pmol and ~3.45 pmol per 10^6 parasites in RhoGC-3xHA and DD-RhoGC-HA strains, respectively, after 5 min illumination. These cGMP levels were clearly sufficient to induce the motility, invasion and egress phenotypes in the tachyzoites. The impact of induced cGMP was also observed as an enhanced motility in proportion, which was also reflected in invasion rates of different strains. Likewise, all optogenetic strains showed an escalated egress in

response to light; however, the efficiency of egress differed across the strains. The egress event was complete in DD-RhoGC-HA strain, which indicates above the threshold cGMP induction in this strain. These results together suggest that different threshold levels of cGMP might be required to regulate individual events of the lytic cycle. It must be noted that the phenotypes observed with optogenetic assays are quite consistent with the genetic knockdown studies of *Tg*ATPase$_P$-GC and *Tg*PKG, which endorses the utility of an optogenetic strain in *T. gondii*.

Based on the existing literature (42,115,123,154), cGMP signaling and Ca^{2+} signaling most likely interact with each other to regulate the lytic cycle of parasite. To investigate the relationship of both pathways, a *T. gondii* strain co-expressing RhoGC (to modulate the cGMP levels) and calcium sensor GCaMP6s (to monitor the dynamics of Ca^{2+}) was engineered in this study. Our initial proof of concept work confirms the hypothesis that cGMP signaling leads to an increase in cytosolic calcium, which also seems to require a minimum threshold of cGMP level as observed for lytic cycle assays. We proposed a model system within the parasite, which illustrates an optogenetic induction of cGMP by activation of RhoGC and synchronously monitoring of Ca^{2+} by GCaMP6s in *T. gondii* (Figure 30). The system shall enable to monitor calcium changes in individual steps of lytic cycle in further assays. It should now be possible to create mutants of intermediate signaling mediators to dissect the pathways leading to the release of calcium. In this regard, PI-PLC-mediated IP_3/ DAG-signaling pathway which connects cGMP and calcium signaling requires a special attention.

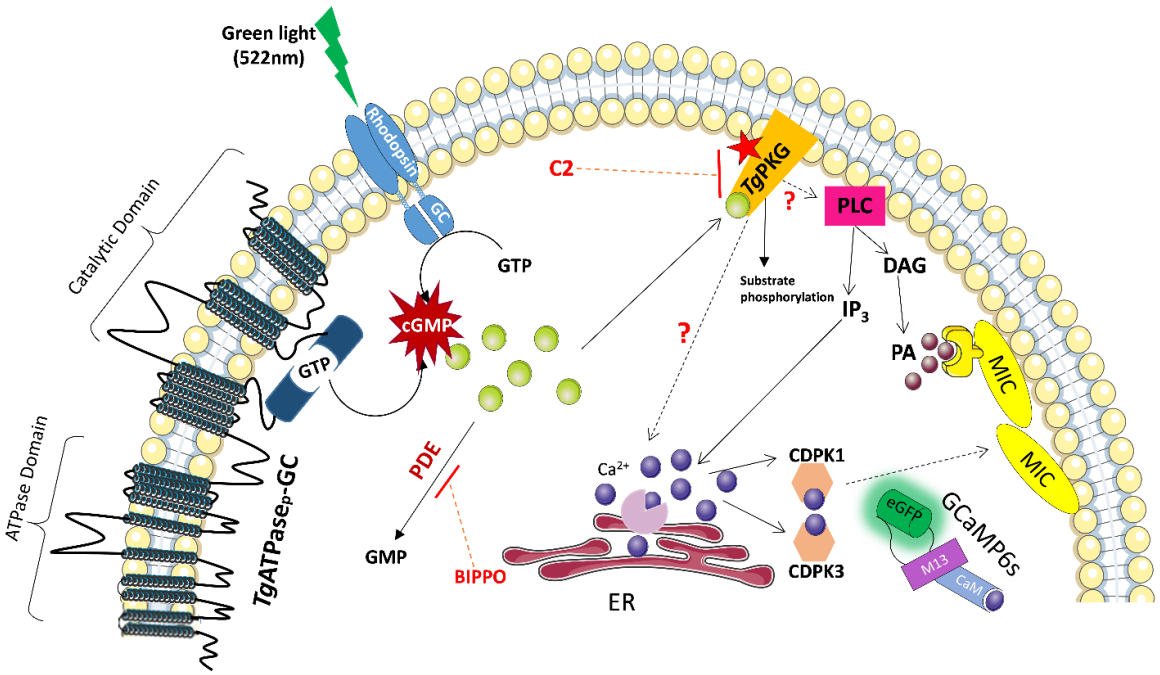

Figure 30. Proposed model for optogenetic induction of cGMP and sensing Ca^{2+} in *T. gondii*. Light-activated RhoGC converts GTP into cGMP when activated by the green light (530 nm) within the parasite. *Tg*ATPase$_P$-GC initiates native cGMP signaling. A rise in cGMP level either *via* *Tg*ATPase$_P$-GC or RhoGC activates *Tg*PKG, which stimulates the calcium signaling *via* an intermediate lipid signaling. Active *Tg*PKG provides the substrates for phosphoinositide phospholipase C (PLC) which in turn produces inositol trisphosphate (IP_3) and diacylglycerol (DAG). IP_3 formation leads to release calcium from the storage organelles, like ER, to the cytosol. It is still an open question whether *Tg*PKG directly or by another pathway can also induce calcium release to the cytosol. Free cytosolic calcium can be detected by genetically-encoded calcium sensor GCaMP6s. An increase in cytosolic calcium induces Ca^{2+}-dependent protein kinases (CDPKs) which regulate microneme secretion. The conversion of DAG to phosphatidic acid (PA) is another way for parasite to promote microneme secretion. The cascade can be regulated by RhoGC in a reversible manner, once the parasite is kept in the dark. The inhibition of *Tg*PKG by compound 2 totally impairs the cascade. However, BIPPO treatment blocking phosphodiesterases (PDEs), can stimulate the pathway again. Straight lines represent known pathways, while hypothetical ones are shown by dashed lines. Ca^{2+}: calcium; cGMP: cyclic guanosine monophosphate; eGFP: enhanced green fluorescent protein; ER: endoplasmic reticulum; GCaMP6s: circularly permuted GFP-calmodulin-M13 peptide 6; GC: guanylate cyclase; GTP: guanosine triphosphate; M13: myosin light-chain kinase; PDE: phosphodiesterase; PKG: protein kinase G.

5 Conclusions and Outlook

This work demonstrates the importance of cGMP signaling on the lytic cycle of obligate intracellular parasite *T. gondii*. An atypical guanylate cyclase fused to a P4-ATPase, *Tg*ATPase$_P$-GC, was characterized in the parasite as an upstream mediator of native cyclic GMP signaling. Genetic knockdown and pharmacological inhibition studies revealed the essentiality of this protein for the successful lytic cycle of parasite. *In silico* analysis provided valuable insights into its membrane topology, complex architecture and possible multifunctioning, however many questions are still awaiting to be answered:

(1) Intermolecular coordination of P4-ATPase and GC domains in *Tg*ATPase$_P$-GC,
(2) The role of P4-ATPase domain on GC function,
(3) Mechanism of lipid-sensing by P4-ATPase domain.

Besides, the integration of an optogenetic approach into the *T. gondii* research by expressing a light-activated guanylate cyclase, RhoGC, enabled to induce cGMP simply by light in fast, spatial and reversible manner. The proof of concept work exhibited a direct linkage between the induction of cGMP in the parasite and its impact on the motility, invasion and egress events. The optogenetic strain co-expressing RhoGC with a calcium sensor, GCaMP6s, sounds promising to selectively modulate and monitor cGMP and calcium levels within the parasite. Having multiple optogenetic strains permits now an objective-oriented usage of them to address following signaling-related researches in the future:

(1) Kinetics of cGMP and Ca^{2+} in intracellular parasites during the lytic cycle,
(2) Real-time monitoring of phenotypes in response to light during the lytic cycle,
(3) Phosphoproteomic analysis of C2-sensitive and C2-resistant optogenetic strains,
(4) Genetic knockouts/knockdowns of PKG-dependent phosphorylated proteins in the optogenetic strains to dissect hierarchical nature of signaling.

6 References

1. Adl, S. M., Leander, B. S., Simpson, A. G., Archibald, J. M., Anderson, O. R., Bass, D., Bowser, S. S., Brugerolle, G., Farmer, M. A., and Karpov, S. *et al.* (2007) Diversity, nomenclature, and taxonomy of protists. *Systematic Biology* **56**, 684-689

2. Organization, W. H. (2018) World Malaria Day 2018" Ready to beat malaria": Key messages. *World Health Organization*

3. Roos, D. S. (2005) Themes and variations in apicomplexan parasite biology. *Science* **309**, 72-73

4. Lucius, R., and Loos-Frank, B. (2008) *Biologie von parasiten*, Springer

5. Striepen, B., Jordan, C. N., Reiff, S., and Van Dooren, G. G. (2007) Building the perfect parasite: Cell division in apicomplexa. *PLoS pathogens* **3**, e78

6. Carruthers, V. B., and Sibley, L. (1997) Sequential protein secretion from three distinct organelles of *Toxoplasma gondii* accompanies invasion of human fibroblasts. *European journal of cell biology* **73**, 114-123

7. Dobrowolski, J. M., and Sibley, L. D. (1996) *Toxoplasma* invasion of mammalian cells is powered by the actin cytoskeleton of the parasite. *Cell* **84**, 933-939

8. Lim, L., and McFadden, G. I. (2010) The evolution, metabolism and functions of the apicoplast. *Philosophical Transactions of the Royal Society B: Biological Sciences* **365**, 749-763

9. Tenter, A. M., Heckeroth, A. R., and Weiss, L. M. (2000) *Toxoplasma gondii:* from animals to humans. *International journal for parasitology* **30**, 1217-1258

10. Sabin, A. B. (1939) Biological and immunological identity of *Toxoplasma* of animal and human origin. *Proceedings of the Society for Experimental Biology and Medicine* **41**, 75-80

11. Dubey, J. P., and Beattie, C. (1988) *Toxoplasmosis of animals and man*, CRC Press, Inc. *Cambridge University Press,* 220

12. Howe, D. K., and Sibley, L. D. (1995) *Toxoplasma gondii* comprises three clonal lineages: correlation of parasite genotype with human disease. *Journal of infectious diseases* **172**, 1561-1566

13. Khan, A., Dubey, J., Su, C., Ajioka, J. W., Rosenthal, B. M., and Sibley, L. D. (2011) Genetic analyses of atypical *Toxoplasma gondii* strains reveal a fourth clonal lineage in North America. *International journal for parasitology* **41**, 645-655

14. Su, C., Khan, A., Zhou, P., Majumdar, D., Ajzenberg, D., Dardé, M.-L., Zhu, X.-Q., Ajioka, J. W., Rosenthal, B. M., and Dubey, J. P. (2012) Globally diverse *Toxoplasma*

gondii isolates comprise six major clades originating from a small number of distinct ancestral lineages. *Proceedings of the National Academy of Sciences* **109**, 5844-5849

15. Lehmann, T., Marcet, P. L., Graham, D. H., Dahl, E. R., Dubey, J. and Sibley, L.D. (2006) Globalization and the population structure of *Toxoplasma gondii*. *Proceedings of the National Academy of Sciences* **103**, 11423-11428

16. Yan, C., Liang, L.-J., Zheng, K.-Y., and Zhu, X.-Q. (2016) Impact of environmental factors on the emergence, transmission and distribution of *Toxoplasma gondii. Parasites & vectors* **9**, 137

17. Sturge, C. R., and Yarovinsky, F. (2014) Complex immune cell interplay in the gamma interferon response during *Toxoplasma gondii* infection. *Infection and immunity* **82**, 3090-3097

18. Hunter, C. A., and Sibley, L. D. (2012) Modulation of innate immunity by *Toxoplasma gondii* virulence effectors. *Nature Reviews Microbiology* **10**, 766

19. Wilking, H., Thamm, M., Stark, K., Aebischer, T., and Seeber, F. (2016) Prevalence, incidence estimations, and risk factors of *Toxoplasma gondii* infection in Germany: A representative, cross-sectional, serological study. *Scientific reports* **6**, 22551

20. Moncada, P. A., and Montoya, J. G. (2012) Toxoplasmosis in the fetus and newborn: An update on prevalence, diagnosis and treatment. *Expert review of anti-infective therapy* **10**, 815-828

21. Jones, J. L., and Dubey, J. (2012) Foodborne toxoplasmosis. *Clinical infectious diseases* **55**, 845-851

22. Buxton, D., and Innes, E. (1995) A commercial vaccine for ovine toxoplasmosis. *Parasitology* **110**, S11-S16

23. Frenkel, J., Pfefferkorn, E., Smith, D., and Fishback, J. (1991) Prospective vaccine prepared from a new mutant of T*oxoplasma gondii* for use in cats. *American journal of veterinary research* **52**, 759-763

24. Ramakrishnan, C., Maier, S., Walker, R. A., Rehrauer, H., Joekel, D. E., Winiger, R. R., Basso, W. U., Grigg, M. E., Hehl, A. B., Deplazes, P., and Smith, N.C. (2019) An experimental genetically attenuated live vaccine to prevent transmission of *Toxoplasma gondii* by cats. *Scientific reports* **9**, 1474

25. Weiss, L. M., and Kim, K. (2011) *Toxoplasma gondii:* The model apicomplexan. *Perspectives and methods*, Elsevier

26. Sullivan Jr, W. J., and Jeffers, V. (2012) Mechanisms of *Toxoplasma gondii* persistence and latency. *FEMS microbiology reviews* **36**, 717-733

27. Frenkel, J., Dubey, J., and Miller, N. L. (1970) *Toxoplasma gondii* in cats: Fecal stages identified as coccidian oocysts. *Science* **167**, 893-896

28. Ferguson, D., and Hutchison, W. (1987) An ultrastructural study of the early development and tissue cyst formation of *Toxoplasma gondii* in the brains of mice. *Parasitology research* **73**, 483-491

29. Dubey, R., Harrison, B., Dangoudoubiyam, S., Bandini, G., Cheng, K., Kosber, A., Agop-Nersesian, C., Howe, D. K., Samuelson, J., Ferguson, D. J., and Gubbels M.J. (2017) Differential Roles for Inner Membrane Complex Proteins across *Toxoplasma gondii* and *Sarcocystis neurona* Development. *mSphere* **2**, e00409-00417

30. Dubey, J., Lindsay, D., and Speer, C. (1998) Structures of *Toxoplasma gondii* tachyzoites, bradyzoites, and sporozoites and biology and development of tissue cysts. *Clinical microbiology reviews* **11**, 267-299

31. Torrey, E. F., and Yolken, R. H. (2013) *Toxoplasma* oocysts as a public health problem. *Trends in parasitology* **29**, 380-384

32. Dubey, J. (1998) Advances in the life cycle of *Toxoplasma gondii. International journal for parasitology* **28**, 1019-1024

33. Black, M. W., and Boothroyd, J. C. (2000) Lytic cycle of *Toxoplasma gondii. Microbiology and Molecular Biology Reviews* **64**, 607-623

34. Blader, I. J., Coleman, B. I., Chen, C.-T., and Gubbels, M.J. (2015) Lytic cycle of *Toxoplasma gondii:* 15 years later. *Annual review of microbiology* **69**, 463-485

35. Morrissette, N. S., and Sibley, L. D. (2002) Cytoskeleton of apicomplexan parasites. *Microbiol. Mol. Biol. Rev.* **66**, 21-38

36. Sibley, L. D. (2010) How apicomplexan parasites move in and out of cells. *Current opinion in biotechnology* **21**, 592-598

37. Hu, K., Johnson, J., Florens, L., Fraunholz, M., Suravajjala, S., DiLullo, C., Yates, J., Roos, D. S., and Murray, J. M. (2006) Cytoskeletal components of an invasion machine—The apical complex of *Toxoplasma gondii*. *PLoS pathogens* **2**, e13

38. Joiner, K. A., Fuhrman, S., Miettinen, H., Kasper, L., and Mellman, I. (1990) *Toxoplasma gondii:* Fusion competence of parasitophorous vacuoles in Fc receptor-transfected fibroblasts. *Science* **249**, 641-646

39. Suss-Toby, E., Zimmerberg, J., and Ward, G. (1996) *Toxoplasma* invasion: The parasitophorous vacuole is formed from host cell plasma membrane and pinches off via a fission pore. *Proceedings of the National Academy of Sciences* **93**, 8413-8418

40. Francia, M. E., and Striepen, B. (2014) Cell division in apicomplexan parasites. *Nature Reviews Microbiology* **12**, 125

41. Blackman, M. J., and Carruthers, V. B. (2013) Recent insights into apicomplexan parasite egress provide new views to a kill. *Current opinion in microbiology* **16**, 459-464

42. Lourido, S., Tang, K., and Sibley, L. D. (2012) Distinct signalling pathways control *Toxoplasma* egress and host-cell invasion. *The EMBO journal* **31**, 4524-4534

43. Zhang, M., Joyce, B. R., Sullivan, W. J., and Nussenzweig, V. (2013) Translational control in *Plasmodium* and *Toxoplasma* parasites. *Eukaryotic cell* **12**, 161-167

44. Cesbron-Delauw, M. F., Gendrin, C., Travier, L., Ruffiot, P., and Mercier, C. (2008) Apicomplexa in mammalian cells: Trafficking to the parasitophorous vacuole. *Traffic* **9**, 657-664

45. Sibley, L. (2004) Intracellular parasite invasion strategies. *Science* **304**, 248-253

46. Schwab, J., Beckers, C., and Joiner, K. A. (1994) The parasitophorous vacuole membrane surrounding intracellular *Toxoplasma gondii* functions as a molecular sieve. *Proceedings of the National Academy of Sciences* **91**, 509-513

47. Bisanz, C., Bastien, O., Grando, D., Jouhet, J., Maréchal, E., and Cesbron-Delauw, M.-F. (2006) *Toxoplasma gondii* acyl-lipid metabolism: *De novo* synthesis from apicoplast-generated fatty acids *versus* scavenging of host cell precursors. *Biochemical Journal* **394**, 197-205

48. Crawford, M. J., Thomsen-Zieger, N., Ray, M., Schachtner, J., Roos, D. S., and Seeber, F. (2006) *Toxoplasma gondii* scavenges host-derived lipoic acid despite its *de novo* synthesis in the apicoplast. *The EMBO journal* **25**, 3214-3222

49. Gupta, N. (2018) An Intimate Dining–Nutritional Interactions between Obligate Intracellular Parasites and Host Cells.

50. Gajria, B., Bahl, A., Brestelli, J., Dommer, J., Fischer, S., Gao, X., Heiges, M., Iodice, J., Kissinger, J. C., and Mackey, A. J. *et al*. (2007) ToxoDB: An integrated *Toxoplasma gondii* database resource. *Nucleic acids research* **36**, D553-D556

51. Pfefferkorn, E., and Pfefferkorn, L. G. (1976) *Toxoplasma gondii*: Isolation and preliminary characterization of temperature-sensitive mutants. *Experimental parasitology* **39**, 365-376

52. Pfefferkorn, L. C., and Pfefferkorn, E. (1980) *Toxoplasma gondii*: Genetic recombination between drug resistant mutants. *Experimental parasitology* **50**, 305-316

53. Sibley, L. D., LeBlanc, A. J., Pfefferkorn, E., and Boothroyd, J. C. (1992) Generation of a restriction fragment length polymorphism linkage map for *Toxoplasma gondii*. *Genetics* **132**, 1003-1015

54. Sibley, L., and Boothroyd, J. C. (1992) Construction of a molecular karyotype for *Toxoplasma gondii. Molecular and biochemical parasitology* **51**, 291-300

55. Soldati, D., and Boothroyd, J. C. (1993) Transient transfection and expression in the obligate intracellular parasite *Toxoplasma gondii. Science* **260**, 349-352

56. Donald, R., and Roos, D. S. (1993) Stable molecular transformation of *Toxoplasma gondii*: A selectable dihydrofolate reductase-thymidylate synthase marker based on drug-resistance mutations in malaria. *Proceedings of the National Academy of Sciences* **90**, 11703-11707

57. Donald, R. G., Carter, D., Ullman, B., and Roos, D. S. (1996) Insertional tagging, cloning, and expression of the *Toxoplasma gondii* hypoxanthine-xanthine-guanine phosphoribosyltransferase gene Use as a selectable marker for stable transformation. *Journal of Biological Chemistry* **271**, 14010-14019

58. Donald, R., and Roos, D. S. (1995) Insertional mutagenesis and marker rescue in a protozoan parasite: cloning of the uracil phosphoribosyltransferase locus from *Toxoplasma gondii*. *Proceedings of the National Academy of Sciences* **92**, 5749-5753

59. Kim, K., Soldati, D., and Boothroyd, J. C. (1993) Gene replacement in *Toxoplasma gondii* with chloramphenicol acetyltransferase as selectable marker. *Science* **262**, 911-914

60. Brecht, S., Erdhart, H., Soete, M., and Soldati, D. (1999) Genome engineering of *Toxoplasma gondii* using the site-specific recombinase Cre. *Gene* **234**, 239-247

61. Huynh, M.-H., and Carruthers, V. B. (2009) Tagging of endogenous genes in a *Toxoplasma gondii* strain lacking Ku80. *Eukaryotic cell* **8**, 530-539

62. Fox, B. A., Ristuccia, J. G., Gigley, J. P., and Bzik, D. J. (2009) Efficient gene replacements in *Toxoplasma gondii* strains deficient for nonhomologous end joining. *Eukaryotic cell* **8**, 520-529

63. Fox, B. A., Falla, A., Rommereim, L. M., Tomita, T., Gigley, J. P., Mercier, C., Cesbron-Delauw, M.-F., Weiss, L. M., and Bzik, D. J. (2011) Type II *Toxoplasma gondii* KU80 knockout strains enable functional analysis of genes required for cyst development and latent infection. *Eukaryotic cell* **10**, 1193-1206

64. Kolev, N. G., Tschudi, C., and Ullu, E. (2011) RNA interference in protozoan parasites: Achievements and challenges. *Eukaryotic cell* **10**, 1156-1163

65. Meissner, M., Schlüter, D., and Soldati, D. (2002) Role of *Toxoplasma gondii* myosin A in powering parasite gliding and host cell invasion. *Science* **298**, 837-840

66. Herm-Götz, A., Agop-Nersesian, C., Münter, S., Grimley, J. S., Wandless, T. J., Frischknecht, F., and Meissner, M. (2007) Rapid control of protein level in the apicomplexan *Toxoplasma gondii. Nature methods* **4**, 1003

67. Banaszynski, L. A., Chen, L.-c., Maynard-Smith, L. A., Ooi, A. L., and Wandless, T. J. (2006) A rapid, reversible, and tunable method to regulate protein function in living cells using synthetic small molecules. *Cell* **126**, 995-1004

68. Barrangou, R., Fremaux, C., Deveau, H., Richards, M., Boyaval, P., Moineau, S., Romero, D. A., and Horvath, P. (2007) CRISPR provides acquired resistance against viruses in prokaryotes. *Science* **315**, 1709-1712

69. Jinek, M., Chylinski, K., Fonfara, I., Hauer, M., Doudna, J. A., and Charpentier, E. (2012) A programmable dual-RNA–guided DNA endonuclease in adaptive bacterial immunity. *Science* **337**, 816-821

70. Shen, B., Brown, K. M., Lee, T. D., and Sibley, L. D. (2014) Efficient gene disruption in diverse strains of *Toxoplasma gondii* using CRISPR/CAS9. *MBio* **5**, e01114-01114

71. Sidik, S. M., Hackett, C. G., Tran, F., Westwood, N. J., and Lourido, S. (2014) Efficient genome engineering of *Toxoplasma gondii* using CRISPR/Cas9. *PloS one* **9**, e100450

72. Brown, K. M., Long, S., and Sibley, L. D. (2017) Plasma membrane association by N-acylation governs PKG function in *Toxoplasma gondii*. *MBio* **8**, e00375-00317

73. Brown, K. M., Long, S., and Sibley, L. D. (2018) Conditional knockdown of proteins using auxin-inducible degron (AID) fusions in *Toxoplasma gondii*. *Bio-protocol* **8**

74. Long, S., Brown, K. M., Drewry, L. L., Anthony, B., Phan, I. Q., and Sibley, L. D. (2017) Calmodulin-like proteins localized to the conoid regulate motility and cell invasion by *Toxoplasma gondii. PLoS pathogens* **13**, e1006379

75. Teale, W. D., Paponov, I. A., and Palme, K. (2006) Auxin in action: Signalling, transport and the control of plant growth and development. *Nature Reviews Molecular Cell Biology* **7**, 847

76. Nishimura, K., Fukagawa, T., Takisawa, H., Kakimoto, T., and Kanemaki, M. (2009) An auxin-based degron system for the rapid depletion of proteins in nonplant cells. *Nature methods* **6**, 917

77. Beavo, J. A., and Brunton, L. L. (2002) Cyclic nucleotide research—Still expanding after half a century. *Nature reviews Molecular cell biology* **3**, 710

78. Berridge, M. J. (1987) Inositol trisphosphate and diacylglycerol: Two interacting second messengers. *Annual review of biochemistry* **56**, 159-193

79. Hall, C. L., and Lee, V. T. (2018) Cyclic-di-GMP regulation of virulence in bacterial pathogens. *Wiley Interdisciplinary Reviews: RNA* **9**, e1454

80. Lucas, K. A., Pitari, G. M., Kazerounian, S., Ruiz-Stewart, I., Park, J., Schulz, S., Chepenik, K. P., and Waldman, S. A. (2000) Guanylyl cyclases and signaling by cyclic GMP. *Pharmacological reviews* **52**, 375-414

81. Pifferi, S., Boccaccio, A., and Menini, A. (2006) Cyclic nucleotide-gated ion channels in sensory transduction. *FEBS letters* **580**, 2853-2859

82. Schmidt, M., Dekker, F. J., and Maarsingh, H. (2013) Exchange protein directly activated by cAMP (EPAC): a multidomain cAMP mediator in the regulation of diverse biological functions. *Pharmacological reviews* **65**, 670-709

83. Beavo, J. A. (1995) Cyclic nucleotide phosphodiesterases: Functional implications of multiple isoforms. *Physiological reviews* **75**, 725-748

84. Potter, L. R. (2011) Guanylyl cyclase structure, function and regulation. *Cellular signalling* **23**, 1921-1926

85. MacFarland, R. T. (1995) Molecular aspects of cyclic GMP signaling. *Zoological science* **12**, 151-164

86. Haynes, L., and Yau, K.-W. (1985) Cyclic GMP-sensitive conductance in outer segment membrane of catfish cones. *Nature* **317**, 61

87. Hanoune, J., and Defer, N. (2001) Regulation and role of adenylyl cyclase isoforms. *Annual review of pharmacology and toxicology* **41**, 145-174

88. Sinclair, M. L., Wang, X. Y., Mattia, M., Conti, M., Buck, J., Wolgemuth, D. J., and Levin, L. R. (2000) Specific expression of soluble adenylyl cyclase in male germ cells. *Molecular Reproduction and Development: Incorporating Gamete Research* **56**, 6-11

89. Linder, J. U., and Schultz, J. E. (2003) The class III adenylyl cyclases: Multi-purpose signalling modules. *Cellular signalling* **15**, 1081-1089

90. Søberg, K., Moen, L. V., Skålhegg, B. S., and Laerdahl, J. K. (2017) Evolution of the cAMP-dependent protein kinase (PKA) catalytic subunit isoforms. *PloS one* **12**, e0181091

91. Vaandrager, A. B., Edixhoven, M., Bot, A. G., Kroos, M. A., Jarchau, T., Lohmann, S., Genieser, H.-G., and de Jonge, H. R. (1997) Endogenous type II cGMP-dependent protein kinase exists as a dimer in membranes and can be functionally distinguished from the type I isoforms. *Journal of Biological Chemistry* **272**, 11816-11823

92. Butt, E., Geiger, J., Jarchau, T., Lohmann, S. M., and Walter, U. (1993) The cGMP-dependent protein kinase-gene, protein, and function. *Neurochemical research* **18**, 27-42

93. Jarchau, T., Häusler, C., Markert, T., Pöhler, D., Vanderkerckhove, J., De Jonge, H. R., Lohmann, S. M., and Walter, U. (1994) Cloning, expression, and in situ localization of rat intestinal cGMP-dependent protein kinase II. *Proceedings of the National Academy of Sciences* **91**, 9426-9430

94. De Jonge, H. (1981) Cyclic GMP-dependent protein kinase in intestinal brushborders. *Advances in cyclic nucleotide research* **14**, 315

95. Gould, M. K., and de Koning, H. P. (2011) Cyclic-nucleotide signalling in protozoa. *FEMS microbiology reviews* **35**, 515-541

96. Hopp, C. S., Bowyer, P. W., and Baker, D. A. (2012) The role of cGMP signalling in regulating life cycle progression of *Plasmodium. Microbes and infection* **14**, 831-837

97. Linder, J. U., Engel, P., Reimer, A., Krüger, T., Plattner, H., Schultz, A., and Schultz, J. E. (1999) Guanylyl cyclases with the topology of mammalian adenylyl cyclases and an N-terminal P-type ATPase-like domain in *Paramecium, Tetrahymena* and *Plasmodium*. *The EMBO Journal* **18**, 4222-4232

98. Baker, D. A., Drought, L. G., Flueck, C., Nofal, S. D., Patel, A., Penzo, M., and Walker, E. M. (2017) Cyclic nucleotide signalling in malaria parasites. *Open biology* **7**, 170213

99. Brown, K. M., and Sibley, L. D. (2018) Essential cGMP signaling in *Toxoplasma* is initiated by a hybrid P-Type ATPase-Guanylate cyclase. *Cell host & microbe* **24**, 804-816. e806

100. Frénal, K., Dubremetz, J.-F., Lebrun, M., and Soldati-Favre, D. (2017) Gliding motility powers invasion and egress in Apicomplexa. *Nature Reviews Microbiology* **15**, 645

101. Govindasamy, K., Jebiwott, S., Jaijyan, D., Davidow, A., Ojo, K., Van Voorhis, W., Brochet, M., Billker, O., and Bhanot, P. (2016) Invasion of hepatocytes by *Plasmodium* sporozoites requires cGMP-dependent protein kinase and Calcium dependent protein kinase 4. *Molecular microbiology* **102**, 349-363

102. Brochet, M., Collins, M. O., Smith, T. K., Thompson, E., Sebastian, S., Volkmann, K., Schwach, F., Chappell, L., Gomes, A. R., and Berriman, M. *et al.* (2014) Phosphoinositide metabolism links cGMP-dependent Protein kinase G to essential Ca^{2+} signals at key decision points in the life cycle of malaria parasites. *PLoS biology* **12**, e1001806

103. Brown, K. M., Lourido, S., and Sibley, L. D. (2016) Serum albumin stimulates Protein kinase G-dependent microneme secretion in *Toxoplasma gondii*. *Journal of Biological Chemistry* **291**, 9554-9565

104. Bullen, H. E., Jia, Y., Yamaryo-Botté, Y., Bisio, H., Zhang, O., Jemelin, N. K., Marq, J.-B., Carruthers, V., Botté, C. Y., and Soldati-Favre, D. (2016) Phosphatidic acid-mediated signaling regulates microneme secretion in *Toxoplasma. Cell host & microbe* **19**, 349-360

105. Moudy, R., Manning, T. J., and Beckers, C. J. (2001) The loss of cytoplasmic potassium upon host cell breakdown triggers egress of *Toxoplasma gondii*. *Journal of Biological Chemistry* **276**, 41492-41501

106. Roiko, M. S., Svezhova, N., and Carruthers, V. B. (2014) Acidification activates *Toxoplasma gondii* motility and egress by enhancing protein secretion and cytolytic activity. *PLoS pathogens* **10**, e1004488

107. Gurnett, A. M., Liberator, P. A., Dulski, P. M., Salowe, S. P., Donald, R. G., Anderson, J. W., Wiltsie, J., Diaz, C. A., Harris, G., and Chang, B. *et al.* (2002) Purification and molecular characterization of cGMP-dependent Protein kinase from apicomplexan parasites a novel chemotherapeutic target. *Journal of Biological Chemistry* **277**, 15913-15922

108. Donald, R. G., and Liberator, P. A. (2002) Molecular characterization of a coccidian parasite cGMP dependent protein kinase. *Molecular and biochemical parasitology* **120**, 165-175

109. Wiersma, H. I., Galuska, S. E., Tomley, F. M., Sibley, L. D., Liberator, P. A., and Donald, R. G. (2004) A role for coccidian cGMP-dependent protein kinase in motility and invasion. *International journal for parasitology* **34**, 369-380

110. Sidik, S. M., Huet, D., Ganesan, S. M., Huynh, M.-H., Wang, T., Nasamu, A. S., Thiru, P., Saeij, J. P., Carruthers, V. B., Niles, J. C. and Lourido, S. (2016) A genome-wide CRISPR screen in *Toxoplasma* identifies essential apicomplexan genes. *Cell* **166**, 1423-1435. e1412

111. Falae, A., Combe, A., Amaladoss, A., Carvalho, T., Menard, R., and Bhanot, P. (2010) Role of *Plasmodium berghei* cGMP-dependent Protein kinase in late liver stage development. *Journal of Biological Chemistry* **285**, 3282-3288

112. Taylor, H. M., McRobert, L., Grainger, M., Sicard, A., Dluzewski, A. R., Hopp, C. S., Holder, A. A., and Baker, D. A. (2010) The malaria parasite cyclic GMP-dependent protein kinase plays a central role in blood-stage schizogony. *Eukaryotic cell* **9**, 37-45

113. Singh, S., Alam, M. M., Pal-Bhowmick, I., Brzostowski, J. A., and Chitnis, C. E. (2010) Distinct external signals trigger sequential release of apical organelles during erythrocyte invasion by malaria parasites. *PLoS pathogens* **6**, e1000746

114. Billker, O., Lourido, S., and Sibley, L. D. (2009) Calcium-dependent signaling and kinases in apicomplexan parasites. *Cell host & microbe* **5**, 612-622

115. Stewart, R. J., Whitehead, L., Nijagal, B., Sleebs, B. E., Lessene, G., McConville, M. J., Rogers, K. L., and Tonkin, C. J. (2017) Analysis of Ca^{2+} mediated signaling regulating *Toxoplasma* infectivity reveals complex relationships between key molecules. *Cellular microbiology* **19**, e12685

116. Carruthers, V. B., Moreno, S. N., and Sibley, D. L. (1999) Ethanol and acetaldehyde elevate intracellular [Ca^{2+}] and stimulate microneme discharge in *Toxoplasma gondii.* *Biochemical journal* **342**, 379-386

117. Wetzel, D. M., Chen, L. A., Ruiz, F. A., Moreno, S. N., and Sibley, L. D. (2004) Calcium-mediated protein secretion potentiates motility in *Toxoplasma gondii*. *Journal of Cell Science* **117**, 5739-5748

118. Vieira, M. C., and Moreno, S. N. (2000) Mobilization of intracellular calcium upon attachment of *Toxoplasma gondii* tachyzoites to human fibroblasts is required for invasion. *Molecular and biochemical parasitology* **106**, 157-162

119. Farrell, A., Thirugnanam, S., Lorestani, A., Dvorin, J. D., Eidell, K. P., Ferguson, D. J., Anderson-White, B. R., Duraisingh, M. T., Marth, G. T., and Gubbels, M.-J. (2012) A DOC2 protein identified by mutational profiling is essential for apicomplexan parasite exocytosis. *Science* **335**, 218-221

120. Jia, Y., Marq, J. B., Bisio, H., Jacot, D., Mueller, C., Yu, L., Choudhary, J., Brochet, M., and Soldati-Favre, D. (2017) Crosstalk between PKA and PKG controls pH-dependent host cell egress of *Toxoplasma gondii*. *The EMBO journal* **36**, 3250-3267

121. Donald, R. G., Allocco, J., Singh, S. B., Nare, B., Salowe, S. P., Wiltsie, J., and Liberator, P. A. (2002) *Toxoplasma gondii* cyclic GMP-dependent kinase: Chemotherapeutic targeting of an essential parasite protein kinase. *Eukaryotic cell* **1**, 317-328

122. Howard, B. L., Harvey, K. L., Stewart, R. J., Azevedo, M. F., Crabb, B. S., Jennings, I. G., Sanders, P. R., Manallack, D. T., Thompson, P. E., and Tonkin, C. J. (2015) Identification of potent phosphodiesterase inhibitors that demonstrate cyclic nucleotide-dependent functions in apicomplexan parasites. *ACS chemical biology* **10**, 1145-1154

123. Uboldi, A. D., Wilde, M.-L., McRae, E. A., Stewart, R. J., Dagley, L. F., Yang, L., Katris, N. J., Hapuarachchi, S. V., Coffey, M. J., and Lehane, A. M. *et al.* (2018) Protein kinase A negatively regulates Ca^{2+} signalling in *Toxoplasma gondii*. *PLoS biology* **16**, e2005642

124. Deisseroth, K., Feng, G., Majewska, A. K., Miesenböck, G., Ting, A., and Schnitzer, M. J. (2006) Next-generation optical technologies for illuminating genetically targeted brain circuits. *Soc Neuroscience,* 26 **(41),** 10380-6.

125. Rost, B. R., Schneider-Warme, F., Schmitz, D., and Hegemann, P. (2017) Optogenetic tools for subcellular applications in neuroscience. *Neuron* **96**, 572-603

126. Miesenböck, G. (2009) The optogenetic catechism. *Science* **326**, 395-399

127. Arroyo-Olarte, R. D., Thurow, L., Kozjak-Pavlovic, V., and Gupta, N. (2018) Illuminating pathogen–host intimacy through optogenetics. *PLoS pathogens* **14**, e1007046

128. Gao, S., Nagpal, J., Schneider, M. W., Kozjak-Pavlovic, V., Nagel, G., and Gottschalk, A. (2015) Optogenetic manipulation of cGMP in cells and animals by the tightly light-regulated guanylyl-cyclase opsin CyclOp. *Nature communications* **6**, 8046

129. Iseki, M., Matsunaga, S., Murakami, A., Ohno, K., Shiga, K., Yoshida, K., Sugai, M., Takahashi, T., Hori, T., and Watanabe, M. (2002) A blue-light-activated adenylyl cyclase mediates photoavoidance in *Euglena gracilis*. *Nature* **415**, 1047

130. Stierl, M., Stumpf, P., Udwari, D., Gueta, R., Hagedorn, R., Losi, A., Gärtner, W., Petereit, L., Efetova, M., and Schwarzel, M. *et al.* (2011) Light modulation of cellular cAMP by a small bacterial photoactivated adenylyl cyclase, bPAC, of the soil bacterium *Beggiatoa. Journal of Biological Chemistry* **286**, 1181-1188

131. Ryu, M.-H., Moskvin, O. V., Siltberg-Liberles, J., and Gomelsky, M. (2010) Natural and engineered photoactivated nucleotidyl cyclases for optogenetic applications. *Journal of Biological Chemistry* **285**, 41501-41508

132. Gasser, C., Taiber, S., Yeh, C.-M., Wittig, C. H., Hegemann, P., Ryu, S., Wunder, F., and Möglich, A. (2014) Engineering of a red-light–activated human cAMP/cGMP-specific phosphodiesterase. *Proceedings of the National Academy of Sciences* **111**, 8803-8808

133. Mei, Y., and Zhang, F. (2012) Molecular tools and approaches for optogenetics. *Biological psychiatry* **71**, 1033-1038

134. Spudich, J. L., Yang, C.-S., Jung, K.-H., and Spudich, E. N. (2000) Retinylidene proteins: Structures and functions from archaea to humans. *Annual review of cell and developmental biology* **16**, 365-392

135. Avelar, G. M., Schumacher, R. I., Zaini, P. A., Leonard, G., Richards, T. A., and Gomes, S. L. (2014) A rhodopsin-guanylyl cyclase gene fusion functions in visual perception in a fungus. *Current Biology* **24**, 1234-1240

136. Scheib, U., Stehfest, K., Gee, C. E., Körschen, H. G., Fudim, R., Oertner, T. G., and Hegemann, P. (2015) The rhodopsin–guanylyl cyclase of the aquatic fungus *Blastocladiella emersonii* enables fast optical control of cGMP signaling. *Sci. Signal.* **8**, rs8-rs8

137. Trieu, M. M., Devine, E. L., Lamarche, L. B., Ammerman, A. E., Greco, J. A., Birge, R. R., Theobald, D. L., and Oprian, D. D. (2017) Expression, purification, and spectral tuning of RhoGC, a retinylidene/guanylyl cyclase fusion protein and optogenetics tool from the aquatic fungus Blastocladiella emersonii. *Journal of Biological Chemistry* **292**, 10379-10389

138. Lamarche, L. B., Kumar, R. P., Trieu, M. M., Devine, E. L., Cohen-Abeles, L. E., Theobald, D. L., and Oprian, D. D. (2017) Purification and characterization of RhoPDE, a retinylidene/phosphodiesterase fusion protein and potential optogenetic tool from the choanoflagellate *Salpingoeca rosetta*. *Biochemistry* **56**, 5812-5822

139. Yoshida, K., Tsunoda, S. P., Brown, L. S., and Kandori, H. (2017) A unique choanoflagellate enzyme rhodopsin exhibits light-dependent cyclic nucleotide phosphodiesterase activity. *Journal of Biological Chemistry* **292**, 7531-7541

140. Paolillo, M., Peters, S., Schramm, A., Schlossmann, J., and Feil, R. (2018) Real-time imaging reveals augmentation of glutamate-induced Ca^{2+} transients by the NO-cGMP pathway in cerebellar granule neurons. *International journal of molecular sciences* **19**, 2185

141. Knöpfel, T., Lin, M. Z., Levskaya, A., Tian, L., Lin, J. Y., and Boyden, E. S. (2010) Toward the second generation of optogenetic tools. *Journal of Neuroscience* **30**, 14998-15004

142. Tantama, M., Hung, Y. P., and Yellen, G. (2012) Optogenetic reporters: Fluorescent protein-based genetically encoded indicators of signaling and metabolism in the brain. in *Progress in brain research*, Elsevier. pp 235-263

143. Russwurm, M., Mullershausen, F., Friebe, A., Jäger, R., Russwurm, C., and Koesling, D. (2007) Design of fluorescence resonance energy transfer (FRET)-based cGMP indicators: A systematic approach. *Biochemical Journal* **407**, 69-77

144. Nausch, L. W., Ledoux, J., Bonev, A. D., Nelson, M. T., and Dostmann, W. R. (2008) Differential patterning of cGMP in vascular smooth muscle cells revealed by single GFP-linked biosensors. *Proceedings of the National Academy of Sciences* **105**, 365-370

145. Akerboom, J., Chen, T.-W., Wardill, T. J., Tian, L., Marvin, J. S., Mutlu, S., Calderón, N. C., Esposti, F., Borghuis, B. G., and Sun, X. R. *et al.* (2012) Optimization of a GCaMP calcium indicator for neural activity imaging. *Journal of neuroscience* **32**, 13819-13840

146. Chen, T.-W., Wardill, T. J., Sun, Y., Pulver, S. R., Renninger, S. L., Baohan, A., Schreiter, E. R., Kerr, R. A., Orger, M. B., and Jayaraman, V. *et al.* (2013) Ultrasensitive fluorescent proteins for imaging neuronal activity. *Nature* **499**, 295

147. Kuchipudi, A., Arroyo-Olarte, R. D., Hoffmann, F., Brinkmann, V., and Gupta, N. (2016) Optogenetic monitoring identifies phosphatidylthreonine-regulated calcium homeostasis in *Toxoplasma gondii*. *Microbial Cell* **3**, 215

148. Nagai, T., Sawano, A., Park, E. S., and Miyawaki, A. (2001) Circularly permuted green fluorescent proteins engineered to sense Ca^{2+}. *Proceedings of the National Academy of Sciences* **98**, 3197-3202

149. Hartmann, A., Arroyo-Olarte, R. D., Imkeller, K., Hegemann, P., Lucius, R., and Gupta, N. (2013) Optogenetic modulation of an adenylate cyclase in *Toxoplasma gondii* demonstrates a requirement of the parasite cAMP for host-cell invasion and stage differentiation. *Journal of Biological Chemistry* **288**, 13705-13717

150. Baker, D. (2004) Adenylyl and guanylyl cyclases from the malaria parasite *Plasmodium falciparum. IUBMB life* **56**, 535-540

151. Carucci, D. J., Witney, A. A., Muhia, D. K., Warhurst, D. C., Schaap, P., Meima, M., Li, J.-L., Taylor, M. C., Kelly, J. M., and Baker, D. A. (2000) Guanylyl cyclase activity associated with putative bifunctional integral membrane proteins in *Plasmodium falciparum*. *Journal of Biological Chemistry* **275**, 22147-22156

152. Gao, H., Yang, Z., Wang, X., Qian, P., Hong, R., Chen, X., Su, X.-z., Cui, H., and Yuan, J. (2018) ISP1-anchored polarization of GCβ/CDC50A complex initiates malaria ookinete gliding motility. *Current Biology* **28**, 2763-2776. e2766

153. Bisio, H., Lunghi, M., Brochet, M., and Soldati-Favre, D. (2019) Phosphatidic acid governs natural egress in *Toxoplasma gondii via* a guanylate cyclase receptor platform. *Nature microbiology* **4**, 420

154. Yang, L., Uboldi, A. D., Seizova, S., Wilde, M.-L., Coffey, M. J., Katris, N. J., Yamaryo-Botté, Y., Kocan, M., Bathgate, R. A., and Stewart, R. J. (2019) An apically

located hybrid guanylate cyclase–ATPase is critical for the initiation of Ca^{2+} signaling and motility in *Toxoplasma gondii*. *Journal of Biological Chemistry* **294**, 8959-8972

155. Dubremetz, J., Rodriguez, C., and Ferreira, E. (1985) *Toxoplasma gondii:* Redistribution of monoclonal antibodies on tachyzoites during host cell invasion. *Experimental parasitology* **59**, 24-32

156. Beck, J. R., Rodriguez-Fernandez, I. A., De Leon, J. C., Huynh, M.-H., Carruthers, V. B., Morrissette, N. S., and Bradley, P. J. (2010) A novel family of *Toxoplasma* IMC proteins displays a hierarchical organization and functions in coordinating parasite division. *PLoS pathogens* **6**, e1001094

157. Plattner, F., Yarovinsky, F., Romero, S., Didry, D., Carlier, M.-F., Sher, A., and Soldati-Favre, D. (2008) *Toxoplasma* profilin is essential for host cell invasion and TLR11-dependent induction of an interleukin-12 response. *Cell host & microbe* **3**, 77-87

158. Sadak, A., Taghy, Z., Fortier, B., and Dubremetz, J.-F. (1988) Characterization of a family of rhoptry proteins of *Toxoplasma gondii. Molecular and biochemical parasitology* **29**, 203-211

159. Echeverria, P. C., Matrajt, M., Harb, O. S., Zappia, M. P., Costas, M. A., Roos, D. S., Dubremetz, J. F., and Angel, S. O. (2005) *Toxoplasma gondii* Hsp90 is a potential drug target whose expression and subcellular localization are developmentally regulated. *Journal of molecular biology* **350**, 723-734

160. Biftu, T., Feng, D., Ponpipom, M., Girotra, N., Liang, G.-B., Qian, X., Bugianesi, R., Simeone, J., Chang, L., and Gurnett, A. (2005) Synthesis and SAR of 2, 3-diarylpyrrole inhibitors of parasite cGMP-dependent protein kinase as novel anticoccidial agents. *Bioorganic & medicinal chemistry letters* **15**, 3296-3301

161. Karimova, G., Pidoux, J., Ullmann, A., and Ladant, D. (1998) A bacterial two-hybrid system based on a reconstituted signal transduction pathway. *Proceedings of the National Academy of Sciences* **95**, 5752-5756

162. Pfefferkorn, E., and Borotz, S. E. (1994) *Toxoplasma gondii:* Characterization of a mutant resistant to 6-thioxanthine. *Experimental parasitology* **79**, 374-382

163. Sonnhammer, E. L., Von Heijne, G., and Krogh, A. (1998) A hidden Markov model for predicting transmembrane helices in protein sequences. in *Ismb,* **6***,* 175-182

164. Letunic, I., Doerks, T., and Bork, P. (2014) SMART: Recent updates, new developments and status in 2015. *Nucleic acids research* **43**, D257-D260

165. Käll, L., Krogh, A., and Sonnhammer, E. L. (2004) A combined transmembrane topology and signal peptide prediction method. *Journal of molecular biology* **338**, 1027-1036

166. Marchler-Bauer, A., and Bryant, S. H. (2004) CD-Search: Protein domain annotations on the fly. *Nucleic acids research* **32**, W327-W331

167. Hofmann, K. (1993) TMbase-A database of membrane spanning proteins segments. *Biol. Chem. Hoppe-Seyler* **374**, 166

168. Sievers, F., Wilm, A., Dineen, D., Gibson, T. J., Karplus, K., Li, W., Lopez, R., McWilliam, H., Remmert, M., and Söding, J. *et al.* (2011) Fast, scalable generation of high-quality protein multiple sequence alignments using Clustal Omega. *Molecular systems biology* **7**, 539

169. Katoh, K., and Standley, D. M. (2013) MAFFT multiple sequence alignment software version 7: Improvements in performance and usability. *Molecular biology and evolution* **30**, 772-780

170. Andersen, J. P., Vestergaard, A. L., Mikkelsen, S. A., Mogensen, L. S., Chalat, M., and Molday, R. S. (2016) P4-ATPases as phospholipid flippases—Structure, function, and enigmas. *Frontiers in physiology* **7**, 275

171. Palmgren, M. G., and Nissen, P. (2011) P-type ATPases. *Annual review of biophysics* **40**, 243-266

172. Bublitz, M., Morth, J. P., and Nissen, P. (2011) P-type ATPases at a glance. *J Cell Sci* **124**, 2515-2519

173. Axelsen, K. B., and Palmgren, M. G. (1998) Evolution of substrate specificities in the P-type ATPase superfamily. *Journal of molecular evolution* **46**, 84-101

174. Lee, S., Uchida, Y., Wang, J., Matsudaira, T., Nakagawa, T., Kishimoto, T., Mukai, K., Inaba, T., Kobayashi, T., and Molday, R. S. *et al.* (2015) Transport through recycling endosomes requires EHD1 recruitment by a phosphatidylserine translocase. *The EMBO journal* **34**, 669-688

175. Sinha, S., and Sprang, S. (2006) Structures, mechanism, regulation and evolution of class III nucleotidyl cyclases. in *Reviews of Physiology Biochemistry and Pharmacology*, Springer. pp 105-140

176. Steegborn, C. (2014) Structure, mechanism, and regulation of soluble adenylyl cyclases—Similarities and differences to transmembrane adenylyl cyclases. *Biochimica Et Biophysica Acta (BBA)-Molecular Basis of Disease* **1842**, 2535-2547

177. Linder, J. U. (2005) Substrate selection by class III adenylyl cyclases and guanylyl cyclases. *IUBMB life* **57**, 797-803

178. Gaskins, E., Gilk, S., DeVore, N., Mann, T., Ward, G., and Beckers, C. (2004) Identification of the membrane receptor of a class XIV myosin in *Toxoplasma gondii*. *The Journal of cell biology* **165**, 383-393

179. Bradley, P. J., Ward, C., Cheng, S. J., Alexander, D. L., Coller, S., Coombs, G. H., Dunn, J. D., Ferguson, D. J., Sanderson, S. J., and Wastling, J. M. (2005) Proteomic analysis of rhoptry organelles reveals many novel constituents for host-parasite interactions in *Toxoplasma gondii. Journal of Biological Chemistry* **280**, 34245-34258

180. Morgens, D. W., Wainberg, M., Boyle, E. A., Ursu, O., Araya, C. L., Tsui, C. K., Haney, M. S., Hess, G. T., Han, K., and Jeng, E. E. *et al*. (2017) Genome-scale measurement of off-target activity using Cas9 toxicity in high-throughput screens. *Nature communications* **8**, 15178

181. Tsai, S. Q., and Joung, J. K. (2016) Defining and improving the genome-wide specificities of CRISPR–Cas9 nucleases. *Nature Reviews Genetics* **17**, 300

182. Wang, T., Birsoy, K., Hughes, N. W., Krupczak, K. M., Post, Y., Wei, J. J., Lander, E. S., and Sabatini, D. M. (2015) Identification and characterization of essential genes in the human genome. *Science* **350**, 1096-1101

183. Donald, R. G., Zhong, T., Wiersma, H., Nare, B., Yao, D., Lee, A., Allocco, J., and Liberator, P. A. (2006) Anticoccidial kinase inhibitors: Identification of protein kinase targets secondary to cGMP-dependent protein kinase. *Molecular and biochemical parasitology* **149**, 86-98

184. Yuasa, K., Mi-Ichi, F., Kobayashi, T., Yamanouchi, M., Kotera, J., Kita, K., and Omori, K. (2005) *Pf*PDE1, a novel cGMP-specific phosphodiesterase from the human malaria parasite *Plasmodium falciparum. Biochemical Journal* **392**, 221-229

185. McCoy, J. M., Whitehead, L., van Dooren, G. G., and Tonkin, C. J. (2012) *Tg*CDPK3 regulates calcium-dependent egress of *Toxoplasma gondii* from host cells. *PLoS pathogens* **8**, e1003066

186. Günay-Esiyok, Ö., Scheib, U., Noll, M., and Gupta, N. (2019) An unusual and vital protein with guanylate cyclase and P4-ATPase domains in a pathogenic protist. *Life Science Alliance* **2**, e201900402

187. Tesmer, J. J., Sunahara, R. K., Gilman, A. G., and Sprang, S. R. (1997) Crystal structure of the catalytic domains of adenylyl cyclase in a complex with Gsα· GTPγS. *Science* **278**, 1907-1916

188. Endo, T., and Yagita, K. (1990) Effect of extracellular ions on motility and cell entry in *Toxoplasma gondii. The Journal of protozoology* **37**, 133-138

189. Rohloff, P., Miranda, K., Rodrigues, J. C., Fang, J., Galizzi, M., Plattner, H., Hentschel, J., and Moreno, S. N. (2011) Calcium uptake and proton transport by acidocalcisomes of *Toxoplasma gondii*. *PLoS One* **6**, e18390

190. Coleman, J. A., and Molday, R. S. (2011) Critical role of the β-subunit CDC50A in the stable expression, assembly, subcellular localization, and lipid transport activity of the P4-ATPase ATP8A2. *Journal of Biological Chemistry* **286**, 17205-17216

191. Pilz, R. B., and Casteel, D. E. (2003) Regulation of gene expression by cyclic GMP. *Circulation research* **93**, 1034-1046

192. Roelofs, J., Snippe, H., Kleineidam, R. G., and Van Haastert, P. J. (2001) Guanylate cyclase in *Dictyostelium discoideum* with the topology of mammalian adenylate cyclase. *Biochemical Journal* **354**, 697-706

193. Samineni, V. K., Yoon, J., Crawford, K. E., Jeong, Y. R., McKenzie, K. C., Shin, G., Xie, Z., Sundaram, S. S., Li, Y., and Yang, M. Y. (2017) Fully implantable, battery-free wireless optoelectronic devices for spinal optogenetics. *Pain* **158**, 2108

194. Yizhar, O., Fenno, L. E., Davidson, T. J., Mogri, M., and Deisseroth, K. (2011) Optogenetics in neural systems. *Neuron* **71**, 9-34

195. Zhang, F., Gradinaru, V., Adamantidis, A. R., Durand, R., Airan, R. D., De Lecea, L., and Deisseroth, K. (2010) Optogenetic interrogation of neural circuits: technology for probing mammalian brain structures. *Nature protocols* **5**, 439

7 Appendices

Appendix 1: Assigned digital values and corresponding light intensities depending on the wavelengths to control constructed 24-well plate compatible illumination device for optogenetic study.

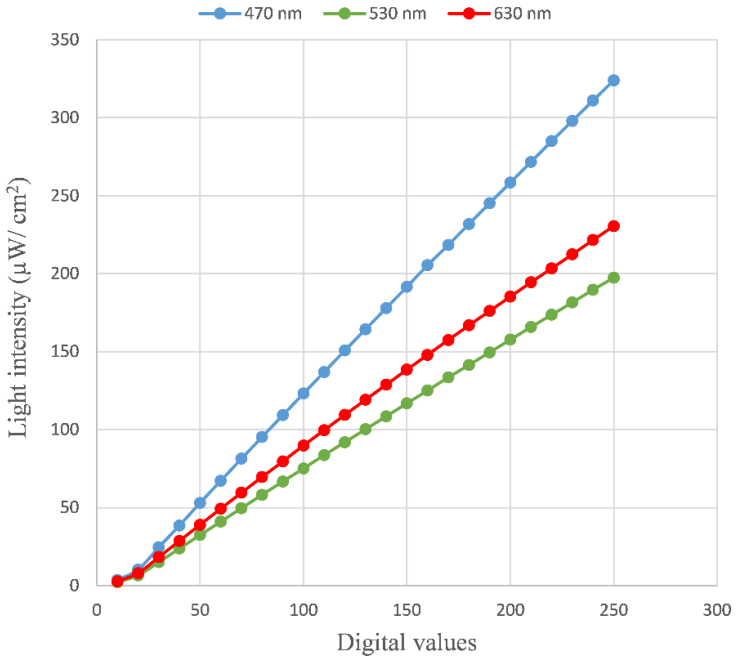

Appendix 2. The alignment of P-type ATPase-like domains of *Tg*ATPase$_P$-GC, *Pf*GCα and *Pf*GCβ with the members of human P4-ATPases. The human P4-ATPases were aligned by MAFFT alignment server (v7) (169), and then merged with the aligned ATPase domains of *Tg*ATPase$_P$-GC, *Pf*GCα and *Pf*GCβ using MAFFT merge. The alignment was trimmed, as indicated by horizontal lines, and signature residues were color-coded with the Clustal Omega program (>30% sequence conservation). Selected amino acids that are essential for ATP binding and phosphorylation, as well as transmembrane helices are boxed in black. Transmembrane topology of ATP8A1 retrieved from TMHMM Server (v2) (163) was used as a reference. Organism abbreviations and accession numbers: P-type ATPase-like domain of *Tg*ATPase$_P$-GC, *Toxoplasma gondii* (EPR59074.1); *Pf*GCα, *Plasmodium falciparum* (AJ245435.1); *Pf*GCβ, *Plasmodium falciparum* (AJ249165.1); and P4-ATPases of *Homo sapiens*: ATP8A1 (Q9Y2Q0.1), ATP8B4 (Q8TF62.3), ATP9A (O75110.3), ATP10A (O60312.2), ATP11C (Q8NB49.3).

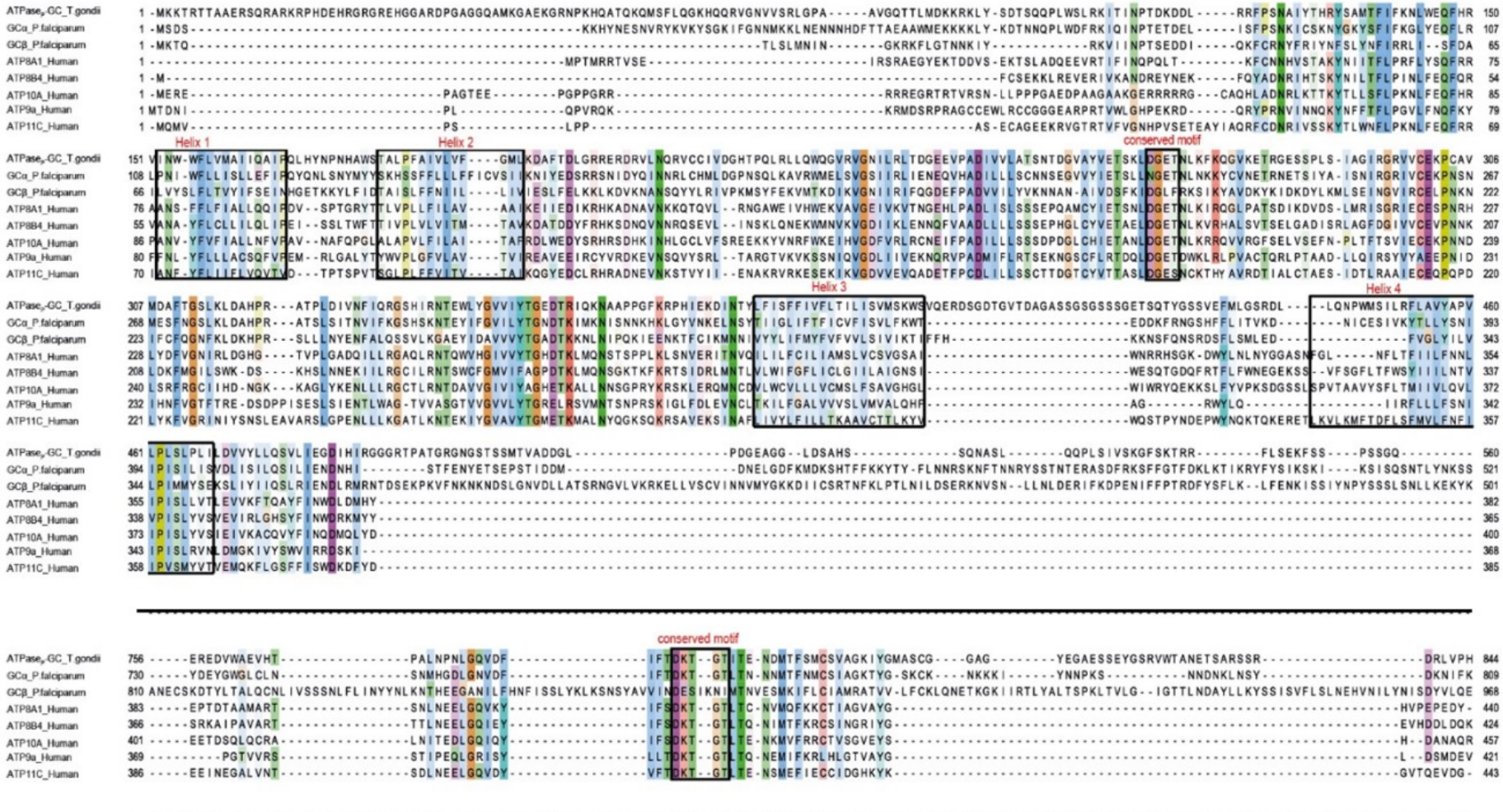
Helix 1
Helix 2
conserved motif
Helix 3
Helix 4
conserved motif


consverded motif
consverded motif
Helix 5
Helix 6
Helix 7
Helix 8
Helix 9
Helix 10

Appendix 3: Protein sequence alignment of GC1 and GC2 domains of *Tg*ATPase$_P$-GC with orthologous GCs/ACs showing a 74- and 40-residues long loop insertions in the GC1 of *Tg*ATPase$_P$-GC and *Pf*GCα, respectively. Both GC1 and GC2 domains are structured with seven-stranded β-sheets surrounded by four α-helices, and conserved residues that are important for the functionality were annotated.

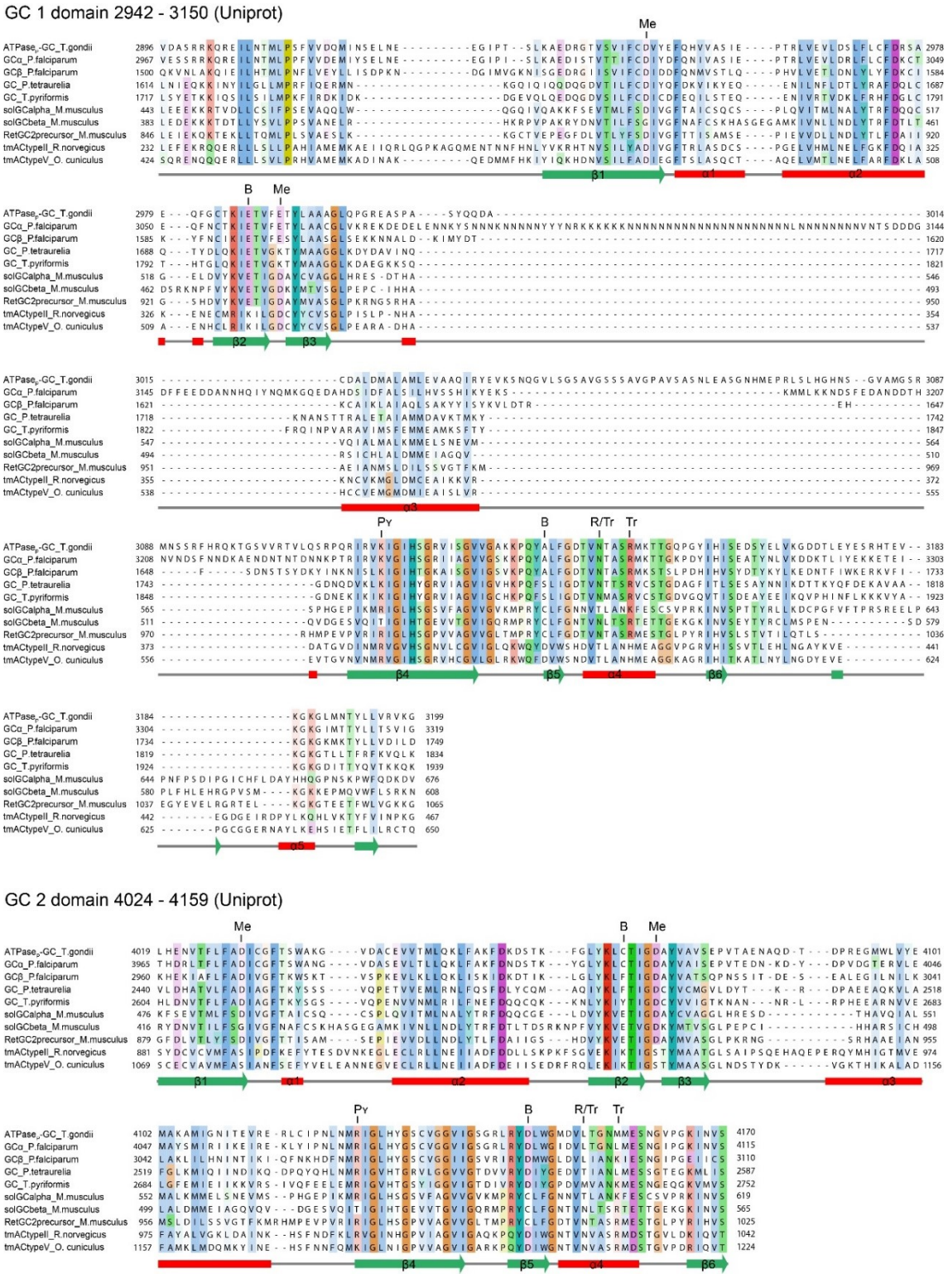

Appendix 4: (A) Expression profiles of GC1 and GC2 domains of *Tg*ATPase$_P$-GC in *E. coli* M15 strain before- and after- IPTG induction as well as in induced bacterial lysates. **(B)** cGMP measurements *via* HPLC following *in vitro* guanylate cyclase assay that was set by bacterial lysates expressing GC1 and GC2 domains as described in *methods* resulted in no cGMP detection.

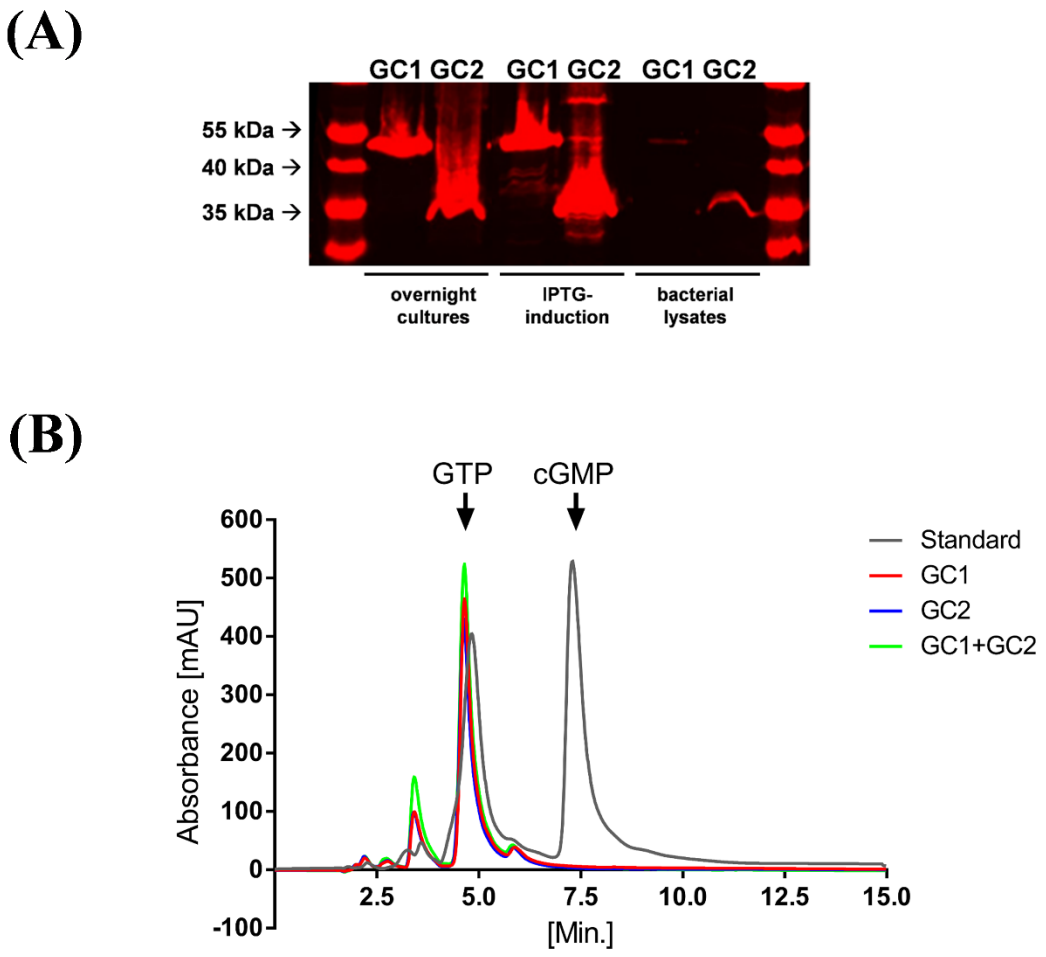

Appendix 5: Efficiency of Cre recombinase-mediated 3'UTR excision in *Tg*ATPase$_P$-GC and *Tg*PKG mutants. Efficiency of 3'UTR excision was quantified by scoring the loss of HA signal **(A)** in the *Tg*ATPase$_P$-GC-HA$_{3'IT}$-3'UTR$_{excised}$ mutant, which was generated as described in Figure 16A **(B)** in the *Tg*PKG mutant, which was generated as described in Figure 21B. Both mutants were immunostained with α-HA and α-*Tg*Gap45 antibodies. 300 vacuoles containing parasites with or without HA signal were counted from three independent immunofluorescence assays (mean with S.E.M.).

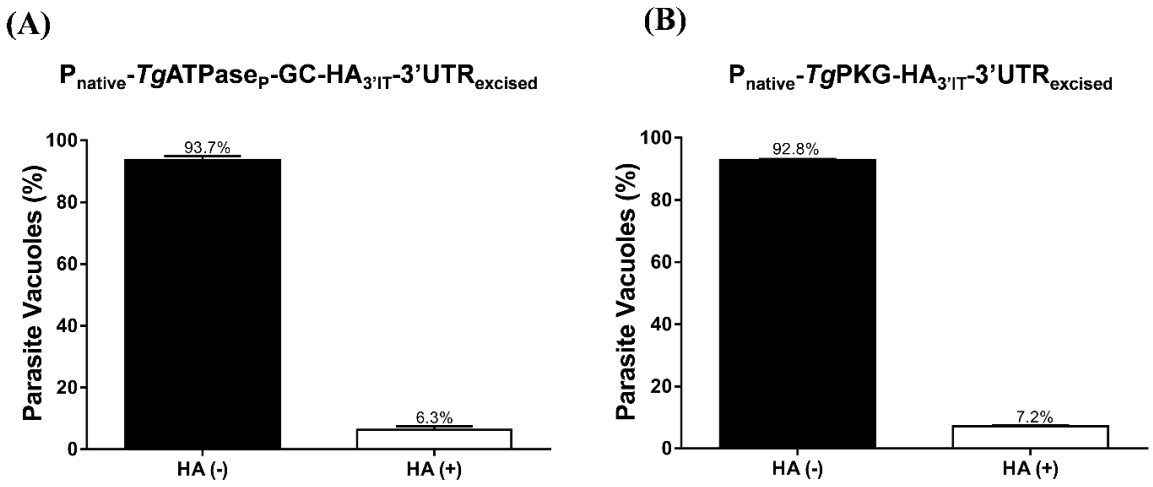

Appendix 6: Inhibition of residual activity in the *Tg*PKG-HA$_{3'IT}$ mutant by compound 2 enhances the defect of motility, invasion and egress. **(A)** Motile fraction and trail lengths of the P$_{native}$-*Tg*PKG-HA$_{3'IT}$-3'UTR$_{excised}$ mutant and P$_{native}$-*Tg*PKG-HA$_{3'IT}$-3'UTR$_{floxed}$ progenitor strains, generated according to Figure 21B, were measured by staining with α-*Tg*Sag1 antibody after Compound 2 treatment (2 µM, 15 min). A total of 500 parasites for each strain were analyzed to calculate the motile fraction. In total, 100 trails were measured for the progenitor strain, whereas only 30 trails could be evaluated for the mutant due to severe defect (n = 3 assays). **(B-C)** Comparative invasion and egress of strains were calculated following α-*Tg*Gap45 and α-*Tg*Sag1 antibody staining. **(B)** Fresh extracellular parasites (10^6) were let to invade to HFF-monolayers for 1 h with or without compound 2 (2 µM) addition. 450-500 parasites were evaluated from 3 independent assays. **(C)** Early parasite cultures (40 hpi) were treated with Compound 2 (2 µM) and incubated 8 hours to follow their attitude against the drug. 500-600 vacuoles were counted for each strain (n=4). (mean with S.E.M., significance with Student's *t*-test. (*, $p \leq 0.05$; **, $p \leq 0.01$; ***, $p \leq 0.001$; ****, $p \leq 0.0001$).

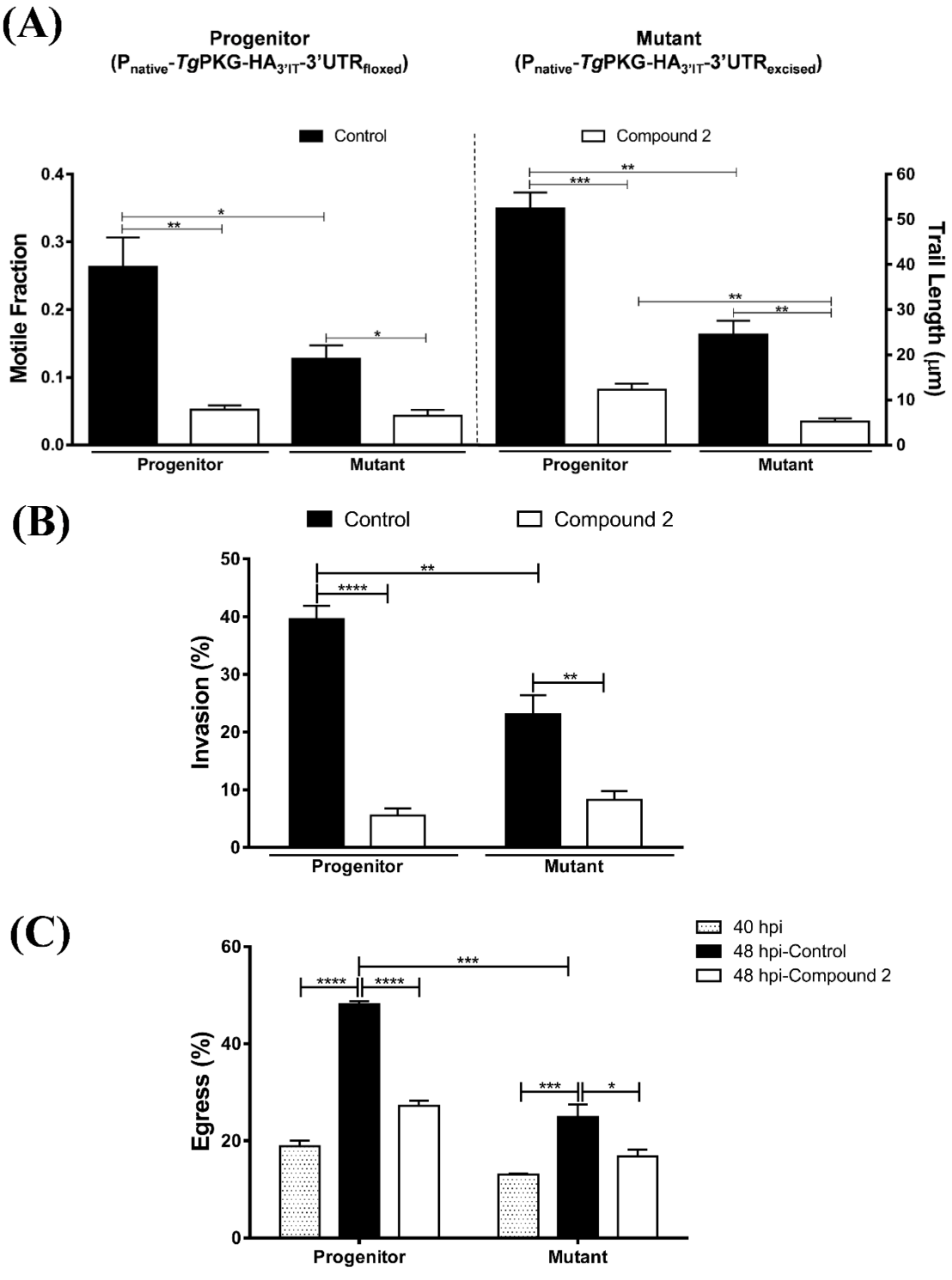
(A)
Progenitor
(P native-TgPKG-HA 3'IT-3'UTR floxed)
Mutant
(P native-TgPKG-HA 3'IT-3'UTR excised)
Control
Compound 2
Motile Fraction
Trail Length (μm)
Progenitor
Mutant
Progenitor
Mutant
(B)
Control
Compound 2
Invasion (%)
Progenitor
Mutant
(C)
40 hpi
48 hpi-Control
48 hpi-Compound 2
Egress (%)
Progenitor
Mutant

Appendix 7: Transcript screening of RhoGC and/or GCaMP6s expressing-optogenetic strains following transfection into *T. gondii* tachyzoites of RHΔ*ku80-hxgprt*$^{-}$ strain. RNAs of transgenic strains were isolated from transgenic strains followed by cDNA synthesis. cDNAs were screened for positive expression of the ORFs using specific primers given in Table 1, resulted in 1900 and 1354 bp amplicons for RhoGC and GCaMP6s, respectively.

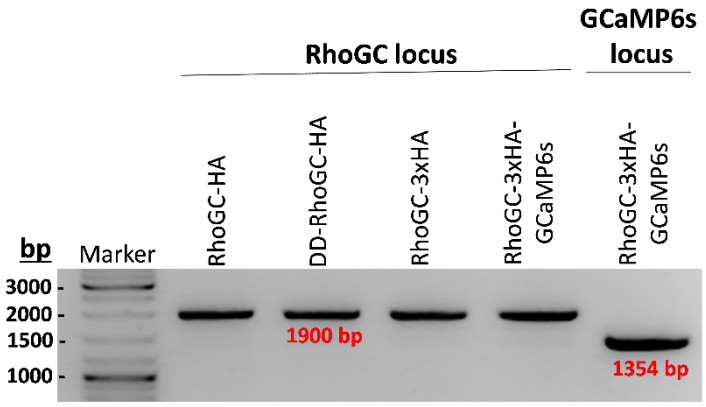

Appendix 8: Maps and sequences of vector constructs used in this study

A) Plasmid of *pQE60-TgATPase$_p$-GC1*

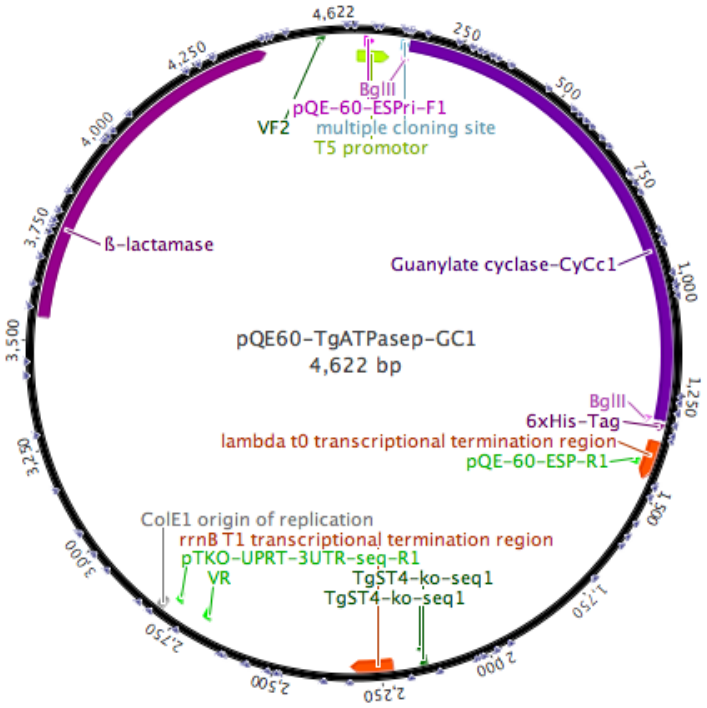

CTCGAGAAATCATAAAAAATTTATTTGCTTTGTGAGCGGATAACAATTATAATAGATTCAATTGTGAGCGGATAACAATTTCACACAGAATT
CATTAAAGAGGAGAAATTAACCATGGGAGGATCCAGATCTATGCTCGATAAGAAGTACTTGCCCCCACTAAATTTCGTCCACTACATTCCAC
TGTTCATTGGCATAGACGTCTTTGTCGCCTTTGTCGGTTATCGCCTGGAGTACAACCAGCGCAAGTCGTTCTTGCTGGACTACTCAGTGGAC
GCGTCTCGCAGGAAGCAACGAGAAATTCTCAACACGATGCTTCCCTCCTTCGTCGTCGACCAGATGATTAACTCGGAACTCAACGAAGAAGG
GATTCCGACGTCCCTCAAGGCCGAAGACAGAGGAACTGTGTCAGTCATTTTCTGCGATGTCTACGAATTCCAGCATGTCGTCGCATCCATCG
AACCGACGCGTCTCGTCGAGGTCTTGGATTCTCTTTTTCTCTGCTTCGACCGCAGTGCCGAACAGTTTGGTTGCACAAAAATCGAGACCGTC
TTCGAAACCTACCTGGCAGCCGCCGGCCTCCAGCCTGGTCGCGAAGCATCACCGGCATCGTACCAGCAAGACGCATGCGACGCCCTCGACAT
GGCACTGGCGATGCTGGAAGTCGCTGCACAGATTCGCTACGAAGTGAAAAGCAATCAGGGAGTTTTATCGGGGTCTGCTGTCGGCTCGAGCT
CAGCCGTCGGCCCCGCGGTGTCTGCCTCCAATCTTGAGGCTTCGGGCAACCACATGGAGCCTCGGCTTTCTCTCCATGGTCACAACTCTGGT
GTCGCCATGGGCAGTCGCATGAACAGCAGCCGGTTCCACCGACAGAAAACAGGCAGTGTCGTGCGCACTGTCCTCCAGTCTCGTCCGCAAAG
AATTCGCGTAAAGATTGGAATTCACTCAGGTCGTGTCATCAGTGGAGTCGTCGGGGCCAAGAAGCCCCAATACGCGCTTTTCGGAGACACTG
TCAACACAGCAAGTCGTATGAAGACCACCGGACAGCCGGGCTACATTCACATTTCGGAGGATTCCTACGAGCTTGTCAAGGGAGACGACACT
CTGGAATATGAATCACGACACACAGAAGTCAAAGGCAAAGGTCTGATGAACACCTATCTTCTCGTCAGAGTCAAAGGTTCGCCTTACCCTCA
CTTCGACGATCAAGAAGCAGACGAGGGAGACGTAATCTCGGAAACAGGAGGCCAAAACGGCGAGTCGCGGCGGTCGACCGCTTCCCTGCCCA
GGCAGCTGGAGACTGCGGGTGCGTCGTCGAGATCTCATCACCATCACCATCACTAAGCTTAATTAGCTGAGCTTGGACTCCTGTTGATAGAT
CCAGTAATGACCTCAGAACTCCATCTGGATTTGTTCAGAACGCTCGGTTGCCGCCGGGCGTTTTTTATTGGTGAGAATCCAAGCTAGCTTGG
CGAGATTTTCAGGAGCTAAGGAAGCTAAAATGGAGAAAAAAATCACTGGATATACCACCGTTGATATATCCCAATGGCATCGTAAAGAACAT
TTTGAGGCATTTCAGTCAGTTGCTCAATGTACCTATAACCAGACCGTTCAGCTGGATATTACGGCCTTTTTAAAGACCGTAAAGAAAAATAA
GCACAAGTTTTATCCGGCCTTTATTCACATTCTTGCCCGCCTGATGAATGCTCATCCGGAATTTCGTATGGCAATGAAAGACGGTGAGCTGG
TGATATGGGATAGTGTTCACCCTTGTTACACCGTTTTCCATGAGCAAACTGAAACGTTTTCATCGCTCTGGAGTGAATACCACGACGATTTC
CGGCAGTTTCTACACATATATTCGCAAGATGTGGCGTGTTACGGTGAAAACCTGGCCTATTTCCCTAAAGGGTTTATTGAGAATATGTTTTT
CGTCTCAGCCAATCCCTGGGTGAGTTTCACCAGTTTTGATTTAAACGTGGCCAATATGGACAACTTCTTCGCCCCCGTTTTCACCATGCATG
GGCAAATATTATACGCAAGGCGACAAGGTGCTGATGCCGCTGGCGATTCAGGTTCATCATGCCGTCTGTGATGGCTTCCATGTCGGCAGAAT
GCTTAATGAATTACAACAGTACTGCGATGAGTGGCAGGGCGGGGCGTAATTTTTTTAAGGCAGTTATTGGTGCCCTTAAACGCCTGGGGTAA
TGACTCTCTAGCTTGAGGCATCAAATAAAACGAAAGGCTCAGTCGAAAGACTGGGCCTTTCGTTTTATCTGTTGTTTGTCGGTGAACGCTCT
CCTGAGTAGGACAAATCCGCCGCTCTAGAGCTGCCTCGCGCGTTTCGGTGATGACGGTGAAAACCTCTGACACATGCAGCTCCCGGAGACGG
TCACAGCTTGTCTGTAAGCGGATGCCGGGAGCAGACAAGCCCGTCAGGGCGCGTCAGCGGGTGTTGGCGGGTGTCGGGGCGCAGCCATGACC
CAGTCACGTAGCGATAGCGGAGTGTATACTGGCTTAACTATGCGGCATCAGAGCAGATTGTACTGAGAGTGCACCATATGCGGTGTGAAATA
CCGCACAGATGCGTAAGGAGAAAATACCGCATCAGGCGCTCTTCCGCTTCCTCGCTCACTGACTCGCTGCGCTCGGTCGTTCGGCTGCGGCG
AGCGGTATCAGCTCACTCAAAGGCGGTAATACGGTTATCCACAGAATCAGGGGATAACGCAGGAAAGAACATGTGAGCAAAAGGCCAGCAAA
AGGCCAGGAACCGTAAAAAGGCCGCGTTGCTGGCGTTTTTCCATAGGCTCCGCCCCCCTGACGAGCATCACAAAAATCGACGCTCAAGTCAG
AGGTGGCGAAACCCGACAGGACTATAAAGATACCAGGCGTTTCCCCCTGGAAGCTCCCTCGTGCGCTCTCCTGTTCCGACCCTGCCGCTTAC
CGGATACCTGTCCGCCTTTCTCCCTTCGGGAAGCGTGGCGCTTTCTCATAGCTCACGCTGTAGGTATCTCAGTTCGGTGTAGGTCGTTCGCT
CCAAGCTGGGCTGTGTGCACGAACCCCCCGTTCAGCCCGACCGCTGCGCCTTATCCGGTAACTATCGTCTTGAGTCCAACCCGGTAAGACAC

GACTTATCGCCACTGGCAGCAGCCACTGGTAACAGGATTAGCAGAGCGAGGTATGTAGGCGGTGCTACAGAGTTCTTGAAGTGGTGGCCTAA
CTACGGCTACACTAGAAGGACAGTATTTGGTATCTGCGCTCTGCTGAAGCCAGTTACCTTCGGAAAAAGAGTTGGTAGCTCTTGATCCGGCA
AACAAACCACCGCTGGTAGCGGTGGTTTTTTTGTTTGCAAGCAGCAGATTACGCGCAGAAAAAAAGGATCTCAAGAAGATCCTTTGATCTTT
TCTACGGGGTCTGACGCTCAGTGGAACGAAAACTCACGTTAAGGGATTTTGGTCATGAGATTATCAAAAAGGATCTTCACCTAGATCCTTTT
AAATTAAAAATGAAGTTTTAAATCAATCTAAAGTATATATGAGTAAACTTGGTCTGACAGTTACCAATGCTTAATCAGTGAGGCACCTATCT
CAGCGATCTGTCTATTTCGTTCATCCATAGTTGCCTGACTCCCCGTCGTGTAGATAACTACGATACGGGAGGGCTTACCATCTGGCCCCAGT
GCTGCAATGATACCGCGAGACCCACGCTCACCGGCTCCAGATTTATCAGCAATAAACCAGCCAGCCGGAAGGGCCGAGCGCAGAAGTGGTCC
TGCAACTTTATCCGCCTCCATCCAGTCTATTAATTGTTGCCGGGAAGCTAGAGTAAGTAGTTCGCCAGTTAATAGTTTGCGCAACGTTGTTG
CCATTGCTACAGGCATCGTGGTGTCACGCTCGTCGTTTGGTATGGCTTCATTCAGCTCCGGTTCCCAACGATCAAGGCGAGTTACATGATCC
CCCATGTTGTGCAAAAAAGCGGTTAGCTCCTTCGGTCCTCCGATCGTTGTCAGAAGTAAGTTGGCCGCAGTGTTATCACTCATGGTTATGGC
AGCACTGCATAATTCTCTTACTGTCATGCCATCCGTAAGATGCTTTTCTGTGACTGGTGAGTACTCAACCAAGTCATTCTGAGAATAGTGTA
TGCGGCGACCGAGTTGCTCTTGCCCGGCGTCAATACGGGATAATACCGCGCCACATAGCAGAACTTTAAAAGTGCTCATCATTGGAAAACGT
TCTTCGGGGCGAAAACTCTCAAGGATCTTACCGCTGTTGAGATCCAGTTCGATGTAACCCACTCGTGCACCCAACTGATCTTCAGCATCTTT
TACTTTCACCAGCGTTTCTGGGTGAGCAAAAACAGGAAGGCAAAATGCCGCAAAAAAGGGAATAAGGGCGACACGGAAATGTTGAATACTCA
TACTCTTCCTTTTTCAATATTATTGAAGCATTTATCAGGGTTATTGTCTCATGAGCGGATACATATTTGAATGTATTTAGAAAAATAAACAA
ATAGGGGTTCCGCGCACATTTCCCCGAAAAGTGCCACCTGACGTCTAAGAAACCATTATTATCATGACATTAACCTATAAAAATAGGCGTAT
CACGAGGCCCTTTCGTCTTCAC

T5 promoter	Ampicillin	rrnB_T1_Terminator	*Tg*ATPase$_p$-GC1
BglII	CAT/CamR	6xHis-tag	

B) Plasmid of *pQE60-TgATPase$_p$-GC2*

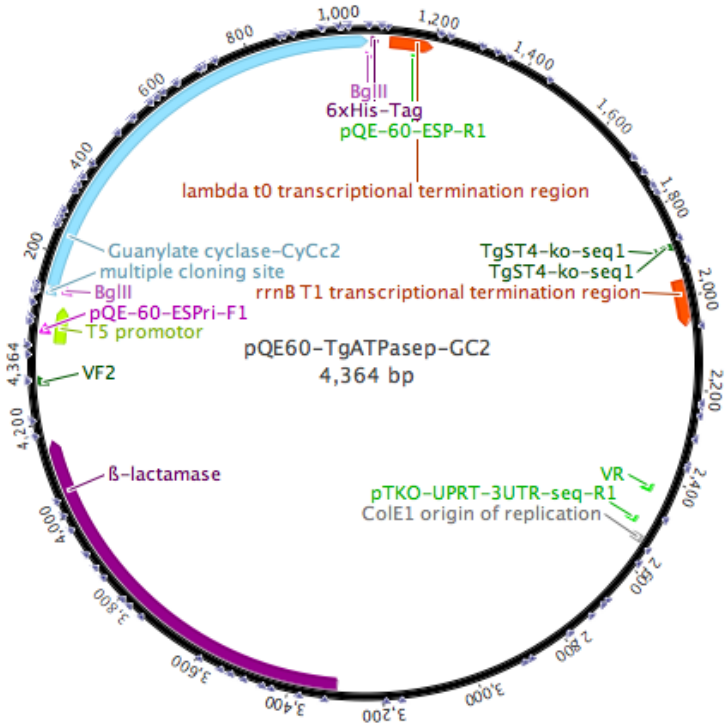

CTCGAGAAATCATAAAAAATTTATTTGCTTTGTGAGCGGATAACAATTATAATAGATTCAATTGTGAGCGGATAACAATTTCACACAGAATT
CATTAAAGAGGAGAAATTAACCATGGGAGGATCCAGATCTATGACGATGAGCTTAACGTTCATCATCACCACAGCCAGGGAAACCGCGTCGA
CAGTCAGCACGATTGCCACCTTCCCCTGCTACGTCTTCTTCAACTTGGTCAGTGCATACTGCAAAGAGTACATCGATCGTCTGACTTTCTAC
GTGAACGAGCATGCCAAGACGACAGAAAGCCGTGCGACGCAGCTTCTCAACGATATGCTTCCGAAGCAGGTTCTGGAGGAGTTTCAGCAGGA
CAAGCTGAAGCTCGCGTACCTCCACGAGAACGTGACTTTCCTTTTCGCAGATATTTGTGGGTTTACAAGTTGGGCAAAGGGTGTCGACGCTT
GCGAGGTCGTAACAATGCTGCAGAAACTCTTTGCGAAGTTCGACAAAGACAGTACCAAGTTCGGCCTGTACAAACTCTGCACCATCGGAGAC
GCTTACGTCGCTGTCTCCGAACCGGTCACAGCAGAGAATGCTCAAGACACAGACCCCCGAGAGGGCATGTGGCTTGTCTACGAGATGGCCAA
GGCGATGATCGGAAACATCACAGAAGTTCGAGAGCGTTTGTGCATTCCCAATCTGAACATGCGCATAGGTCTGCACTACGGAAGCTGCGTAG

GAGGCGTTATCGGGAGTGGACGCCTTCGTTACGATTTGTGGGGAATGGATGTCTTGACGGGGAACATGATGGAGAGCAACGGAGTTCCTGGA
AAAATCAATGTCTCGGAAATCCTGAAAAACGAAATGGAAAAAGGCTTTCCAGGAGAATTCGTTTTCAAGTTCAACAAGACAGTAGCGGTCTT
GCAAAGCACCGTCGACTCGTACCTCATTCGCCCTGCGAAGGATTTCGACGAAGACGAAGAACTTGCGGCAGCGGCGGCGACGATGGCTGTTG
CAGGTCCCTCTGCCTCTCTTCAGCAGGGCGGCGGTGCGATCCCTCAAAGATCTCATCACCATCACCATCACTAAGCTTAATTAGCTGAGCTT
GGACTCCTGTTGATAGATCCAGTAATGACCTCAGAACTCCATCTGGATTTGTTCAGAACGCTCGGTTGCCGCCGGGCGTTTTTTATTGGTGA
GAATCCAAGCTAGCTTGGCGAGATTTTCAGGAGCTAAGGAAGCTAAAATGGAGAAAAAAATCACTGGATATACCACCGTTGATATATCCCAA
TGGCATCGTAAAGAACATTTTGAGGCATTTCAGTCAGTTGCTCAATGTACCTATAACCAGACCGTTCAGCTGGATATTACGGCCTTTTTAAA
GACCGTAAAGAAAAATAAGCACAAGTTTTATCCGGCCTTTATTCACATTCTTGCCCGCCTGATGAATGCTCATCCGGAATTTCGTATGGCAA
TGAAAGACGGTGAGCTGGTGATATGGGATAGTGTTCACCCTTGTTACACCGTTTTCCATGAGCAAACTGAAACGTTTTCATCGCTCTGGAGT
GAATACCACGACGATTTCCGGCAGTTTCTACACATATATTCGCAAGATGTGGCGTGTTACGGTGAAAACCTGGCCTATTTCCCTAAAGGGTT
TATTGAGAATATGTTTTTCGTCTCAGCCAATCCCTGGGTGAGTTTCACCAGTTTTGATTTAAACGTGGCCAATATGGACAACTTCTTCGCCC
CCGTTTTCACCATGCATGGGCAAATATTATACGCAAGGCGACAAGGTGCTGATGCCGCTGGCGATTCAGGTTCATCATGCCGTCTGTGATGG
CTTCCATGTCGGCAGAATGCTTAATGAATTACAACAGTACTGCGATGAGTGGCAGGGCGGGGCGTAATTTTTTTAAGGCAGTTATTGGTGCC
CTTAAACGCCTGGGGTAATGACTCTCTAGCTTGAGGCATCAAATAAAACGAAAGGCTCAGTCGAAAGACTGGGCCTTTCGTTTTATCTGTTG
TTTGTCGGTGAACGCTCTCCTGAGTAGGACAAATCCGCCGCTCTAGAGCTGCCTCGCGCGTTTCGGTGATGACGGTGAAAACCTCTGACACA
TGCAGCTCCCGGAGACGGTCACAGCTTGTCTGTAAGCGGATGCCGGGAGCAGACAAGCCCGTCAGGGCGCGTCAGCGGGTGTTGGCGGGTGT
CGGGGCGCAGCCATGACCCAGTCACGTAGCGATAGCGGAGTGTATACTGGCTTAACTATGCGGCATCAGAGCAGATTGTACTGAGAGTGCAC
CATATGCGGTGTGAAATACCGCACAGATGCGTAAGGAGAAAATACCGCATCAGGCGCTCTTCCGCTTCCTCGCTCACTGACTCGCTGCGCTC
GGTCGTTCGGCTGCGGCGAGCGGTATCAGCTCACTCAAAGGCGGTAATACGGTTATCCACAGAATCAGGGGATAACGCAGGAAAGAACATGT
GAGCAAAAGGCCAGCAAAAGGCCAGGAACCGTAAAAAGGCCGCGTTGCTGGCGTTTTTCCATAGGCTCCGCCCCCCTGACGAGCATCACAAA
AATCGACGCTCAAGTCAGAGGTGGCGAAACCCGACAGGACTATAAAGATACCAGGCGTTTCCCCCTGGAAGCTCCCTCGTGCGCTCTCCTGT
TCCGACCCTGCCGCTTACCGGATACCTGTCCGCCTTTCTCCCTTCGGGAAGCGTGGCGCTTTCTCATAGCTCACGCTGTAGGTATCTCAGTT
CGGTGTAGGTCGTTCGCTCCAAGCTGGGCTGTGTGCACGAACCCCCCGTTCAGCCCGACCGCTGCGCCTTATCCGGTAACTATCGTCTTGAG
TCCAACCCGGTAAGACACGACTTATCGCCACTGGCAGCAGCCACTGGTAACAGGATTAGCAGAGCGAGGTATGTAGGCGGTGCTACAGAGTT
CTTGAAGTGGTGGCCTAACTACGGCTACACTAGAAGGACAGTATTTGGTATCTGCGCTCTGCTGAAGCCAGTTACCTTCGGAAAAAGAGTTG
GTAGCTCTTGATCCGGCAAACAAACCACCGCTGGTAGCGGTGGTTTTTTTGTTTGCAAGCAGCAGATTACGCGCAGAAAAAAAGGATCTCAA
GAAGATCCTTTGATCTTTTCTACGGGGTCTGACGCTCAGTGGAACGAAAACTCACGTTAAGGGATTTTGGTCATGAGATTATCAAAAAGGAT
CTTCACCTAGATCCTTTTAAATTAAAAATGAAGTTTTAAATCAATCTAAAGTATATATGAGTAAACTTGGTCTGACAGTTACCAATGCTTAA
TCAGTGAGGCACCTATCTCAGCGATCTGTCTATTTCGTTCATCCATAGTTGCCTGACTCCCCGTCGTGTAGATAACTACGATACGGGAGGGC
TTACCATCTGGCCCCAGTGCTGCAATGATACCGCGAGACCCACGCTCACCGGCTCCAGATTTATCAGCAATAAACCAGCCAGCCGGAAGGGC
CGAGCGCAGAAGTGGTCCTGCAACTTTATCCGCCTCCATCCAGTCTATTAATTGTTGCCGGGAAGCTAGAGTAAGTAGTTCGCCAGTTAATA
GTTTGCGCAACGTTGTTGCCATTGCTACAGGCATCGTGGTGTCACGCTCGTCGTTTGGTATGGCTTCATTCAGCTCCGGTTCCCAACGATCA
AGGCGAGTTACATGATCCCCCATGTTGTGCAAAAAAGCGGTTAGCTCCTTCGGTCCTCCGATCGTTGTCAGAAGTAAGTTGGCCGCAGTGTT
ATCACTCATGGTTATGGCAGCACTGCATAATTCTCTTACTGTCATGCCATCCGTAAGATGCTTTTCTGTGACTGGTGAGTACTCAACCAAGT
CATTCTGAGAATAGTGTATGCGGCGACCGAGTTGCTCTTGCCCGGCGTCAATACGGGATAATACCGCGCCACATAGCAGAACTTTAAAAGTG
CTCATCATTGGAAAACGTTCTTCGGGGCGAAAACTCTCAAGGATCTTACCGCTGTTGAGATCCAGTTCGATGTAACCCACTCGTGCACCCAA
CTGATCTTCAGCATCTTTTACTTTCACCAGCGTTTCTGGGTGAGCAAAAACAGGAAGGCAAAATGCCGCAAAAAAGGGAATAAGGGCGACAC
GGAAATGTTGAATACTCATACTCTTCCTTTTTCAATATTATTGAAGCATTTATCAGGGTTATTGTCTCATGAGCGGATACATATTTGAATGT
ATTTAGAAAAATAAACAAATAGGGGTTCCGCGCACATTTCCCCGAAAAGTGCCACCTGACGTCTAAGAAACCATTATTATCATGACATTAAC
CTATAAAAATAGGCGTATCACGAGGCCCTTTCGTCTTCAC

T5 promoter	Ampicillin	rrnB_T1_Terminator	*Tg*ATPase$_p$-GC2
BglII	CAT/CamR	6xHis-tag	

C) Plasmid of *pQE60-TgATPase$_p$-GC1+GC2*

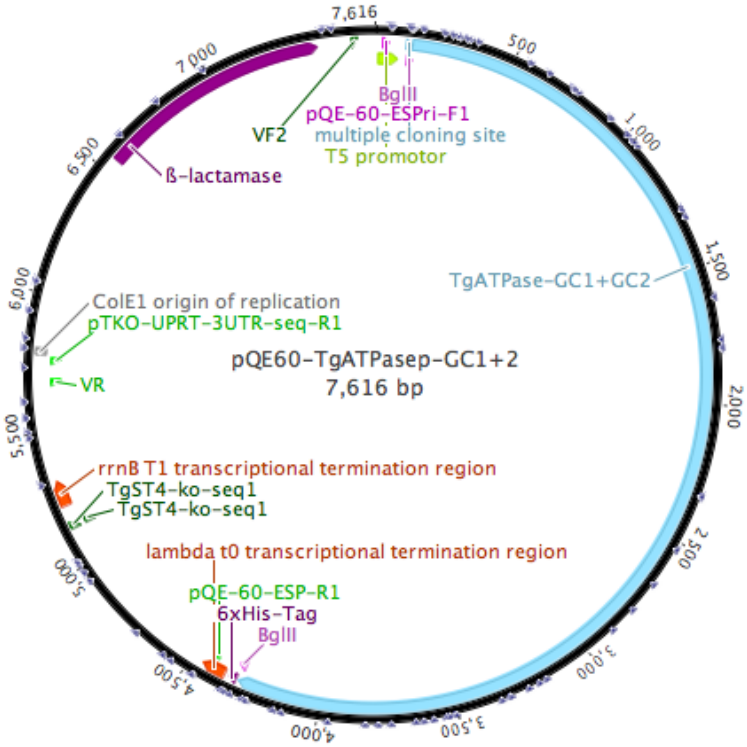

CTCGAGAAATCATAAAAAATTTATTTGCTTTGTGAGCGGATAACAATTATAATAGATTCAATTGTGAGCGGATAACAATTTCACACAGAATT
CATTAAAGAGGAGAAATTAACCATGGGAGGATCCAGATCTATGCTCGATAAGAAGTACTTGCCCCCACTAAATTTCGTCCACTACATTCCAC
TGTTCATTGGCATAGACGTCTTTGTCGCCTTTGTCGGTTATCGCCTGGAGTACAACCAGCGCAAGTCGTTCTTGCTGGACTACTCAGTGGAC
GCGTCTCGCAGGAAGCAACGAGAAATTCTCAACACGATGCTTCCCTCCTTCGTCGTCGACCAGATGATTAACTCGGAACTCAACGAAGAAGG
GATTCCGACGTCCCTCAAGGCCGAAGACAGAGGAACTGTGTCAGTCATTTTCTGCGATGTCTACGAATTCCAGCATGTCGTCGCATCCATCG
AACCGACGCGTCTCGTCGAGGTCTTGGATTCTCTTTTTCTCTGCTTCGACCGCAGTGCCGAACAGTTTGGTTGCACAAAAATCGAGACCGTC
TTCGAAACCTACCTGGCAGCCGCCGGCCTCCAGCCTGGTCGCGAAGCATCACCGGCATCGTACCAGCAAGACGCATGCGACGCCCTCGACAT
GGCACTGGCGATGCTGGAAGTCGCTGCACAGATTCGCTACGAAGTGAAAAGCAATCAGGGAGTTTTATCGGGGTCTGCTGTCGGCTCGAGCT
CAGCCGTCGGCCCCGCGGTGTCTGCCTCCAATCTTGAGGCTTCGGGCAACCACATGGAGCCTCGGCTTTCTCTCCATGGTCACAACTCTGGT
GTCGCCATGGGCAGTCGCATGAACAGCAGCCGGTTCCACCGACAGAAAACAGGCAGTGTCGTGCGCACTGTCCTCCAGTCTCGTCCGCAAAG
AATTCGCGTAAAGATTGGAATTCACTCAGGTCGTGTCATCAGTGGAGTCGTCGGGGCCAAGAAGCCCCAATACGCGCTTTTCGGAGACACTG
TCAACACAGCAAGTCGTATGAAGACCACCGGACAGCCGGGCTACATTCACATTTCGGAGGATTCCTACGAGCTTGTCAAGGGAGACGACACT
CTGGAATATGAATCACGACACACAGAAGTCAAAGGCAAAGGTCTGATGAACACCTATCTTCTCGTCAGAGTCAAAGGTTCGCCTTACCCTCA
CTTCGACGATCAAGAAGCAGACGAGGGAGACGTAATCTCGGAAACAGGAGGCCAAAACGGCGAGTCGCGGCGGTCGACCGCTTCCCTGCCCA
GGCAGCTGGAGACTGCGGGTGCGTCGTCGGGTGTACATACGGGCGAGGCGATGGGCTGTTTCGCATCTGTGGGGTCTCGGGGAGAGAGTCAG
ACAGCGGCAGATGCGGCGGCGGCCGAGGCCATCGAAGAGGACATCCAAGTGGAGATCGACGAGGAAGGCGTCGTGGAAGACACCGTCGAAAA
GGCAGTGGAAGATGTGCGACGTCTCAGGAACGAAGGGTCGCACGCAGTCGCGAGCGACGACTTCCCAGTCTCTCAGGCCGGTGCAGCGCAGC
CGCGACGCTGCTCCCGCTTCCTCTTCCAAAATGCGGAGGAGCATGGAGCTGCAGAGCCTCAACGAGGAGAGGGCGCGCGCTTGATTCTCTCC
CCTGGACAGACAGAGGGAACGCGTCAAAGCGAGAAAGAGGGATCGGCTCTCGGCAGCAACATCGCTGCGAGTGCACGCGCAGATCGCAGGCC
TGCCGGGCGGCGAGAGGATTCGAGAGGAGACAGCCGCTTCGACTACGAGTCCATGACAACACAGCAGCTTCTGCGAATCTACAGGAGACAAC
AGAAGGTCGCCAAGGTTCTCCAGTGGATCGACGAAGAACTGAGAGGGCAGCGCGATACAGCGCACAGACACGCAAGGACAGCGGACATCGTC
GCGAAGCTCCTCGCTTCGTCGGGAGACGAGCAGGCAGCTGGAGAGAGTTCGGAGGCAGACCACGACGAAGTGCCTCTGGACGAGATCAAGGA
GGAACTGCGGCGACAAGCTCGGGAGGCGAACGAGCAGGAATCCGCGAAGAGGTCCGGGGGAGACGCTCCACCCCACACACCCACACGCAAGG
CCCTTCTCAAGGCCTTTCGCAGCGAAATCGTGCATGGATGCGCGGCTCCCACGGAAGAAGAGAAGACTGCAAAGGAAGGCAGAGAGTCTGAA
GTGGCTCTCGCCTCTCCAGAAACCGAATCTCGAGACGCCAATGGCCAGCGAGTTTCCGAAAGGGATGCGTCAGATGCCCGAGAGGGCAGCGC
GTCTCCGCAACCGGACCACGCGGCGCCTCCGTCAGGGCTACCGCAGGGATTGAAAGGACAAGAGACAGAGAAGCAGCAAGGCTGGAAACTGT
TTCGTTCTGCGAGTCTTGTGCGCGCCGCCGGCCAGTCGTTTGCTTCTCTCTTCAGGCGGCGCAAACCGGCCGCTCCTTCTGAAGCTGCGAGC
CCCTCAAGTGCGGACACACCCATGGATAGCCGCGTCTCGCCGACGTCGGTCGATGACGAAGACCTGGAGCAAAACAGAGTGACGCGAATCGG
CGTATCGAGTGAGTGGCTGCTTCTCAAATTCAAAGACAAGAATCTCGAGGCGCGCTATCGAACGCACTTTTACAACAACAAGTCCAACATTA
ACACAATTGAACAAGCCCTCATCATCTTTCTTGTGACCTTTTGCGTTCAAACGCTGACACGGCTGGCGCTGCCGCGCTTCTACGTTGTTTGC
TCTCATCACACGATCAACCTCCACGTCTGCACAGGCCTTTACTGGGCGGTTCGCGCGACGTACACCTTAGCCGCGTTCGTCCTCTGGATGTT
GTTCCACTACCGAAACCGAAAGGAGGTGGCGACATGTTTGGAGCTTCGCTGGATGGTTTTCCTTCTGAATTTGCTGTTTATTTCTGCGTCGT
GTGTCTTCGCACTCTCGAACTCCTGGGGTGTCTGCGGACAGCAGCAGGAAGACCATGGGGCGTCCGAGACCGCCGTGGAGAACACCCTGGTC
GCTCTCTCGCATCTTGCGAAAGACGGCAGCTTCCCGGCCGACGACGCAGAAGTGAACAGCGTCGCCGGCTCGCCTCTCGCTCAGGCCATGCA
CTCTCCCTTCACCACGGCAGGCGTCTCACGAGCCTCCCGAATGCTGAGGAGTGGAGGCGTCAGTGTCTCCGGAGGAACGGATTGCACGGGTG

TCGGCACCTCGGGTGAAGAGGGATCCGACCTCGTGACTGCCAACGGGAGGGCCTACACCTACTGGCTTCTCAGCGACACGATTGAGCTCTTC
TTCTACATCGTCATTCTCCACCACAACACCGGTCTCTTGTTCCAAAACTGCATCCTCGTCGATGTCCTGCTGATGACGATGAGCTTAACGTT
CATCATCACCACAGCCAGGGAAACCGCGTCGACAGTCAGCACGATTGCCACCTTCCCCTGCTACGTCTTCTTCAACTTGGTCAGTGCATACT
GCAAAGAGTACATCGATCGTCTGACTTTCTACGTGAACGAGCATGCCAAGACGACAGAAAGCCGTGCGACGCAGCTTCTCAACGATATGCTT
CCGAAGCAGGTTCTGGAGGAGTTTCAGCAGGACAAGCTGAAGCTCGCGTACCTCCACGAGAACGTGACTTTCCTTTTCGCAGATATTTGTGG
GTTTACAAGTTGGGCAAAGGGTGTCGACGCTTGCGAGGTCGTAACAATGCTGCAGAAACTCTTTGCGAAGTTCGACAAAGACAGTACCAAGT
TCGGCCTGTACAAACTCTGCACCATCGGAGACGCTTACGTCGCTGTCTCCGAACCGGTCACAGCAGAGAATGCTCAAGACACAGACCCCCGA
GAGGGCATGTGGCTTGTCTACGAGATGGCCAAGGCGATGATCGGAAACATCACAGAAGTTCGAGAGCGTTTGTGCATTCCCAATCTGAACAT
GCGCATAGGTCTGCACTACGGAAGCTGCGTAGGAGGCGTTATCGGGAGTGGACGCCTTCGTTACGATTTGTGGGGAATGGATGTCTTGACGG
GGAACATGATGGAGAGCAACGGAGTTCCTGGAAAAATCAATGTCTCGGAAATCCTGAAAAACGAAATGGAAAAAGGCTTTCCAGGAGAATTC
GTTTTCAAGTTCAACAAGACAGTAGCGGTCTTGCAAAGCACCGTCGACTCGTACCTCATTCGCCCTGCGAAGGATTTCGACGAAGACGAAGA
ACTTGCGGCAGCGGCGGCGACGATGGCTGTTGCAGGTCCCTCTGCCTCTCTTCAGCAGGGCGGCGGTGCGATCCCTCAAAGATCTCATCACC
ATCACCATCACTAAGCTTAATTAGCTGAGCTTGGACTCCTGTTGATAGATCCAGTAATGACCTCAGAACTCCATCTGGATTTGTTCAGAACG
CTCGGTTGCCGCCGGGCGTTTTTTATTGGTGAGAATCCAAGCTAGCTTGGCGAGATTTTCAGGAGCTAAGGAAGCTAAAATGGAGAAAAAAA
TCACTGGATATACCACCGTTGATATATCCCAATGGCATCGTAAAGAACATTTTGAGGCATTTCAGTCAGTTGCTCAATGTACCTATAACCAG
ACCGTTCAGCTGGATATTACGGCCTTTTTAAAGACCGTAAAGAAAAATAAGCACAAGTTTTATCCGGCCTTTATTCACATTCTTGCCCGCCT
GATGAATGCTCATCCGGAATTTCGTATGGCAATGAAAGACGGTGAGCTGGTGATATGGGATAGTGTTCACCCTTGTTACACCGTTTTCCATG
AGCAAACTGAAACGTTTTCATCGCTCTGGAGTGAATACCACGACGATTTCCGGCAGTTTCTACACATATATTCGCAAGATGTGGCGTGTTAC
GGTGAAAACCTGGCCTATTTCCCTAAAGGGTTTATTGAGAATATGTTTTTCGTCTCAGCCAATCCCTGGGTGAGTTTCACCAGTTTTGATTT
AAACGTGGCCAATATGGACAACTTCTTCGCCCCCGTTTTCACCATGCATGGGCAAATATTATACGCAAGGCGACAAGGTGCTGATGCCGCTG
GCGATTCAGGTTCATCATGCCGTCTGTGATGGCTTCCATGTCGGCAGAATGCTTAATGAATTACAACAGTACTGCGATGAGTGGCAGGGCGG
GGCGTAATTTTTTTAAGGCAGTTATTGGTGCCCTTAAACGCCTGGGGTAATGACTCTCTAGCTTGAGGCATCAAATAAAACGAAAGGCTCAG
TCGAAAGACTGGGCCTTTCGTTTTATCTGTTGTTTGTCGGTGAACGCTCTCCTGAGTAGGACAAATCCGCCGCTCTAGAGCTGCCTCGCGCG
TTTCGGTGATGACGGTGAAAACCTCTGACACATGCAGCTCCCGGAGACGGTCACAGCTTGTCTGTAAGCGGATGCCGGGAGCAGACAAGCCC
GTCAGGGCGCGTCAGCGGGTGTTGGCGGGTGTCGGGGCGCAGCCATGACCCAGTCACGTAGCGATAGCGGAGTGTATACTGGCTTAACTATG
CGGCATCAGAGCAGATTGTACTGAGAGTGCACCATATGCGGTGTGAAATACCGCACAGATGCGTAAGGAGAAAATACCGCATCAGGCGCTCT
TCCGCTTCCTCGCTCACTGACTCGCTGCGCTCGGTCGTTCGGCTGCGGCGAGCGGTATCAGCTCACTCAAAGGCGGTAATACGGTTATCCAC
AGAATCAGGGGATAACGCAGGAAAGAACATGTGAGCAAAAGGCCAGCAAAAGGCCAGGAACCGTAAAAAGGCCGCGTTGCTGGCGTTTTTCC
ATAGGCTCCGCCCCCCTGACGAGCATCACAAAAATCGACGCTCAAGTCAGAGGTGGCGAAACCCGACAGGACTATAAAGATACCAGGCGTTT
CCCCCTGGAAGCTCCCTCGTGCGCTCTCCTGTTCCGACCCTGCCGCTTACCGGATACCTGTCCGCCTTTCTCCCTTCGGGAAGCGTGGCGCT
TTCTCATAGCTCACGCTGTAGGTATCTCAGTTCGGTGTAGGTCGTTCGCTCCAAGCTGGGCTGTGTGCACGAACCCCCCGTTCAGCCCGACC
GCTGCGCCTTATCCGGTAACTATCGTCTTGAGTCCAACCCGGTAAGACACGACTTATCGCCACTGGCAGCAGCCACTGGTAACAGGATTAGC
AGAGCGAGGTATGTAGGCGGTGCTACAGAGTTCTTGAAGTGGTGGCCTAACTACGGCTACACTAGAAGGACAGTATTTGGTATCTGCGCTCT
GCTGAAGCCAGTTACCTTCGGAAAAAGAGTTGGTAGCTCTTGATCCGGCAAACAAACCACCGCTGGTAGCGGTGGTTTTTTTGTTTGCAAGC
AGCAGATTACGCGCAGAAAAAAAGGATCTCAAGAAGATCCTTTGATCTTTTCTACGGGGTCTGACGCTCAGTGGAACGAAAACTCACGTTAA
GGGATTTTGGTCATGAGATTATCAAAAAGGATCTTCACCTAGATCCTTTTAAATTAAAAATGAAGTTTTAAATCAATCTAAAGTATATATGA
GTAAACTTGGTCTGACAGTTACCAATGCTTAATCAGTGAGGCACCTATCTCAGCGATCTGTCTATTTCGTTCATCCATAGTTGCCTGACTCC
CCGTCGTGTAGATAACTACGATACGGGAGGGCTTACCATCTGGCCCCAGTGCTGCAATGATACCGCGAGACCCACGCTCACCGGCTCCAGAT
TTATCAGCAATAAACCAGCCAGCCGGAAGGGCCGAGCGCAGAAGTGGTCCTGCAACTTTATCCGCCTCCATCCAGTCTATTAATTGTTGCCG
GGAAGCTAGAGTAAGTAGTTCGCCAGTTAATAGTTTGCGCAACGTTGTTGCCATTGCTACAGGCATCGTGGTGTCACGCTCGTCGTTTGGTA
TGGCTTCATTCAGCTCCGGTTCCCAACGATCAAGGCGAGTTACATGATCCCCCATGTTGTGCAAAAAAGCGGTTAGCTCCTTCGGTCCTCCG
ATCGTTGTCAGAAGTAAGTTGGCCGCAGTGTTATCACTCATGGTTATGGCAGCACTGCATAATTCTCTTACTGTCATGCCATCCGTAAGATG
CTTTTCTGTGACTGGTGAGTACTCAACCAAGTCATTCTGAGAATAGTGTATGCGGCGACCGAGTTGCTCTTGCCCGGCGTCAATACGGGATA
ATACCGCGCCACATAGCAGAACTTTAAAAGTGCTCATCATTGGAAAACGTTCTTCGGGGCGAAAACTCTCAAGGATCTTACCGCTGTTGAGA
TCCAGTTCGATGTAACCCACTCGTGCACCCAACTGATCTTCAGCATCTTTTACTTTCACCAGCGTTTCTGGGTGAGCAAAAACAGGAAGGCA
AAATGCCGCAAAAAAGGGAATAAGGGCGACACGGAAATGTTGAATACTCATACTCTTCCTTTTTCAATATTATTGAAGCATTTATCAGGGTT
ATTGTCTCATGAGCGGATACATATTTGAATGTATTTAGAAAAATAAACAAATAGGGGTTCCGCGCACATTTCCCCGAAAAGTGCCACCTGAC
GTCTAAGAAACCATTATTATCATGACATTAACCTATAAAAATAGGCGTATCACGAGGCCCTTTCGTCTTCAC

T5 promoter	Ampicillin	rrnB_T1_Terminator	*Tg*ATPase$_p$-GC1+GC2
BglII	CAT/CamR	6xHis-tag	

D) Plasmid of *p3'IT-HXGPRT-TgATPase$_P$-GC-HA$_{3'IT}$-TgGra1-3'UTR*

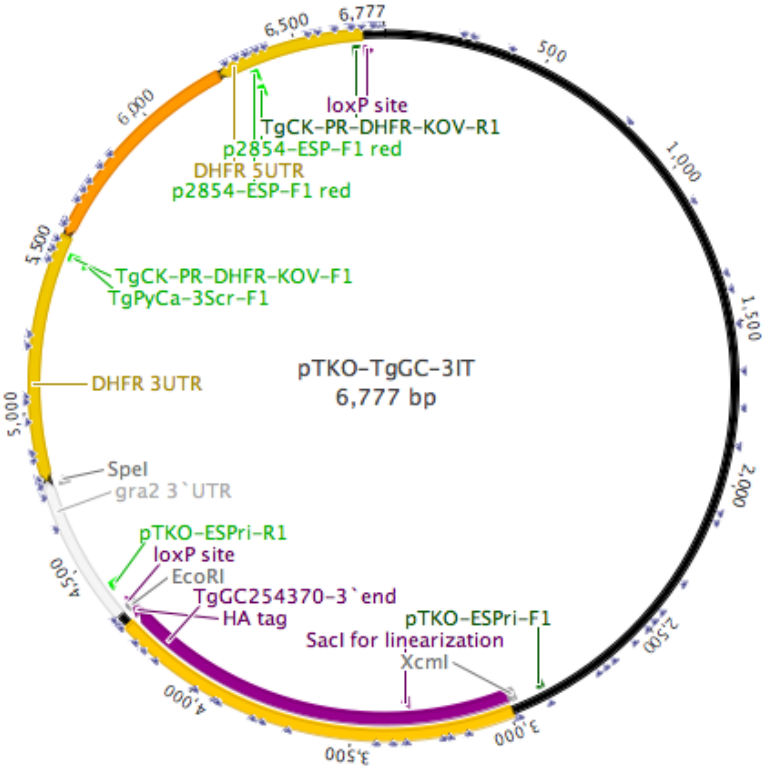

CAGCTTTTGTTCCCTTTAGTGAGGGTTAATTGCGCGCTTGGCGTAATCATGGTCATAGCTGTTTCCTGTGTGAAATTGTTATCCGCTCACAA
TTCCACACAACATACGAGCCGGAAGCATAAAGTGTAAAGCCTGGGGTGCCTAATGAGTGAGCTAACTCACATTAATTGCGTTGCGCTCACTG
CCCGCTTTCCAGTCGGGAAACCTGTCGTGCCAGCTGCATTAATGAATCGGCCAACGCGCGGGGAGAGGCGGTTTGCGTATTGGGCGCTCTTC
CGCTTCCTCGCTCACTGACTCGCTGCGCTCGGTCGTTCGGCTGCGGCGAGCGGTATCAGCTCACTCAAAGGCGGTAATACGGTTATCCACAG
AATCAGGGGATAACGCAGGAAAGAACATGTGAGCAAAAGGCCAGCAAAAGGCCAGGAACCGTAAAAAGGCCGCGTTGCTGGCGTTTTTCCAT
AGGCTCCGCCCCCCTGACGAGCATCACAAAAATCGACGCTCAAGTCAGAGGTGGCGAAACCCGACAGGACTATAAAGATACCAGGCGTTTCC
CCCTGGAAGCTCCCTCGTGCGCTCTCCTGTTCCGACCCTGCCGCTTACCGGATACCTGTCCGCCTTTCTCCCTTCGGGAAGCGTGGCGCTTT
CTCATAGCTCACGCTGTAGGTATCTCAGTTCGGTGTAGGTCGTTCGCTCCAAGCTGGGCTGTGTGCACGAACCCCCCGTTCAGCCCGACCGC
TGCGCCTTATCCGGTAACTATCGTCTTGAGTCCAACCCGGTAAGACACGACTTATCGCCACTGGCAGCAGCCACTGGTAACAGGATTAGCAG
AGCGAGGTATGTAGGCGGTGCTACAGAGTTCTTGAAGTGGTGGCCTAACTACGGCTACACTAGAAGGACAGTATTTGGTATCTGCGCTCTGC
TGAAGCCAGTTACCTTCGGAAAAAGAGTTGGTAGCTCTTGATCCGGCAAACAAACCACCGCTGGTAGCGGTGGTTTTTTTGTTTGCAAGCAG
CAGATTACGCGCAGAAAAAAAGGATCTCAAGAAGATCCTTTGATCTTTTCTACGGGGTCTGACGCTCAGTGGAACGAAAACTCACGTTAAGG
GATTTTGGTCATGAGATTATCAAAAAGGATCTTCACCTAGATCCTTTTAAATTAAAAATGAAGTTTTAAATCAATCTAAAGTATATATGAGT
AAACTTGGTCTGACAGTTACCAATGCTTAATCAGTGAGGCACCTATCTCAGCGATCTGTCTATTTCGTTCATCCATAGTTGCCTGACTCCCC
GTCGTGTAGATAACTACGATACGGGAGGGCTTACCATCTGGCCCCAGTGCTGCAATGATACCGCGAGACCCACGCTCACCGGCTCCAGATTT
ATCAGCAATAAACCAGCCAGCCGGAAGGGCCGAGCGCAGAAGTGGTCCTGCAACTTTATCCGCCTCCATCCAGTCTATTAATTGTTGCCGGG
AAGCTAGAGTAAGTAGTTCGCCAGTTAATAGTTTGCGCAACGTTGTTGCCATTGCTACAGGCATCGTGGTGTCACGCTCGTCGTTTGGTATG
GCTTCATTCAGCTCCGGTTCCCAACGATCAAGGCGAGTTACATGATCCCCCATGTTGTGCAAAAAAGCGGTTAGCTCCTTCGGTCCTCCGAT
CGTTGTCAGAAGTAAGTTGGCCGCAGTGTTATCACTCATGGTTATGGCAGCACTGCATAATTCTCTTACTGTCATGCCATCCGTAAGATGCT
TTTCTGTGACTGGTGAGTACTCAACCAAGTCATTCTGAGAATAGTGTATGCGGCGACCGAGTTGCTCTTGCCCGGCGTCAATACGGGATAAT
ACCGCGCCACATAGCAGAACTTTAAAAGTGCTCATCATTGGAAAACGTTCTTCGGGGCGAAAACTCTCAAGGATCTTACCGCTGTTGAGATC
CAGTTCGATGTAACCCACTCGTGCACCCAACTGATCTTCAGCATCTTTTACTTTCACCAGCGTTTCTGGGTGAGCAAAAACAGGAAGGCAAA
ATGCCGCAAAAAAGGGAATAAGGGCGACACGGAAATGTTGAATACTCATACTCTTCCTTTTTCAATATTATTGAAGCATTTATCAGGGTTAT
TGTCTCATGAGCGGATACATATTTGAATGTATTTAGAAAAATAAACAAATAGGGGTTCCGCGCACATTTCCCCGAAAAGTGCCACCTGACGC
GCCCTGTAGCGGCGCATTAAGCGCGGCGGGTGTGGTGGTTACGCGCAGCGTGACCGCTACACTTGCCAGCGCCCTAGCGCCCGCTCCTTTCG
CTTTCTTCCCTTCCTTTCTCGCCACGTTCGCCGGCTTTCCCCGTCAAGCTCTAAATCGGGGGCTCCCTTTAGGGTTCCGATTTAGTGCTTTA
CGGCACCTCGACCCCAAAAAACTTGATTAGGGTGATGGTTCACGTAGTGGGCCATCGCCCTGATAGACGGTTTTTCGCCCTTTGACGTTGGA
GTCCACGTTCTTTAATAGTGGACTCTTGTTCCAAACTGGAACAACACTCAACCCTATCTCGGTCTATTCTTTTGATTTATAAGGGATTTTGC
CGATTTCGGCCTATTGGTTAAAAAATGAGCTGATTTAACAAAAATTTAACGCGAATTTTAACAAAATATTAACGCTTACAATTTCCATTCGC
CATTCAGGCTGCGCAACTGTTGGGAAGGGCGATCGGTGCGGGCCTCTTCGCTATTACGCCAGCTGGCGAAAGGGGGATGTGCTGCAAGGCGA
TTAAGTTGGGTAACGCCAGGGTTTTCCCAGTCACGACGTTGTAAAACGACGGCCAGTGAGCGCGCGTAATACGACTCACTATAGGGCGAATT
GGAGCTTCGAAGGCTGTAGTACTGGTGCTCGTATGCGACACGCGGATTCACGGCGTATGCGACAAGCGGGATTGCTGATGAGCGTCGTTCCC
CACTGAAGCGCGCGGAGTGGTGGGCGACCACCGGTCACCTGGGCATGAGTGTGGCGGAGTCGCGCTGTGAGTTTTTGCTCTTTTCCTCGCCC
TGTGTGTTCTTCTTTTGCGCAGCATTCGAGGAAATTACCGCAGGAGATTCACCATTCTTGGCAGTGCGCCGCGCGTTCTGGGACGCCGACAG
TCTCTCAGGGGTCACCAGTTCAGTGCACTCGCTCTCGCGTCACACGTAAGTTCAGATGCATGCGCACCGAATTGAGAAAAGGCGCTCCGGAC

GCAAATTGAGACAAACATGCAACAAAACCTACCGAGTCTGCTTTTCTCCTGTGTCGGCAGGGACTTCCCGCTACACAGACGTCGTCACAGAT
CCGTTTCACGAGCTCTCTACTTGGATACTGAACATATATATTTATACATATATCGATTGCTATTTGGATTTGGATGTCTGTATGTTCTCAAA
CGTACAGACAAGTTGATCACTCTTGTTCGATAAATCGGTATATGTGTGGGTGTGCGTATATGGATGTTTGTGTCTTCAACGAGGCAATACTT
GGTGGATAGGTGATTTTTTCGAGATGTCGGCACCTGTGCAGAGCTGTGGTGAGATGTTTGGCGCGTATCCTTGCGCGTTGTTTGTGTTTTTT
TCTCGCAGGGCGATTCTGGACCCAGCGACGAACCGCGCCACCTGGGAGACGAAGGGCAAGCAGCTGGCTCTGTCACTTCGCATGATGGACCA
CTGCGTGAGGAGGTTGAGGACGATGAGATCGACGGCCTCAAGCAACTGAGGAAGGAAATCGAGCGTGCTGGAGGTAGGTTCGAAAGACTAAA
GTCTTCGTAAATTTTTTTCCACACTTTTGGCGTGCATCTCGGCATCGCAGATCCTCGTTTCCAGTCGCAGCATCGGTCCTCACAAAGACACC
TTCGCTGTCGATTGTGTTGAGTCTTCTCACTCCTATTGTTCATACTTGTACATATGCATCTACGTATATATACAGATGTTCATGTTTGTATA
TATATATATATATAGATATAGATATAGATATACGTACGCGGTTTGATATTCTGCGTCGACTTGAGTCGTCTACGTGCATCGCGCCGAGAAGA
TTCTTCTCCACAGTTAAATGTATATATGTATGCATAAAAACATATATATACATATATATGTATATATGTGCATCTATATACATTTACGCATG
CCTAAATGTTTTTTTGTATTTTCATGGGATTCCGAGAGATATTGGTATGTGAGACAACGGCTGTGGTTTTCTCGTAGGTCTCGGTTTGGACG
CGTCGCCTTCGGATATAGGGTCGACACCTGGCTCTGCACTCGGGTCGTACCCGTACGACGTCCCGGACTACGCGTAGGAATTCATAACTTCG
TATAGCATACATTATACGAAGTTATGACTACGACGAAAGTGATGCGCAGGCTGGAAAGCCGCTGAAGGGAGAAGTCTACAAAGCCGATCAGT
GAAAAATGTGTGGGGAGGTGGTCTTGTTGCAGGAATGCAATGGTGTTAAGCATCGTGTTCGAATGCAGTGCGTGTATCAGTTGTGCGCGGAA
GGACACTGCTTCAATGTTAAGAACCTGTTTTCTCCGTAGAGAGGACCAAAAGACGATTGCAAAACTGGTATGTACGCAATAGCCCAATGCCG
GACGTCAGTTGGTTGTATGTGACGCTCCCAGATGTCATATGCCTTGTGAGTGTGTCTGGGATGCAAGTTTTTGGTGTGCGTTGATTTCGCCA
GCTTATGACAGTGGCAGACGAATTATTGACATGATACAAGGACGCAGAAAGGAACAAACACCGTAGTTCCAGTCGACGGATCCACTAGTGGA
TCCCCCTCCACCGCGGTGTCACTGTAGCCTGCCAGAACACTTGTCAACCGACTGTGTCCACATTTTTATGCGCACTGACTGGCATGAATGGC
CAGAGGCAGGCATCAGCAAGTCACGTAGGCCAACGCGTGCGCAGAAACGCTCAAGGCTCGATTGTGGGTGGGGGTTGGTAGCATTTTATCGA
CCTAAACAAGGTTTACACTTAGGTGGTGCGGTTTTACTGATCTGGACGGATTCAGCGGTCGCAGATTATCGATCTGCAAATGGTGTACACTT
AGGTGTCGCGGCTTATTTAGTTAAGGGAGCTTCGTGGTCGGAGCCTAACAAGTCAACAGAGACGTATCGCCAATCGTTCGCGGTGAAGAGTC
GAAACTGACAGCACATCGTAGGGAAACTGAGAGGGTGCTCCTTTCTCTCCGTCGTTTGCGCTGCACCATCCTGCAAGTGCATAGAAGGAAAG
TTGTCTGCTGTCGTGGGCAGACAGCAACAGTCCAGCACTCTAGCGGCATACAGAACGATAACGCATTCACGAGTGGATACACGCACATCTGC
GTCACCCGCAACTCGCTTTCGTTCTGATTGACAAAAAGAAAACAAGGCGAGGTGAGACTGTGTGAAATGCCACATGAAGAGTCATCCCTTTT
CTTCGATAAAGGACACAGGGGTCTCTGGCACCCCCTCGTCAGCTCTCTCCGACCCGAGGCACTCTCCCTGATCCCTCCGAAAAGAGAGGAAA
ACGAGAGACGGGCAGCTTCTGTAGGGCTATGCAGGGTTTACTTCTCGAACTTTTTGCGAGCGGCGTCGCTCAGGACGGCGACGTGGTCGAAG
TCGCGGAACATCTCGTTGAAGTCGTAGCAGCAACCAACGATCCAGACGTCTTCAATGCTGAAGCCGACGAAGTCGCCCTTCAAGCTGTTGGA
GCGATCTGTGCGCTTCTCGACGAGGGTGGCGATTCTCATCGACTTGGGACCGACGGCTTTCAGGCGCTCACCGAACTCGGTGAGGGTGAAAC
CGGTGTCGACGATGTCCTCAACAATCAGAACGTGCTTGTCGCGAAAGATTGACAAGTCGTCGCTCAAGACGGTGAGCTGGCCTGTGCTGTTG
TCGTTCTGGTAGGACTTCAGGCGGACATAGTGCTCGAAGAAGGGGGGCACGCTGGACTCACGACCACTGTACTTCTGTATGGTGGCAAGGTA
GTCGATCAGAAGGTTGAAGAAGCCGCGAGAGCCTTTCAGGATGCAAATGATGTGCAACTCCTCGCCGAAGTAAGTTCTGTGGATGTCATACG
CCAACTTCTCAACTCTGTCCTTGACCAATCCACCAGGGAGGAGGATTTTGTCAATGTAGGGCTTGCAGTGGGGGGGCACAAGAAAGTCATCA
GCGTTGTAGAAGGTGTTGTCGGGGATATACATGGGCTCAATACGGCCCTTGCCCTTGCCGTAGTCTTCAATGGGTTTGGACGCCATTTTGGA
TCTGACAACGCCCCGTAGAGCAGAAACGCACTACTAAAGCGAAACTTCACCCGTCCCTGCTGCACTCAGAGCAGTGCTCCGCACTGCCGTGT
GGTAAAATGAAAAGGTTCTACGAGACACGCGTCTCCGGATCGACAAGCGAAGGATCTGCACACCTGGTCTCGATGTCGAACAAAGCACGGAG
GAGAGACGGAAAGTGCTTACATCGAACACGGTTATCAAACCCGAGAAAAAGAAACGAACAGAAGAAAAAGGAAACCTCCGCATACTTTTAAA
GAATGAAGTTCCCCGATTTTCCCAAAAATGGCGTCATTTTCGCGCACGGCAGTCAGATAACAGGTGTAGCGGCTGCCCACCAACAGAGACGG
CGCGGCCGACAGGACGCTACTGGGACTGCGAACAGCAGCAAGATCGGATCTTCCGCGGGCGGGTTTGAATGCAAGGTTTCGTGCTGATCATA
ACTTCGTATAGCATACATTATACGAAGTTATAAGCTTGCTAGCGTTAACGGGCCCCGTACC

XcmI	EcoRI
*Tg*Gra2-3'UTR	*Tg*ATPase$_P$-3`end
HXGPRT ORF	HA-epitope tag
5`and 3`UTRs of *Tg*DHFR/TS	

E) Plasmid of *p3'IT-HXGPRT-TgATPase$_P$-GC-HA$_{3'IT}$-3'UTR$_{floxed}$*

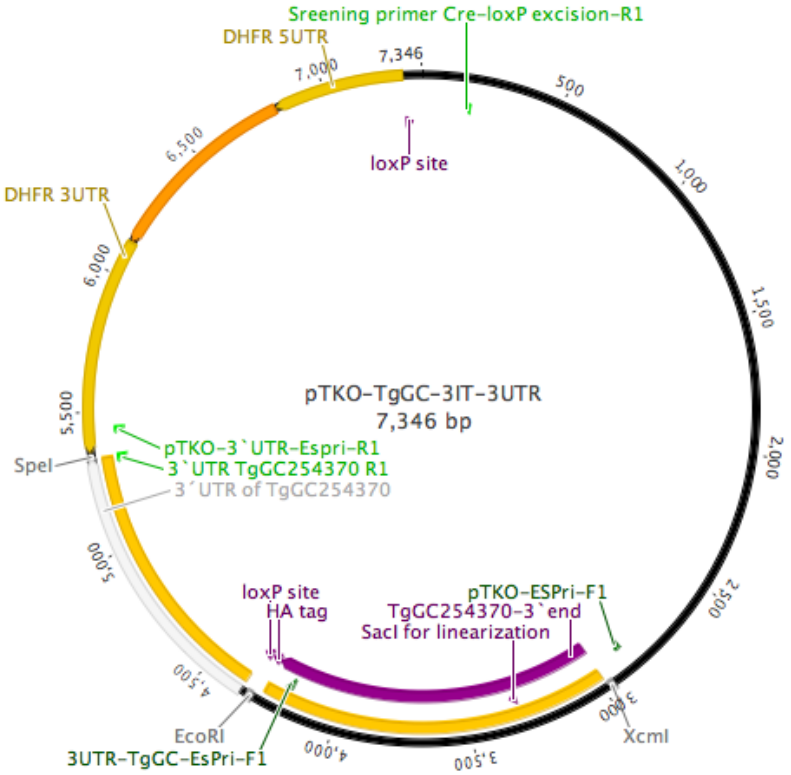

CAGCTTTTGTTCCCTTTAGTGAGGGTTAATTGCGCGCTTGGCGTAATCATGGTCATAGCTGTTTCCTGTGTGAAATTGTTATCCGCTCACAA
TTCCACACAACATACGAGCCGGAAGCATAAAGTGTAAAGCCTGGGGTGCCTAATGAGTGAGCTAACTCACATTAATTGCGTTGCGCTCACTG
CCCGCTTTCCAGTCGGGAAACCTGTCGTGCCAGCTGCATTAATGAATCGGCCAACGCGCGGGGAGAGGCGGTTTGCGTATTGGGCGCTCTTC
CGCTTCCTCGCTCACTGACTCGCTGCGCTCGGTCGTTCGGCTGCGGCGAGCGGTATCAGCTCACTCAAAGGCGGTAATACGGTTATCCACAG
AATCAGGGGATAACGCAGGAAAGAACATGTGAGCAAAAGGCCAGCAAAAGGCCAGGAACCGTAAAAAGGCCGCGTTGCTGGCGTTTTTCCAT
AGGCTCCGCCCCCCTGACGAGCATCACAAAAATCGACGCTCAAGTCAGAGGTGGCGAAACCCGACAGGACTATAAAGATACCAGGCGTTTCC
CCCTGGAAGCTCCCTCGTGCGCTCTCCTGTTCCGACCCTGCCGCTTACCGGATACCTGTCCGCCTTTCTCCCTTCGGGAAGCGTGGCGCTTT
CTCATAGCTCACGCTGTAGGTATCTCAGTTCGGTGTAGGTCGTTCGCTCCAAGCTGGGCTGTGTGCACGAACCCCCCGTTCAGCCCGACCGC
TGCGCCTTATCCGGTAACTATCGTCTTGAGTCCAACCCGGTAAGACACGACTTATCGCCACTGGCAGCAGCCACTGGTAACAGGATTAGCAG
AGCGAGGTATGTAGGCGGTGCTACAGAGTTCTTGAAGTGGTGGCCTAACTACGGCTACACTAGAAGGACAGTATTTGGTATCTGCGCTCTGC
TGAAGCCAGTTACCTTCGGAAAAAGAGTTGGTAGCTCTTGATCCGGCAAACAAACCACCGCTGGTAGCGGTGGTTTTTTTGTTTGCAAGCAG
CAGATTACGCGCAGAAAAAAAGGATCTCAAGAAGATCCTTTGATCTTTTCTACGGGGTCTGACGCTCAGTGGAACGAAAACTCACGTTAAGG
GATTTTGGTCATGAGATTATCAAAAAGGATCTTCACCTAGATCCTTTTAAATTAAAAATGAAGTTTTAAATCAATCTAAAGTATATATGAGT
AAACTTGGTCTGACAGTTACCAATGCTTAATCAGTGAGGCACCTATCTCAGCGATCTGTCTATTTCGTTCATCCATAGTTGCCTGACTCCCC
GTCGTGTAGATAACTACGATACGGGAGGGCTTACCATCTGGCCCCAGTGCTGCAATGATACCGCGAGACCCACGCTCACCGGCTCCAGATTT
ATCAGCAATAAACCAGCCAGCCGGAAGGGCCGAGCGCAGAAGTGGTCCTGCAACTTTATCCGCCTCCATCCAGTCTATTAATTGTTGCCGGG
AAGCTAGAGTAAGTAGTTCGCCAGTTAATAGTTTGCGCAACGTTGTTGCCATTGCTACAGGCATCGTGGTGTCACGCTCGTCGTTTGGTATG
GCTTCATTCAGCTCCGGTTCCCAACGATCAAGGCGAGTTACATGATCCCCCATGTTGTGCAAAAAAGCGGTTAGCTCCTTCGGTCCTCCGAT
CGTTGTCAGAAGTAAGTTGGCCGCAGTGTTATCACTCATGGTTATGGCAGCACTGCATAATTCTCTTACTGTCATGCCATCCGTAAGATGCT
TTTCTGTGACTGGTGAGTACTCAACCAAGTCATTCTGAGAATAGTGTATGCGGCGACCGAGTTGCTCTTGCCCGGCGTCAATACGGGATAAT
ACCGCGCCACATAGCAGAACTTTAAAAGTGCTCATCATTGGAAAACGTTCTTCGGGGCGAAAACTCTCAAGGATCTTACCGCTGTTGAGATC
CAGTTCGATGTAACCCACTCGTGCACCCAACTGATCTTCAGCATCTTTTACTTTCACCAGCGTTTCTGGGTGAGCAAAAACAGGAAGGCAAA
ATGCCGCAAAAAAGGGAATAAGGGCGACACGGAAATGTTGAATACTCATACTCTTCCTTTTTCAATATTATTGAAGCATTTATCAGGGTTAT
TGTCTCATGAGCGGATACATATTTGAATGTATTTAGAAAAATAAACAAATAGGGGTTCCGCGCACATTTCCCCGAAAAGTGCCACCTGACGC
GCCCTGTAGCGGCGCATTAAGCGCGGCGGGTGTGGTGGTTACGCGCAGCGTGACCGCTACACTTGCCAGCGCCCTAGCGCCCGCTCCTTTCG
CTTTCTTCCCTTCCTTTCTCGCCACGTTCGCCGGCTTTCCCCGTCAAGCTCTAAATCGGGGGCTCCCTTTAGGGTTCCGATTTAGTGCTTTA
CGGCACCTCGACCCCAAAAAACTTGATTAGGGTGATGGTTCACGTAGTGGGCCATCGCCCTGATAGACGGTTTTTCGCCCTTTGACGTTGGA
GTCCACGTTCTTTAATAGTGGACTCTTGTTCCAAACTGGAACAACACTCAACCCTATCTCGGTCTATTCTTTTGATTTATAAGGGATTTTGC
CGATTTCGGCCTATTGGTTAAAAAATGAGCTGATTTAACAAAAATTTAACGCGAATTTTAACAAAATATTAACGCTTACAATTTCCATTCGC
CATTCAGGCTGCGCAACTGTTGGGAAGGGCGATCGGTGCGGGCCTCTTCGCTATTACGCCAGCTGGCGAAAGGGGGATGTGCTGCAAGGCGA
TTAAGTTGGGTAACGCCAGGGTTTTCCCAGTCACGACGTTGTAAAACGACGGCCAGTGAGCGCGCGTAATACGACTCACTATAGGGCGAATT
GGAGCTTCGAAGGCTGTAGTACTGGTGCTCGTATGCGACACGCGGATTCACGGCGTATGCGACAAGCGGGATTGCTGATGAGCGTCGTTCCC
CACTGAAGCGCGCGGAGTGGTGGGCGACCACCGGTCACCTGG**GCATGAGTGTGGCGGAGTCGCGCTGTGAGTTTTTGCTCTTTTCCTCGCCC**

TGTGTGTTCTTCTTTTGCGCAGCATTCGAGGAAATTACCGCAGGAGATTCACCATTCTTGGCAGTGCGCCGCGCGTTCTGGGACGCCGACAG
TCTCTCAGGGGTCACCAGTTCAGTGCACTCGCTCTCGCGTCACACGTAAGTTCAGATGCATGCGCACCGAATTGAGAAAAGGCGCTCCGGAC
GCAAATTGAGACAAACATGCAACAAAACCTACCGAGTCTGCTTTTCTCCTGTGTCGGCAGGGACTTCCCGCTACACAGACGTCGTCACAGAT
CCGTTTCACGAGCTCTCTACTTGGATACTGAACATATATATTTATACATATATCGATTGCTATTTGGATTTGGATGTCTGTATGTTCTCAAA
CGTACAGACAAGTTGATCACTCTTGTTCGATAAATCGGTATATGTGTGGGTGTGCGTATATGGATGTTTGTGTCTTCAACGAGGCAATACTT
GGTGGATAGGTGATTTTTTCGAGATGTCGGCACCTGTGCAGAGCTGTGGTGAGATGTTTGGCGCGTATCCTTGCGCGTTGTTTGTGTTTTTT
TCTCGCAGGGCGATTCTGGACCCAGCGACGAACCGCGCCACCTGGGAGACGAAGGGCAAGCAGCTGGCTCTGTCACTTCGCATGATGGACCA
CTGCGTGAGGAGGTTGAGGACGATGAGATCGACGGCCTCAAGCAACTGAGGAAGGAAATCGAGCGTGCTGGAGGTAGGTTCGAAAGACTAAA
GTCTTCGTAAATTTTTTTCCACACTTTTGGCGTGCATCTCGGCATCGCAGATCCTCGTTTCCAGTCGCAGCATCGGTCCTCACAAAGACACC
TTCGCTGTCGATTGTGTTGAGTCTTCTCACTCCTATTGTTCATACTTGTACATATGCATCTACGTATATATACAGATGTTCATGTTTGTATA
TATATATATATATAGATATAGATATAGATATACGTACGCGGTTTGATATTCTGCGTCGACTTGAGTCGTCTACGTGCATCGCGCCGAGAAGA
TTCTTCTCCACAGTTAAATGTATATATGTATGCATAAAAACATATATATACATATATATGTATATATGTGCATCTATATACATTTACGCATG
CCTAAATGTTTTTTTTGTATTTTCATGGGATTCCGAGAGATATTGGTATGTGAGACAACGGCTGTGGTTTTCTCGTAGGTCTCGGTTTGGACG
CGTCGCCTTCGGATATAGGGTCGACACCTGGCTCTGCACTCGGGTCGTACCCGTACGACGTCCCGGACTACGCGTAGGAATTCATAACTTCG
TATAGCATACATTATACGAAGTTATAACGCAGCTTTTGTCAGCGTTTCTTTTTTCATTTCATTCTCCACTTCTTCGCGAAAAGCCGTCTTCC
TTCGACAGGGCGACTGCTCCAAGGTTCTGCGTTGCTCCAGAGGCGGGTCTGTGTCCTGCCGCTTCGGGCAGTCGAGACAGACAGAGGCGGCA
GGTGTCTCGTCACGGCCGGAGGAACCAGAAGAGGAAAGGAGAAAAGGAACAGGACTGTGCGCACCCGGGAGAGAGAAGAGCGCTGCCAGCTT
CGTCAACGCAAAAGGCAAAAGGAAGGCAGAAGCAGGGAGGTGGAGAGACTGCGGATGTGCCGAATTACCTGTTGTGCCATGTTTTCCTGTTT
CCAAACACGGTTGCTGTGTGCATTGACCGCAGCGGCGAGTCGCCCCTAGCAGGTTCCAGTATCCTGCCTCCACGGTAGCGCTCGCTGGCTCG
CATTCGGTCGTTTTTCCGATTTTATTTTGCTTTCATTCTGCGCCTTTTTCCTTCCGTGTGGCATCATCTCTTCTGATGAGTCAGCGTCCTTC
GATGTTCCGCTTGCTCTCGTCGTCTTCTGGCTAGGGAAACCTCTCGCACTTGTCGTATGGCCCTCTTGATTCCTGTCGTCGCTCGCGATGCG
CCCCGCGTGACCGTGCGCGCTGTATGTACACCTCAGACGCGCTTGCGTAGTCTTGTGCCACTGAACAGGGTCAAGGCGAATGCGCTTCTGTC
AGTAAACGTCCATAAATGCATTTGCAGAGAGAACGTGTGCAAACGCATGTTGTCGCTTCCTGAACATTCCTCAAAAAAAATCCGTTTTCTCG
AATTGGGTCAGGAAGACCCCACACCTCTCGTCTTGTTCCCCACCTCTCACACTGGAGAAAACGCCGACTTCCTAAAATATGGCGGAGTCCGC
TCTTCGTACCAAAACGTTCGATGCCAAACTGTCACATGCACGCAGTTTACACACGCACGTACAGACGTTCACACATACATGTGCGTATATAC
GTACATAAACTAGTGGATCCCCCTCCACCGCGGTGTCACTGTAGCCTGCCAGAACACTTGTCAACCGACTGTGTCCACATTTTTATGCGCAC
TGACTGGCATGAATGGCCAGAGGCAGGCATCAGCAAGTCACGTAGGCCAACGCGTGCGCAGAAACGCTCAAGGCTCGATTGTGGGTGGGGGT
TGGTAGCATTTTATCGACCTAAACAAGGTTTACACTTAGGTGGTGCGGTTTTACTGATCTGGACGGATTCAGCGGTCGCAGATTATCGATCT
GCAAATGGTGTACACTTAGGTGTCGCGGCTTATTTAGTTAAGGGAGCTTCGTGGTCGGAGCCTAACAAGTCAACAGAGACGTATCGCCAATC
GTTCGCGGTGAAGAGTCGAAACTGACAGCACATCGTAGGGAAACTGAGAGGGTGCTCCTTTCTCTCCGTCGTTTGCGCTGCACCATCCTGCA
AGTGCATAGAAGGAAAGTTGTCTGCTGTCGTGGGCAGACAGCAACAGTCCAGCACTCTAGCGGCATACAGAACGATAACGCATTCACGAGTG
GATACACGCACATCTGCGTCACCCGCAACTCGCTTTCGTTCTGATTGACAAAAAGAAAACAAGGCGAGGTGAGACTGTGTGAAATGCCACAT
GAAGAGTCATCCCTTTTCTTCGATAAAGGACACAGGGGTCTCTGGCACCCCCTCGTCAGCTCTCTCCGACCCGAGGCACTCTCCCTGATCCC
TCCGAAAAGAGAGGAAAACGAGAGACGGGCAGCTTCTGTAGGGCTATGCAGGGTTTACTTCTCGAACTTTTTGCGAGCGGCGTCGCTCAGGA
CGGCGACGTGGTCGAAGTCGCGGAACATCTCGTTGAAGTCGTAGCAGCAACCAACGATCCAGACGTCTTCAATGCTGAAGCCGACGAAGTCG
CCCTTCAAGCTGTTGGAGCGATCTGTGCGCTTCTCGACGAGGGTGGCGATTCTCATCGACTTGGGACCGACGGCTTTCAGGCGCTCACCGAA
CTCGGTGAGGGTGAAACCGGTGTCGACGATGTCCTCAACAATCAGAACGTGCTTGTCGCGAAAGATTGACAAGTCGTCGCTCAAGACGGTGA
GCTGGCCTGTGCTGTTGTCGTTCTGGTAGGACTTCAGGCGGACATAGTGCTCGAAGAAGGGGGGCACGCTGGACTCACGACCACTGTACTTC
TGTATGGTGGCAAGGTAGTCGATCAGAAGGTTGAAGAAGCCGCGAGAGCCTTTCAGGATGCAAATGATGTGCAACTCCTCGCCGAAGTAAGT
TCTGTGGATGTCATACGCCAACTTCTCAACTCTGTCCTTGACCAATCCACCAGGGAGGAGGATTTTGTCAATGTAGGGCTTGCAGTGGGGGG
GCACAAGAAAGTCATCAGCGTTGTAGAAGGTGTTGTCGGGGATATACATGGGCTCAATACGGCCCTTGCCCTTGCCGTAGTCTTCAATGGGT
TTGGACGCCATTTTGGATCTGACAACGCCCCGTAGAGCAGAAACGCACTACTAAAGCGAAACTTCACCCGTCCCTGCTGCACTCAGAGCAGT
GCTCCGCACTGCCGTGTGGTAAAATGAAAAGGTTCTACGAGACACGCGTCTCCGGATCGACAAGCGAAGGATCTGCACACCTGGTCTCGATG
TCGAACAAAGCACGGAGGAGAGACGGAAAGTGCTTACATCGAACACGGTTATCAAACCCGAGAAAAAGAAACGAACAGAAGAAAAAGGAAAC
CTCCGCATACTTTTAAAGAATGAAGTTCCCCGATTTTCCCAAAAATGGCGTCATTTTCGCGCACGGCAGTCAGATAACAGGTGTAGCGGCTG
CCCACCAACAGAGACGGCGCGGCCGACAGGACGCTACTGGGACTGCGAACAGCAGCAAGATCGGATCTTCCGCGGGCGGGTTTGAATGCAAG
GTTTCGTGCTGATCATAACTTCGTATAGCATACATTATACGAAGTTATAAGCTTGCTAGCGTTAACGGGCCCCGTACC

XcmI	EcoRI
*Tg*ATPase$_P$-GC-3'UTR	*Tg*ATPase$_P$-GC-3`end
HXGPRT ORF	HA-epitope tag
5`and 3`UTRs of *Tg*DHFR/TS	loxP sites
SpeI	

F) Plasmid of *p3'IT-HXGPRT-TgPKG-HA$_{3'IT}$-3'UTR$_{floxed}$*

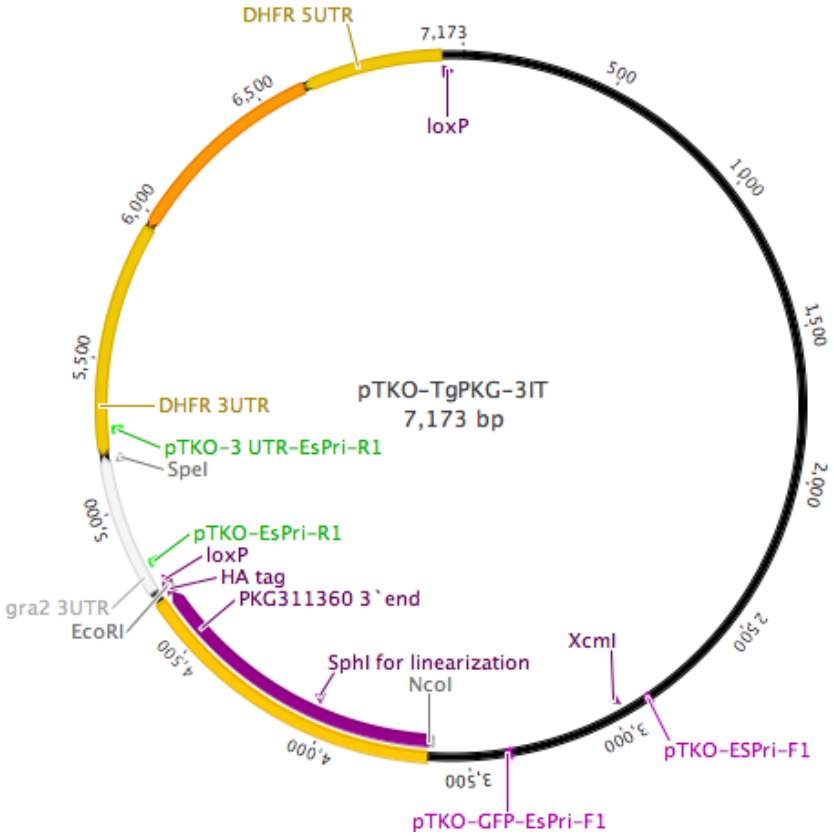

CAGCTTTTGTTCCCTTTAGTGAGGGTTAATTGCGCGCTTGGCGTAATCATGGTCATAGCTGTTTCCTGTGTGAAATTGTTATCCGCTCACAA
TTCCACACAACATACGAGCCGGAAGCATAAAGTGTAAAGCCTGGGGTGCCTAATGAGTGAGCTAACTCACATTAATTGCGTTGCGCTCACTG
CCCGCTTTCCAGTCGGGAAACCTGTCGTGCCAGCTGCATTAATGAATCGGCCAACGCGCGGGGAGAGGCGGTTTGCGTATTGGGCGCTCTTC
CGCTTCCTCGCTCACTGACTCGCTGCGCTCGGTCGTTCGGCTGCGGCGAGCGGTATCAGCTCACTCAAAGGCGGTAATACGGTTATCCACAG
AATCAGGGGATAACGCAGGAAAGAACATGTGAGCAAAAGGCCAGCAAAAGGCCAGGAACCGTAAAAAGGCCGCGTTGCTGGCGTTTTTCCAT
AGGCTCCGCCCCCCTGACGAGCATCACAAAAATCGACGCTCAAGTCAGAGGTGGCGAAACCCGACAGGACTATAAAGATACCAGGCGTTTCC
CCCTGGAAGCTCCCTCGTGCGCTCTCCTGTTCCGACCCTGCCGCTTACCGGATACCTGTCCGCCTTTCTCCCTTCGGGAAGCGTGGCGCTTT
CTCATAGCTCACGCTGTAGGTATCTCAGTTCGGTGTAGGTCGTTCGCTCCAAGCTGGGCTGTGTGCACGAACCCCCCGTTCAGCCCGACCGC
TGCGCCTTATCCGGTAACTATCGTCTTGAGTCCAACCCGGTAAGACACGACTTATCGCCACTGGCAGCAGCCACTGGTAACAGGATTAGCAG
AGCGAGGTATGTAGGCGGTGCTACAGAGTTCTTGAAGTGGTGGCCTAACTACGGCTACACTAGAAGGACAGTATTTGGTATCTGCGCTCTGC
TGAAGCCAGTTACCTTCGGAAAAAGAGTTGGTAGCTCTTGATCCGGCAAACAAACCACCGCTGGTAGCGGTGGTTTTTTTGTTTGCAAGCAG
CAGATTACGCGCAGAAAAAAAGGATCTCAAGAAGATCCTTTGATCTTTTCTACGGGGTCTGACGCTCAGTGGAACGAAAACTCACGTTAAGG
GATTTTGGTCATGAGATTATCAAAAAGGATCTTCACCTAGATCCTTTTAAATTAAAAATGAAGTTTTAAATCAATCTAAAGTATATATGAGT
AAACTTGGTCTGACAGTTACCAATGCTTAATCAGTGAGGCACCTATCTCAGCGATCTGTCTATTTCGTTCATCCATAGTTGCCTGACTCCCC
GTCGTGTAGATAACTACGATACGGGAGGGCTTACCATCTGGCCCCAGTGCTGCAATGATACCGCGAGACCCACGCTCACCGGCTCCAGATTT
ATCAGCAATAAACCAGCCAGCCGGAAGGGCCGAGCGCAGAAGTGGTCCTGCAACTTTATCCGCCTCCATCCAGTCTATTAATTGTTGCCGGG
AAGCTAGAGTAAGTAGTTCGCCAGTTAATAGTTTGCGCAACGTTGTTGCCATTGCTACAGGCATCGTGGTGTCACGCTCGTCGTTTGGTATG
GCTTCATTCAGCTCCGGTTCCCAACGATCAAGGCGAGTTACATGATCCCCCATGTTGTGCAAAAAAGCGGTTAGCTCCTTCGGTCCTCCGAT
CGTTGTCAGAAGTAAGTTGGCCGCAGTGTTATCACTCATGGTTATGGCAGCACTGCATAATTCTCTTACTGTCATGCCATCCGTAAGATGCT
TTTCTGTGACTGGTGAGTACTCAACCAAGTCATTCTGAGAATAGTGTATGCGGCGACCGAGTTGCTCTTGCCCGGCGTCAATACGGGATAAT
ACCGCGCCACATAGCAGAACTTTAAAAGTGCTCATCATTGGAAAACGTTCTTCGGGGCGAAAACTCTCAAGGATCTTACCGCTGTTGAGATC
CAGTTCGATGTAACCCACTCGTGCACCCAACTGATCTTCAGCATCTTTTACTTTCACCAGCGTTTCTGGGTGAGCAAAAACAGGAAGGCAAA
ATGCCGCAAAAAAGGGAATAAGGGCGACACGGAAATGTTGAATACTCATACTCTTCCTTTTTCAATATTATTGAAGCATTTATCAGGGTTAT
TGTCTCATGAGCGGATACATATTTGAATGTATTTAGAAAAATAAACAAATAGGGGTTCCGCGCACATTTCCCCGAAAAGTGCCACCTGACGC
GCCCTGTAGCGGCGCATTAAGCGCGGCGGGTGTGGTGGTTACGCGCAGCGTGACCGCTACACTTGCCAGCGCCCTAGCGCCCGCTCCTTTCG
CTTTCTTCCCTTCCTTTCTCGCCACGTTCGCCGGCTTTCCCCGTCAAGCTCTAAATCGGGGGCTCCCTTTAGGGTTCCGATTTAGTGCTTTA
CGGCACCTCGACCCCAAAAAACTTGATTAGGGTGATGGTTCACGTAGTGGGCCATCGCCCTGATAGACGGTTTTTCGCCCTTTGACGTTGGA
GTCCACGTTCTTTAATAGTGGACTCTTGTTCCAAACTGGAACAACACTCAACCCTATCTCGGTCTATTCTTTTGATTTATAAGGGATTTTGC
CGATTTCGGCCTATTGGTTAAAAAATGAGCTGATTTAACAAAAATTTAACGCGAATTTTAACAAAATATTAACGCTTACAATTTCCATTCGC
CATTCAGGCTGCGCAACTGTTGGGAAGGGCGATCGGTGCGGGCCTCTTCGCTATTACGCCAGCTGGCGAAAGGGGGATGTGCTGCAAGGCGA
TTAAGTTGGGTAACGCCAGGGTTTTCCCAGTCACGACGTTGTAAAACGACGGCCAGTGAGCGCGCGTAATACGACTCACTATAGGGCGAATT
GGAGCTTCGAAGGCTGTAGTACTGGTGCTCGTATGCGACACGCGGATTCACGGCGTATGCGACAAGCGGGATTGCTGATGAGCGTCGTTCCC
CACTGAAGCGCGCGGAGTGGTGGGCGACCACCGGTCACCTGGCGTCTCAGCTGCGCGAGGCACCCCTCTCATAGCGTGGTACTCGTCACGAA
TACCAATCGCTGGGGTCGCGGCGGGAGGAATATGCTGTTTGTTGACCATACGATCACGCTGAACGAAAACATGGTATGAGACGCCGTAAGCG

GGCACAGGTTGTTTGCCCTCGTCTCATTGCGGACCAATTCCCGGTCCACCGCTGCGTCTCGACTCGACGGTTGTGACCACCCCACTTCGCAT
TGGGCAGTCGGTAAAGCCACAACATTACTTTGCAATTTTATCGGTTGAAACTGCCGAGCGAGCTTGCGTTTTTGGGTGCTATCTTCTCCCAC
CTTTTATCAGTTAAGTTGTACAGTGAGTGTCAGCTTGTTTCGACACGTCTGTATAGACGCAACTCGGTTTGCTTGTGTTGGTTGGTGGCTGG
CCAAATCAAAGGCTATTCATTTTTCACTTGCTGTGTTCTTTGAAGAAATCAAGCAAGATGCATAAAGGAGAAGAACTTTTCACTGGAGTTGT
CCCAATTCTTGTTGAATTAGATGGTGATGTTAATGGGCACAAATTTTCTGTCAGTGGAGAGGGTGAAGGTGATGCAACATACGGAAAACTTA
CCCTTAAATTTATTTGCACTACTGGAAAACTACCTGTTCCATGGGAAAACTCGTTTTCCCGCACTATGTCACCGACCAAGATGCGATCAACC
TGATGAAGAGGCTTTTGTGTCGTCTCCCTGAGGTCCGAATCGGATGCTCCATCAACGGCTACAAGGTGGGTGAAGATTCGCCGTTCTGCCGG
GCTACACAGACTCCGGGGAACTCTGTATGCACGCTGTTTGCCGCGGAATCTGTGTAAAGAATGTGTTTCCCGTTCCTCAAAGCGAAGCTTCC
ACACCGCTTTTGGTGCACGTCAATCTTCTCCCGCTGCCTTTCTCTCTGTTTCTCTCTCGATATATATACATACATGTGTATGTATATGTATA
ATACGTATGTGCATGTGTGTGTAGATGTGTGTGTGTGTATATGCAGGGCGGTGCCTGTGCCTACGGTGTGTGTTTGTATCTTGGCATGCTTC
GCCTTACATAAGGAGGGGCGCGGGCAGACTTACGTTCCGTTTTGGTGAGGACTGTTCTGGCTTTTTAGGACATCAAGGAGCACGCATTTTTC
GGAGACTTCGACTGGGACAAACTGGCAGGTCGTGGCTTGCCGCCACCCCTCGCACCGAAAGGCGAAACCTACGCAGAAGATACTGAACAAGT
GAGAAAAATTCCATCTCTCTCCTCATTCACAGGAGTCTCCCACACACACTCTTTGTATGTACAAATAGATATGCATATATATAAATAGATAG
ATATGGACATGCATTTAGCCGCATACACACGTAGATGCATCGTATACATCGACGTACATATATGTATGTATGCATGTACGTGTGTGTATAAG
TTGTGGTCAGTGTTTTTAACGGAGATGCCCTATTCAAGGATATCTGTTCCTATATACGTGCATAGGATGACTTGATTTTTTGACAGCAGGTT
GTTCAGAAGAGATGCAAGGGGGAGGTTGTCGGATTTTTACAGTTAAGATAGAAATGCGTTTGCGTTTTTGTGTGCGTTCCGGTGTGTATGGC
GTTCAGTCCTCTTTCGAGCTGGACGAGGATGACACGATCGTTTTGGAAGACGAGTATGACTGGGACAAGGATTTCTACCCGTACGACGTCCC
GGACTACGCGTAGGAATTCATAACTTCGTATAGCATACATTATACGAAGTTATTTTTTCAGCTTAGGTGTTTGTTCCCCGTCAGTGCTGAAA
GTGCCGCTCCTTCTCTCTTCTGACTCTTCTGTGGACCTGCAACTTCCTGCATGACGAAACGATCCGTGCATAAGCATGAGCGCGATGTTCCT
CGCCCGAAATCCTTCGGCGAGGCCGGAGCCGGTGTCGGGACCGGACAGACGCAGGCAGAACATGAGAGACACACAGCAAACGACCGAAGGGG
GAGTCCGTTCGTCCGCGTGTGCGTGAATTAAAACGAGAAAGGAAAGAGACGGCGCTCTGTGCAACCTAAGGAGTCTCGTTCTTTAGCTTTAT
TCGAGGAAATAGCGAATGATTCCTCTCTCGTGAGAGAAAGTGTGAGAGCACAACGTAGACGTACGTGAGGTTTTGCGTTGCTCCACAATCTA
GCGGGAGAGAACATCGGGCATGAGATAGGTGTACGTTTCTCGAAGTCACCGTTTCACGCCATGTTCCCTCTCGCTCTGTTTTCGTGAAAGCG
GGCGTGGTCTGGGGAGCATAAAATTGGAGTCGAAGTCTGATTCGATCTGGAAGGACTTTGCTTACCGGACTCAAGTACTGCTTTCTGTAGAT
ACTCATTTCAAAGTTCGTTCCTACTCGTTTCCTCAGTTCAAGTCAACAAATCCTTTGTTCACAGTTTGCGCCGTTACCTTCAGAGGAGCGTA
CTGACAAGCATCTCTGCGTATTTAGCGGTGCATAACGCACGCACAATAAGCATGATAGGGAGATACGTGTGTGTATAGTATGGGTGACACAT
GTTTTTATACAGATTTATATTTATGTATTTGAGTTTGTGGCCACGGTGCACTGCACTACACCAAAATAGCGATGCTGCGCGCGTAAAAGACG
TCGCTTTTCTCTACGATGGGAGAGTTCAGGAGTGCTTGGGAGGGGCAACTTCGAGGCGAAATCGGATTTTCGGGGTGTGGAAGGCCAAGTTG
AATGTGTCGTTTTTCTACAAGGAGCAGAGTCGCAGAAAAGCACTAGTGGATCCCCCTCCACCGCGGTGTCACTGTAGCCTGCCAGAACACTT
GTCAACCGACTGTGTCCACATTTTTATGCGCACTGACTGGCATGAATGGCCAGAGGCAGGCATCAGCAAGTCACGTAGGCCAACGCGTGCGC
AGAAACGCTCAAGGCTCGATTGTGGGTGGGGGTTGGTAGCATTTTATCGACCTAAACAAGGTTTACACTTAGGTGGTGCGGTTTTACTGATC
TGGACGGATTCAGCGGTCGCAGATTATCGATCTGCAAATGGTGTACACTTAGGTGTCGCGGCTTATTTAGTTAAGGGAGCTTCGTGGTCGGA
GCCTAACAAGTCAACAGAGACGTATCGCCAATCGTTCGCGGTGAAGAGTCGAAACTGACAGCACATCGTAGGGAAACTGAGAGGGTGCTCCT
TTCTCTCCGTCGTTTGCGCTGCACCATCCTGCAAGTGCATAGAAGGAAAGTTGTCTGCTGTCGTGGGCAGACAGCAACAGTCCAGCACTCTA
GCGGCATACAGAACGATAACGCATTCACGAGTGGATACACGCACATCTGCGTCACCCGCAACTCGCTTTCGTTCTGATTGACAAAAAGAAAA
CAAGGCGAGGTGAGACTGTGTGAAATGCCACATGAAGAGTCATCCCTTTTCTTCGATAAAGGACACAGGGGTCTCTGGCACCCCCTCGTCAG
CTCTCTCCGACCCGAGGCACTCTCCCTGATCCCTCCGAAAAGAGAGGAAAACGAGAGACGGGCAGCTTCTGTAGGGCTATGCAGGGTTTACT
TCTCGAACTTTTTGCGAGCGGCGTCGCTCAGGACGGCGACGTGGTCGAAGTCGCGGAACATCTCGTTGAAGTCGTAGCAGCAACCAACGATC
CAGACGTCTTCAATGCTGAAGCCGACGAAGTCGCCCTTCAAGCTGTTGGAGCGATCTGTGCGCTTCTCGACGAGGGTGGCGATTCTCATCGA
CTTGGGACCGACGGCTTTCAGGCGCTCACCGAACTCGGTGAGGGTGAAACCGGTGTCGACGATGTCCTCAACAATCAGAACGTGCTTGTCGC
GAAAGATTGACAAGTCGTCGCTCAAGACGGTGAGCTGGCCTGTGCTGTTGTCGTTCTGGTAGGACTTCAGGCGGACATAGTGCTCGAAGAAG
GGGGGCACGCTGGACTCACGACCACTGTACTTCTGTATGGTGGCAAGGTAGTCGATCAGAAGGTTGAAGAAGCCGCGAGAGCCTTTCAGGAT
GCAAATGATGTGCAACTCCTCGCCGAAGTAAGTTCTGTGGATGTCATACGCCAACTTCTCAACTCTGTCCTTGACCAATCCACCAGGGAGGA
GGATTTTGTCAATGTAGGGCTTGCAGTGGGGGGGCACAAGAAAGTCATCAGCGTTGTAGAAGGTGTTGTCGGGGATATACATGGGCTCAATA
CGGCCCTTGCCCTTGCCGTAGTCTTCAATGGGTTTGGACGCCATTTTGGATCTGACAACGCCCCGTAGAGCAGAAACGCACTACTAAAGCGA
AACTTCACCCGTCCCTGCTGCACTCAGAGCAGTGCTCCGCACTGCCGTGTGGTAAAATGAAAAGGTTCTACGAGACACGCGTCTCCGGATCG
ACAAGCGAAGGATCTGCACACCTGGTCTCGATGTCGAACAAAGCACGGAGGAGAGACGGAAAGTGCTTACATCGAACACGGTTATCAAACCC
GAGAAAAAGAAACGAACAGAAGAAAAAGGAAACCTCCGCATACTTTTAAAGAATGAAGTTCCCCGATTTTCCCAAAAATGGCGTCATTTTCG
CGCACGGCAGTCAGATAACAGGTGTAGCGGCTGCCCACCAACAGAGACGGCGCGGCCGACAGGACGCTACTGGGACTGCGAACAGCAGCAAG
ATCGGATCTTCCGCGGGCGGGTTTGAATGCAAGGTTTCGTGCTGATCATAACTTCGTATAGCATACATTATACGAAGTTATAAGCTTGCTAG
CGTTAACGGGCCCCGTACC

NcoI	EcoRI
*Tg*PKG-3'UTR	*Tg*PKG-3`end
HXGPRT ORF	HA-epitope tag
5`and 3`UTRs of *Tg*DHFR/TS	loxP sites
SpeI	

G) Plasmid of *pTKO-DHFR/TS-RhoGC-HA*

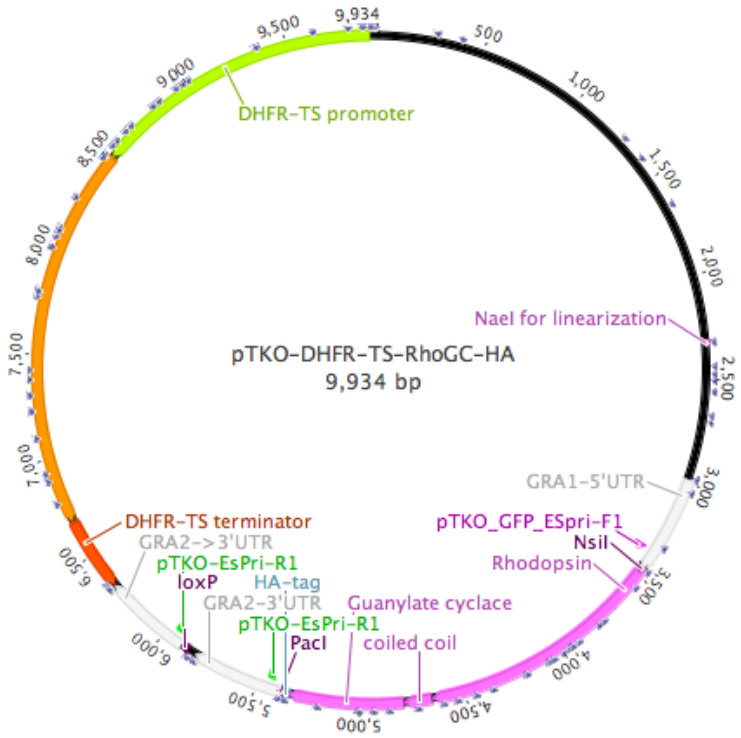

CAGCTTTTGTTCCCTTTAGTGAGGGTTAATTGCGCGCTTGGCGTAATCATGGTCATAGCTGTTTCCTGTGTGAAATTGTTATCCGCTCACAA
TTCCACACAACATACGAGCCGGAAGCATAAAGTGTAAAGCCTGGGGTGCCTAATGAGTGAGCTAACTCACATTAATTGCGTTGCGCTCACTG
CCCGCTTTCCAGTCGGGAAACCTGTCGTGCCAGCTGCATTAATGAATCGGCCAACGCGCGGGGAGAGGCGGTTTGCGTATTGGGCGCTCTTC
CGCTTCCTCGCTCACTGACTCGCTGCGCTCGGTCGTTCGGCTGCGGCGAGCGGTATCAGCTCACTCAAAGGCGGTAATACGGTTATCCACAG
AATCAGGGGATAACGCAGGAAAGAACATGTGAGCAAAAGGCCAGCAAAAGGCCAGGAACCGTAAAAAGGCCGCGTTGCTGGCGTTTTTCCAT
AGGCTCCGCCCCCCTGACGAGCATCACAAAAATCGACGCTCAAGTCAGAGGTGGCGAAACCCGACAGGACTATAAAGATACCAGGCGTTTCC
CCCTGGAAGCTCCCTCGTGCGCTCTCCTGTTCCGACCCTGCCGCTTACCGGATACCTGTCCGCCTTTCTCCCTTCGGGAAGCGTGGCGCTTT
CTCATAGCTCACGCTGTAGGTATCTCAGTTCGGTGTAGGTCGTTCGCTCCAAGCTGGGCTGTGTGCACGAACCCCCCGTTCAGCCCGACCGC
TGCGCCTTATCCGGTAACTATCGTCTTGAGTCCAACCCGGTAAGACACGACTTATCGCCACTGGCAGCAGCCACTGGTAACAGGATTAGCAG
AGCGAGGTATGTAGGCGGTGCTACAGAGTTCTTGAAGTGGTGGCCTAACTACGGCTACACTAGAAGGACAGTATTTGGTATCTGCGCTCTGC
TGAAGCCAGTTACCTTCGGAAAAAGAGTTGGTAGCTCTTGATCCGGCAAACAAACCACCGCTGGTAGCGGTGGTTTTTTTGTTTGCAAGCAG
CAGATTACGCGCAGAAAAAAAGGATCTCAAGAAGATCCTTTGATCTTTTCTACGGGGTCTGACGCTCAGTGGAACGAAAACTCACGTTAAGG
GATTTTGGTCATGAGATTATCAAAAAGGATCTTCACCTAGATCCTTTTAAATTAAAAATGAAGTTTTAAATCAATCTAAAGTATATATGAGT
AAACTTGGTCTGACAGTTACCAATGCTTAATCAGTGAGGCACCTATCTCAGCGATCTGTCTATTTCGTTCATCCATAGTTGCCTGACTCCCC
GTCGTGTAGATAACTACGATACGGGAGGGCTTACCATCTGGCCCCAGTGCTGCAATGATACCGCGAGACCCACGCTCACCGGCTCCAGATTT
ATCAGCAATAAACCAGCCAGCCGGAAGGGCCGAGCGCAGAAGTGGTCCTGCAACTTTATCCGCCTCCATCCAGTCTATTAATTGTTGCCGGG
AAGCTAGAGTAAGTAGTTCGCCAGTTAATAGTTTGCGCAACGTTGTTGCCATTGCTACAGGCATCGTGGTGTCACGCTCGTCGTTTGGTATG
GCTTCATTCAGCTCCGGTTCCCAACGATCAAGGCGAGTTACATGATCCCCCATGTTGTGCAAAAAAGCGGTTAGCTCCTTCGGTCCTCCGAT
CGTTGTCAGAAGTAAGTTGGCCGCAGTGTTATCACTCATGGTTATGGCAGCACTGCATAATTCTCTTACTGTCATGCCATCCGTAAGATGCT
TTTCTGTGACTGGTGAGTACTCAACCAAGTCATTCTGAGAATAGTGTATGCGGCGACCGAGTTGCTCTTGCCCGGCGTCAATACGGGATAAT
ACCGCGCCACATAGCAGAACTTTAAAAGTGCTCATCATTGGAAAACGTTCTTCGGGGCGAAAACTCTCAAGGATCTTACCGCTGTTGAGATC
CAGTTCGATGTAACCCACTCGTGCACCCAACTGATCTTCAGCATCTTTTACTTTCACCAGCGTTTCTGGGTGAGCAAAAACAGGAAGGCAAA
ATGCCGCAAAAAAGGGAATAAGGGCGACACGGAAATGTTGAATACTCATACTCTTCCTTTTTCAATATTATTGAAGCATTTATCAGGGTTAT
TGTCTCATGAGCGGATACATATTTGAATGTATTTAGAAAAATAAACAAATAGGGGTTCCGCGCACATTTCCCCGAAAAGTGCCACCTGACGC
GCCCTGTAGCGGCGCATTAAGCGCGGCGGGTGTGGTGGTTACGCGCAGCGTGACCGCTACACTTGCCAGCGCCCTAGCGCCCGCTCCTTTCG
CTTTCTTCCCTTCCTTTCTCGCCACGTTCGCCGGCTTTCCCCGTCAAGCTCTAAATCGGGGGCTCCCTTTAGGGTTCCGATTTAGTGCTTTA
CGGCACCTCGACCCCAAAAAACTTGATTAGGGTGATGGTTCACGTAGTGGGCCATCGCCCTGATAGACGGTTTTTCGCCCTTTGACGTTGGA
GTCCACGTTCTTTAATAGTGGACTCTTGTTCCAAACTGGAACAACACTCAACCCTATCTCGGTCTATTCTTTTGATTTATAAGGGATTTTGC
CGATTTCGGCCTATTGGTTAAAAAATGAGCTGATTTAACAAAAATTTAACGCGAATTTTAACAAAATATTAACGCTTACAATTTCCATTCGC
CATTCAGGCTGCGCAACTGTTGGGAAGGGCGATCGGTGCGGGCCTCTTCGCTATTACGCCAGCTGGCGAAAGGGGGATGTGCTGCAAGGCGA
TTAAGTTGGGTAACGCCAGGGTTTTCCCAGTCACGACGTTGTAAAACGACGGCCAGTGAGCGCGCGTAATACGACTCACTATAGGGCGAATT
GGAGCTTCGAAGGCTGTAGTACTGGTGCTCGTATGCGACACGCGGATTCACGGCGTATGCGACAAGCGGGATTGCTGATGAGCGTCGTTCCC
CACTGAAGCGCGCGGAGTGGTGGGCGACCACCGGTCACCTGGCGTCTCAGCTGCGCGAGGCACCCCTCTCATAGCGTGGTACTCGTCACGAA
TACCAATCGCTGGGGTCGCGGCGGGAGGAATATGCTGTTTGTTGACCATACGATCACGCTGAACGAAAACATGGTATGAGACGCCGTAAGCG
GGCACAGGTTGTTTGCCCTCGTCTCATTGCGGACCAATTCCCGGTCCACCGCTGCGTCTCGACTCGACGGTTGTGACCACCCCACTTCGCAT
TGGGCAGTCGGTAAAGCCACAACATTACTTTGCAATTTTATCGGTTGAAACTGCCGAGCGAGCTTGCGTTTTTGGGTGCTATCTTCTCCCAC

CTTTTATCAGTTAAGTTGTACAGTGAGTGTCAGCTTGTTTCGACACGTCTGTATAGACGCAACTCGGTTTGCTTGTGTTGGTTGGTGGCTGG
CCAAATCAAAGGCTATTCATTTTTCACTTGCTGTGTTCTTTGAAGAAATCAAGCAAGATGCATATGAAAGATAAGGATAATAACCTGAGAGG
AGCTTGTTCTAGCTGTAACTGCCCTGAATACTGTTTTAGCCCAACTTCCACCCTGTGCGACGATTGCAAGTGTTCCGTGACCAAACACCCAA
TCGTCGAACAGCCCCTGTCCCGAAACGGATCTTTCCGGAGCTCCGGAGCAAGTCTGCTGCCATCACCTTCTAGTCCCAATGTGAAGATTACC
TCTACAGTCGGCCTGCGGAGTAGAAAAAGCGAGTCCCAGGCAAACGTGCGCGGGTCTATGATCTCTAACAGTAATTCAGGAAGCCGATCCAA
CAATAGTGGAGGAGCAGGAGGAGGGTCAGGAGGCTCAAGCTCCTCTAAGGGGGGCAGCGCCCTGGCTAACTACCAGTCCGCTATGTCTGAGC
TGTGGTCTTGGAATATGATGCTGAGTACTCCTTCACTGAAATTCCTGACCGTGCAGTTTACCACATGGATTGTGCTGACTACCGTCGGCGCC
ATCTACACTCTGTTCTTTCATGAAAGACAGGCTTATAATAGGGGGTGGGCAGACATCTGGTACGGCTATGGGGCTTTCGGATTTGGCCTGGG
GCTGAGCTTCGCATATATGGGCTTCACCGGCGCCAGAAACCCAGAGAAGAAAGCTCTGAGCCTGTGCCTGCTGGGGGTGAATTTCATTAGCT
TTATGTCCTACATCATCATCATGCTGCGGCTGACTCCCACCATCGAAGGCACCATGGCCAACCCAGTGGAGCCCGCTAGATATCTGGAATGG
ATCGCCACTTGCCCTGTCCTGATCCTGCTGATTAGCGAGATCACCCAGTACCCTCACGACCCATATAAAGTGATCGTCAATGATTACGCCCT
GTGCCTGGCAGGATTCGTGGGAGCAATCAGCGCCCAGCAGCCATGGGGCGACCTGGCACATTTCGTGAGCTGCCTGTGCTTTTCCTACGTGG
TCTATTCTCTGTGGAGTTGCTTCACAGGGGCTATCGATGGAGAGACTCAGTGTAACGTGGAAAAAAGCGGCCTGAGGTGGATTCGCTTTTCA
ACAATCACAACTTGGAGCCTGTTCCCCATTACCTGGTTTTCATATACAAGCGGCCTGATCTCTTTCACTGTGGCAGAGGCCGGGTTTAGTAT
GATTGACATCGGAGCCAAGGTCTTCCTGACCCTGGTGCTGGTCAACAGCACAGTGGAACAGGCACAGAATCAGAAAGTCGACGCCATTACCG
CTATCGCAGAGGAACTGGAGAACCAGATTAACAATTGTGATGCCATCCTGCAGAAGATGATGCCCGAGGGCGTGCTGGAACAGCTGAAGAAT
GGGCAGGCTACTGAGGCAAAAGAGTACGAATCCGTGACCGTCTTCTTTTCTGATATTACTAACTTTACCGTGATCAGTTCAAGGACATCCAC
TAAGGACATGATGGCCACCCTGAACAAGCTGTGGCTGGAATATGATGCCATTGCTAAGCGGTGGGGAGTGTATAAAGTCGAGACAATCGGCG
ACGCTTATCTGGGAGTGACTGGAGCACCAGACGTGGTCCCTGATCACGCAGAGCGAGCTTGCAACTTCGCCGTGGATATCATCGAAATGATT
AAGAGCTTTAAAACCATCACAGGCGAGTCCATTAACATCCGCATTGGCCTGAATAGCGGACCTGTGACCGCAGGAGTCCTGGGCGACCTGAA
CCCACACTGGTGTCTGGTGGGAGATACAGTCAATACTGCCTCCCGGATGGAATCTACAAGTAAAGCTGGCCACATCCATATTTCAGAGAGCA
CCTACCATTTCATCAAGTCTAAATTTGTGACACAGCCTCTGGATGTGATGGAGGTGAAAGGCAAAGGCAAAATGCAGACTTATTGGGTGCTG
GGCAGAAAATACCCGTACGACGTCCCGGACTACGCGTAGTTAATTAAGACTACGACGAAAGTGATGCGCAGGCTGGAAAGCCGCTGAAGGGA
GAAGTCTACAAAGCCGATCAGTGAAAAATGTGTGGGGAGGTGGTCTTGTTGCAGGAATGCAATGGTGTTAAGCATCGTGTTCGAATGCAGTG
CGTGTATCAGTTGTGCGCGGAAGGACACTGCTTCAATGTTAAGAACCTGTTTTCTCCGTAGAGAGGACCAAAAGACGATTGCAAAACTGGTA
TGTACGCAATAGCCCAATGCCGGACGTCAGTTGGTTGTATGTGACGCTCCCAGATGTCATATGCCTTGTGAGTGTGTCTGGGATGCAAGTTT
TTGGTGTGCGTTGATTTCGCCAGCTTATGACAGTGGCAGACGAATTATTGACATGATACAAGGACGCAGAAAGGAACAAACACCGTAGTTCC
AGTCGACGGATCCCACCGCGGTGGCGGCCGCACTGCAGGGTACCCTCGAGGATATCGAATTCATAACTTCGTATAGCATACATTATACGAAG
TTATGACTACGACGAAAGTGATGCGCAGGCTGGAAAGCCGCTGAAGGGAGAAGTCTACAAAGCCGATCAGTGAAAAATGTGTGGGGAGGTGG
TCTTGTTGCAGGAATGCAATGGTGTTAAGCATCGTGTTCGAATGCAGTGCGTGTATCAGTTGTGCGCGGAAGGACACTGCTTCAATGTTAAG
AACCTGTTTTCTCCGTAGAGAGGACCAAAAGACGATTGCAAAACTGGTATGTACGCAATAGCCCAATGCCGGACGTCAGTTGGTTGTATGTG
ACGCTCCCAGATGTCATATGCCTTGTGAGTGTGTCTGGGATGCAAGTTTTTGGTGTGCGTTGATTTCGCCAGCTTATGACAGTGGCAGACGA
ATTATTGACATGATACAAGGACGCAGAAAGGAACAAACACCGTAGTTCCAGTCGACGGATCCACTAGTGGATCGATCCCCCGGGCTGCAGGA
ATTCATCCTGCAAGTGCATAGAAGGAAAGTTGTCTGCTGTCGTGGGCAGACAGCAACAGTCCAGCACTCTAGCGGCATACAGAACGATAACG
CATTCACGAGTGGATACACGCACATCTGCGTCACCCGCAACTCGCTTTCGTTCTGATTGACAAAAAGAAAACAAGGCGAGGTGAGACTGTGT
GAAATGCCACATGAAGAGTCATCCCTTTTCTTCGATAAAGGACACAGGGGTCTCTGGCACCCCCTCGTCAGCTCTCTCCGACCCGAGGCACT
CTCCCTGATCCCTCCGAAAAGAGAGGAAAACGAGAGACGGGCAGCTTCTGTATTTCCGCTAGACAGCCATCTCCATCTGGATTCGTCCGTGC
GGGACGTAGCCCACGACCTCAAAATCCTCGGCGGTGAAATCGTCGATTTCCTTGATGCGTTCCTTGTTGAGGATGTTCACAATGGGGAACGG
TCTCGGTTCTCTCCGCAGCTGCTCTTTTAAAGCCTCGACATGGTTCGTGTAGACATGCGTGTTCCCCATGAAGTGAATGAACTCCTTAGGTT
TTAGGTTGCAGACGTGTGCAACCATGAGCGTCAAAAGCGAATAGGAAGCGATGTTGAAGGGGACGCCGAGGCCGACATCGCACGACCGCTGA
TACATGATGCACGACAGCTCCTTCTGGTCGTTCACGTAGAACTGGCACAACAAGTGACAAGGCGGCAGCGCCATTTCGTCCAGCGCTGCAGG
ATTCCAGGCAGTCATGAGCATGCGACGATCTGTTGGATTCGTTCTCAGCATCTGGATCACATTCTTCAGCTGGTCGACGCCCTGCCCTGTGT
AGTCTGTGTGCATGTCTTTGTATGCCGCGCCGAAGTGTCTCCACTGGAAGCCGTAGCCCGGGCCGATGTCTCCGACCTCTCGGTGGGGGAGA
TTGCGCGAATCGAGGAACTCGCGTGTCACATTCTTGTCCCAGATCTTCACGCCCTTCTCAGAAAGATGGTTTGCGTTCGTGTCGCCGCGAAT
GAACCACAGCAACTCTTCGAGGACCCCTTTCCAGAACACACGCTTTGTGGTGAGAAGTGGAAAGGCCTGATCCAGCGAGTAGCGCATAGTGC
AGCCGAATTTGGAGATGACACCAACGCCCGTTCGGTCATCCATTGTCCTTCCATTGTTAATAATGTCGGCAATGAGATCAAGGTACTGGAAT
TCTTCATGGCCTCTAAAGTGAACATGCGGAACGGCCCGAATCAGTTCCTTTTGCTCGCGTTTTTTCCGGTCTTCTTCGTCCATCCACGCCAA
CACCGGGGCAATGGCTGCGGCCGAAGAAGGAGCCTGCAACCCGTGCACGGGAGTTGTCTCCCTCGTGGACGTCAAGGAGCTCATTGCGTTGC
TCGGTTCCGCAGTGGCTGCGTCGTCAGTCTTCCTTCTCTTCTCGAGAACCACAAAGTCGTAGGGTACCCCGTTGTCTGAGAAGGTCTTGGAA
ATGAAGATGGGTCGATACGTCGCTTCATTGTCCTTCTCTCTTCCGAGCTCCGGACAAAAGGGAACGAACACAGACTCGGCAGGAGCTGCAGC
CTGCGCAGCAGTTGATTTGTTTGAAAGAATGTCATCTCCGGGGAACGCAGGGAAGAAAACGTCGCACGGAAACTCGCGGGCTACACGCGTGA
TGTACAGGTGAGAGGCAACGCCCAGAGACAGCGCTGCCTCGTACAGTCCCGCTCCTCCCACGACAAAAATCTGGTCGACAGAATCCTTGTAC
TCTTCCTCCAGAAGGCTGAGAGCTGCTGGGAGTGAAGCACAGACTCGGACGCGCTGCTGGCCTTCAGCTTGAGGCTTCTCCGCCGCAATGTC
TTCTTCTTTGAGGGAAGAGGAAACGACGATGTTCAATCTGTCCACGAGGGGTCTAAACTTTCGAGGCATGCTTTCCCAGGTTTTCCGTCCCA
TGACAACGGCGTTGAATCTCTTGCCGACTGATGGAGAGGGAAGTCCAGAGTCGCCCGTCTTTGCAAATTTCCTGGGAAGCCACCCGTTCAGG
CGACTGGCTTCTTCGGGCGTCGTTTTTGTCACACGAGAAAAGTGTTTGAAATCTGTGGTCAAGTGGGGCCACGGGAGGCCGTTGTTGATGCC
GATGCCCCTCTTGGGGGTCATCGCGACGACCAGACACACCGGTTTCTGCATCTTCCCAGACACGACAACGCCCCGTAGAGCAGAAACGCACT
ACTAAAGCGAAACTTCACCCGTCCCTGCTGCACTCAGAGCAGTGCTCCGCACTGCCGTGTGGTAAAATGAAAAGGTTCTACGAGACACGCGT
CTCCGGATCGACAAGCGAAGGATCTGCACACCTGGTCTCGATGTCGAACAAAGCACGGAGGAGAGACGGAAAGTGCTTACATCGAACACGGT
TATCAAACCCGAGAAAAAGAAACGAACAGAAGAAAAAGGAAACCTCCGCATACTTTTAAAGAATGAAGTTCCCCGATTTTCCCAAAAATGGC
GTCATTTTCGCGCACGGCAGTCAGATAACAGGTGTAGCGGCTGCCCACCAACAGAGACGGCGCGGCCGACAGGACGCTACTGGGACTGCGAA
CAGCAGCAAGATCGGATCTTCCGCGGGCGGGTTTGAATGCAAGGTTTCGTGCTGTCGAAAAAGAGAATGGAACTTAATGTCCACGTAGTTCG
CGCATGAAAAGCGTCCTACCACTCAAAAAAGACAAAAACCGCACTCGCGGCGTTGAATGTGCGGGGGAACGGATGGCTCTCTTTTTTGGAAA
GCGAATGCAAAAAGACAAGACGCAGACGCATACAACGTTAGTCCCCTGGCACGAGAGATAGAGGTGCTGGGGGCCATTGCGGTGTCGTGGAT
TTACCAGTCATGGACGAGATCGTTCCGGAGCCTGTCTTTCCTGAAAGTCTGAAAAAATTGCGGGAAAGTCACGCATATGGAACAGCACCGGG
GCGGGACAGAGTTGTCTCGACAACGAATGACACACAGGAACTACGCGGGGGGTGAAAATCGAATGACATGCTAGCGTTCAACTTCTGGAAAG
GTGGTGGCTTCTCGATCAGGAAACTCCGTTTTCTAGTGTTGAACAGGTGCGCTCCGAGAAATCGCACGCGGGCTAATACGTGGTAAGACAAA

AGACCAGCCTGTCGCCGGATTTAGAAGTCGTGGCACTACATACGGACCTCTGTACGAGACATGCCGATGCCAAGGGCGTTATCTGGTGCCTG
TGACCGCCAGTTTCAGACAGTACGCGTCTACTAAGTTTGAAAACGCATATGAACGCGTTTGTCGGTTACCATTCATTCTGCAACTGTCTCAG
GCATTGCGTGAGCAAAGCGAGCGCCTCGCTGGTAGTCCCAACTGAATATTATCGAGTAAGCACACTACTCCACGGACATCCCTAGCGCTCTT
ACCTGTTCGTAGGGCTAGAGAAATGATTCGGATATGGTTACACGTGACCACGCCAAAGTAGAAAGGAATTAGCATAACTCAGTCAGGCAGTC
TCCCTGAGGACACCTGCTTGATGATTTGTGAGGACGACTCACGGGATTTACAGCCTGGCGAAGCTTGCTAGCGTTAACGGGCCCCGTACC

*Tg*Gra1-5'UTR	HA-tag	DHFR/TS selection cassette
Rhodopsin domain	*Tg*Gra2-3'UTR	(ORF underlined)
Coiled Coil	PacI	
Guanylate Cyclase domain	NsiI	

H) Plasmid of *pTKO-DD-DHFR/TS-RhoGC-HA*

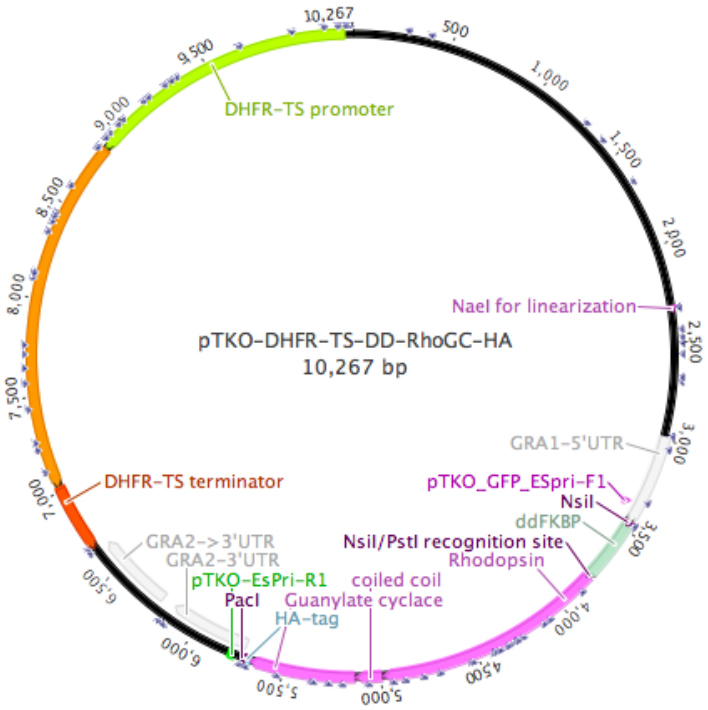

CAGCTTTTGTTCCCTTTAGTGAGGGTTAATTGCGCGCTTGGCGTAATCATGGTCATAGCTGTTTCCTGTGTGAAATTGTTATCCGCTCACAA
TTCCACACAACATACGAGCCGGAAGCATAAAGTGTAAAGCCTGGGGTGCCTAATGAGTGAGCTAACTCACATTAATTGCGTTGCGCTCACTG
CCCGCTTTCCAGTCGGGAAACCTGTCGTGCCAGCTGCATTAATGAATCGGCCAACGCGCGGGGAGAGGCGGTTTGCGTATTGGGCGCTCTTC
CGCTTCCTCGCTCACTGACTCGCTGCGCTCGGTCGTTCGGCTGCGGCGAGCGGTATCAGCTCACTCAAAGGCGGTAATACGGTTATCCACAG
AATCAGGGGATAACGCAGGAAAGAACATGTGAGCAAAAGGCCAGCAAAAGGCCAGGAACCGTAAAAAGGCCGCGTTGCTGGCGTTTTTCCAT
AGGCTCCGCCCCCCTGACGAGCATCACAAAAATCGACGCTCAAGTCAGAGGTGGCGAAACCCGACAGGACTATAAAGATACCAGGCGTTTCC
CCCTGGAAGCTCCCTCGTGCGCTCTCCTGTTCCGACCCTGCCGCTTACCGGATACCTGTCCGCCTTTCTCCCTTCGGGAAGCGTGGCGCTTT
CTCATAGCTCACGCTGTAGGTATCTCAGTTCGGTGTAGGTCGTTCGCTCCAAGCTGGGCTGTGTGCACGAACCCCCCGTTCAGCCCGACCGC
TGCGCCTTATCCGGTAACTATCGTCTTGAGTCCAACCCGGTAAGACACGACTTATCGCCACTGGCAGCAGCCACTGGTAACAGGATTAGCAG
AGCGAGGTATGTAGGCGGTGCTACAGAGTTCTTGAAGTGGTGGCCTAACTACGGCTACACTAGAAGGACAGTATTTGGTATCTGCGCTCTGC
TGAAGCCAGTTACCTTCGGAAAAAGAGTTGGTAGCTCTTGATCCGGCAAACAAACCACCGCTGGTAGCGGTGGTTTTTTTGTTTGCAAGCAG
CAGATTACGCGCAGAAAAAAAGGATCTCAAGAAGATCCTTTGATCTTTTCTACGGGGTCTGACGCTCAGTGGAACGAAAACTCACGTTAAGG
GATTTTGGTCATGAGATTATCAAAAAGGATCTTCACCTAGATCCTTTTAAATTAAAAATGAAGTTTTAAATCAATCTAAAGTATATATGAGT
AAACTTGGTCTGACAGTTACCAATGCTTAATCAGTGAGGCACCTATCTCAGCGATCTGTCTATTTCGTTCATCCATAGTTGCCTGACTCCCC

GTCGTGTAGATAACTACGATACGGGAGGGCTTACCATCTGGCCCCAGTGCTGCAATGATACCGCGAGACCCACGCTCACCGGCTCCAGATTT
ATCAGCAATAAACCAGCCAGCCGGAAGGGCCGAGCGCAGAAGTGGTCCTGCAACTTTATCCGCCTCCATCCAGTCTATTAATTGTTGCCGGG
AAGCTAGAGTAAGTAGTTCGCCAGTTAATAGTTTGCGCAACGTTGTTGCCATTGCTACAGGCATCGTGGTGTCACGCTCGTCGTTTGGTATG
GCTTCATTCAGCTCCGGTTCCCAACGATCAAGGCGAGTTACATGATCCCCCATGTTGTGCAAAAAAGCGGTTAGCTCCTTCGGTCCTCCGAT
CGTTGTCAGAAGTAAGTTGGCCGCAGTGTTATCACTCATGGTTATGGCAGCACTGCATAATTCTCTTACTGTCATGCCATCCGTAAGATGCT
TTTCTGTGACTGGTGAGTACTCAACCAAGTCATTCTGAGAATAGTGTATGCGGCGACCGAGTTGCTCTTGCCCGGCGTCAATACGGGATAAT
ACCGCGCCACATAGCAGAACTTTAAAAGTGCTCATCATTGGAAAACGTTCTTCGGGGCGAAAACTCTCAAGGATCTTACCGCTGTTGAGATC
CAGTTCGATGTAACCCACTCGTGCACCCAACTGATCTTCAGCATCTTTTACTTTCACCAGCGTTTCTGGGTGAGCAAAAACAGGAAGGCAAA
ATGCCGCAAAAAAGGGAATAAGGGCGACACGGAAATGTTGAATACTCATACTCTTCCTTTTTCAATATTATTGAAGCATTTATCAGGGTTAT
TGTCTCATGAGCGGATACATATTTGAATGTATTTAGAAAAATAAACAAATAGGGGTTCCGCGCACATTTCCCCGAAAAGTGCCACCTGACGC
GCCCTGTAGCGGCGCATTAAGCGCGGCGGGTGTGGTGGTTACGCGCAGCGTGACCGCTACACTTGCCAGCGCCCTAGCGCCCGCTCCTTTCG
CTTTCTTCCCTTCCTTTCTCGCCACGTTCGCCGGCTTTCCCCGTCAAGCTCTAAATCGGGGGCTCCCTTTAGGGTTCCGATTTAGTGCTTTA
CGGCACCTCGACCCCAAAAAACTTGATTAGGGTGATGGTTCACGTAGTGGGCCATCGCCCTGATAGACGGTTTTTCGCCCTTTGACGTTGGA
GTCCACGTTCTTTAATAGTGGACTCTTGTTCCAAACTGGAACAACACTCAACCCTATCTCGGTCTATTCTTTTGATTTATAAGGGATTTTGC
CGATTTCGGCCTATTGGTTAAAAAATGAGCTGATTTAACAAAAATTTAACGCGAATTTTAACAAAATATTAACGCTTACAATTTCCATTCGC
CATTCAGGCTGCGCAACTGTTGGGAAGGGCGATCGGTGCGGGCCTCTTCGCTATTACGCCAGCTGGCGAAAGGGGGATGTGCTGCAAGGCGA
TTAAGTTGGGTAACGCCAGGGTTTTCCCAGTCACGACGTTGTAAAACGACGGCCAGTGAGCGCGCGTAATACGACTCACTATAGGGCGAATT
GGAGCTTCGAAGGCTGTAGTACTGGTGCTCGTATGCGACACGCGGATTCACGGCGTATGCGACAAGCGGGATTGCTGATGAGCGTCGTTCCC
CACTGAAGCGCGCGGAGTGGTGGGCGACCACCGGTCACCTGGCGTCTCAGCTGCGCGAGGCACCCCTCTCATAGCGTGGTACTCGTCACGAA
TACCAATCGCTGGGGTCGCGGCGGGAGGAATATGCTGTTTGTTGACCATACGATCACGCTGAACGAAAACATGGTATGAGACGCCGTAAGCG
GGCACAGGTTGTTTGCCCTCGTCTCATTGCGGACCAATTCCCGGTCCACCGCTGCGTCTCGACTCGACGGTTGTGACCACCCCACTTCGCAT
TGGGCAGTCGGTAAAGCCACAACATTACTTTGCAATTTTATCGGTTGAAACTGCCGAGCGAGCTTGCGTTTTTGGGTGCTATCTTCTCCCAC
CTTTTATCAGTTAAGTTGTACAGTGAGTGTCAGCTTGTTTCGACACGTCTGTATAGACGCAACTCGGTTTGCTTGTGTTGGTTGGTGGCTGG
CCAAATCAAAGGCTATTCATTTTTCACTTGCTGTGTTCTTTGAAGAAATCAAGCAAGATGCATATGGGAGTGCAGGTGGAAACCATCTCCCC
AGGAGACGGGCGCACCTTCCCCAAGCGCGGCCAGACCTGTGTGGTGCACTACACCGGGATGCTTGAAGATGGAAAGAAAGTCGATTCCTCCC
GGGACAGAAACAAGCCCTTTAAGTTTATGCTAGGCAAGCAGGAGGTGATCCGAGGCTGGGAAGAAGGGGTTGCCCAGATGAGTGTGGGTCAG
AGAGCCAAACTGACTATATCTCCAGATTATGCCTATGGTGCCACTGGGCACCCAGGCATCATCCCACCACATGCCACTCTCGTCTTCGATGT
GGAGCTTCTAAAACCGGAACCTCTGCAGATGAAAGATAAGGATAATAACCTGAGAGGAGCTTGTTCTAGCTGTAACTGCCCTGAATACTGTT
TTAGCCCAACTTCCACCCTGTGCGACGATTGCAAGTGTTCCGTGACCAAACACCCAATCGTCGAACAGCCCCTGTCCCGAAACGGATCTTTC
CGGAGCTCCGGAGCAAGTCTGCTGCCATCACCTTCTAGTCCCAATGTGAAGATTACCTCTACAGTCGGCCTGCGGAGTAGAAAAAGCGAGTC
CCAGGCAAACGTGCGCGGGTCTATGATCTCTAACAGTAATTCAGGAAGCCGATCCAACAATAGTGGAGGAGCAGGAGGAGGGTCAGGAGGCT
CAAGCTCCTCTAAGGGGGGCAGCGCCCTGGCTAACTACCAGTCCGCTATGTCTGAGCTGTGGTCTTGGAATATGATGCTGAGTACTCCTTCA
CTGAAATTCCTGACCGTGCAGTTTACCACATGGATTGTGCTGACTACCGTCGGCGCCATCTACACTCTGTTCTTTCATGAAAGACAGGCTTA
TAATAGGGGGTGGGCAGACATCTGGTACGGCTATGGGGCTTTCGGATTTGGCCTGGGGCTGAGCTTCGCATATATGGGCTTCACCGGCGCCA
GAAACCCAGAGAAGAAAGCTCTGAGCCTGTGCCTGCTGGGGGTGAATTTCATTAGCTTTATGTCCTACATCATCATCATGCTGCGGCTGACT
CCCACCATCGAAGGCACCATGGCCAACCCAGTGGAGCCCGCTAGATATCTGGAATGGATCGCCACTTGCCCTGTCCTGATCCTGCTGATTAG
CGAGATCACCCAGTACCCTCACGACCCATATAAAGTGATCGTCAATGATTACGCCCTGTGCCTGGCAGGATTCGTGGGAGCAATCAGCGCCC
AGCAGCCATGGGGCGACCTGGCACATTTCGTGAGCTGCCTGTGCTTTTCCTACGTGGTCTATTCTCTGTGGAGTTGCTTCACAGGGGCTATC
GATGGAGAGACTCAGTGTAACGTGGAAAAAAGCGGCCTGAGGTGGATTCGCTTTTCAACAATCACAACTTGGAGCCTGTTCCCCATTACCTG
GTTTTCATATACAAGCGGCCTGATCTCTTTCACTGTGGCAGAGGCCGGGTTTAGTATGATTGACATCGGAGCCAAGGTCTTCCTGACCCTGG
TGCTGGTCAACAGCACAGTGGAACAGGCACAGAATCAGAAAGTCGACGCCATTACCGCTATCGCAGAGGAACTGGAGAACCAGATTAACAAT
TGTGATGCCATCCTGCAGAAGATGATGCCCGAGGGCGTGCTGGAACAGCTGAAGAATGGGCAGGCTACTGAGGCAAAAGAGTACGAATCCGT
GACCGTCTTCTTTTCTGATATTACTAACTTTACCGTGATCAGTTCAAGGACATCCACTAAGGACATGATGGCCACCCTGAACAAGCTGTGGC
TGGAATATGATGCCATTGCTAAGCGGTGGGGAGTGTATAAAGTCGAGACAATCGGCGACGCTTATCTGGGAGTGACTGGAGCACCAGACGTG
GTCCCTGATCACGCAGAGCGAGCTTGCAACTTCGCCGTGGATATCATCGAAATGATTAAGAGCTTTAAAACCATCACAGGCGAGTCCATTAA
CATCCGCATTGGCCTGAATAGCGGACCTGTGACCGCAGGAGTCCTGGGCGACCTGAACCCACACTGGTGTCTGGTGGGAGATACAGTCAATA
CTGCCTCCCGGATGGAATCTACAAGTAAAGCTGGCCACATCCATATTTCAGAGAGCACCTACCATTTCATCAAGTCTAAATTTGTGACACAG
CCTCTGGATGTGATGGAGGTGAAAGGCAAAGGCAAAATGCAGACTTATTGGGTGCTGGGCAGAAAATACCCGTACGACGTCCCGGACTACGC
GTAGTTAATTAAGACTACGACGAAAGTGATGCGCAGGCTGGAAAGCCGCTGAAGGGAGAAGTCTACAAAGCCGATCAGTGAAAAATGTGTGG
GGAGGTGGTCTTGTTGCAGGAATGCAATGGTGTTAAGCATCGTGTTCGAATGCAGTGCGTGTATCAGTTGTGCGCGGAAGGACACTGCTTCA
ATGTTAAGAACCTGTTTTCTCCGTAGAGAGGACCAAAAGACGATTGCAAAACTGGTATGTACGCAATAGCCCAATGCCGGACGTCAGTTGGT
TGTATGTGACGCTCCCAGATGTCATATGCCTTGTGAGTGTGTCTGGGATGCAAGTTTTTGGTGTGCGTTGATTTCGCCAGCTTATGACAGTG
GCAGACGAATTATTGACATGATACAAGGACGCAGAAAGGAACAAACACCGTAGTTCCAGTCGACGGATCCCACCGCGGTGGCGGCCGCACTG
CAGGGTACCCTCGAGGATATCGAATTCATAACTTCGTATAGCATACATTATACGAAGTTATGACTACGACGAAAGTGATGCGCAGGCTGGAA
AGCCGCTGAAGGGAGAAGTCTACAAAGCCGATCAGTGAAAAATGTGTGGGGAGGTGGTCTTGTTGCAGGAATGCAATGGTGTTAAGCATCGT
GTTCGAATGCAGTGCGTGTATCAGTTGTGCGCGGAAGGACACTGCTTCAATGTTAAGAACCTGTTTTCTCCGTAGAGAGGACCAAAAGACGA
TTGCAAAACTGGTATGTACGCAATAGCCCAATGCCGGACGTCAGTTGGTTGTATGTGACGCTCCCAGATGTCATATGCCTTGTGAGTGTGTC
TGGGATGCAAGTTTTTGGTGTGCGTTGATTTCGCCAGCTTATGACAGTGGCAGACGAATTATTGACATGATACAAGGACGCAGAAAGGAACA
AACACCGTAGTTCCAGTCGACGGATCCACTAGTGGATCGATCCCCCGGGCTGCAGGAATTCATCCTGCAAGTGCATAGAAGGAAAGTTGTCT
GCTGTCGTGGGCAGACAGCAACAGTCCAGCACTCTAGCGGCATACAGAACGATAACGCATTCACGAGTGGATACACGCACATCTGCGTCACC
CGCAACTCGCTTTCGTTCTGATTGACAAAAAGAAAACAAGGCGAGGTGAGACTGTGTGAAATGCCACATGAAGAGTCATCCCTTTTCTTCGA
TAAAGGACACAGGGGTCTCTGGCACCCCCTCGTCAGCTCTCTCCGACCCGAGGCACTCTCCCTGATCCCTCCGAAAAGAGAGGAAAACGAGA
GACGGGCAGCTTCTGTATTTCCGCTAGACAGCCATCTCCATCTGGATTCGTCCGTGCGGGACGTAGCCCACGACCTCAAAATCCTCGGCGGT
GAAATCGTCGATTTCCTTGATGCGTTCCTTGTTGAGGATGTTCACAATGGGGAACGGTCTCGGTTCTCTCCGCAGCTGCTCTTTTAAAGCCT
CGACATGGTTCGTGTAGACATGCGTGTTCCCCATGAAGTGAATGAACTCCTTAGGTTTTAGGTTGCAGACGTGTGCAACCATGAGCGTCAAA
AGCGAATAGGAAGCGATGTTGAAGGGGACGCCGAGGCCGACATCGCACGACCGCTGATACATGATGCACGACAGCTCCTTCTGGTCGTTCAC
GTAGAACTGGCACAACAAGTGACAAGGCGGCAGCGCCATTTCGTCCAGCGCTGCAGGATTCCAGGCAGTCATGAGCATGCGACGATCTGTTG

GATTCGTTCTCAGCATCTGGATCACATTCTTCAGCTGGTCGACGCCCTGCCCTGTGTAGTCTGTGTGCATGTCTTTGTATGCCGCGCCGAAG
TGTCTCCACTGGAAGCCGTAGCCCGGGCCGATGTCTCCGACCTCTCGGTGGGGGAGATTGCGCGAATCGAGGAACTCGCGTGTCACATTCTT
GTCCCAGATCTTCACGCCCTTCTCAGAAAGATGGTTTGCGTTCGTGTCGCCGCGAATGAACCACAGCAACTCTTCGAGGACCCCTTTCCAGA
ACACACGCTTTGTGGTGAGAAGTGGAAAGGCCTGATCCAGCGAGTAGCGCATAGTGCAGCCGAATTTGGAGATGACACCAACGCCCGTTCGG
TCATCCATTGTCCTTCCATTGTTAATAATGTCGGCAATGAGATCAAGGTACTGGAATTCTTCATGGCCTCTAAAGTGAACATGCGGAACGGC
CCGAATCAGTTCCTTTTGCTCGCGTTTTTTCCGGTCTTCTTCGTCCATCCACGCCAACACCGGGGCAATGGCTGCGGCCGAAGAAGGAGCCT
GCAACCCGTGCACGGGAGTTGTCTCCCTCGTGGACGTCAAGGAGCTCATTGCGTTGCTCGGTTCCGCAGTGGCTGCGTCGTCAGTCTTCCTT
CTCTTCTCGAGAACCACAAAGTCGTAGGGTACCCCGTTGTCTGAGAAGGTCTTGGAAATGAAGATGGGTCGATACGTCGCTTCATTGTCCTT
CTCTCTTCCGAGCTCCGGACAAAAGGGAACGAACACAGACTCGGCAGGAGCTGCAGCCTGCGCAGCAGTTGATTTGTTTGAAAGAATGTCAT
CTCCGGGGAACGCAGGGAAGAAAACGTCGCACGGAAACTCGCGGGCTACACGCGTGATGTACAGGTGAGAGGCAACGCCCAGAGACAGCGCT
GCCTCGTACAGTCCCGCTCCTCCCACGACAAAAATCTGGTCGACAGAATCCTTGTACTCTTCCTCCAGAAGGCTGAGAGCTGCTGGGAGTGA
AGCACAGACTCGGACGCGCTGCTGGCCTTCAGCTTGAGGCTTCTCCGCCGCAATGTCTTCTTCTTTGAGGGAAGAGGAAACGACGATGTTCA
ATCTGTCCACGAGGGGTCTAAACTTTCGAGGCATGCTTTCCCAGGTTTTCCGTCCCATGACAACGGCGTTGAATCTCTTGCCGACTGATGGA
GAGGGAAGTCCAGAGTCGCCCGTCTTTGCAAATTTCCTGGGAAGCCACCCGTTCAGGCGACTGGCTTCTTCGGGCGTCGTTTTTGTCACACG
AGAAAAGTGTTTGAAATCTGTGGTCAAGTGGGGCCACGGGAGGCCGTTGTTGATGCCGATGCCCCTCTTGGGGGTCATCGCGACGACCAGAC
ACACCGGTTTCTGCATCTTCCCAGACACGACAACGCCCCGTAGAGCAGAAACGCACTACTAAAGCGAAACTTCACCCGTCCCTGCTGCACTC
AGAGCAGTGCTCCGCACTGCCGTGTGGTAAAATGAAAAGGTTCTACGAGACACGCGTCTCCGGATCGACAAGCGAAGGATCTGCACACCTGG
TCTCGATGTCGAACAAAGCACGGAGGAGAGACGGAAAGTGCTTACATCGAACACGGTTATCAAACCCGAGAAAAAGAAACGAACAGAAGAAA
AAGGAAACCTCCGCATACTTTTAAAGAATGAAGTTCCCCGATTTTCCCAAAAATGGCGTCATTTTCGCGCACGGCAGTCAGATAACAGGTGT
AGCGGCTGCCCACCAACAGAGACGGCGCGGCCGACAGGACGCTACTGGGACTGCGAACAGCAGCAAGATCGGATCTTCCGCGGGCGGGTTTG
AATGCAAGGTTTCGTGCTGTCGAAAAAGAGAATGGAACTTAATGTCCACGTAGTTCGCGCATGAAAAGCGTCCTACCACTCAAAAAAGACAA
AAACCGCACTCGCGGCGTTGAATGTGCGGGGGAACGGATGGCTCTCTTTTTTGGAAAGCGAATGCAAAAAGACAAGACGCAGACGCATACAA
CGTTAGTCCCCTGGCACGAGAGATAGAGGTGCTGGGGGCCATTGCGGTGTCGTGGATTTACCAGTCATGGACGAGATCGTTCCGGAGCCTGT
CTTTCCTGAAAGTCTGAAAAAATTGCGGGAAAGTCACGCATATGGAACAGCACCGGGGCGGGACAGAGTTGTCTCGACAACGAATGACACAC
AGGAACTACGCGGGGGGTGAAAATCGAATGACATGCTAGCGTTCAACTTCTGGAAAGGTGGTGGCTTCTCGATCAGGAAACTCCGTTTTCTA
GTGTTGAACAGGTGCGCTCCGAGAAATCGCACGCGGGCTAATACGTGGTAAGACAAAAGACCAGCCTGTCGCCGGATTTAGAAGTCGTGGCA
CTACATACGGACCTCTGTACGAGACATGCCGATGCCAAGGGCGTTATCTGGTGCCTGTGACCGCCAGTTTCAGACAGTACGCGTCTACTAAG
TTTGAAAACGCATATGAACGCGTTTGTCGGTTACCATTCATTCTGCAACTGTCTCAGGCATTGCGTGAGCAAAGCGAGCGCCTCGCTGGTAG
TCCCAACTGAATATTATCGAGTAAGCACACTACTCCACGGACATCCCTAGCGCTCTTACCTGTTCGTAGGGCTAGAGAAATGATTCGGATAT
GGTTACACGTGACCACGCCAAAGTAGAAAGGAATTAGCATAACTCAGTCAGGCAGTCTCCCTGAGGACACCTGCTTGATGATTTGTGAGGAC
GACTCACGGGATTTACAGCCTGGCGAAGCTTGCTAGCGTTAACGGGCCCCGTACC

*Tg*Gra1-5'UTR	HA-tag	NsiI/PstI
Rhodopsin domain	*Tg*Gra2-3'UTR	DHFR/TS selection cassette
Coiled Coil	PacI	(ORF underlined)
Guanylate Cyclase domain	ddFKBP domain	

I) Plasmid of *pDHFR-UPKO-RhoGC-3xHA* (generated by Claudia Ufermann)

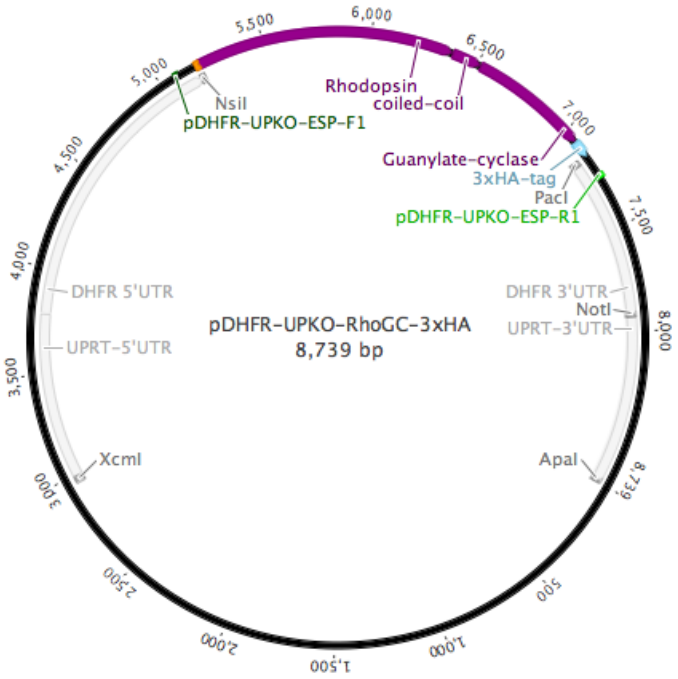

CAGCTTTTGTTCCCTTTAGTGAGGGTTAATTGCGCGCTTGGCGTAATCATGGTCATAGCTGTTTCCTGTGTGAAATTGTTATCCGCTCACAA
TTCCACACAACATACGAGCCGGAAGCATAAAGTGTAAAGCCTGGGGTGCCTAATGAGTGAGCTAACTCACATTAATTGCGTTGCGCTCACTG
CCCGCTTTCCAGTCGGGAAACCTGTCGTGCCAGCTGCATTAATGAATCGGCCAACGCGCGGGGAGAGGCGGTTTGCGTATTGGGCGCTCTTC
CGCTTCCTCGCTCACTGACTCGCTGCGCTCGGTCGTTCGGCTGCGGCGAGCGGTATCAGCTCACTCAAAGGCGGTAATACGGTTATCCACAG
AATCAGGGGATAACGCAGGAAAGAACATGTGAGCAAAAGGCCAGCAAAAGGCCAGGAACCGTAAAAAGGCCGCGTTGCTGGCGTTTTTCCAT
AGGCTCCGCCCCCCTGACGAGCATCACAAAAATCGACGCTCAAGTCAGAGGTGGCGAAACCCGACAGGACTATAAAGATACCAGGCGTTTCC
CCCTGGAAGCTCCCTCGTGCGCTCTCCTGTTCCGACCCTGCCGCTTACCGGATACCTGTCCGCCTTTCTCCCTTCGGGAAGCGTGGCGCTTT
CTCATAGCTCACGCTGTAGGTATCTCAGTTCGGTGTAGGTCGTTCGCTCCAAGCTGGGCTGTGTGCACGAACCCCCCGTTCAGCCCGACCGC
TGCGCCTTATCCGGTAACTATCGTCTTGAGTCCAACCCGGTAAGACACGACTTATCGCCACTGGCAGCAGCCACTGGTAACAGGATTAGCAG
AGCGAGGTATGTAGGCGGTGCTACAGAGTTCTTGAAGTGGTGGCCTAACTACGGCTACACTAGAAGGACAGTATTTGGTATCTGCGCTCTGC
TGAAGCCAGTTACCTTCGGAAAAAGAGTTGGTAGCTCTTGATCCGGCAAACAAACCACCGCTGGTAGCGGTGGTTTTTTTGTTTGCAAGCAG
CAGATTACGCGCAGAAAAAAAGGATCTCAAGAAGATCCTTTGATCTTTTCTACGGGGTCTGACGCTCAGTGGAACGAAAACTCACGTTAAGG
GATTTTGGTCATGAGATTATCAAAAAGGATCTTCACCTAGATCCTTTTAAATTAAAAATGAAGTTTTAAATCAATCTAAAGTATATATGAGT
AAACTTGGTCTGACAGTTACCAATGCTTAATCAGTGAGGCACCTATCTCAGCGATCTGTCTATTTCGTTCATCCATAGTTGCCTGACTCCCC
GTCGTGTAGATAACTACGATACGGGAGGGCTTACCATCTGGCCCCAGTGCTGCAATGATACCGCGAGACCCACGCTCACCGGCTCCAGATTT
ATCAGCAATAAACCAGCCAGCCGGAAGGGCCGAGCGCAGAAGTGGTCCTGCAACTTTATCCGCCTCCATCCAGTCTATTAATTGTTGCCGGG
AAGCTAGAGTAAGTAGTTCGCCAGTTAATAGTTTGCGCAACGTTGTTGCCATTGCTACAGGCATCGTGGTGTCACGCTCGTCGTTTGGTATG
GCTTCATTCAGCTCCGGTTCCCAACGATCAAGGCGAGTTACATGATCCCCCATGTTGTGCAAAAAAGCGGTTAGCTCCTTCGGTCCTCCGAT
CGTTGTCAGAAGTAAGTTGGCCGCAGTGTTATCACTCATGGTTATGGCAGCACTGCATAATTCTCTTACTGTCATGCCATCCGTAAGATGCT
TTTCTGTGACTGGTGAGTACTCAACCAAGTCATTCTGAGAATAGTGTATGCGGCGACCGAGTTGCTCTTGCCCGGCGTCAATACGGGATAAT
ACCGCGCCACATAGCAGAACTTTAAAAGTGCTCATCATTGGAAAACGTTCTTCGGGGCGAAAACTCTCAAGGATCTTACCGCTGTTGAGATC
CAGTTCGATGTAACCCACTCGTGCACCCAACTGATCTTCAGCATCTTTTACTTTCACCAGCGTTTCTGGGTGAGCAAAAACAGGAAGGCAAA
ATGCCGCAAAAAAGGGAATAAGGGCGACACGGAAATGTTGAATACTCATACTCTTCCTTTTTCAATATTATTGAAGCATTTATCAGGGTTAT
TGTCTCATGAGCGGATACATATTTGAATGTATTTAGAAAAATAAACAAATAGGGGTTCCGCGCACATTTCCCCGAAAAGTGCCACCTGACGC
GCCCTGTAGCGGCGCATTAAGCGCGGCGGGTGTGGTGGTTACGCGCAGCGTGACCGCTACACTTGCCAGCGCCCTAGCGCCCGCTCCTTTCG
CTTTCTTCCCTTCCTTTCTCGCCACGTTCGCCGGCTTTCCCCGTCAAGCTCTAAATCGGGGGCTCCCTTTAGGGTTCCGATTTAGTGCTTTA
CGGCACCTCGACCCCAAAAAACTTGATTAGGGTGATGGTTCACGTAGTGGGCCATCGCCCTGATAGACGGTTTTTCGCCCTTTGACGTTGGA
GTCCACGTTCTTTAATAGTGGACTCTTGTTCCAAACTGGAACAACACTCAACCCTATCTCGGTCTATTCTTTTGATTTATAAGGGATTTTGC
CGATTTCGGCCTATTGGTTAAAAAATGAGCTGATTTAACAAAAATTTAACGCGAATTTTAACAAAATATTAACGCTTACAATTTCCATTCGC
CATTCAGGCTGCGCAACTGTTGGGAAGGGCGATCGGTGCGGGCCTCTTCGCTATTACGCCAGCTGGCGAAAGGGGGATGTGCTGCAAGGCGA
TTAAGTTGGGTAACGCCAGGGTTTTCCCAGTCACGACGTTGTAAAACGACGGCCAGTGAGCGCGCGTAATACGACTCACTATAGGGCGAATT
GGAGCTTCGAAGGCTGTAGTACTGGTGCTCGTATGCGACACGCGGATTCACGGCGTATGCGACAAGCGGGATTGCTGATGAGCGTCGTTCCC
CACTGAAGCGCGCGGAGTGGTGGGCGACCACCGGTCACCTGGTTGTAAGCGGCAAAAGGACGCGAAAATGGTGGGAGCAGCAAAGACAGCTA
AAACGCCACAGCATTAATATTCTCCATTAAGACTCATATGCCGAAGAAAGATGCAGTGTGTAGAAACCTGTGAAGTCCGTATTCTCATCTGT
AACAGAGAGACTAGCTTTAGTTGTTTTCCGACACGTCCTGGATCACCCGCGTTACTTTGTCTTCTAACCGTTCTGTCACTACTGGCTCTCTC
CCTGAGCTGCACGTGAGCTCATGCTGGAGCTTCGTATGGATAGGGTTACCCTGGTACACTCGGAAATGTTCTTTGAACGCGGCTGGTGTGGC
TTCTTGTCCCTGGGTGTTTCCTCTCCTCCTTCGACACGTGTTTTTTTCTGCTTTTTCCTGCGCCATCCGCTGTGCCTAGTATCGAAAGCTGT
AGAGTTGCCACCCTGATCTTCTCCCTTCCAACTCTCCGCTTCGACACACCCCCCAACGACTTGTTGTGAAGCTCTGGCCCCCCTGTTTCGGT
TGTGACAGGCTCTCCAGGTGCTCTTGCACTCTCCAGTCCAGCTGGTGTCATAGAACCGTTATCTCTAGAGTGCCCCGAAAGAGCCCCCTCCT

TTTATTCGTTGTTTCCCCTGGGTACGAGCTATCTTGTGGCTTTCTTTGCTTGGGGATGACCCTTGTCGTGACCTTCTATGCGTTCTCGATGA
GAAACCGTCGAGTCTTCGTTGCATGCAGGGGTTTCTGCGCGAAGATACTCTCCCACAGAGCCACAGAAAGTGGTAGCCGCTGTTTTCCAACG
CAGCGTACGTACCTATGCAAAGCTTCGCCAGGCTGTAAATCCCGTGAGTCGTCCTCACAAATCATCAAGCAGGTGTCCTCAGGGAGACTGCC
TGACTGAGTTATGCTAATTCCTTTCTACTTTGGCGTGGTCACGTGTAACCATATCCGAATCATTTCTCTAGCCCTACGAACAGGTAAGAGCG
CTAGGGATGTCCGTGGAGTAGTGTGCTTACTCGATAATATTCAGTTGGGACTACCAGCGAGGCGCTCGCTTTGCTCACGCAATGCCTGAGAC
AGTTGCAGAATGAATGGTAACCGACAAACGCGTTCATATGCGTTTTCAAACTTAGTAGACGCGGTACTGTCTGAAACTGGCGGTCACGCAGC
ACCAGATAACGCCCTTGGCATCGGCATGTCTCGTACAGAGGTCCGTATGTAGTGCCACGACTTCTAAATCCGGCGACAGGCTGGTCTTTTGT
CTTACCACGTATTAGCCCGCGTGCGATTTCTCGGAGCGCACCTGTTCAACACTAGAAAACGGAGTTTCCTGATCGAGAAGCCACCACCTTTC
CAGAAGTTGAACGCTAGCATGTCATTCGATTTTCACCCCCCGCGTAGTTCCTGTGTGTCATTCGTTGTCGAGACAACTCTGTCCCGCCCCGG
TGCTGTTCCATATGCGTGACTTTCCCGCAATTTTTTCAGACTTTCAGGAAAGACAGGCTCCGGAACGATCTCGTCCATGACTGGTAAATCCA
CGACACCGCAATGGCCCCCAGCACCTCTATCTCTCGTGCCAGGGGACTAACGTTGTATGCGTCTGCGTCTTGTCTTTTTGCATTCGCTTTCC
AAAAAAGAGAGCCATCCGTTCCCCCGCACATTCAACGCCGCGAGTGCGGTTTTTGTCTTTTTTGAGTGGTAGGACGCTTTTCATGCGCGAAC
TACGTGGACATTAAGTTCCATTCTCTTTTTCGACAGCACGAAACCTTGCATTCAAACCCGCCCGCGGAAGATCCGATCTTGCTGCTGTTCGC
AGTCCCAGTAGCGTCCTGTCGGCCGCGCCGTCTCTGTTGGTGGGCAGCCGCTACACCTGTTATCTGACTGCCGTGCGCGAAAATGACGCCAT
TTTTGGGAAAATCGGGGAACTTCATTCTTTAAAAGTATGCGGAGGTTTCCTTTTTCTTCTGTTCGTTTCTTTTTCTCGGGTTTGATAACCGT
GTTCGATGTAAGCACTTTCCGTCTCTCCTCCGTGCTTTGTTCGACATCGAGACCAGGTGTGCAGATCCTTCGCTTGTCGATCCGGAGACGCG
TGTCTCGTAGAACCTTTTCATTTTACCACACGGCAGTGCGGAGCACTGCTCTGAGTGCAGCAGGGACGGGTGAAGTTTCGCTTTAGTAGTGC
GTTTCTGCTCTACGGGGCGTTGTCGTGTCTGGGAAGATGCATATGAAAGATAAGGATAATAACCTGAGAGGAGCTTGTTCTAGCTGTAACTG
CCCTGAATACTGTTTTAGCCCAACTTCCACCCTGTGCGACGATTGCAAGTGTTCCGTGACCAAACACCCAATCGTCGAACAGCCCCTGTCCC
GAAACGGATCTTTCCGGAGCTCCGGAGCAAGTCTGCTGCCATCACCTTCTAGTCCCAATGTGAAGATTACCTCTACAGTCGGCCTGCGGAGT
AGAAAAAGCGAGTCCCAGGCAAACGTGCGCGGGTCTATGATCTCTAACAGTAATTCAGGAAGCCGATCCAACAATAGTGGAGGAGCAGGAGG
AGGGTCAGGAGGCTCAAGCTCCTCTAAGGGGGGCAGCGCCCTGGCTAACTACCAGTCCGCTATGTCTGAGCTGTGGTCTTGGAATATGATGC
TGAGTACTCCTTCACTGAAATTCCTGACCGTGCAGTTTACCACATGGATTGTGCTGACTACCGTCGGCGCCATCTACACTCTGTTCTTTCAT
GAAAGACAGGCTTATAATAGGGGGTGGGCAGACATCTGGTACGGCTATGGGGCTTTCGGATTTGGCCTGGGGCTGAGCTTCGCATATATGGG
CTTCACCGGCGCCAGAAACCCAGAGAAGAAAGCTCTGAGCCTGTGCCTGCTGGGGGTGAATTTCATTAGCTTTATGTCCTACATCATCATCA
TGCTGCGGCTGACTCCCACCATCGAAGGCACCATGGCCAACCCAGTGGAGCCCGCTAGATATCTGGAATGGATCGCCACTTGCCCTGTCCTG
ATCCTGCTGATTAGCGAGATCACCCAGTACCCTCACGACCCATATAAAGTGATCGTCAATGATTACGCCCTGTGCCTGGCAGGATTCGTGGG
AGCAATCAGCGCCCAGCAGCCATGGGGCGACCTGGCACATTTCGTGAGCTGCCTGTGCTTTTCCTACGTGGTCTATTCTCTGTGGAGTTGCT
TCACAGGGGCTATCGATGGAGAGACTCAGTGTAACGTGGAAAAAAGCGGCCTGAGGTGGATTCGCTTTTCAACAATCACAACTTGGAGCCTG
TTCCCCATTACCTGGTTTTCATATACAAGCGGCCTGATCTCTTTCACTGTGGCAGAGGCCGGGTTTAGTATGATTGACATCGGAGCCAAGGT
CTTCCTGACCCTGGTGCTGGTCAACAGCACAGTGGAACAGGCACAGAATCAGAAAGTCGACGCCATTACCGCTATCGCAGAGGAACTGGAGA
ACCAGATTAACAATTGTGATGCCATCCTGCAGAAGATGATGCCCGAGGGCGTGCTGGAACAGCTGAAGAATGGGCAGGCTACTGAGGCAAAA
GAGTACGAATCCGTGACCGTCTTCTTTTCTGATATTACTAACTTTACCGTGATCAGTTCAAGGACATCCACTAAGGACATGATGGCCACCCT
GAACAAGCTGTGGCTGGAATATGATGCCATTGCTAAGCGGTGGGGAGTGTATAAAGTCGAGACAATCGGCGACGCTTATCTGGGAGTGACTG
GAGCACCAGACGTGGTCCCTGATCACGCAGAGCGAGCTTGCAACTTCGCCGTGGATATCATCGAAATGATTAAGAGCTTTAAAACCATCACA
GGCGAGTCCATTAACATCCGCATTGGCCTGAATAGCGGACCTGTGACCGCAGGAGTCCTGGGCGACCTGAACCCACACTGGTGTCTGGTGGG
AGATACAGTCAATACTGCCTCCCGGATGGAATCTACAAGTAAAGCTGGCCACATCCATATTTCAGAGAGCACCTACCATTTCATCAAGTCTA
AATTTGTGACACAGCCTCTGGATGTGATGGAGGTGAAAGGCAAAGGCAAAATGCAGACTTATTGGGTGCTGGGCAGAAAATACCCGTACGAC
GTCCCGGACTACGCTGGCTATCCCTATGATGTGCCCGATTATGCGTATCCTTACGATGTTCCAGATTATGCCTAATTAATTAAAGCCCTACA
GAAGCTGCCCGTCTCTCGTTTTCCTCTCTTTTCGGAGGGATCAGGGAGAGTGCCTCGGGTCGGAGAGAGCTGACGAGGGGGTGCCAGAGACC
CCTGTGTCCTTTATCGAAGAAAAGGGATGACTCTTCATGTGGCATTTCACACAGTCTCACCTCGCCTTGTTTTCTTTTTGTCAATCAGAACG
AAAGCGAGTTGCGGGTGACGCAGATGTGCGTGTATCCACTCGTGAATGCGTTATCGTTCTGTATGCCGCTAGAGTGCTGGACTGTTGCTGTC
TGCCCACGACAGCAGACAACTTTCCTTCTATGCACTTGCAGGATGGTGCAGCGCAAACGACGGAGAGAAAGGAGCACCCTCTCAGTTTCCCT
ACGATGTGCTGTCAGTTTCGACTCTTCACCGCGAACGATTGGCGATACGTCTCTGTTGACTTGTTAGGCTCCGACCACGAAGCTCCCTTAAC
TAAATAAGCCGCGACACCTAAGTGTACACCATTTGCAGATCCATAATCTGCGACCGCTGAATCCGTCCAGATCAGTAAAACCGCACCACCTA
AGTGTAAACCTTGTTTAGGTCGATAAAATGCTACCAACCCCCACCCACAATCGAGCCTTGAGCGTTTCTGCGCACGCGTTGGCCTACGTGAC
TTGCTGATGCCTGCCTCTGGCCATTCATGCCAGTCAGTGCGCATAAAAATGTGGACACAGTCGGTTGACAAGTGTTCTGGCAGGCTACAGTG
ACAGCGGCCGCCAGTACCAAGTCTGCTCTGATGAAGTGCGCCACCAGCATTCTGTTTTTTCGCTCCCACGAGGGTGGAACCTCTAGCACACA
ACTTCTCTCTTCTGAGGTTGCCGAAAAACTGTCTGCTAATTTATCGAGTTATTTGAACTACGGGACCAACGGGCAGAGACTGTTTTCACTCG
GATGTCGTACAGTTGACGTCGCGACGAAAGGCACATGACCAAGGCGATTTTTTTTATTTTCTGGTTCATCCGGCTATCCACCAGTGTTGCTT
CGGTCGATCGAACGCCAGAAACCAAAACACCTGTTAGTAACATCTGACCAGTGTCGAACCTGGAAGAAACGCAGCAGTTTGCTTACAACGAA
ATTTTCATTCCACCGGAGACGAGGGTCTGATTCCCGTGGCAATCATTGCAAGGCATCCCGTAGGAAAGGTAGGCAATATCGAAATAGATCCA
GTCGTGCTATGCAGCGTGTCCCTCGACGTTACTACGCACATCCTGTGAACAATTGCCAGGCAGCTGAACGGGTGGTGTGCTGAAGACGTATT
CCAAGATAACAAACCTCCCTGCACGGTCACTGTTTGCTTCCTGGCGATCAGATGTCGTGTGTACGGATAGCAGGTGTCTTCTGCGGTCATTT
CTCTCTCGGTGTACACAGAAAAGAGAGAAATGTAGAGCGTGGCCTGGGTACGCGTGAAAACACGCAACCGGAGGTTCTGGGAGGTACTCCAA
GGAAGCCTGTTCCGCTCAGGATTCCGAGTGGCATTCTATTTTCTGCTACACTGCATTTCCTCGGCAAAAGTGTAAGCAGGGGCCCCGTACC

Guanylate Cyclase	Rhodopsin domain	PacI	NsiI
*Tg*UPRT-5'UTR	Coiled Coil	*Tg*DHFR-3'UTR	3xHA-tag
*Tg*DHFR-5'UTR	NotI	*Tg*UPRT-3'UTR	

J) Plasmid of *pUPKO-pTgDHFR-RhoGC-3xHA-pTgGra1-GCaMP6s*

(generated by Elena Pies under my lab supervision)

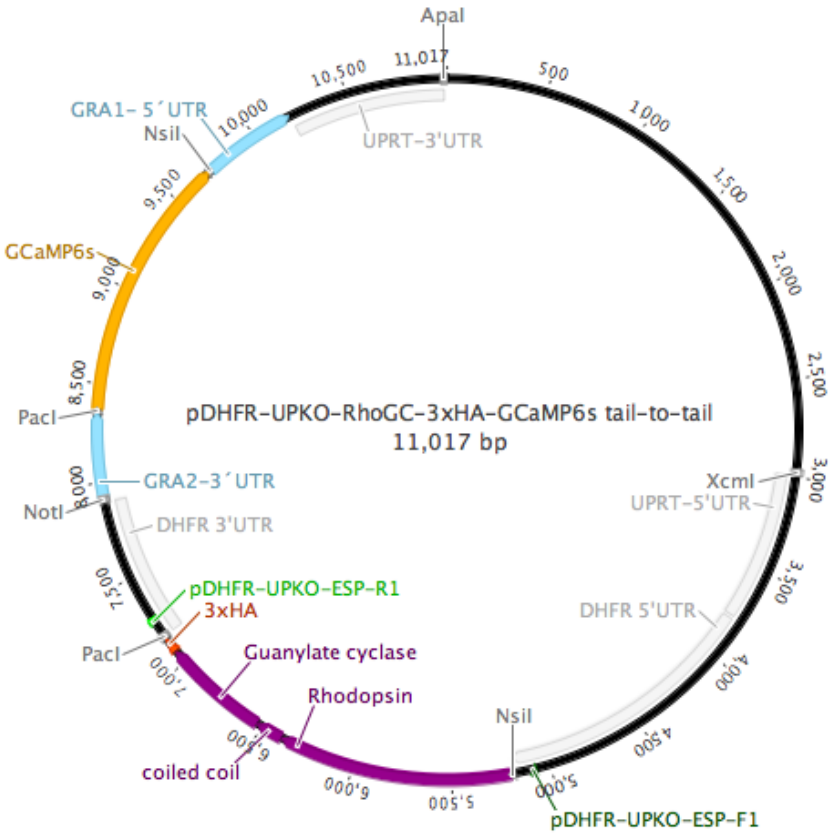

CAGCTTTTGTTCCCTTTAGTGAGGGTTAATTGCGCGCTTGGCGTAATCATGGTCATAGCTGTTTCCTGTGTGAAATTGTTATCCGCTCACAA
TTCCACACAACATACGAGCCGGAAGCATAAAGTGTAAAGCCTGGGGTGCCTAATGAGTGAGCTAACTCACATTAATTGCGTTGCGCTCACTG
CCCGCTTTCCAGTCGGGAAACCTGTCGTGCCAGCTGCATTAATGAATCGGCCAACGCGCGGGGAGAGGCGGTTTGCGTATTGGGCGCTCTTC
CGCTTCCTCGCTCACTGACTCGCTGCGCTCGGTCGTTCGGCTGCGGCGAGCGGTATCAGCTCACTCAAAGGCGGTAATACGGTTATCCACAG
AATCAGGGGATAACGCAGGAAAGAACATGTGAGCAAAAGGCCAGCAAAAGGCCAGGAACCGTAAAAAGGCCGCGTTGCTGGCGTTTTTCCAT
AGGCTCCGCCCCCCTGACGAGCATCACAAAAATCGACGCTCAAGTCAGAGGTGGCGAAACCCGACAGGACTATAAAGATACCAGGCGTTTCC
CCCTGGAAGCTCCCTCGTGCGCTCTCCTGTTCCGACCCTGCCGCTTACCGGATACCTGTCCGCCTTTCTCCCTTCGGGAAGCGTGGCGCTTT
CTCATAGCTCACGCTGTAGGTATCTCAGTTCGGTGTAGGTCGTTCGCTCCAAGCTGGGCTGTGTGCACGAACCCCCCGTTCAGCCCGACCGC
TGCGCCTTATCCGGTAACTATCGTCTTGAGTCCAACCCGGTAAGACACGACTTATCGCCACTGGCAGCAGCCACTGGTAACAGGATTAGCAG
AGCGAGGTATGTAGGCGGTGCTACAGAGTTCTTGAAGTGGTGGCCTAACTACGGCTACACTAGAAGGACAGTATTTGGTATCTGCGCTCTGC
TGAAGCCAGTTACCTTCGGAAAAAGAGTTGGTAGCTCTTGATCCGGCAAACAAACCACCGCTGGTAGCGGTGGTTTTTTTGTTTGCAAGCAG
CAGATTACGCGCAGAAAAAAAGGATCTCAAGAAGATCCTTTGATCTTTTCTACGGGGTCTGACGCTCAGTGGAACGAAAACTCACGTTAAGG
GATTTTGGTCATGAGATTATCAAAAAGGATCTTCACCTAGATCCTTTTAAATTAAAAATGAAGTTTTAAATCAATCTAAAGTATATATGAGT
AAACTTGGTCTGACAGTTACCAATGCTTAATCAGTGAGGCACCTATCTCAGCGATCTGTCTATTTCGTTCATCCATAGTTGCCTGACTCCCC
GTCGTGTAGATAACTACGATACGGGAGGGCTTACCATCTGGCCCCAGTGCTGCAATGATACCGCGAGACCCACGCTCACCGGCTCCAGATTT
ATCAGCAATAAACCAGCCAGCCGGAAGGGCCGAGCGCAGAAGTGGTCCTGCAACTTTATCCGCCTCCATCCAGTCTATTAATTGTTGCCGGG
AAGCTAGAGTAAGTAGTTCGCCAGTTAATAGTTTGCGCAACGTTGTTGCCATTGCTACAGGCATCGTGGTGTCACGCTCGTCGTTTGGTATG
GCTTCATTCAGCTCCGGTTCCCAACGATCAAGGCGAGTTACATGATCCCCCATGTTGTGCAAAAAAGCGGTTAGCTCCTTCGGTCCTCCGAT
CGTTGTCAGAAGTAAGTTGGCCGCAGTGTTATCACTCATGGTTATGGCAGCACTGCATAATTCTCTTACTGTCATGCCATCCGTAAGATGCT
TTTCTGTGACTGGTGAGTACTCAACCAAGTCATTCTGAGAATAGTGTATGCGGCGACCGAGTTGCTCTTGCCCGGCGTCAATACGGGATAAT
ACCGCGCCACATAGCAGAACTTTAAAAGTGCTCATCATTGGAAAACGTTCTTCGGGGCGAAAACTCTCAAGGATCTTACCGCTGTTGAGATC
CAGTTCGATGTAACCCACTCGTGCACCCAACTGATCTTCAGCATCTTTTACTTTCACCAGCGTTTCTGGGTGAGCAAAAACAGGAAGGCAAA
ATGCCGCAAAAAAGGGAATAAGGGCGACACGGAAATGTTGAATACTCATACTCTTCCTTTTTCAATATTATTGAAGCATTTATCAGGGTTAT
TGTCTCATGAGCGGATACATATTTGAATGTATTTAGAAAAATAAACAAATAGGGGTTCCGCGCACATTTCCCCGAAAAGTGCCACCTGACGC
GCCCTGTAGCGGCGCATTAAGCGCGGCGGGTGTGGTGGTTACGCGCAGCGTGACCGCTACACTTGCCAGCGCCCTAGCGCCCGCTCCTTTCG
CTTTCTTCCCTTCCTTTCTCGCCACGTTCGCCGGCTTTCCCCGTCAAGCTCTAAATCGGGGGCTCCCTTTAGGGTTCCGATTTAGTGCTTTA
CGGCACCTCGACCCCAAAAAACTTGATTAGGGTGATGGTTCACGTAGTGGGCCATCGCCCTGATAGACGGTTTTTCGCCCTTTGACGTTGGA
GTCCACGTTCTTTAATAGTGGACTCTTGTTCCAAACTGGAACAACACTCAACCCTATCTCGGTCTATTCTTTTGATTTATAAGGGATTTTGC
CGATTTCGGCCTATTGGTTAAAAAATGAGCTGATTTAACAAAAATTTAACGCGAATTTTAACAAAATATTAACGCTTACAATTTCCATTCGC
CATTCAGGCTGCGCAACTGTTGGGAAGGGCGATCGGTGCGGGCCTCTTCGCTATTACGCCAGCTGGCGAAAGGGGGATGTGCTGCAAGGCGA
TTAAGTTGGGTAACGCCAGGGTTTTCCCAGTCACGACGTTGTAAAACGACGGCCAGTGAGCGCGCGTAATACGACTCACTATAGGGCGAATT

GGAGCTTCGAAGGCTGTAGTACTGGTGCTCGTATGCGACACGCGGATTCACGGCGTATGCGACAAGCGGGATTGCTGATGAGCGTCGTTCCC
CACTGAAGCGCGCGGAGTGGTGGGCGACCACCGGTCACCTGGTTGTAAGCGGCAAAAGGACGCGAAAATGGTGGGAGCAGCAAAGACAGCTA
AAACGCCACAGCATTAATATTCTCCATTAAGACTCATATGCCGAAGAAAGATGCAGTGTGTAGAAACCTGTGAAGTCCGTATTCTCATCTGT
AACAGAGAGACTAGCTTTAGTTGTTTTCCGACACGTCCTGGATCACCCGCGTTACTTTGTCTTCTAACCGTTCTGTCACTACTGGCTCTCTC
CCTGAGCTGCACGTGAGCTCATGCTGGAGCTTCGTATGGATAGGGTTACCCTGGTACACTCGGAAATGTTCTTTGAACGCGGCTGGTGTGGC
TTCTTGTCCCTGGGTGTTTCCTCTCCTCCTTCGACACGTGTTTTTTTCTGCTTTTTCCTGCGCCATCCGCTGTGCCTAGTATCGAAAGCTGT
AGAGTTGCCACCCTGATCTTCTCCCTTCCAACTCTCCGCTTCGACACACCCCCCAACGACTTGTTGTGAAGCTCTGGCCCCCCTGTTTCGGT
TGTGACAGGCTCTCCAGGTGCTCTTGCACTCTCCAGTCCAGCTGGTGTCATAGAACCGTTATCTCTAGAGTGCCCCGAAAGAGCCCCCTCCT
TTTATTCGTTGTTTCCCCTGGGTACGAGCTATCTTGTGGCTTTCTTTGCTTGGGGATGACCCTTGTCGTGACCTTCTATGCGTTCTCGATGA
GAAACCGTCGAGTCTTCGTTGCATGCAGGGGTTTCTGCGCGAAGATACTCTCCCACAGAGCCACAGAAAGTGGTAGCCGCTGTTTTCCAACG
CAGCGTACGTACCTATGCAAAGCTTCGCCAGGCTGTAAATCCCGTGAGTCGTCCTCACAAATCATCAAGCAGGTGTCCTCAGGGAGACTGCC
TGACTGAGTTATGCTAATTCCTTTCTACTTTGGCGTGGTCACGTGTAACCATATCCGAATCATTTCTCTAGCCCTACGAACAGGTAAGAGCG
CTAGGGATGTCCGTGGAGTAGTGTGCTTACTCGATAATATTCAGTTGGGACTACCAGCGAGGCGCTCGCTTTGCTCACGCAATGCCTGAGAC
AGTTGCAGAATGAATGGTAACCGACAAACGCGTTCATATGCGTTTTCAAACTTAGTAGACGCGGTACTGTCTGAAACTGGCGGTCACGCAGC
ACCAGATAACGCCCTTGGCATCGGCATGTCTCGTACAGAGGTCCGTATGTAGTGCCACGACTTCTAAATCCGGCGACAGGCTGGTCTTTTGT
CTTACCACGTATTAGCCCGCGTGCGATTTCTCGGAGCGCACCTGTTCAACACTAGAAAACGGAGTTTCCTGATCGAGAAGCCACCACCTTTC
CAGAAGTTGAACGCTAGCATGTCATTCGATTTTCACCCCCCGCGTAGTTCCTGTGTGTCATTCGTTGTCGAGACAACTCTGTCCCGCCCCGG
TGCTGTTCCATATGCGTGACTTTCCCGCAATTTTTTCAGACTTTCAGGAAAGACAGGCTCCGGAACGATCTCGTCCATGACTGGTAAATCCA
CGACACCGCAATGGCCCCCAGCACCTCTATCTCTCGTGCCAGGGGACTAACGTTGTATGCGTCTGCGTCTTGTCTTTTTGCATTCGCTTTCC
AAAAAAGAGAGCCATCCGTTCCCCCGCACATTCAACGCCGCGAGTGCGGTTTTTGTCTTTTTTGAGTGGTAGGACGCTTTTCATGCGCGAAC
TACGTGGACATTAAGTTCCATTCTCTTTTTCGACAGCACGAAACCTTGCATTCAAACCCGCCCGCGGAAGATCCGATCTTGCTGCTGTTCGC
AGTCCCAGTAGCGTCCTGTCGGCCGCGCCGTCTCTGTTGGTGGGCAGCCGCTACACCTGTTATCTGACTGCCGTGCGCGAAAATGACGCCAT
TTTTGGGAAAATCGGGGAACTTCATTCTTTAAAAGTATGCGGAGGTTTCCTTTTTCTTCTGTTCGTTTCTTTTTCTCGGGTTTGATAACCGT
GTTCGATGTAAGCACTTTCCGTCTCTCCTCCGTGCTTTGTTCGACATCGAGACCAGGTGTGCAGATCCTTCGCTTGTCGATCCGGAGACGCG
TGTCTCGTAGAACCTTTTCATTTTACCACACGGCAGTGCGGAGCACTGCTCTGAGTGCAGCAGGGACGGGTGAAGTTTCGCTTTAGTAGTGC
GTTTCTGCTCTACGGGGCGTTGTCGTGTCTGGGAAGATGCATATGAAAGATAAGGATAATAACCTGAGAGGAGCTTGTTCTAGCTGTAACTG
CCCTGAATACTGTTTTAGCCCAACTTCCACCCTGTGCGACGATTGCAAGTGTTCCGTGACCAAACACCCAATCGTCGAACAGCCCCTGTCCC
GAAACGGATCTTTCCGGAGCTCCGGAGCAAGTCTGCTGCCATCACCTTCTAGTCCCAATGTGAAGATTACCTCTACAGTCGGCCTGCGGAGT
AGAAAAAGCGAGTCCCAGGCAAACGTGCGCGGGTCTATGATCTCTAACAGTAATTCAGGAAGCCGATCCAACAATAGTGGAGGAGCAGGAGG
AGGGTCAGGAGGCTCAAGCTCCTCTAAGGGGGGCAGCGCCCTGGCTAACTACCAGTCCGCTATGTCTGAGCTGTGGTCTTGGAATATGATGC
TGAGTACTCCTTCACTGAAATTCCTGACCGTGCAGTTTACCACATGGATTGTGCTGACTACCGTCGGCGCCATCTACACTCTGTTCTTTCAT
GAAAGACAGGCTTATAATAGGGGGTGGGCAGACATCTGGTACGGCTATGGGGCTTTCGGATTTGGCCTGGGGCTGAGCTTCGCATATATGGG
CTTCACCGGCGCCAGAAACCCAGAGAAGAAAGCTCTGAGCCTGTGCCTGCTGGGGGTGAATTTCATTAGCTTTATGTCCTACATCATCATCA
TGCTGCGGCTGACTCCCACCATCGAAGGCACCATGGCCAACCCAGTGGAGCCCGCTAGATATCTGGAATGGATCGCCACTTGCCCTGTCCTG
ATCCTGCTGATTAGCGAGATCACCCAGTACCCTCACGACCCATATAAAGTGATCGTCAATGATTACGCCCTGTGCCTGGCAGGATTCGTGGG
AGCAATCAGCGCCCAGCAGCCATGGGGCGACCTGGCACATTTCGTGAGCTGCCTGTGCTTTTCCTACGTGGTCTATTCTCTGTGGAGTTGCT
TCACAGGGGCTATCGATGGAGAGACTCAGTGTAACGTGGAAAAAAGCGGCCTGAGGTGGATTCGCTTTTCAACAATCACAACTTGGAGCCTG
TTCCCCATTACCTGGTTTTCATATACAAGCGGCCTGATCTCTTTCACTGTGGCAGAGGCCGGGTTTAGTATGATTGACATCGGAGCCAAGGT
CTTCCTGACCCTGGTGCTGGTCAACAGCACAGTGGAACAGGCACAGAATCAGAAAGTCGACGCCATTACCGCTATCGCAGAGGAACTGGAGA
ACCAGATTAACAATTGTGATGCCATCCTGCAGAAGATGATGCCCGAGGGCGTGCTGGAACAGCTGAAGAATGGGCAGGCTACTGAGGCAAAA
GAGTACGAATCCGTGACCGTCTTCTTTTCTGATATTACTAACTTTACCGTGATCAGTTCAAGGACATCCACTAAGGACATGATGGCCACCCT
GAACAAGCTGTGGCTGGAATATGATGCCATTGCTAAGCGGTGGGGAGTGTATAAAGTCGAGACAATCGGCGACGCTTATCTGGGAGTGACTG
GAGCACCAGACGTGGTCCCTGATCACGCAGAGCGAGCTTGCAACTTCGCCGTGGATATCATCGAAATGATTAAGAGCTTTAAAACCATCACA
GGCGAGTCCATTAACATCCGCATTGGCCTGAATAGCGGACCTGTGACCGCAGGAGTCCTGGGCGACCTGAACCCACACTGGTGTCTGGTGGG
AGATACAGTCAATACTGCCTCCCGGATGGAATCTACAAGTAAAGCTGGCCACATCCATATTTCAGAGAGCACCTACCATTTCATCAAGTCTA
AATTTGTGACACAGCCTCTGGATGTGATGGAGGTGAAAGGCAAAGGCAAAATGCAGACTTATTGGGTGCTGGGCAGAAAATACCCGTACGAC
GTCCCGGACTACGCTGGCTATCCCTATGATGTGCCCGATTATGCGTATCCTTACGATGTTCCAGATTATGCCTAATTAATTAAAGCCCTACA
GAAGCTGCCCGTCTCTCGTTTTCCTCTCTTTTCGGAGGGATCAGGGAGAGTGCCTCGGGTCGGAGAGAGCTGACGAGGGGGTGCCAGAGACC
CCTGTGTCCTTTATCGAAGAAAAGGGATGACTCTTCATGTGGCATTTCACACAGTCTCACCTCGCCTTGTTTTCTTTTTGTCAATCAGAACG
AAAGCGAGTTGCGGGTGACGCAGATGTGCGTGTATCCACTCGTGAATGCGTTATCGTTCTGTATGCCGCTAGAGTGCTGGACTGTTGCTGTC
TGCCCACGACAGCAGACAACTTTCCTTCTATGCACTTGCAGGATGGTGCAGCGCAAACGACGGAGAGAAAGGAGCACCCTCTCAGTTTCCCT
ACGATGTGCTGTCAGTTTCGACTCTTCACCGCGAACGATTGGCGATACGTCTCTGTTGACTTGTTAGGCTCCGACCACGAAGCTCCCTTAAC
TAAATAAGCCGCGACACCTAAGTGTACACCATTTGCAGATCCATAATCTGCGACCGCTGAATCCGTCCAGATCAGTAAAACCGCACCACCTA
AGTGTAAACCTTGTTTAGGTCGATAAAATGCTACCAACCCCCACCCACAATCGAGCCTTGAGCGTTTCTGCGCACGCGTTGGCCTACGTGAC
TTGCTGATGCCTGCCTCTGGCCATTCATGCCAGTCAGTGCGCATAAAAATGTGGACACAGTCGGTTGACAAGTGTTCTGGCAGGCTACAGTG
ACAGCGGCCGCCACCGCGGTGGGATCCGTCGACTGGAACTACGGTGTTTGTTCCTTTCTGCGTCCTTGTATCATGTCAATAATTCGTCTGCC
ACTGTCATAAGCTGGCGAAATCAACGCACACCAAAAACTTGCATCCCAGACACACTCACAAGGCATATGACATCTGGGAGCGTCACATACAA
CCAACTGACGTCCGGCATTGGGCTATTGCGTACATACCAGTTTTGCAATCGTCTTTTGGTCCTCTCTACGGAGAAAACAGGTTCTTAACATT
GAAGCAGTGTCCTTCCGCGCACAACTGATACACGCACTGCATTCGAACACGATGCTTAACACCATTGCATTCCTGCAACAAGACCACCTCCC
CACACATTTTTCACTGATCGGCTTTGTAGACTTCTCCCTTCAGCGGCTTTCCAGCCTGCGCATCACTTTCGTCGTAGTCTTAATTAATCACT
TCGCTGTCATCATTTGTACAAACTCTTCGTAGTTTACCTGACCATCCCCATCGATGTCTGCTTCCCTGATCATTTCATCAACCTCTTCATCT
GTTAACTTCTCTCCAAGGTTTGTCATCACGTGGCGAAGCTCTGCTGCACTGATGTAGCCATTGCCATCCTTATCAAACACACCGAACGCTTC
TCTAATTTCTTCTTCCGTGTCCCTGTATTTCATTTTTCTTGCCATCATTGTCAGGAACTCAGGGAAGTCGATTGTGCCGTCACCGTCGGCAT
CTACTTCATTGATCATGTCCTGCAGCTCTGCTTCTGTGGGGTTCTGCCCCAGAGACCGCATCACCGTCCCCAGCTCCTTGGTTGTTATTGTC
CCATCCCCGTCCTTGTCAAATAGGGAGAAAGCCTCTTTAAATTCTGCGATCTGCTCTTCAGTCAGTTGGTCCGGCAGGTTGTACTCCAGCTT
GTGCCCCAGGATGTTGCCGTCCTCCTTGAAGTCGATGCCCTTCAGCTCGATGCGGTTCACCAGGGTGTCGCCCTCGAACTTCACCTCGGCGC
GGGTCTTGTAGTTGCCGTCGTCCTTGAAGAAGATGGTGCGCTCCTGGATGTAGCCTTCGGGCATGGCGGACTTGAAGAAGTCGTGCTGCTTC

ATGTGGTCGGGGTAGCGGCTGAAGCACTGCACGCCGTAGGTCAGGGTGGTCACGAGGGTGGGCCAGGGCACGGGCAGCTTGCCGGTGGTGCA
GATGAACTTCAGGGTCAGCTTGCCGTAGGTGGCATCGCCCTCACCCTCGCCGGACACGCTGAACTTGTGGCCGTTTACGTCGCCGTCCAGCT
CGACCAGGATGGGCACCACCCCGGTGAACAGCTCCTCGCCCTTGCTCACCATGCTCCCTCCGGTACCGCCCTTGTACAGCTCGTCCATGCCG
AGAGTGATCCCGGCGGCGGTCACGAACTCCAGCAGGACCATGTGATCGCGCTTCTCGTTGGGGTCTTTCGAAAGTTTGGACTGCACGCTCAG
GTAGTGGTTGTCGGGCAGCAGCACGGGGCCGTCGCCGATGGGGGTGTTCTGCTGGTAGTGGTAGGCGAGCTGCACGCCGCCGTCCTCGATGT
TGTGGCGGATGTGGAAGTTCGCCTTGATGCCGTTCTTCTGCTTGTCGGCCTTGATATAGACGTTCTCGAGTGAGCTCAGCCGACCTATAGCT
CTGACTGCGTGACCTGTCTTATTCCACTTACGACGTGATGAGTCGACCATGGTGGCGAGATCCTTATCGTCATCGTCGTACAGATCCCGACC
CATTTGCTGTCCACCAGTCATGCTAGCCATACCATGATGATGATGATGATGAGAATGCATATGCATCTTGCTTGATTTCTTCAAAGAACACA
GCAAGTGAAAAATGAATAGCCTTTGATTTGGCCAGCCACCAACCAACACAAGCAAACCGAGTTGCGTCTATACAGACGTGTCGAAACAAGCT
GACACTCACTGTACAACTTAACTGATAAAAGGTGGGAGAAGATAGCACCCAAAAACGCAAGCTCGCTCGGCAGTTTCAACCGATAAAATTGC
AAAGTAATGTTGTGGCTTTACCGACTGCCCAATGCGAAGTGGGGTGGTCACAACCGTCGAGTCGAGACGCAGCGGTGGACCGGGAATTGGTC
CGCAATGAGACGAGGGCAAACAACCTGTGCCCGCTTACGGCGTCTCATACCATGTTTTCGTTCAGCGTGATCGTATGGTCAACAAACAGCAT
ATTCCTCCCGCCGCGACCCCAGCGATTGGTATTCGTGACGAGTACCACGCTATGAGAGGGGTGCCTCGCGCAGCTGAGACGCAGTACCAAGT
CTGCTCTGATGAAGTGCGCCACCAGCATTCTGTTTTTTCGCTCCCACGAGGGTGGAACCTCTAGCACACAACTTCTCTCTTCTGAGGTTGCC
GAAAAACTGTCTGCTAATTTATCGAGTTATTTGAACTACGGGACCAACGGGCAGAGACTGTTTTCACTCGGATGTCGTACAGTTGACGTCGC
GACGAAAGGCACATGACCAAGGCGATTTTTTTTATTTTCTGGTTCATCCGGCTATCCACCAGTGTTGCTTCGGTCGATCGAACGCCAGAAAC
CAAAACACCTGTTAGTAACATCTGACCAGTGTCGAACCTGGAAGAAACGCAGCAGTTTGCTTACAACGAAATTTTCATTCCACCGGAGACGA
GGGTCTGATTCCCGTGGCAATCATTGCAAGGCATCCCGTAGGAAAGGTAGGCAATATCGAAATAGATCCAGTCGTGCTATGCAGCGTGTCCC
TCGACGTTACTACGCACATCCTGTGAACAATTGCCAGGCAGCTGAACGGGTGGTGTGCTGAAGACGTATTCCAAGATAACAAACCTCCCTGC
ACGGTCACTGTTTGCTTCCTGGCGATCAGATGTCGTGTGTACGGATAGCAGGTGTCTTCTGCGGTCATTTCTCTCTCGGTGTACACAGAAAA
GAGAGAAATGTAGAGCGTGGCCTGGGTACGCGTGAAAACACGCAACCGGAGGTTCTGGGAGGTACTCCAAGGAAGCCTGTTCCGCTCAGGAT
TCCGAGTGGCATTCTATTTTCTGCTACACTGCATTTCCTCGGCAAAAGTGTAAGCAGGGGCCCCGTACC

NsiI	Rhodopsin domain	PacI	GCaMP6s
*Tg*UPRT-5'UTR	Coiled Coil	*Tg*Gra1-5'UTR	NotI
*Tg*DHFR-5'UTR	Guanylate Cyclase domain	3xHA-tag	
*TgD*HFR-3'UTR	*Tg*UPRT-3'UTR	*Tg*Gra2-3'UTR	

List of Publications

The following publications and presentations resulted from this work:

- **Publication**

Günay-Esiyok Ö., Scheib U., Noll M., Gupta N. An unusual and vital protein with guanylate cyclase and P-4 ATPase domains in pathogenic protist. *Life Science Alliance*, 2019; **2(3):** e201900402

- **Presentations**

An unusual multifunctional protein with P-type ATPase and guanylate cyclase motifs located at the apical end governs the lytic cycle of *Toxoplasma gondii*. *ICOPA 2018, 14th International Congress of Parasitology*, Daegu, South Korea, 19-24 August, 2018

An exclusive guanylate cyclase governs the lytic cycle of *Toxoplasma gondii*. *28th Annual Meeting of the German Society for Parasitology,* Berlin, Germany. 21-24 March, 2018

- **Posters**

Günay-Esiyok Ö., Scheib U., Gupta N. An unusual and physiologically vital protein with guanylate cyclase and P-type ATPase domains in the parasitic protozoan *Toxoplasma gondii*. *Hot topics in Signal transduction and cGMP research*, Tübingen, Germany. **Poster 8**, 08-10 October, 2018.

Günay-Esiyok Ö., Ufermann C., Pies E., Gupta N. Optogenetic regulation of cGMP signaling in *Toxoplasma gondii*. *28th Annual Meeting of the German Society for Parasitology,* Berlin, Germany. **CBS-P-07,** 21-24 March, 2018.

Günay-Esiyok Ö., Gupta N. Physiological importance of the cyclic GMP signaling in *Toxoplasma gondii. The 14th biennial conference of the Toxoplasma gondii research community,* Tomar, Portugal. **255**, 31 May-4 June 2017.

Günay-Esiyok Ö., Gupta N. Cyclic GMP-mediated signaling in the apicomplexan parasite *Toxoplasma gondii. 27th Annual Meeting of the German Society for Parasitology,* Göttingen, Germany. **P CEL 1**, 9-12 March 2016.

Other publications outside the scope of this thesis:

- **Publications**

Nitzsce R., **Günay-Esiyok Ö.**, Tischer M., Zagoriy V., Gupta N.A plant/fungal-type phosphoenolpyruvate carboxykinase located in the parasite mitochondrion ensures glucoseindependent survival of *Toxoplasma gondii*. *Journal of Biological Chemistry*, 2017; **292-(237):** 15225-15239.

Gunay Esiyok O., Akcelik N., Akcelik M. Identification of Genomic Heterogeneity among *Lactococcus lactis* Strains by Plasmid Profiling, PFGE and 16S rDNA Sequence Analysis. *Polish Journal of Microbiology*, 2014; **63-(2):** 157-166.

Diani M., **Gunay Esiyok O.**, Ariafar M.N., Yuksel F.N., Gunes Altuntas E., Akcelik N. The Interactions between *esp*, *fsr*, *gelE* Genes and Biofilm Formation and PFGE Analysis of Clinical *Enterococcus faecium* Strains. *African Journal of Microbiology Research*, 2014; **8-(2):** 129-137.

- **Posters**

Günay-Esiyok Ö., Noll M., Randle N., Xia D., Gupta N. Optogenetic illumination of cAMP signaling in *Toxoplasma gondii. 15th biennial meeting on Toxoplasma Biology and Toxoplasmosis,* Quimbaya, Quindio, Colombia. **Poster 243**, 19-21 June, 2019.

Gunay Esiyok O., Yuksel F.N., Diani M., Ariafar M.N., Akcelik N. Determination of genetic diversity among vancomycin-resistant *Enterococcus faecium* isolates by pulsed field gel electrophoresis (PFGE) and virulence genes by polymerase chain reactions (PCR). *ESCMID-24th European Congress of Clinical Microbiology and Infectious Diseases*, Barcelona, Spain. **R255,** 10-13 May 2014.

Diani M., **Gunay O**., Badali M.N., Yuksel F.N., Buyer B., Gunes Altuntas E., Akcelik N. Difference in biofilm-forming abilities among fecal, urine and blood enterococcal isolates of human origin, *ESCMID – 23rd European Congress of Clinical Microbiology and Infectious Diseases*, Berlin, Germany. **R2538**, 27-30 April 2013.

Akcelik N., Sanlıbaba P., **Gunay O**., Yıldız N., Akcelik M. Bonding Characteristics of MisL Autotransporter Protein to Fibronectin. XXXV. *Turkish Microbiology Congress,* Kusadasi, Aydin, Turkey. **P341,** 03-07 November 2012

Karaca B.*, Yuksel F.N., **Gunay O**., Diani M., Badali M.N., Yavas B., Akcelik N., Akcelik M. Biofilm Producing Ability of *Salmonella typhimurium* BK4, Isolated from Turkey. ESCMID – *22nd European Congress of Clinical Microbiology and Infectious Diseases*, London, UK. **R2436,** 31.03.2012 - 03.04.2012

Acknowledgements

First of all, I would like to thank to my mentor PD. Dr. Nishith Gupta for giving me a chance to work on my PhD topic and his constant support during my PhD period.

I also want to express my sincere thanks to Prof. Dr. Richard Lucius and Prof. Dr. Friedrich W. Herberg for rewieving my thesis, as well as Prof. Dr. Kai Matuschewski and Prof. Dr. Maik Lehmann for being part of my thesis committee.

In addition, I would like to express my appreciation to the Elsa-Neumann-Scholarship by the state of Berlin for funding me three years in this context of study.

I am grateful to all our collaborators, Dr. Ulrike Scheib, Dr. Daniel Lauster, Dr. Shatanik Mukherjee and Willi Weber for their valuable contributions into this work. Besides, I would like to thank to Prof. Dr. Stefan Tenzer as well as Thomas Michna for the opportunity to collaborate in proteomics research.

Furthemore, I particularly thank to Claudia Ufermann, Elena Pies and Anika Freitag for their hard work in lab and contributions to this study during their master and project studies. I really enjoyed working with them, learned a lot and improved my skills during lab supervision.

Thanks to all members of Molecular Parasitology Department, especially to my dear colleagues Matthias, Arun, Bingjian, Pengfei and Richard, for creating a friendly working environment, sharing the knowledge and ideas. And of course special thanks to our technical assistance Grit Meusel for her helpful and support whenever I needed.

Last but not least, I would like to express my deepest gratitude to my family. I always felt their support through my education. I feel depted to specially and deeply thank to my husband. All of this would not have been possible without his extensive and unconditional support.

Eigenstandigkeitserklarung

Hiermit erkläre ich, die vorliegende Dissertation

"Cyclic GMP signaling during the lytic cycle of *Toxoplasma gondii*"

selbständig angefertigt und nur unter Verwendung der angegebenen Hilfen und Hilfsmittel angefertigt zu haben.

_____

Ort, Datum Unterschrift